

Tailored Epoxide Monomers as Building Units for Multifunctional Poly(ethylene glycol)

Dissertation zur Erlangung des Grades

"Doktor der Naturwissenschaften"

im Promotionsfach Makromolekulare Chemie

am Fachbereich Chemie, Pharmazie und Geowissenschaften

der Johannes Gutenberg-Universität in Mainz

Christine Elisabeth Mangold

geboren am 16.01.1985 in Karlsruhe

Mainz, April 2012

Tag der mündlichen Prüfung: 06.06.2012

Hiermit versichere ich gemäß § 10 Abs. 3d der Promotionsordnung vom 24.07.2007, dass ich die als Dissertation vorgelegte Arbeit selbst angefertigt und alle benutzten Hilfsmittel (Literatur, Apparaturen, Material) in der Arbeit angegeben habe.

Die als Dissertation vorgelegte Arbeit wurde in der Zeit vom September 2009 bis April 2012 am Institut für Organische Chemie der Johannes Gutenberg-Universität Mainz im Arbeitskreis von Univ.-Prof. Dr. Holger Frey angefertigt.

Ich bin immer noch verwirrt, aber auf einem höheren Niveau.

Enrico Fermi

Table of Contents

Motivation and Objectives	12
Abstract	16
Graphical Abstract	19
Functional PEG-based Polymers with Reactive Groups via Anionic ROP of Tailor-made Epoxides	24
Hetero-Multifunctional Poly(ethylene glycol) Copolymers with Multiple Hydroxyl Groups and a Single Terminal Functionality	42
Supporting Information	53
“Functional Poly(ethylene glycol)”: PEG-based Random Copolymers with 1,2-Diol Side Chains and Terminal Amino Functionality	64
Supporting Information	81
PEG-based Multifunctional Polyethers with Highly Reactive Vinyl-Ether Side Chains for Click-type Functionalization	88
Supporting Information	104
From an Epoxide Monomer Toolkit to Functional PEG Copolymers with Adjustable LCST Behavior.	112
Supporting Information	122
In Vitro Toxicity Evaluation of mf-PEGs with Varying Microstructure and Architecture	131
Thermo-Responsive Ferrocene-Containing Poly(ethylene glycol)	149
Supporting Information	162
Asymmetric Micellization of Organometallic Polyether Block Copolymers.....	171
Branched Acid-Degradable, Biocompatible Polyether-Based Copolymers by Anionic Ring-Opening Polymerization Using an Epoxide Inimer.....	187
Supporting Information	203

Motivation and Objectives

Motivation and Objectives

Poly(ethylene glycol) (PEG) also named Poly(ethylene oxide) (PEO) is one of the most important biocompatible polymers known today. It is chemically inert, shows good antigenicity and does not generate an immune response *in vivo*. Besides its valuable characteristics regarding pronounced biocompatibility, the excellent water solubility of PEG plays an important role. These features have led to applications in an immense variety of products, in areas as diverse as cosmetics and as food additive, either as homo-oligomer/polymer or as derivative in surfactants. PEG is also important in the pharmaceutical industry, as it can serve as a basis for creams and ointments as well as laxatives. PEG can be synthesized by anionic ring-opening polymerization (AROP) of ethylene oxide (EO), which is produced on a million ton scale per year. Besides its use in daily life applications, PEG is an important industrial product and can serve for example as a lubricant.

One sophisticated application for PEG is its use in biomedical applications, with the most prominent example being PEGylation, i.e., the covalent attachment of PEG to small drug molecules or proteins, vesicles and nanoparticles, which brings along several advantages. In some cases, PEG can serve as a solubilizing agent of hydrophobic molecules or solubilize metal/metal oxide nanoparticles, which might be used in magnetic resonance imaging (MRI). Furthermore, PEG can increase the stability of vesicles used for controlled release of pharmaceutically active agents in physiological environment, the so-called “stealth”-effect. This describes the shielding effects of PEG chains that prolong the blood circulation time of active compounds, such as proteins. This effect is one of the main reasons for the recent success of the PEGylation strategy.

One major drawback of PEG with respect to multiple covalent attachments of molecules is that commercially available PEG exhibits a maximum of two reactive sites viz. the hydroxyl groups at the polymer termini. Although PEG has been known and used in a variety of the above-mentioned applications for several decades, there has been no effort to modify PEG in such a way that the functionality is increased significantly without the implementation of a second, chemically different polymer block. The use of block copolymers can be advantageous in some applications, if phase separation between the blocks, i.e., the formation of micellar structures is required, but this should be avoided, when amphiphilicity leads to unwanted side effects. Generally, the introduction of multiple functional groups at the PEG backbone using functional oxirane comonomers in AROP has not been realized so far.

The first objective of this thesis is to establish a general route for the synthesis of multifunctional PEGs (*mf*-PEGs), avoiding block copolymer formation. This affords the synthesis of novel epoxide derivatives, which are easily accessible and carry suitable functionalities. To achieve this objective, different glycidyl ethers can be copolymerized as comonomers with EO via anionic ring-opening

polymerization. The introduction of different functionalities can be realized employing two different strategies.

On the one hand comonomers carrying functional groups which are stable toward the highly basic conditions applied in AROP can be used. On the other hand protecting group chemistry can be utilized to introduce functionalities, such as hydroxyl-groups, which would usually serve as initiator themselves. In this context the following important questions need to be answered:

i) Are the newly introduced functionalities randomly distributed along the PEG chain?

The random distribution of the functional groups/side chains is important for two reasons: First of all, fundamental ideas on the relative glycidyl ether reactivity can be derived from an investigation of this type, which is useful for further syntheses. Secondly, if gradient type polymers are obtained, they might form undesired aggregates and/ or micellar structures.

Another question which arises especially with respect to biomedical applications is:

ii) Is it possible to obtain mf-PEGs, by simultaneous retention of the good water solubility and excellent biocompatibility known from PEG?

Therefore, one major objective of this thesis was to study the temperature-dependent water solubility of several, newly synthesized glycidyl ether containing copolymers, followed by toxicity tests to establish, whether these materials show PEG like biocompatibility.

The third objective of this thesis is to prove the addressability of the functional groups and the possibility to use the newly synthesized copolymers either as precursor for sophisticated architectures, e.g., brush-copolymers, or in the synthesis of organometallic polyethers.

Following the general concept of functional glycidyl ethers, which can be used to overcome the low loading capacity of PEG, the final question asked is:

iii) Is it possible to synthesize degradable PEG?

The synthesis of a suitable monomer with an acid-labile group incorporated and the subsequent anionic polymerization of this newly developed compound are the main tasks of the last part of this thesis.

Abstract

Abstract

This thesis aims at the development of novel functional polyethers based on the combination of ethylene oxide with other functional epoxide comonomers. In **Chapter 1** functional epoxide monomers that are suitable for controlled ring-opening polymerization (ROP) are discussed. In this short review the recent renaissance in the field of epoxide polymerization is highlighted, with a special focus on living and controlled polymerization of functional epoxide monomers. The combination of i) easily accessible monomers and ii) the possibility to obtain well-defined materials, which are water-soluble in most cases and biocompatible as well as chemically robust, bears promising potential for different uses. Potential applications including biomedical aspects are also discussed in this context.

In **Chapter 2** the introduction of versatile functional groups into the poly(ethylene glycol) (PEG)-based polyether backbone is shown. Among the oxiranes it is possible to distinguish between two different classes of functional epoxide-based monomers: the first class carries a functional group that is stable under the polymerization conditions, and the second class bears a group that needs to be protected. In this thesis different glycidyl ether monomers carrying both, protected (Chapter 2.1 and 2.2) and directly usable (Chapter 2.3), functionalities are employed to implement reactive moieties, yielding multifunctional (*mf*)-PEG.

In **Chapter 2.1** polyethers with multiple hydroxyl groups and one orthogonal terminal moiety are presented. A series of polymers with varying comonomer ratio is synthesized by copolymerization of ethylene oxide (EO) and ethoxy ethyl glycidyl ether (EEGE), resulting in linear glycerol units with one hydroxyl group per monomer unit after acidic deprotection. The polymerization is followed by the removal of the terminal benzyl residues, resulting in an orthogonally addressable terminal functionality viz. an amine moiety. Molecular characterization is conducted by ^1H and ^{13}C NMR as well as size exclusion chromatography (SEC). Random incorporation of the two monomers was probed using ^{13}C NMR, analyzing the triad sequence distribution and differential scanning calorimetry (DSC). In addition investigations of the thermal behavior of the series of polyethers with different comonomer ratios have been carried out.

In **Chapter 2.2** polyethers with vicinal diols in the side chain are introduced. A series of random copolymers with different fractions of EO and 1,2-isopropylidene glyceryl glycidyl ether (IGG) units is synthesized. Besides the introduction of an additional hydroxyl moiety the 1,2 diol-component of the side chains allows for attachment and facile acid-catalyzed release of molecules bearing ketone/aldehyde functionalities via reversible formation of cyclic acetals. This renders the materials potentially useful as support for reagents, drugs or catalysts. Random incorporation of both comonomers is verified by monitoring the copolymerization kinetics via real-time ^1H NMR

spectroscopy during the polymerization in DMSO and by characterization of the triad sequence distribution, relying on ^{13}C NMR analysis, as stated above.

In **Chapter 2.3** polyethers carrying highly reactive vinyl ether moieties along the PEG backbone are presented, employing the novel monomer ethoxy vinyl glycidyl ether (EVGE). The facile transformation of the vinyl ether side chains in click type reactions is verified by two different post polymerization modification reactions: (i) thiol-ene addition and (ii) acetal formation, using various model compounds. It can be shown that both strategies are very efficient, resulting in quantitative conversion. The rapid acetal formation with alcohols results in an acid-labile bond and is thus highly interesting with respect to biomedical applications that require slow or controlled release of a drug, while the thiol-ene addition to vinyl ether moieties prevents cross-linking efficiently, in contrast to other types of double bonds. Again the random incorporation of the EVGE comonomer can be proven by the methods employed in Chapter 2.1 and 2.2.

Regarding the key issue concerning the structural constitution of these polymers:

- i) *Are the newly introduced functionalities randomly distributed along the PEG chain?*

It can be stated that all three different polymer classes studied exhibit random incorporation, as it can be derived from NMR kinetics, triad analysis and is also indirectly confirmed by the thermal properties. Nevertheless, it should be mentioned that the results might vary in dependence on solvent, temperature, and counter ion. However, the statistical distribution of the glycidyl ether moieties is in accordance with other polymers investigated.

In **Chapter 3** another important question is targeted:

- ii) *Is it possible to generate mf-PEGs preserving the good water-solubility and excellent biocompatibility known from PEG?*

This is investigated in two different studies. In **Chapter 3.1** the water-solubility of the novel mf-PEGs is examined. Variable comonomer ratios of EO and the above mentioned oxiranes IGG, EVGE, as well as other monomers such as allyl glycidyl ether (AGE) and dibenzyl amino glycidol (DBAG) are found to influence the lower critical solution temperature (LCST) behavior. Sharp transitions from translucent to opaque solutions, comparable to other well-established stimuli-responsive polymers, are observed at temperatures ranging from 9 to 82 °C. The influence of the side group hydrophobicity as well as the comonomer ratios can be quantified by comparison of the different copolymer systems observed.

In **Chapter 3.2** the biocompatibility of the novel polymers is under investigation. Cytotoxicity of several mf-PEG-analogues is studied against chinese hamster ovary cells (CHO). Beside the random mf-PEG copolymers with different glycidyl ether-based comonomers also block copolymers with varying polymer architectures are studied. The data is evaluated via the Alamar Blue staining technique and the packed cell volume (PCV) method. Both methods prove that the random

copolymers exhibit similar toxicity compared to PEG, while block copolymers show a slightly higher toxicity, which can be assigned to the aggregation behavior. In addition, the data prove that the experimentally more convenient PCV method provides reliable results for the cytotoxicity of the investigated polymers.

In **Chapter 4** the previously introduced concept is used to synthesize metal-containing polyethers. In **Chapter 4.1** anionic ring-opening polymerization is applied for the synthesis of several di- and triblock (PPO-*b*-PEO-*b*-PEVGE) copolymers bearing a variable amount of vinyl ether moieties using the above mentioned EVGE monomer. These vinyl ethers are reacted with Grubbs' catalyst to generate organometallic copolymers via stable Fischer carbenes. The ruthenium containing block copolymers are investigated by transmission electron microscopy (TEM) for their aggregation behavior.

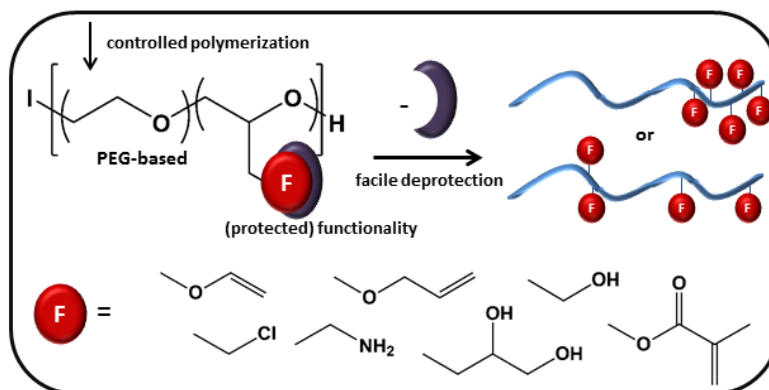
In **Chapter 4.2** EO is copolymerized with ferrocenyl glycidyl ether (fcGE) to generate water-soluble and thermo-responsive copolyethers with ferrocenyl moieties in the side chain. Up to 10% of fcGE can be introduced before the water-solubility at room temperature is lost. Interestingly, the thermo-responsiveness, which is present in all copolymers can be switched off by oxidation of the iron centers, as the hydrophobicity is altered. In addition the LCST behavior can be recovered by reduction of the iron(III) species. For a low fcGE copolymer content the toxicity tests reveal biocompatibility of the newly developed materials, while the polymers with higher fc content show toxicity and might be interesting as cytostatics.

In **Chapter 5**, the copolymerization strategy introduced throughout Chapter 1 and 2, is used to overcome another disadvantage of PEG, viz. its non-biodegradability. The introduction of acid degradable acetal moieties into a hyperbranched polymer backbone is realized by the design of a novel epoxide-based degradable inimer. This new compound, viz. glycoloxy ethyl glycidyl ether (GEGE) is copolymerized in the anionic ring opening polymerization (AROP) with either EO or glycidol, yielding branched degradable polyethers, i.e. (P(EO-*co*-GEGE) and P(G-*co*-GEGE)) with varying structure and an adjustable amount of acid-cleavable acetal units incorporated. An additional class of polymers P(G-*co*-GEGE-*g*-EO) is synthesized by using the P(G-*co*-GEGE) copolymers as macroinitiators for AROP of EO. The new materials are characterized in detail and the degradation kinetic of these polymers is analyzed via SEC and ¹H NMR spectroscopy.

Graphical Abstract

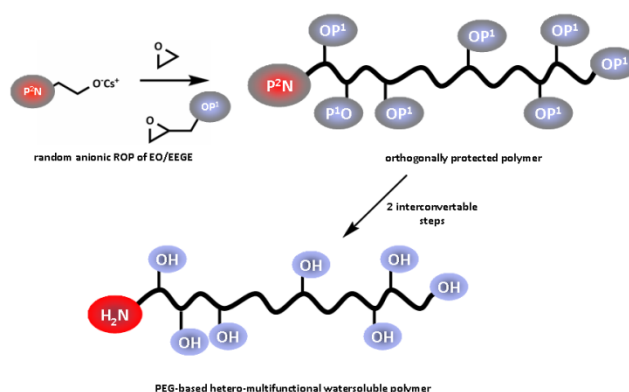
Chapter 1:

Functional PEG-based Polymers with Reactive Groups via Anionic ROP of Tailor-made Epoxides



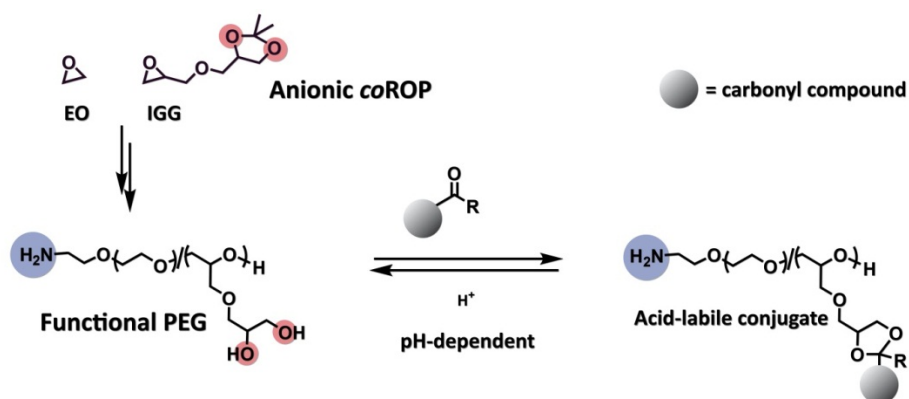
Chapter 2.1:

Hetero-Multifunctional Poly(ethylene glycol) Copolymers with Multiple Hydroxyl Groups and a Single Terminal Functionality



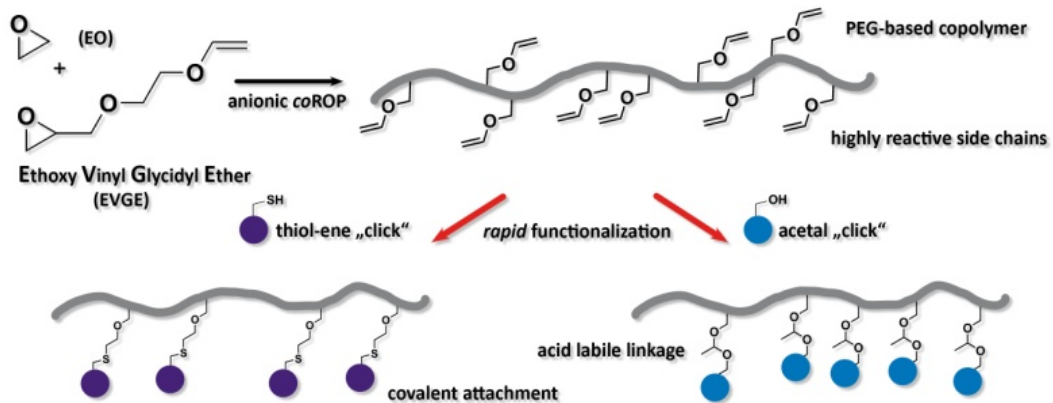
Chapter 2.2:

"Functional Poly(ethylene glycol)": PEG-based Random Copolymers with 1,2-Diol Side Chains and Terminal Amino Functionality



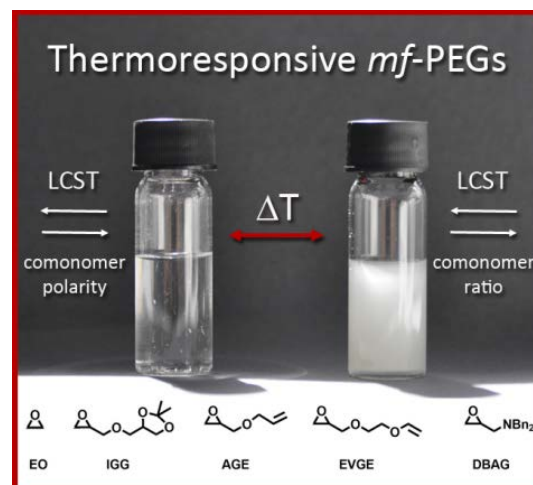
Chapter 2.3:

PEG-based Multifunctional Polyethers with Highly Reactive Vinyl-Ether Side Chains for Click-type Functionalization



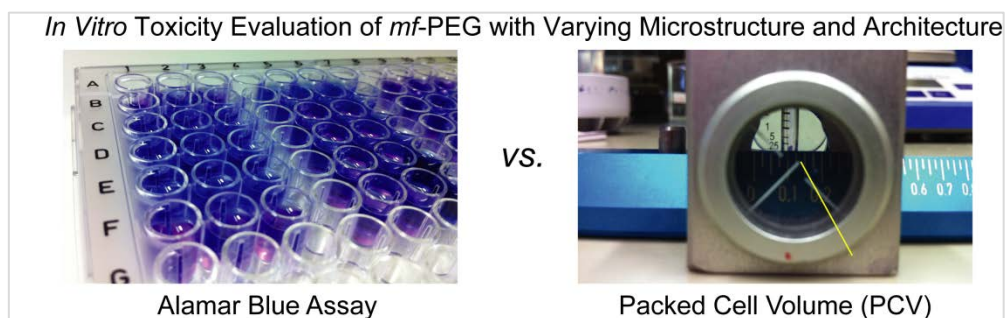
Chapter 3.1:

From an Epoxide Monomer Toolkit to Functional PEG Copolymers With Adjustable LCST Behavior



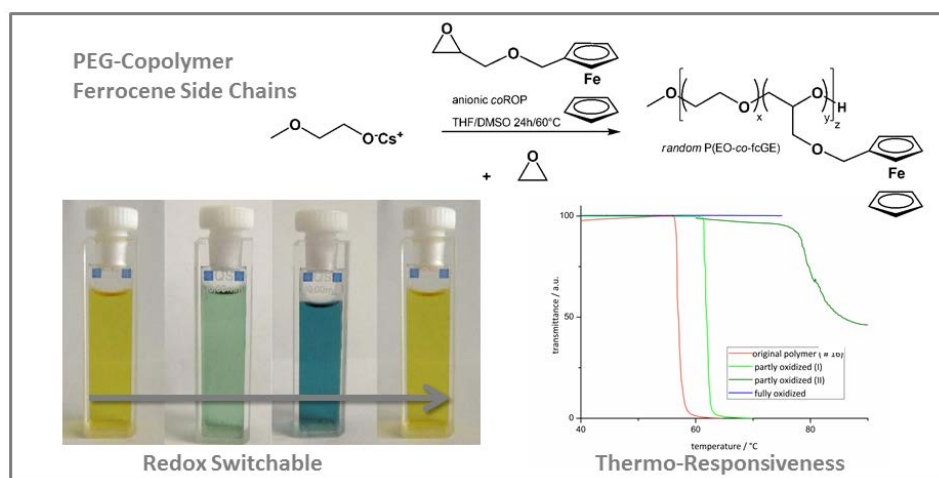
Chapter 3.2:

In Vitro Toxicity Evaluation of *mf*-PEGs with Varying Microstructure and Architecture



Chapter 4.1:

Thermo-Responsive Ferrocene-Containing Poly(ethylene glycol)



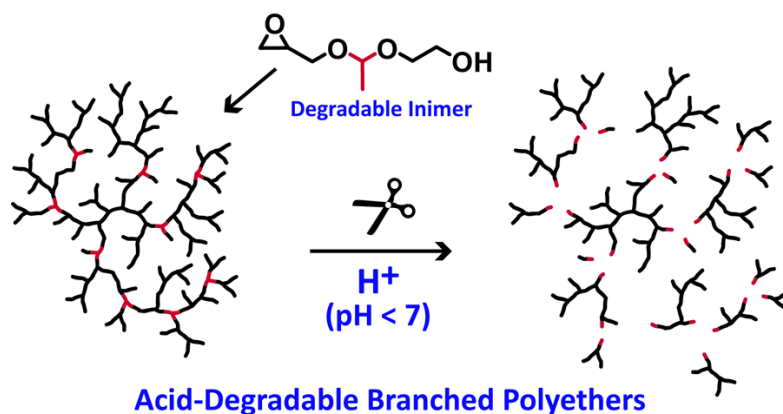
Chapter 4.2:

Asymmetric Micellization of Organometallic Polyether Block Copolymers



Chapter 5:

Branched Acid-Degradable, Biocompatible Polyether-Based Copolymers by Anionic Ring-Opening Polymerization Using an Epoxide Inimer



Chapter 1:

***Functional PEG-based Polymers with Reactive Groups via Anionic ROP of
Tailor-made Epoxides***

this article. It should be noted that the functionality of PEG can also be increased by varying the polymer architecture, e.g., by the synthesis of branched structures (using latent AB₂-comonomers such as glycidol),³ star-like,⁴ or PEG-based dendrimer-like structures.⁵ However, this interesting field will not be highlighted in this article, since the main focus lies on linear polymer structures and tailor-made epoxide monomers.

The synthesis of functional epoxides bearing either a functional group that is stable towards the polymerization conditions or which is protected with a suitable protective group allows for the introduction of versatile functionalities, such as double bonds, hydroxyl groups or vicinal diols and amines. However, the combination of living polymerization and the systematic introduction of functionalities at a poly(ethylene glycol)/(PEG)-based backbone had only been realized for some limited systems until recently.⁶ The typical building blocks for functional epoxides are epichlorohydrin (ECH) or glycidol as well as an alcohol or amine carrying the (protected) functional group. Glycidol, ECH and a majority of the corresponding alcohols are common reagents in the chemical industry and a major fraction of the monomer syntheses are one- or two-step reactions. The monomers are typically synthesized via nucleophilic attack of the (functional) alcohol or amine of choice on the methylene group of ECH, followed by ring-closure through intramolecular nucleophilic substitution (S_{Ni}). In some cases the intermediate chlorhydrin can be isolated (e.g. for di-benzyl amino glycidol (DBAG))⁷, while if phase transfer catalysis conditions are applied the desired monomers are obtained in one step (e.g. 1,2-isopropylidene glyceryl glycidyl ether (IGG)⁸ or ethoxy vinyl glycidyl ether (EVGE)⁹ see below). Another strategy relies on the hydroxyl group of glycidol, which can be protected with ethyl vinyl ether under acidic catalysis.¹⁰ An overview of all fundamental reaction types is given in Figure 1.

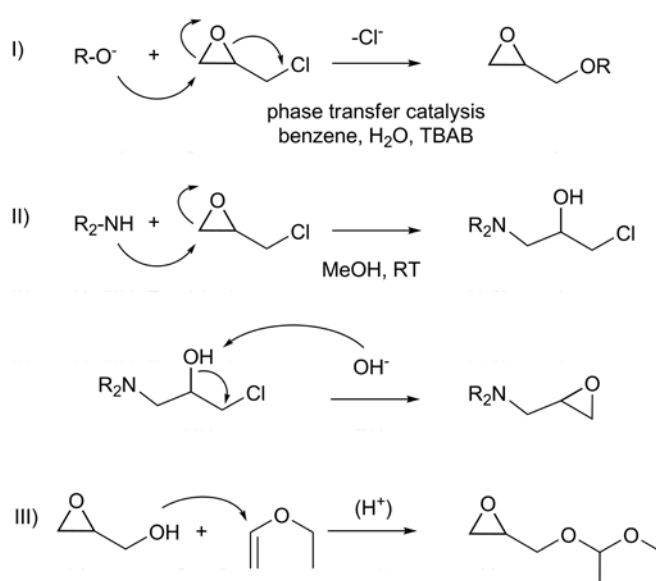


Figure 1. Overview of the fundamental synthetic methods I-III yielding (functional) epoxides, suitable for (anionic) ROP.

The combination of i) easily accessible monomers and ii) the possibility to obtain well-defined materials, which are water-soluble in most cases and biocompatible as well as chemically robust, bears promising potential for different applications. Figure 2 gives an overview of the different functional epoxides discussed in the context of this article.

Synthetic Strategies

The controlled synthesis of functional polyethers is an important issue, since well-defined materials with narrow molecular weight distributions are desirable not only for biomedical uses, but also for a large number of other applications.

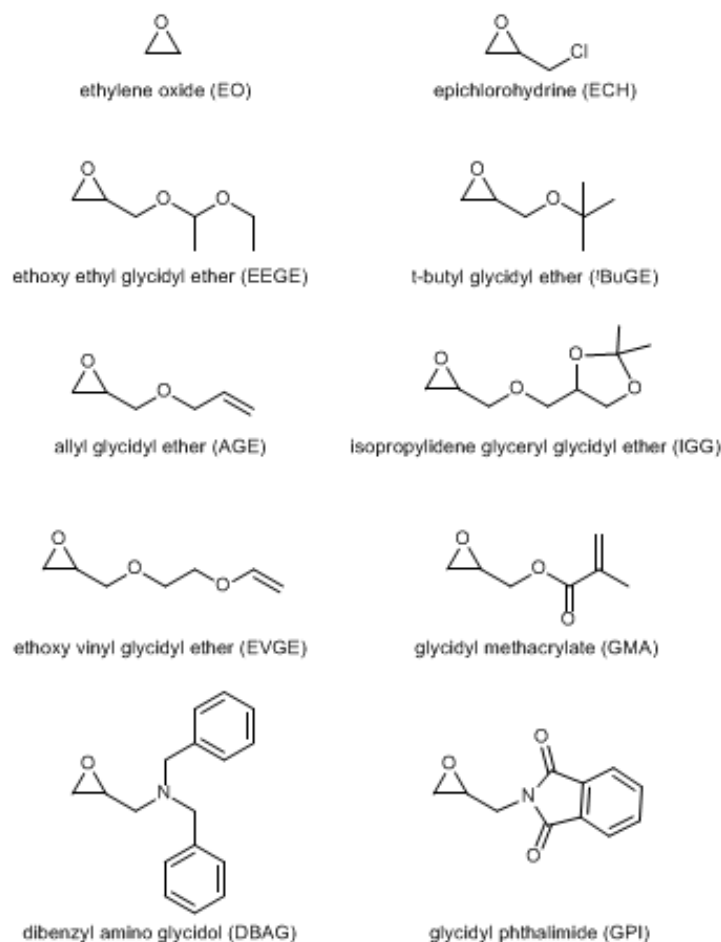


Figure 2. Overview of the different (functional) epoxides, suitable for (anionic) ROP, as discussed in this review article.

Not all of the different functional oxiranes presented in Figure 2 fulfil the necessary criteria for (an)ionic polymerization, but might be suitable for the quasi-living activated monomer mechanism (detailed discussion see below).

Polymerization Methods

The oldest,¹¹ but not out-dated living polymerization technique is anionic polymerization.¹² Anionic ring-opening polymerization (AROP) of ethylene oxide was carried out as early as 1933 by Staudinger¹³ and 1940 by Flory,¹⁴ who established its controlled character. It is until today the most important method for epoxide polymerization, which is also widely used on industrial scale (e.g., for the polymerization of EO). Typically, the polymerization is initiated by an alcohol, activated (i.e. deprotonated) by a metal-ion forming an alkoxide. Versatile alcohols have been used to introduce functionalities or labels in a terminal position.^{15, 16} Intensive studies have been carried out focussing on the role of the counter ion, which is an alkaline metal in most cases. In the case of Li⁺ cations (the smallest counter ion possible) usually no polymerization occurs.^{17, 18} In the presence of a phosphazene base,^{19, 20} which acts like a chelating ligand, polymerization can take place. However, polymerization of glycidyl ethers (e.g. EEGE) employing the phosphazene base method is less common, since the obtained secondary alcohol affords increased reaction time and proton abstraction (compare Fig. 3) can take place.²¹ Very recently, Carlotti and coworkers²² reported that the addition of tri *iso*-butyl aluminium to a living polystyryl lithium (PS-Li) chain end allows the direct polymerization of ethylene oxide as a second block with Li⁺ as a counter ion. This effect was explained by the presence of an “ate” complex formed by the aluminium salt and the PS-Li. Although the diblock formation efficiency stays below 90%, this approach represents an interesting method to combine carb- and oxy-anionic polymerization. Apart from these two exceptions the strong Li-O interaction prevents insertion of the oxirane.²³ The polymerization rate constants increase with increasing size of the counter ion (Na⁺<K⁺<Cs⁺),²⁴ as it can be derived from the hard and soft acid and base (HSAB) concept.²⁵ The concept allows predicting a decreasing affinity to the comparably “hard” oxygen atom with increasing atomic radius of the counter ion, which translates to increasing “softness”. Most commonly, potassium is applied, due to reasonable polymerization results and lower cost (in comparison to Cs⁺). However, it has been shown that cesium counter ions exhibit not only a higher polymerization rate, but moreover in the case of substituted oxiranes, such as propylene oxide (PO),²⁶ the occurrence of transfer reactions resulting in unsaturated species (see Fig. 3) can be reduced. This proton abstraction, or chain transfer reaction, can occur at all substituted oxiranes²⁷, such as ethoxy ethyl glycidyl ether (EEGE). Möller and co-workers studied this chain transfer reaction to the monomer (in this case: EEGE) at various temperatures and different initiating systems (3-phenylpropanol/potassium 3-phenylpropanolate, potassium *tert*-butoxide and *sec*-butyllithium/phosphazene base).²⁸ It was shown that with K⁺ as the counter ion the extent of proton abstraction in comparison with the Li⁺ phosphazene base initiator is decreased, especially when moderate reaction temperatures (60°C) were applied. The authors conclude that there is an upper molecular weight limit for PEEGE (M_n) of 30,000 g/mol.

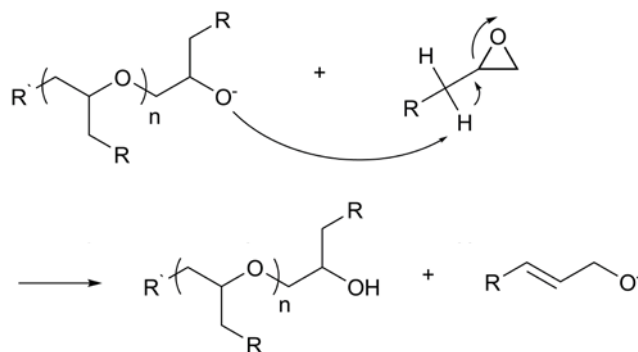


Figure 3. Mechanism of undesired proton abstraction for the AROP of substituted epoxides, as proposed.²⁸

Another method for the controlled polymerization of (functional) oxiranes, relying on an anionic coordination mechanism,²⁹⁻³¹ has been revitalised and investigated in elegant work by Deffieux and co-workers within the last decade. By the addition of triisobutylaluminium to either a metal (Na^+) alkoxide³² or tetraalkylammonium salts³³ as the respective initiators, two different complexes are formed. The authors propose that one species obtained is the initiating complex (I) and the other one is formed by the excess of aluminium salt and the corresponding monomer resulting in an activated monomer mechanism (II, compare Figure 4)³². With this approach it has been possible to obtain different copolymers (of EO/PO³³, EEGE/PO and ^tBuGE/butylene oxide (BO)³⁴, as well as AGE/ECH³⁵, EEGE/ECH³⁶ and AGE/EEGE³⁷) and high molecular weight PEEGE³⁴, with M_n exceeding the 30,000 g/mol limit. In addition, this strategy broadens the toolkit of possible initiators, since bromides or even azides are sufficiently nucleophilic in the complex with the aluminiumalkylate to open the strained epoxide ring. Versatile initiators have been used to polymerize EO, PO, ECH and EEGE yielding α -azido or bromo, α -hydroxypolyethers.³⁸

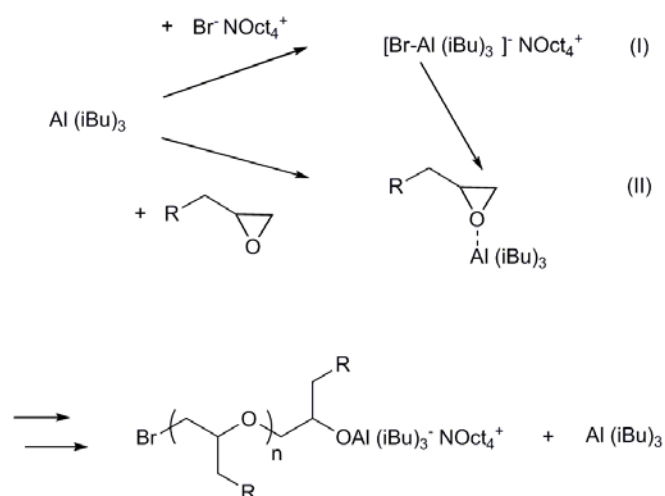


Figure 4: Proposed monomer activation mechanism for the “living” polymerization using tetraoctylammonium salts and triisobutyl-aluminum.³²

Very recently, Taton and co-workers presented a straightforward living polymerization technique for EO³⁹ activated by N-heterocyclic carbenes (NHC), widely used in different organic catalysis reactions. This approach represents not only a metal-free alternative to the abovementioned protocols, but also generates the opportunity to obtain α,ω -functional polymers.⁴⁰ However, to date this polymerization technique has not been applied for the (co)polymerization of functional monomers, but represents a very promising method and might be suitable for substituted oxiranes as well.

Functional Epoxides

The synthesis of multifunctional polyethers with either block or random structure can be conducted via two different strategies: the first one relies on polymer modification reactions of “common” precursor polymers, such as *lin*PG or PECH (compare Fig. 4). These functionalization reactions are often accompanied by non-quantitative conversion³² or require multi-step syntheses.⁵⁶ The focus of this article, however, is the expansion of these “common” materials toward a detailed description of specialized monomers allowing the introduction of the respective functional group via direct (co)polymerization of the oxirane carrying the desired functionality.

Among the oxiranes it is possible to distinguish between two different classes of functional epoxide based monomers. The first class of oxiranes carries a functional group that is stable under the polymerization conditions applied, and the second class of functional epoxide bears a group that needs to be protected. In the two sections below, first monomers carrying a ROP-stable functional group will be highlighted, followed by epoxide monomers requiring a deprotection step to obtain the functional polymer.

Several oxiranes do not need to be protected and thus lead to a functional group that is addressable right after polymerization, without the need for a further deprotection or activation step. Functional groups that are generally stable toward the highly basic conditions applied in AROP are double bonds. A typical example is AGE which is commercially available, easy to purify (distillation) and introduces an allylic double bond into the polymer backbone.^{2, 41} AGE can easily be homopolymerized, for example with PEG as a starting block,⁴²⁻⁴⁴ or copolymerized with other oxiranes, such as EO⁴⁵ or ECH³⁵ and glycidol, yielding branched structures.⁴⁶ Furthermore, the double bond can be post-modified via thiol-ene coupling reactions to attach biomolecules^{47, 48} or to build complex architectures using hydrosilylation.⁴⁴ However, one major aspect which has to be considered in the case of AGE (co)polymerization is the tendency of the allyl double bond towards isomerization.^{45, 49} It was found that this isomerization is directly related to the polymerization temperature. This was studied intensively by Lee and coworkers,⁵⁰ who varied the polymerization temperature from 40 to 140 °C, obtaining polymers with 1.5 to 16.6% of *cis*-prop-1-enyl (isomeric structure) side chains. The resulting internal (and therefore less accessible) vinyl double bond has a different reactivity or does

not take part in subsequent reactions or can be even lost during the work-up procedure, as it is not stable toward acidic media and can be cleaved to release hydroxyl groups. However, this (usually) unwanted side reaction can not only be promoted by the reaction temperature, but also by palladium catalysts (i.e. Pd(PPh₃)₄ in DCM) and utilized for orthogonal deprotection of linear polyglycerol (*linPG*).⁵¹

Introduction of vinyl ether moieties at the PEG backbone can be realized by the newly established monomer EVGE, which can serve as a (co)monomer in the polymerization with EO and has recently been carried out by our group. The resulting polymers cannot only be deprotected to afford a polyol, as mentioned above, but can in addition be used for thiol-ene click reactions and acetal formation.⁹ The thiol-ene reaction with the vinyl ether double bond is very efficient and does not require an excess of the thiol component, since the vinyl ether radical formed in the transitional state is too stable to attack other double bonds. Therefore the undesired and often observed side-reaction of crosslinking does not occur, which allows for stoichiometric control over the thiol-ene click. In addition, the possibility to attach alcohols via an acid-labile acetal bond is interesting with regard to drug carrier applications as the corresponding alcohol can be released in acidic media, present for example in lysosomes or cancer cells. EVGE can also be homo-polymerized and the terminal vinyl ether can be used for the attachment of Grubbs' catalyst via the formation of a stable Fischer carbene.^{52 53}

The activated monomer method developed by Carlotti and Deffieux permits the polymerization of functional monomers, which cannot be used in anionic polymerization, since they would suffer from nucleophilic attack of the propagating alkoxide. Therefore PECH⁵⁴, which was available before only by cationic ROP,^{55, 56} is now accessible with this approach.^{33, 35, 36} Very recently, Carlotti and co-workers were able to polymerize another interesting monomer, viz. glycidyl methacrylate (GMA), by selective ring-opening of the epoxide group and simultaneous conservation of the methacrylate functionality, which was then used for crosslinking reactions.⁵⁷ The conventional anionic ROP of GMA would lead to highly branched or crosslinked structures as the carbonylic C-atom of the acrylate also reacts.⁵⁸

In the ensuing section functional oxiranes are presented which necessitate the use of protective groups. Especially functional groups that can undergo nucleophilic attack and can in principle initiate AROP themselves (OH, NH₂) require protection. The protective group at a monomer/polymer backbone needs to fulfil two criteria: first, the monomer synthesis needs to be feasible. Secondly, and even more important the release of the functional group should be a facile, quantitative one-step or a one-pot polymer transformation, such as hydrolysis or hydrogenation.

Especially the introduction of hydroxyl groups into the polyether backbone is important, since alcohols show versatile reactivity and are essential for biomedical applications as they are nontoxic.⁵⁹ The protection of a single hydroxyl group can be realized by the ethoxy ethyl⁻¹⁰, the *tert*-butyl⁶⁰- or

the allyl- protective group. EEGE^{1, 61} has been used in the synthesis of PEG copolymers with either random⁶²⁻⁶⁴ or block-like⁶⁵⁻⁶⁸ structures, serving as precursor for other sophisticated architectures.^{15, 63, 69-76} The *tert*-butyl protective group has been less frequently employed until very recently,^{77, 78} although the monomer *t*-butyl glycidyl ether is commercially available. This might be due to the harsh conditions (trifluoroacetic acid, TFA) which are needed for the deprotection of the homopolymers.^{79,67} A combination of protected allyl-, ethoxy ethyl and *tert*-butyl glycidyl ethers was carried out in an important work by Möller and co-workers, yielding *lin*PG with orthogonal protected hydroxyl groups.⁷⁹

The introduction of two vicinal hydroxyl groups per monomer unit has first been realized by our group employing two different methods.⁸ In the first approach AGE was polymerized followed by the subsequent dihydroxylation (with osmium tetroxide). In the second approach a novel functional epoxide, viz. IGG was polymerized, which can easily be deprotected with diluted acids to release glyceryl glycerol units. It was also shown that IGG can be copolymerized with EO⁸⁰ and the 1,2-diol can easily be reacted with aldehydes or ketones forming the cyclic acetals, as it is also known for hyperbranched PG.⁸¹ This reversible reaction allows the pH-controlled attachment or release of small molecules.

Besides the introduction of hydroxyl groups, which is by now well-established, there have been only few attempts to introduce multiple amine functionalities, which is astonishing as they are highly interesting especially with respect to biomedical applications. In a polymer modification approach by Koyama and co-workers,² the introduction of amines at the PEG-backbone has first been realized, accompanied with the before mentioned problematic aspects of post-polymerization reactions. An amine-carrying protected, functional epoxide has been employed by our group, the newly developed epoxide DBAG.⁷ The amine groups were released by hydrogenation with Pearlman's catalyst (Pd(OH)₂/C) and their addressability was proven by different model reactions. Another interesting amine-inhabiting oxirane (glycidyl phthalimide) was first mentioned by Meyer et al..³⁶ Unfortunately, the sterically demanding phthalimide group only allows for single addition of the epoxide, i.e. quenching of the polymeric chain with a single amine.

Other protective groups and interesting functional moieties have rarely been investigated, but as the demand for functional polyethers increases steadily, it is a safe bet that other functional epoxides will be developed.

Properties and Applications

Poly(ethylene glycol) (PEG) exhibits unusual properties that are exploited in a vast number of applications. The polymer backbone with –CH₂CH₂O– repeating units is flexible and in contrast to its smaller homologues (compare poly(oxymethylene)) water-soluble.⁸² PEG is also chemically robust

and due to its biocompatibility,⁸³ it is widely used in medical and pharmaceutical formulations as well as specific applications, such as PEGylation.⁸⁴ In addition, PEG is employed as soluble support in organic synthesis.⁸⁵ Using functional epoxides to synthesize PEG-based homo-, block- or random copolymers some of these material properties are retained and some are significantly altered. In the following some uses and possible applications of functional polyethers will be discussed, with a focus on two different aspects. The first is related to general material properties and the second relies on the use of certain functionalities.

One interesting, general feature, which is not directly related to the use of the functional groups introduced, is the (temperature dependent) water solubility of many polyethers. Polymerization, but also polymer modification reactions in water will be a highly relevant topic in the future, both with respect to technical aspects, but of course all biomedical uses require water soluble polymers, as they always take place in aqueous media. PEG itself exhibits a lower critical solution temperature (LCST) behavior, however, the cloud point temperature is approximately 100 °C.⁸⁶ In addition, a variety of PEG-containing structures such as OEGMA⁸⁷⁻⁹⁰ as well as more sophisticated architectures^{91, 92} show thermo-responsive behavior, and it can be assumed that also other polyethers behave in a similar manner. Watanabe and co-workers showed that different homopolymers based on (functional and non-functional) glycidyl ethers exhibit LCSTs in the range of 14 °C to 57 °C, dependent on the side chain hydrophobicity.⁹³ Various (tri)block-copolymers containing PEEGE and PPO blocks were also found to show thermo-responsiveness, which was mainly assigned to the PEEGE or PPO building blocks.⁶⁸ Additionally, star-like polyethers with temperature dependent water solubility based on *t*-butyl glycidyl ether were investigated by Dworak and coworkers.^{77, 78} Very recently, we have been able to show that the random incorporation of the oxiranes IGG, EVGE, AGE, and DBAG into the PEG-backbone permits to tailor the LCST behavior. Sharp transitions from translucent to opaque solutions were observed at temperatures ranging from 9 to 82 °C. Plotting the LCST versus comonomer content provided a linear relationship with varying slopes, dependent on the comonomer hydrophobicity.⁹⁴ The results were in good agreement with earlier reports on random PEO-co-PPO copolymers.^{95, 96}

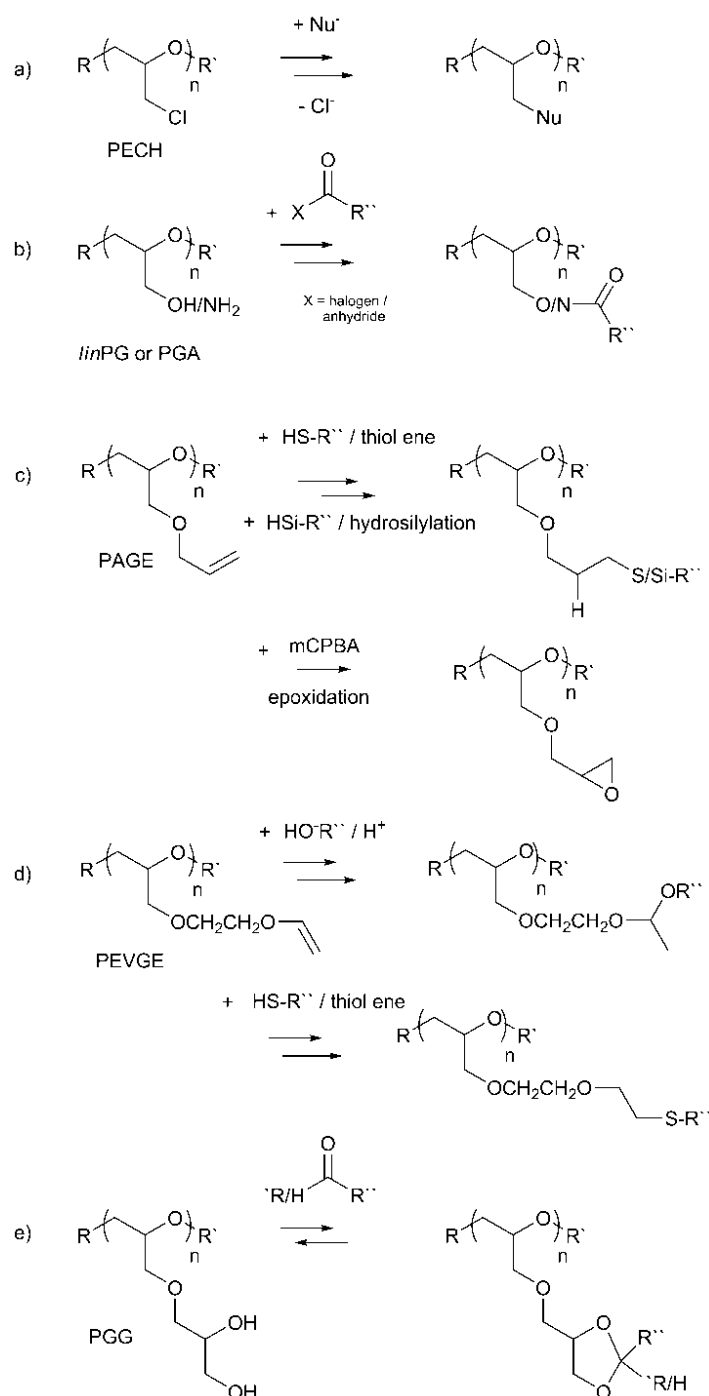


Figure 5. Some possible reactions for the functionalities introduced in PEG copolymers by the oxiranes presented. Literature for the displayed reactions: a)^{36, 59, 64, 97} b)^{36, 37, 45, 60, 96} c)^{7, 37, 42, 43, 98, 99,35} d)⁹ e)⁸⁰.

Potential applications for stimuli-responsive polyethers are in the field of bioconjugation.¹⁰⁰ Haag and coworkers employed different random copolymers based on glycidyl methyl ether, glycidyl ethyl ether as well as EEGE to obtain self-assembled monolayers on gold¹⁰¹, aiming at protein resistant surfaces.¹⁰² Another possible application for poly(glycidyl ether)s could be their use as functional polyurethane (PU) precursors, replacing the well-known polyether polyols as reactive compounds.

This application with great potential for new promising PU-materials has been investigated in one single example only. Brocas et al.³⁵ used an isocyanate-free approach to synthesize cross-linked PUs from PECH-co-PAGE copolymers. One application related to PECH homopolymer was reported by Mohana Raju et al. The modification of the chlorides to azide-functionalities resulted in poly(glycidyl azide) (GAP), which can be used as energetic material (propellant).¹⁰³

The second class of applications is related to the utilization of the functional groups. A majority of these uses are biomedical, especially if PEG represents the major component of the copolymer, and biocompatibility is assured. The attachment of drugs via the novel functionalities⁵⁹ has been demonstrated in several cases, and also pharmaceutical activity has been demonstrated.^{9, 42, 43, 104} A detailed description on *mf*-PEGs with respect to their pharmaceutical applications can be found in a recently published review article by Obermeier et al.⁶ and is therefore only mentioned briefly in this overview.

The possibilities for potential applications strongly depend on the nature of the functional groups and the feasibility of the post-polymerization reaction. Figure 4 presents an overview of different reactions. Especially reaction b) and c) have been employed intensively to attach small molecules onto the polyether structure, while d) and e) have only been carried out as model reactions. However, the opportunity for the reversible attachment of drugs, but also for example catalysts or reagents in soluble support applications, bears potential for future applications.

Beside the addition of small molecules the functionalities can be used to gain more sophisticated architectures. Employing the protected hydroxyl group(s) of EEGE/IGG/^tBuGE it is possible to obtain star-like-,^{77, 78} long-term branched/ arborescent-,⁷⁵ hyperbranched-¹⁰⁵ or linear-hyperbranched^{15, 106-108} block structures based on glycidol and its derivatives. Amphiphilic linear-hyperbranched structures using PEO-PAGE as a platform and subsequent hydrosilylation of different Si-H-containing AB₂ monomers were synthesized by Wurm et al.⁴⁴ Beside the (hyper) branched copolymers, different graft structures have been synthesized and investigated. Huang and co-workers presented versatile methods to obtain graft-copolymers based on linear PEO-co-PG, either using the multiple hydroxyl groups to directly initiate the polymerization (e.g., of ϵ -caprolactone⁶³) or to attach an ATRP initiator and use this complex as macroinitiator.^{71, 73, 74} Very recently Ozdemir et al. reported the synthesis of amphiphilic double-comb copolymers using PEEGE-co-PAGE as starting molecule.³⁷

Conclusions

The use of functional oxiranes has recently led to a renaissance of the area of PEG-derived polyethers, synthesized by living polymerization methods. This is due to the easily available starting materials with a broad variety of functionalities that can be introduced. Relying on well-known protective group chemistry, halogens, hydroxyl groups and amines as well as vicinal diols, vinyl- and

allyl-ethers can be incorporated into the PEG-backbone. Some applications employing the newly emerging general material properties or the now accessible functional moieties are already in practice or subject of current investigations. However, with respect to potential future applications as well as novel (protected) functional oxiranes the growing field of functional polyethers is by no means a mature area yet, which motivates the search for other functional epoxide monomers.

1. Taton, D.; Le Borgne, A.; Sepulchre, M.; Spassky, N. *Macromol. Chem. Phys.* **1994**, 195, (1), 139-148.
2. Koyama, Y.; Umehara, M.; Mizuno, A.; Itaba, M.; Yasukouchi, T.; Natsume, K.; Suginaka, A.; Watanabe, K. *Bioconjugate Chem.* **1996**, 7, (3), 298-301.
3. Wilms, D.; Schömer, M.; Wurm, F.; Hermanns, M. I.; Kirkpatrick, C. J.; Frey, H. *Macromol. Rapid Commun.* **2010**, 31, (20), 1811-1815.
4. Grzegorz, L. *Prog. Polym. Sci.* **2009**, 34, (9), 852-892.
5. Feng, X.-S.; Taton, D.; Chaikof, E. L.; Gnanou, Y. *J. Am. Chem. Soc.* **2005**, 127, (31), 10956-10966.
6. Obermeier, B.; Wurm, F.; Mangold, C.; Frey, H. *Angew. Chem.* **2011**, 123, (35), 8136-8146.
7. Obermeier, B.; Wurm, F.; Frey, H. *Macromolecules* **2010**, 43, (5), 2244-2251.
8. Wurm, F.; Nieberle, J.; Frey, H. *Macromolecules* **2008**, 41, (6), 1909-1911.
9. Mangold, C.; Dingels, C.; Obermeier, B.; Frey, H.; Wurm, F. *Macromolecules* **2011**, 44, (16), 6326-6334.
10. Fitton, A. O.; Hill, J.; Jane, D. E.; Millar, R. *Synthesis* **1987**, (12), 1140-1142.
11. Swarc, M. *Nature* **1956**, 178, (4543), 1168-1169.
12. Hadjichristidis, N.; Pitsikalis, M.; Pispas, S.; Iatrou, H. *Chem. Rev.* **2001**, 101, (12), 3747-3792.
13. Staudinger, H.; Lohmann, H. *Liebigs Ann. Chem.* **1933**, 505, (1), 41-51.
14. Flory, P. J. *J. Am. Chem. Soc.* **1940**, 62, (6), 1561-1565.
15. Wurm, F.; Klos, J.; Räder, H. J.; Frey, H. *J. Am. Chem. Soc.* **2009**, 131, 7954-7955.
16. Thompson, M. S.; Vadala, T. P.; Vadala, M. L.; Lin, Y.; Riffle, J. S. *Polymer* **2008**, 49, (2), 345-373.
17. Tonhauser, C.; Frey, H. *Macromol. Rapid Commun.* **2010**, 31, (22), 1938-1947.
18. Quirk, R. P.; Hsieh, H. L., *Anionic Polymerization: Principles And Practical Applications*. Marcel Dekker Inc: New York, 1996.
19. Boileau, S.; Illy, N. *Prog. Polym. Sci.* **2011**, 36, (9), 1132-1151.
20. Schwesinger, R.; Schlemper, H.; Hasenfratz, C.; Willaredt, J.; Dambacher, T.; Breuer, T.; Ottaway, C.; Fletschinger, M.; Boele, J.; Fritz, H.; Putzas, D.; Rotter, H. W.; Bordwell, F. G.;

- Satish, A. V.; Ji, G.-Z.; Peters, E.-M.; Peters, K.; von Schnering, H. G.; Walz, L. *Liebigs Annalen* **1996**, 1996, (7), 1055-1081.
21. Toy, A. A.; Reinicke, S.; Müller, A. H. E.; Schmalz, H. *Macromolecules* **2007**, 40, (15), 5241-5244.
22. Rejsek, V.; Desbois, P.; Deffieux, A.; Carlotti, S. p. *Polymer* **2010**, 51, (24), 5674-5679.
23. Tonhauser, C.; Obermeier, B.; Mangold, C.; Lowe, H.; Frey, H. *Chem. Commun.* **2011**, 47, (31), 8964-8966.
24. Eßwein, B.; Möller, M. *Angew. Chem. Int. Ed.* **1996**, 35, (6), 623-625.
25. Pearson, R. G. *J. Am. Chem. Soc.* **1963**, 85, (22), 3533-3539.
26. de Lucas, A.; Rodríguez, L.; Pérez-Collado, M.; Sánchez, P.; Rodríguez, J. F. *Polym. Int.* **2002**, 51, (10), 1066-1071.
27. Stolarzewicz, A.; Morejko-Buz, B.; Grobelny, Z.; Pisarski, W.; Frey, H. *Polymer* **2004**, 45, (21), 7047-7051.
28. Hans, M.; Keul, H.; Möller, M. *Polymer* **2009**, 50, (5), 1103-1108.
29. Jedliński, Z.; Bero, M.; Szewczyk, P.; Dworak, A. *J. Polym. Sci. Polym. Chem. Ed.* **1981**, 19, (3), 749-757.
30. Price, C. C.; Brecker, L. R. *J. Polym. Sci., Part A: Polym. Chem.* **1969**, 7, (2), 575-582.
31. Bansleben, D. A.; Hersman, M. J.; Vogl, O. *J. Polym. Sci. Polym. Chem. Ed.* **1984**, 22, (10), 2489-2500.
32. Billouard, C.; Carlotti, S.; Desbois, P.; Deffieux, A. *Macromolecules* **2004**, 37, (11), 4038-4043.
33. Rejsek, V.; Sauvanier, D.; Billouard, C.; Desbois, P.; Deffieux, A.; Carlotti, S. *Macromolecules* **2007**, 40, (18), 6510-6514.
34. Gervais, M.; Brocas, A.-L.; Cendejas, G.; Deffieux, A.; Carlotti, S. *Macromolecules* **2010**, 43, (4), 1778-1784.
35. Brocas, A.-L.; Cendejas, G.; Caillol, S.; Deffieux, A.; Carlotti, S. *J. Polym. Sci., Part A: Polym. Chem.* **2011**, 49, (12), 2677-2684.
36. Meyer, J.; Keul, H.; Möller, M. *Macromolecules* **2011**, 44, (11), 4082-4091.
37. Ozdemir, F.; Keul, H.; Mourran, A.; Möller, M. *Macromol. Rapid Commun.* **2011**, 32, (13), 1007-1013.
38. Gervais, M.; Labbé, A.; Carlotti, S.; Deffieux, A. *Macromolecules* **2009**, 42, (7), 2395-2400.
39. Raynaud, J.; Absalon, C.; Gnanou, Y.; Taton, D. *J. Am. Chem. Soc.* **2009**, 131, (9), 3201-3209.
40. Raynaud, J.; Absalon, C.; Gnanou, Y.; Taton, D. *Macromolecules* **2010**, 43, (6), 2814-2823.
41. Vandenberg, E. J. *J. Polym. Sci., Part A: Polym. Chem.* **1986**, 24, (7), 1423-1431.
42. Hrubý, M.; Konák, C.; Ulbrich, K. *J. Controlled Release* **2005**, 103, (1), 137-148.

43. Vetvicka, D.; Hruby, M.; Hovorka, O.; Etrych, T.; Vetrik, M.; Kovar, L.; Kovar, M.; Ulbrich, K.; Rihova, B. *Bioconjugate Chem.* **2009**, 20, (11), 2090-2097.
44. Wurm, F.; Schüle, H.; Frey, H. *Macromolecules* **2008**, 41, (24), 9602-9611.
45. Obermeier, B.; Frey, H. *Bioconjugate Chem.* **2011**, 22, (3), 436-444.
46. Sunder, A.; Turk, H.; Haag, R.; Frey, H. *Macromolecules* **2000**, 33, (21), 7682-7692.
47. Hashimoto, M.; Koyama, Y.; Sato, T. *Chem. Lett.* **2008**, 37, (3), 266-267.
48. Yoshihara, C.; Shew, C.-Y.; Ito, T.; Koyama, Y. *Biophys. J.* **2010**, 98, (7), 1257-1266.
49. Lee, B. F.; Kade, M. J.; Chute, J. A.; Gupta, N.; Campos, L. M.; Fredrickson, G. H.; Kramer, E. J.; Lynd, N. A.; Hawker, C. J. *J. Polym. Sci., Part A: Polym. Chem.* **2011**, 49, (20), 4498-4504.
50. Lee, B. F.; Kade, M. J.; Chute, J. A.; Gupta, N.; Campos, L. M.; Fredrickson, G. H.; Kramer, E. J.; Lynd, N. A.; Hawker, C. J. *J. Polym. Sci., Part A: Polym. Chem.* **2011**, 49, (20), 4498-4504.
51. Erberich, M.; Keul, H.; Möller, M. *Macromolecules* **2007**, 40, (9), 3070-3079.
52. Mangold, C.; Wurm, F.; Kilbinger Andreas, F. M., Asymmetric Micellization of Organometallic Polyether Block Copolymers. In *Non-Conventional Functional Block Copolymers*, American Chemical Society: 2011; Vol. 1066, pp 103-115.
53. Wurm, F.; König, H. M.; Hilf, S.; Kilbinger, A. F. M. *J. Am. Chem. Soc.* **2008**, 130, (18), 5876-5877.
54. Vandenberg, E. J. *J. Polym. Sci., Part A: Polym. Chem.* **1972**, 10, (10), 2903-2912.
55. Xie, H.-Q.; Guo, J.-S.; Yu, G.-Q.; Zu, J. *J. Appl. Polym. Sci.* **2001**, 80, (13), 2446-2454.
56. Royappa, A. T.; Dalal, N.; Giese, M. W. *J. Appl. Polym. Sci.* **2001**, 82, (9), 2290-2299.
57. Labbé, A.; Brocas, A.-L.; Ibarboure, E.; Ishizone, T.; Hirao, A.; Deffieux, A.; Carlotti, S. *Macromolecules* **2011**, 44, (16), 6356-6364.
58. Jia, Z.; Yan, D. *J. Polym. Sci., Part A: Polym. Chem.* **2005**, 43, (16), 3502-3509.
59. Zhou, P.; Li, Z.; Chau, Y. *European Journal of Pharmaceutical Sciences* **2010**, 41, (3-4), 464-472.
60. Vandenberg, E. J. *J. Polym. Sci., Part A: Polym. Chem.* **1985**, 23, (4), 915-949.
61. Dworak, A.; Panchev, I.; Trzebicka, B.; Walach, W. *Macromol. Symp.* **2000**, 153, (1), 233-242.
62. Mangold, C.; Wurm, F.; Obermeier, B.; Frey, H. *Macromol. Rapid Commun.* **2010**, 31, (3), 258-264.
63. Huang, J.; Li, Z.; Xu, X.; Ren, Y.; Huang, J. *J. Polym. Sci., Part A: Polym. Chem.* **2006**, 44, (11), 3684-3691.
64. Li, Z.; Chau, Y. *Bioconjugate Chem.* **2009**, 20, (4), 780-789.
65. Dimitrov, P.; Utrata-Wesolek, A.; Rangelov, S.; Walach, W.; Trzebicka, B.; Dworak, A. *Polymer* **2006**, 47, (14), 4905-4915.

66. Mendrek, S.; Mendrek, A.; Adler, H.-J.; Walach, W.; Dworak, A.; Kuckling, D., Synthesis of poly(glycidol)-block-poly(N-isopropylacrylamide) copolymers using new hydrophilic poly(glycidol) macroinitiator. In Wiley Subscription Services, Inc., A Wiley Company: 2008; Vol. 46, pp 2488-2499.
67. Backes, M.; Messenger, L.; Mourran, A.; Keul, H.; Möller, M. *Macromolecules* **2010**, 43, (7), 3238-3248.
68. Dimitrov, P.; Rangelov, S.; Dworak, A.; Tsvetanov, C. B. *Macromolecules* **2004**, 37, (3), 1000-1008.
69. Wurm, F.; Nieberle, J.; Frey, H. *Macromolecules* **2008**, 41, (4), 1184-1188.
70. Jamróz-Piegza, M.; Walach, W.; Dworak, A.; Trzebicka, B. *J. Colloid Interface Sci.* **2008**, 325, (1), 141-148.
71. Li, Z.; Li, P.; Huang, J. *J. Polym. Sci., Part A: Polym. Chem.* **2006**, 44, (15), 4361-4371.
72. Pang, X.; Jing, R.; Huang, J. *Polymer* **2008**, 49, (4), 893-900.
73. Pang, X.; Wang, G.; Jia, Z.; Liu, C.; Huang, J. *J. Polym. Sci., Part A: Polym. Chem.* **2007**, 45, (24), 5824-5837.
74. Sun, R.; Wang, G.; Liu, C.; Huang, J. *J. Polym. Sci., Part A: Polym. Chem.* **2009**, 47, (7), 1930-1938.
75. Walach, W.; Kowalczyk, A.; Trzebicka, B.; Dworak, A. *Macromol. Rapid Commun.* **2001**, 22, (15), 1272-1277.
76. Hans, M.; Mourran, A.; Henke, A.; Keul, H.; Möller, M. *Macromolecules* **2009**, 42, (4), 1031-1036.
77. Libera, M.; Trzebicka, B.; Kowalczyk, A.; Walach, W.; Dworak, A. *Polymer* **2011**, 52, (2), 250-257.
78. Libera, M.; Walach, W.; Trzebicka, B.; Rangelov, S.; Dworak, A. *Polymer* **2011**, 52, (16), 3526-3536.
79. Erberich, M.; Keul, H.; Möller, M. *Macromolecules* **2007**, 40, (9), 3070-3079.
80. Mangold, C.; Wurm, F.; Obermeier, B.; Frey, H. *Macromolecules* **2010**, 43, (20), 8511-8518.
81. Haag, R.; Stumbe, J. F.; Sunder, A.; Frey, H.; Hebel, A. *Macromolecules* **2000**, 33, (22), 8158-8166.
82. Kjellander, R.; Florin, E. *J. Chem. Soc., Faraday Trans. 1* **1981**, 77, (9), 2053-2077.
83. Abuchowski, A.; McCoy, J. R.; Palczuk, N. C.; van Es, T.; Davis, F. F. *J. Biol. Chem.* **1977**, 252, (11), 3582-3586.
84. Zalipsky, S. *Adv. Drug Delivery Rev.* **1995**, 16, (2-3), 157-182.
85. Lu, J.; Toy, P. H. *Chem. Rev.* **2009**, 109, (2), 815-838.
86. Saeki, S.; Kuwahara, N.; Nakata, M.; Kaneko, M. *Polymer* **1976**, 17, (8), 685-689.

87. Lutz, J.-F. *Adv. Mater.* **2011**, 23, 2237-2243.
88. Lutz, J.-F.; Weichenhan, K.; Akdemir, Ö.; Hoth, A. *Macromolecules* **2007**, 40, (7), 2503-2508.
89. Lutz, J.-F. o.; Hoth, A. *Macromolecules* **2005**, 39, (2), 893-896.
90. Sugihara, S.; Hashimoto, K.; Okabe, S.; Shibayama, M.; Kanaoka, S.; Aoshima, S. *Macromolecules* **2003**, 37, (2), 336-343.
91. Junk, M. J. N.; Li, W.; Schlüter, A. D.; Wegner, G.; Spiess, H. W.; Zhang, A.; Hinderberger, D. *Macromol. Chem. Phys.* **2011**, 212, (12), 1229-1235.
92. Li, W.; Wu, D.; Schlüter, A. D.; Zhang, A. *J. Polym. Sci., Part A: Polym. Chem.* **2009**, 47, (23), 6630-6640.
93. Aoki, S.; Koide, A.; Imabayashi, S.-i.; Watanabe, M. *Chem. Lett.* **2002**, 31, (11), 1128-1129.
94. Mangold, C.; Obermeier, B.; Wurm, F.; Frey, H. *Macromol. Rapid Commun.* **2002**, 23, (23), 1930-1934.
95. Bailey, F. E.; Callard, R. W. *J. Appl. Polym. Sci.* **1959**, 1, (1), 56-62.
96. Louai, A.; Sarazin, D.; Pollet, G.; François, J.; Moreaux, F. *Polymer* **1991**, 32, (4), 703-712.
97. Stoica, D.; Ogier, L.; Akrou, L.; Alloin, F.; Fauvarque, J. F. *Electrochim. Acta* **2007**, 53, (4), 1596-1603.
98. Giguère, G.; Zhu, X. X. *Biomacromolecules* **2010**, 11, (1), 201-206.
99. Hu, Z.; Fan, X.; Wang, H.; Wang, J. *Polymer* **2009**, 50, (17), 4175-4181.
100. Gil, E. S.; Hudson, S. M. *Prog. Polym. Sci.* **2004**, 29, (12), 1173-1222.
101. Inoue, S.; Kakikawa, H.; Nakadan, N.; Imabayashi, S.-i.; Watanabe, M. *Langmuir* **2009**, 25, (5), 2837-2841.
102. Weinhart, M.; Becherer, T.; Haag, R. *Chem. Commun.* **2011**, 47, (5), 1553-1555.
103. Murali Mohan, Y.; Padmanabha Raju, M.; Mohana Raju, K. *J. Appl. Polym. Sci.* **2004**, 93, (5), 2157-2163.
104. Zhou, L.; Cheng, R.; Tao, H.; Ma, S.; Guo, W.; Meng, F.; Liu, H.; Liu, Z.; Zhong, Z. *Biomacromolecules* **2011**, 12, (5), 1460-1467.
105. Hofmann, A. M.; Wurm, F.; Frey, H. *Macromolecules* **2010**, 44, (12), 4648-4657.
106. Wurm, F.; Kemmer-Jonas, U.; Frey, H. *Polym. Int.* **2009**, 58, (9), 989-995.
107. Wurm, F.; Hofmann, A. M.; Thomas, A.; Dingels, C.; Frey, H. *Macromol. Chem. Phys.* **2010**, 211, (8), 932-939.
108. Hofmann, A. M.; Wurm, F.; Hühn, E.; Nawroth, T.; Langguth, P.; Frey, H. *Biomacromolecules* **2010**, 11, (3), 568-574.

Chapter 2.1:

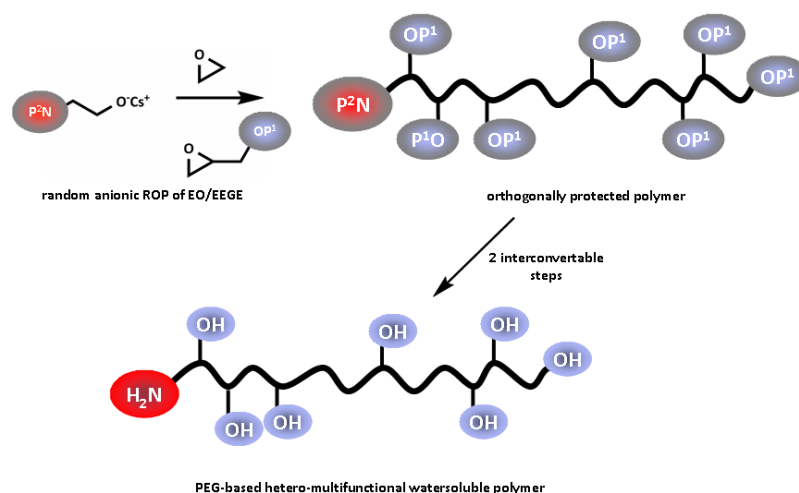
Hetero-Multifunctional Poly(ethylene glycol) Copolymers with Multiple Hydroxyl Groups and a Single Terminal Functionality

Hetero-Multifunctional Poly(ethylene glycol) Copolymers with Multiple Hydroxyl Groups and a Single Terminal Functionality

Christine Mangold, Frederik Wurm, Boris Obermeier, Holger Frey

Published in *Macromol. Rapid Commun.* **2010**, 31, (3), 258-264.

Multifunctional Poly(ethylene glycol-co-glycerol) polyethers with multiple hydroxyl groups and orthogonal terminal moiety have been prepared. A series of polymers with varying comonomer ratio was obtained by copolymerization of ethylene oxide and ethoxy ethyl glycidyl ether, followed by the removal of the orthogonal protecting groups. The materials are promising for bioconjugation and PEGylation.



Keywords: biopolymers; monofunctional PEGs; polyethers; PEGylations; random copolymers

Abstract

Hetero-multifunctional poly(ethylene glycol-co-glycerol) random copolymers with multiple hydroxyl functionalities and a single terminal functionality have been prepared by copolymerization of ethylene oxide (EO) and ethoxy ethyl glycidyl ether (EEGE) with the use of a suitable initiator, introducing a protected amino group or a double bond, respectively. Acidic deprotection was used for removal of the acetal protecting groups in the chain, and the terminal amino group was regenerated by catalytic hydrogenation. A series of copolymers with narrow polydispersity was obtained, varying comonomer fractions from 3-67% and molecular weights in the range of 5 000 to 32 000 g/mol ($1.05 < M_w/M_n < 1.25$). Molecular and thermal characterization was carried out using 1H - and ^{13}C NMR, SEC and differential scanning calorimetry.

Introduction

Poly(ethylene glycol) (PEG) is probably the most important and most widely used biocompatible polymer known today, which is not only due to its very low toxicity and excellent solubility in aqueous solutions, but also to its extremely low immunogenicity and antigenicity.¹⁻³ PEGylation is an established and valuable method for increasing protein stability or solubilizing hydrophobic biomolecules.⁴⁻⁶ In order to link PEG to biomolecules (e.g., proteins, peptides, lipids or drugs) it is essential to introduce functional groups to realize a covalent linkage. There is a variety of synthetic routes to monofunctional PEG derivatives, mainly relying on either a functional initiator or a suitable terminating agent in the anionic polymerization of ethylene oxide (EO). Furthermore, various hetero-bifunctional PEGs⁷ with two different termini have been reported that offer additional possibilities for bioconjugation.

In a recent publication we reported α,ω_n -heteromultifunctional PEG-*b*-polyglycerols with linear-hyperbranched block copolymer structure.⁸ The application of a novel protected initiator, namely *N,N*-dibenzylaminoethanol, permits facile introduction of a terminal amino group, which can be recovered by catalytic hydrogenation subsequent to the polymerization.

The use of poly(glycerol) for biomedical applications is a field of current interest, since both *in vitro* and *in vivo* studies have shown excellent biocompatibility and non-toxicity of both (hyper)branched and linear PG (*linPG*).⁹⁻¹¹ While hyperbranched poly(glycerol)s can be synthesized by cationic^{12, 13} or anionic^{10, 14-16} ring-opening multibranching polymerization of glycidol, for the synthesis of *linPG* a protected glycidyl monomer has to be used, such as ethoxy ethyl glycidyl ether (EEGE), which can be polymerized in a living manner.^{17, 18} Subsequent acidic hydrolysis affords linear poly(glycerol). Use of EEGE as a comonomer for the synthesis of random or block copolymers has attracted increased attention recently and has been employed in several works.¹⁹⁻²³ For instance, Erberich et al. have reported an elegant synthesis of copolymers using various glycidyl ethers, permitting orthogonal deprotection of the hydroxyl functionality.²⁴ Block copolymers consisting of PEG block and *linPG* segments have first been reported by Dworak et al.,²⁵ and now represent well-studied systems. However, rather surprisingly the random copolymers poly(EO-*co*-EEGE) and poly(EO-*co*-G) obtained after removal of the acetal protective groups, which can be viewed as PEGs with an adjustable number of randomly distributed hydroxyl groups at the polymer backbone,^[5] have almost been unnoticed until very recently²⁶⁻²⁸ and the few existing reports lack characterization regarding copolymer microstructure, thermal behaviour and degree of crystallization.

In this Communication we describe the synthesis and characterization of a series of random P(EO-*co*-G) copolymers with narrow molecular weight distributions $M_w/M_n < 1.2$ and varying compositions, ranging from 3 to 67 % glycerol incorporation. These copolymers represent functional PEG analogues. By the use of functional initiators, i.e., the cesium salt of either *N,N*-dibenzylamino-

ethanol or 2-(allyloxy-ethanol) linear, orthogonally reactive, heteromultifunctional PEG-copolymers have been prepared that possess a single, discrete attachment site for bioconjugation.

Experimental Part

Materials

All reagents and solvents were purchased from Acros and used as received, if not otherwise mentioned. Deuterated DMSO- d_6 and $CDCl_3$ were purchased from Deutero GmbH. Ethoxy ethyl glycidyl ether (EEGE) was prepared as described by Fitton et al.,²⁹ dried over CaH_2 and freshly distilled before use. *N,N*-Dibenzyl-2-aminoethanol was synthesized as reported previously.⁸

Instrumentation

1H and ^{13}C nuclear magnetic resonance spectra were recorded using a Bruker AC 300 spectrometer, operated at 300MHz for 1H NMR spectra. ^{13}C NMR spectra (referenced internally to solvent signals) were measured at 100.15 MHz. SEC measurements were performed in dimethylformamide (DMF) containing 0.25 g/L of lithium bromide. An Agilent 1100 Series GPC Setup (gel permeation chromatography) was used, including a PSS HEMA column ($10^6/10^5/10^4$ g/mol), and both a UV (254 nm) and RI detector. Calibration was carried out with poly(ethylene oxide) standards provided by Polymer Standards Service (PSS). The eluent was generally used at 50°C and at a flow rate of 1mL/min. DSC measurements were carried out using a Perkin-Elmer 7 series thermal analysis system and a Perkin-Elmer Thermal Analysis Controller TAC 7/DX in the temperature range from -80 to 100 °C, using heating rates of 4 and 10 K·min⁻¹.

Synthesis

General procedure: Copolymerization. *N,N*-Dibenzyl-2-aminoethanol or 2-allyloxy-ethanol, respectively, was dissolved in benzene in a Schlenk flask and an equivalent amount of cesium hydroxide was added. The mixture was stirred at 60 °C under argon for 1 h and evacuated at 90°C (10^{-2} mbar) for 2 h to remove benzene and water, forming the cesium alkoxide, which was then dissolved in dry DMSO (20 wt%). In a separate setup, dry THF was cryo-transferred into a 250 mL-Schlenk flask. EO was cryo-transferred to a graduated ampoule, dried over CaH_2 and then cryo-transferred into the flask containing THF to produce an approximately 50 weight % solution. Subsequently EEGE was added via syringe and the mixture was warmed to room temperature. The initiator was introduced via canula and the reaction solution was immediately heated to 90 °C and stirred for 12 h. The reagents were introduced *in vacuo* and the reaction is carried out in the sealed flask. After polymerization of the monomers again low pressure is present in the flask.

Caution: in very few cases the pressure evolving in the early stages of the reaction in the flask led to the spontaneous removal of the septum and release of EO. Thus, the reaction has to be carried out in an appropriate fume hood and appropriate safety precautions should be taken. In general the

amount of EO used did not exceed 10 g per batch in a 250 mL flask (conc. of the comonomers ca. 20%) to guarantee a safe reaction.

Precipitation in cold diethyl ether resulted in the pure (co)polymers. For polymers with a high fraction of EEGE, polymer solution was dried *in vacuo*, since precipitation failed due to the amorphous nature of these materials. Yields: generally 95% to quantitative. *N,N*-Dibenzyl-poly(EO-*co*-EEGE): ^1H NMR (300 MHz, CDCl_3): δ = 7.31 (m, C_6H_5), 4.69 (br, acetal-H), 3.78-3.37 (polyether backbone) 1.28-1.15 (br, CH_3 acetal). ^{13}C NMR see Supporting Information.

Allyloxy-poly(EO-*co*-EEGE): ^1H NMR (300 MHz, CDCl_3): δ = 5.85 (m, $\text{H}_2\text{C}=\underline{\text{C}}\text{H}$), 5.21 (dd, $\underline{\text{H}}_2\text{C}=\text{CH}$), 4.69 (br, acetal-H), 3.85-3.37 (polyether backbone) 1.28-1.15 (br, $-\text{CH}_3$ acetal). ^{13}C NMR see Supp. Inf.

N,N-Dibenzyl-poly(ethylene oxide-*co*-glycerol): The acetal protecting groups were removed by the addition of 1N hydrochloric acid to a 20% solution of the polymer in methanol and stirring at room temperature for a period ranging from 30 min up to 2 h, depending on the amount of EEGE-monomer incorporated. The reaction solution was concentrated *in vacuo* and then precipitated from a concentrated methanol solution in diethyl ether. Yields: 80-90%. ^1H NMR (300 MHz, $\text{DMSO}-d_6$): δ = 7.62, 7.40 (br, C_6H_5), 4.51 (br, OH), 3.59-3.27 (polyether backbone).

Allyloxy-poly(ethylene oxide-*co*-glycerol): The copolymer was dissolved in methanol to form an approximately 20% solution. A strongly acidic ion exchange resin was added and the solution was stirred for 5 h at RT. After filtration the reaction solution was concentrated *in vacuo* and then precipitated in diethyl ether. Yields: 80-90%. ^1H NMR (300 MHz, CDCl_3): δ = 5.85 (m, $\text{H}_2\text{C}=\underline{\text{C}}\text{H}$), 5.21 (dd, $\underline{\text{H}}_2\text{C}=\text{CH}$), 4.51 (OH), 3.85-3.37 (polyether backbone).

H_2N -poly(ethylene oxide-*co*-glycerol): *N,N*-Dibenzyl-poly(ethylene oxide-*co*-glycerol) was dissolved in methanol, and palladium on activated charcoal (10%) was added. The reaction vessel was flushed with hydrogen (8 bar) and the reaction was allowed to stir for 72 h at room temperature. The solution was filtered, concentrated and precipitated into cold diethyl ether. Yields: quantitative; ^1H NMR (300 MHz, $\text{DMSO}-d_6$): δ = 4.79-4.42 (OH), 3.59-3.27 (polyether backbone).

Results and Discussion

Synthesis of the Hetero-Multifunctional PEGs

The synthetic strategy developed to obtain the polyfunctional PEG structures with precisely one terminal functionality is depicted in Figure 1. The synthesis was either carried out using a three step (route I) or a two step (route II) procedure. For both routes the synthesis commences with the copolymerization of EO/EEGE, using the protected initiator and subsequent acidic deprotection of the hydroxyl groups. The hydrolysis can be conducted without further purification of the polymer obtained. To regenerate the terminal amino functionality, the benzyl protective groups were finally removed by catalytic hydrogenation with Pd/C.

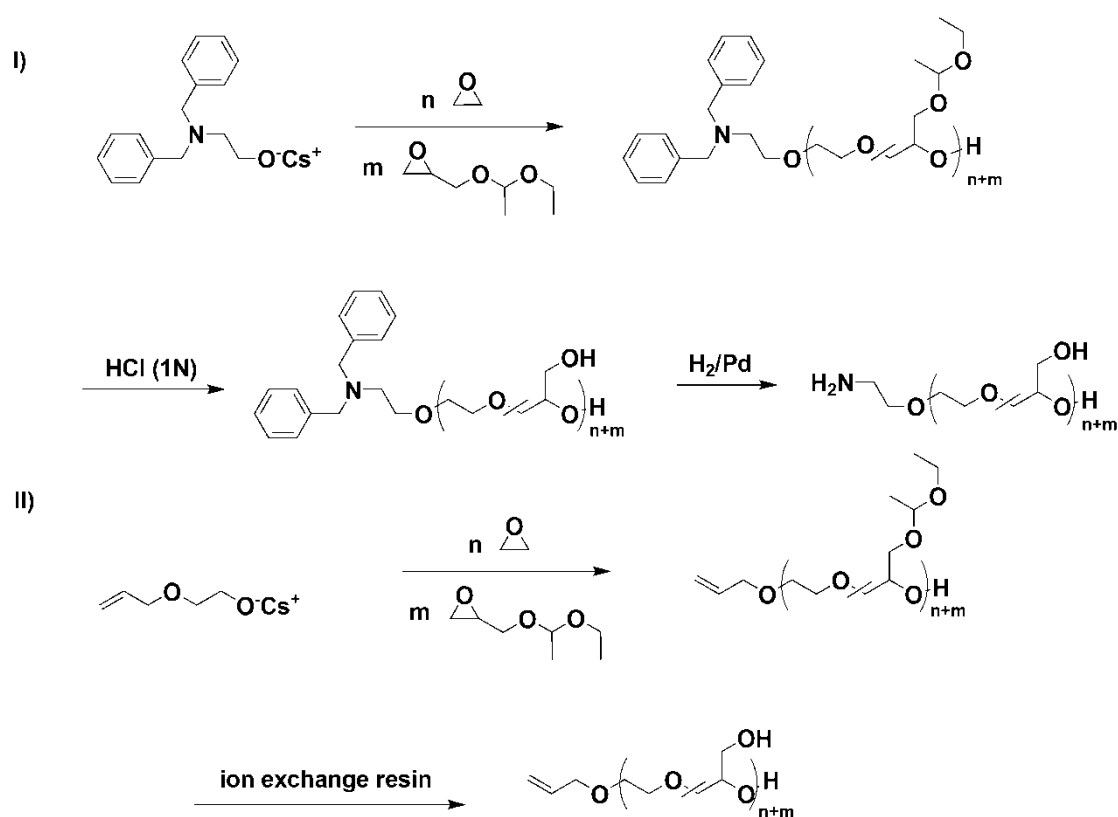


Figure 1. Reaction sequence for random P(EO-co-G) with a terminal amino functionality or allyl group.

In contrast to previously reported procedures for copolymerization of EO and EEGE²⁸ our setup relies on controlling the amounts of monomers by cryo-transfer, subsequent rapid heating and polymerization at 90 °C *in vacuo*. Characterization data for the series of copolymers obtained from the copolymerization of EO and varying fractions of EEGE (3% to 67%) is given in Table 1 (samples 1-8). The theoretical molecular weights of sample 1 to 6 were calculated on the basis of 227

monomer units, referring to a molecular weight of 10 000 g/mol for a PEG homopolymer. Since EEGE exhibits a higher molecular weight than EO, the theoretical molecular weights of the polymers increase with increasing amount of EEGE incorporated, starting from 10 900 g/mol for sample 1 (3%) up to 21 700 g/mol for sample 6 (67%). The targeted M_n of samples 7 and 8 was 5 000 g/mol. In general polymers with a slightly higher molecular weight (in comparison with the theoretical values) were obtained. This is explained by experimental inaccuracies, such as residual initiator solution remaining in the flask or the syringe used for transfer of the solution to the polymerization vessel.

Size exclusion chromatography (SEC) DMF referenced to PEG-standards showed generally narrow molecular weight distributions with polydispersity indices in the range of 1.05 to 1.25 for all samples. However, the molecular weights, ranging from 5 000 to 30 000 g/mol determined by ^1H NMR-spectroscopy differ from the values obtained by SEC. SEC-values are approximately 65% of the actual molecular weight calculated from the NMR-data. This deviation becomes increasingly pronounced, when the amount of EEGE increases and can most likely be explained by the different chemical structure of the polymers investigated in comparison to the calibration standard applied (PEG). The more EEGE-units are incorporated, the more side chains are introduced and the hydrodynamic radius, which determines the elution volume, changes compared to PEG-standards. Therefore an increasing deviation is observed. Polymerization yields were quantitative, and no residual monomer was observed in the reaction mixture. Thus, the ratio of EO to EEGE in the copolymers was found to reflect the composition of the monomer feed. The targeted fractions were 3, 10, 15, 25, 40, and 65% for samples 1 to 6 and 3, 5%, respectively for sample 7 and 8. The incorporated monomer ratios determined by NMR can be found in Table 1. Detailed studies on reaction kinetics are in progress to determine the respective reactivity of the two comonomers.

Deprotection of the hydroxyl groups of P(EO-co-EEGE) by hydrolysis with dilute hydrochloric acid resulted in the linear multifunctional PEGs (deprotected samples 1d-8d). For lower EEGE fractions (up to 14 %, sample 3) the deprotection was carried out using a strongly acidic ion exchange resin, such as Dowex 50WX8, while for higher fractions of EEGE (sample 4 to 6) complete removal of the acetal protective groups was only achieved using 1M hydrochloric acid. Full deprotection was confirmed by ^1H NMR-spectroscopy, and SEC characterization was carried out for all samples. Molecular weights determined by SEC are underestimated, but the results obtained by NMR correspond to the values targeted for the protected polymers (Table 1).

To obtain the α -deprotected PEG-copolymers bearing a single terminal amino functionality and several OH-groups (samples 1da and 3da in Table 1), catalytic hydrogenation was carried out in a pressure vessel at 8 bar for 72 h. Deprotection was followed by ^1H NMR, monitoring the disappearance of the aromatic protons. Related ^1H and ^{13}C NMR data as well as SEC-diagrams of the polymers are given in the Supporting Information.

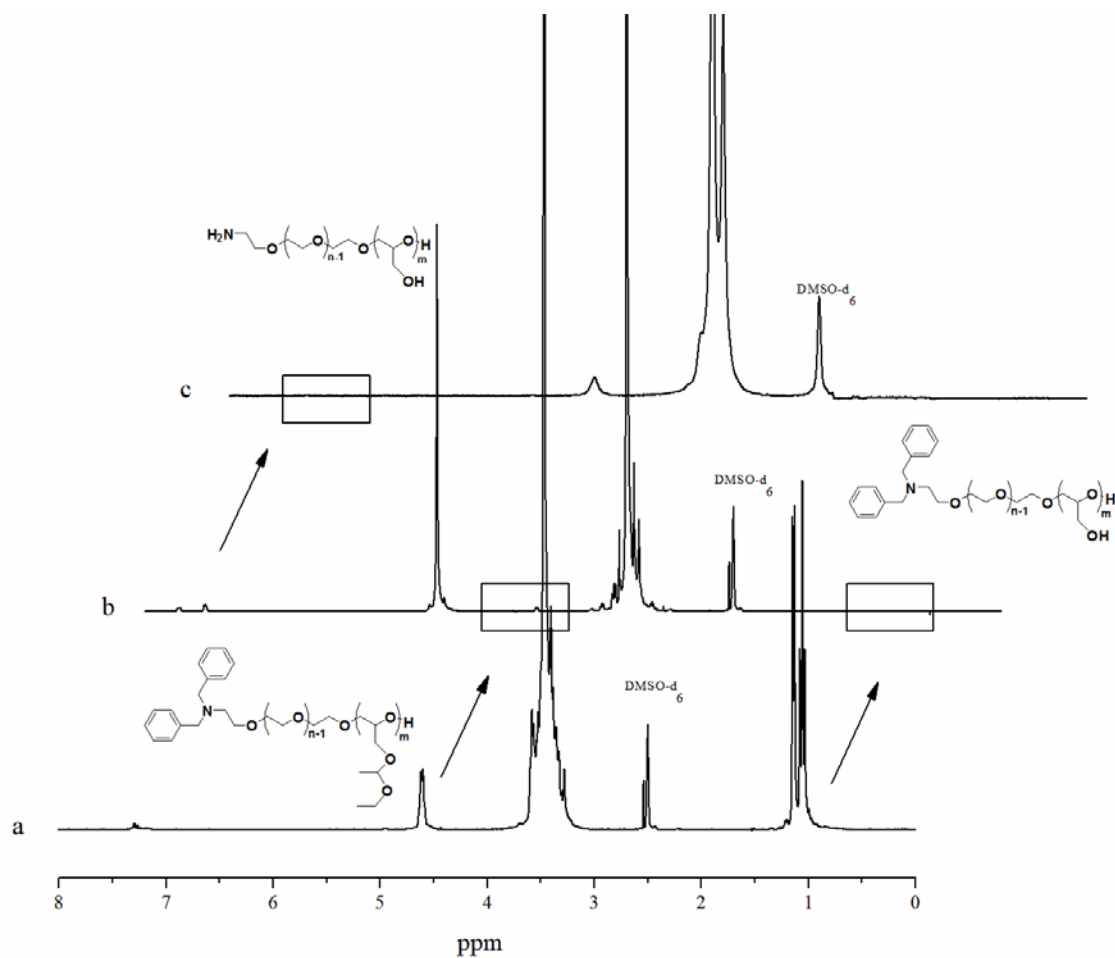


Figure 2. Comparison of ^1H NMR spectra of polymer sample 3 as obtained after polymerization with the benzyl-protected amino-ethanol initiator (a); after deprotection of the hydroxyl side chains 3d (b), and after removal of the benzyl protecting groups after catalytic hydrogenation 3da (c).

Figure 2 shows a comparison of the ^1H NMR spectra of the initial EO-EEGE-copolymer with the final, desired amino- and hydroxyfunctional $\text{H}_2\text{NP}(\text{EO-co-G})$ -copolymers. As it can be seen, the acidic deprotection (a to b) as well as the cleavage of the benzylic protecting groups (b to c) can be followed conveniently.

Table 1. Characterization data for the series of PEG-co-PEEGE copolymers prepared

Sample	EEGE ^{a)}	Mn ^{b)} (NMR)	Mn ^{c)} (SEC)	PDI ^{c)} (SEC)	T _g ^{d)}	T _m ^{e)}	ΔH _m ^{f)}	ΔH _{recryst} ^{g)}	
		g/mol	g/mol		°C	°C	J/g	J/g	
1	Bn ₂ NP(EO ₃₃₅ -CO-EEGE ₁₁)	3%	16 600	10 000	1.11	-64*	41	85	-
2	Bn ₂ NP(EO ₂₃₄ -CO-EEGE ₂₆)	10%	14 100	7 600	1.13	-71	23	42	-
3	Bn ₂ NP(EO ₁₉₃ -CO-EEGE ₃₂)	14%	13 400	6 700	1.19	-69	10	33	-28
4	Bn ₂ NP(EO ₃₀₇ -CO-EEGE ₉₀)	23%	26 600	10 000	1.18	-68	-2	9	-12
5	Bn ₂ NP(EO ₂₄₅ -CO-EEGE ₁₅₄)	39%	23 700	9 200	1.20	-68	-	-	-
6	Bn ₂ NP(EO ₉₅ -CO-EEGE ₁₉₀)	67%	31 900	9 000	1.15	-67	-	-	-
7	Allyl-P(EO ₁₂₀ -CO-EEGE ₃)	3%	5 700	3 900	1.07	- ^{h)}	45	90	-
8	Allyl-P(EO ₁₀₁ -CO-EEGE ₆)	5%	5 500	3 100	1.06	-65 ^{h)}	26	46	-
1d	Bn ₂ NP(EO ₃₃₅ -CO-G ₁₁)	3%	15 800	9 200	1.09	-48 ^{h)}	47	110	-
2d	Bn ₂ NP(EO ₂₃₄ -CO-G ₂₆)	10%	12 500	7 200	1.15	-59	35	71	-2
3d	Bn ₂ NP(EO ₁₉₃ -CO-G ₃₂)	14%	10 900	6 500	1.23	-56	20	42	-
4d	Bn ₂ NP(EO ₃₀₇ -CO-G ₉₀)	23%	20 100	7 800	1.15	-53	-	-	-
5d	Bn ₂ NP(EO ₂₄₅ -CO-G ₁₅₄)	39%	16 700	7 500	1.20	-52	-	-	-
6d	Bn ₂ NP(EO ₉₅ -CO-G ₁₉₀)	67%	17 900	7 600	1.21	-50	-	-	-
7d	Allyl-P(EO ₁₂₀ -CO-G ₃)	3%	5 500	3 900	1.07	- ^{h)}	46	143	-
8d	Allyl-P(EO ₁₀₁ -CO-G ₆)	5%	5 000	3 000	1.09	-59 ⁱ⁾	38	113	-
1da	H ₂ NP(EO ₃₃₅ -CO-G ₁₁)	3%	15 600 ⁱ⁾	7 000	1.25	-	-	-	-
3da	H ₂ NP(EO ₁₉₃ -CO-G ₃₂)	14%	10 700 ⁱ⁾	4 200	1.31	-	-	-	-

^{a)}comonomer content (EEGE or G); ^{b)}determined by ¹H NMR-spectroscopy; ^{c)}determined via size exclusion chromatography in dimethylformamide vs. PEG-standards; ^{d)}glass transition temperature obtained from DSC; ^{e)} T_m= melting point obtained from DSC-measurements; ^{f)}melting enthalpy obtained from DSC; ^{g)}recrystallization enthalpy (DSC); ^{h)}estimated (peak too shallow for analysis) ⁱ⁾theoretical value.

¹³C NMR analysis of copolymer microstructure

Random distribution of the functional EEGE units within the PEG backbone is an important issue with respect to a variety of future applications of the functional PEG copolymers. ¹³C NMR analysis permits to investigate the triad sequence distribution, giving information on the distribution of the EEGE units. To keep abbreviations short, in Figure 3, EEGE-units will be referred to as “G”, while EO-units are indicated by the letter “E”. Figure 3 shows enhanced regions of the ¹³C NMR spectra related to the signals of the PEO (E) backbone for copolymers with EEGE (G) fractions of 3% (a) in Bn₂NP(EO₃₃₅-*co*-EEGE₁₁), 23% (b) in Bn₂NP(EO₃₀₇-*co*-EEGE₉₀) and 67% (c) in Bn₂NP(EO₉₅-*co*-EEGE₁₉₀). The intensity of signals I-V corresponds to the sequence distribution of EO-centered triads, of which signal I is assigned to an overlap of the EEGE methylene backbone signal and the G-E-G triad. Additionally, signal II is due to an overlap of at least two triad signals. Clearly, in contrast to the established signal assignment for random copolymers of propylene oxide and ethylene oxide,³⁰⁻³² for EEGE/EO copolymers the analysis is severely complicated by the presence of overlapping resonances of the EEGE backbone. However, most importantly, signal III can be unequivocally assigned to the E-E-E homo-triad, the signal for both methylene groups of an EO unit adjacent to two other EO units. As expected, for 3% EEGE content (a) the E-E-E-triad signal shows the highest intensity, compared to the other triad signals of low intensity. An increase of EEGE incorporation up to 23% (spectrum b) directly results in a lower ratio of signal III in comparison to signals I, II, IV and VI, evidencing the increased amount of EO linked to EEGE comonomer units.

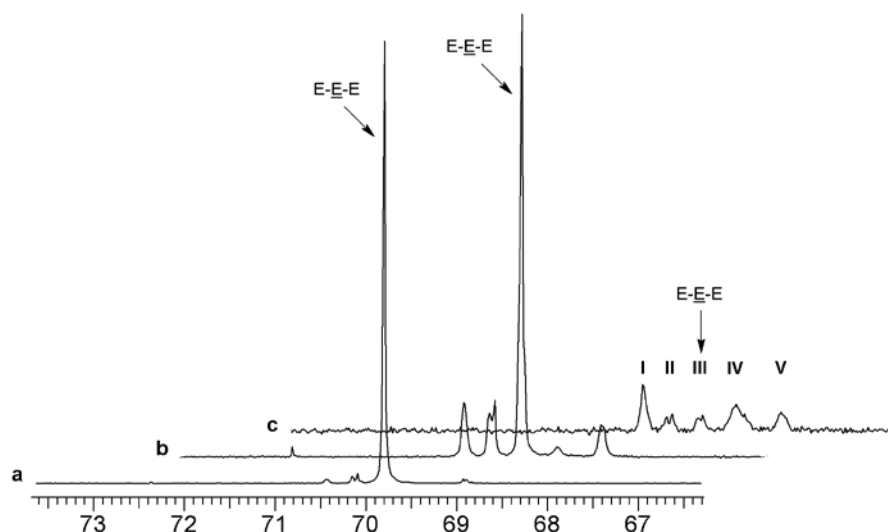


Figure 3. ¹³C NMR (75.5 MHz, DMSO-*d*₆) region for EO backbone signals Bn₂NP(EO₃₃₅-*co*-EEGE₁₁) (a), Bn₂NP(EO₃₀₇-*co*-EEGE₉₀) (b), and Bn₂NP(EO₉₅-*co*-EEGE₁₉₀) (c) with relevant EO centered triads E-E-E (apparent signal shift for different composition is a result of overlay image, exact shifts are given in the Supporting Information).

The lower fraction of EO units adjacent to other EO-units results in a reduced relative intensity of the E-E-E triad. For the highest EEGE content of 67% investigated in this study the E-E-E triad signal decreases further. For this sample, the intensities are similar for all triad signals observed. In summary, the analysis of the triad sequence distribution, focusing on the important EO homo-triad, supports a random distribution of EEGE units along the polymer chain, since the evolution of the triad sequence distribution from a to c would not be observed, if copolymerization led to block or strong gradient block formation. Nevertheless, it is likely that the random distribution is slightly tapered due to the lower reactivity of EEGE compared to EO, based on the comparison with other comonomers with a certain structural analogy, such as propylene oxide.

Thermal behavior

The thermal behavior of the random copolymers is of crucial importance with respect to possible applications that are related to potential crystallization. To the best of our knowledge, the thermal properties of random copolymers of P(EO-co-EEGE) and P(EO-co-G) have not been studied to date. The thermal behaviour has been quantified by differential scanning calorimetry (DSC). Glass transition temperatures (T_g) of all P(EO-co-EEGE) samples are close to the literature value of PEG and are observed in the range of -65 ± 5 °C. With disregard to sample 1, which only shows a hardly detectable T_g due to the predominant crystalline domains, the T_g s of the other samples showed a slight decrease for increasing EEGE/EO-ratios. The same tendency was observed for the deprotected samples, but their glass transition temperatures (1d - 8d) are approximately 10 to 15 °C higher than those of the respective protected precursors, which we attribute to the interaction of the hydroxyl groups in these systems. These values are close to those reported for PEO-*lin*PG- block copolymers.³³ The melting temperature of 66 °C of PEG³⁴ is gradually lowered upon incorporation of the EEGE-comonomers. Already 3% EEGE comonomer incorporation leads to a significantly lowered melting point of 41 °C, which further decreases to -2 °C for sample 4 (25% EEGE). As expected, samples 5 and 6 (40 and 65% EEGE incorporated, respectively) showed no melting endotherms, since they are amorphous. The deprotected, hydroxyfunctional samples show the same trend, however, melting temperatures are generally higher for all deprotected analogues. The related decrease of the degree of crystallization can be quantified by determination of the melting enthalpy ΔH_m , (in J/g), which decreases with increasing comonomer fraction. An additional issue is worth mentioning in this context: while samples 1, 1d, 2, 2d, 7, 7d, 8 and 8d only show a single melting endotherm, samples 3, 4 as well as sample 3d in addition exhibited a pronounced recrystallization peak upon heating. Cooling rates of 10 K/min were too rapid for copolymers with larger fraction of EEGE to permit crystallization, leading to recrystallization events in subsequent heating runs. It is worth noting that the degree of crystallization generally increased after deprotection.

Considering the larger steric hindrance of the ethoxy ethyl side groups in comparison with the hydroxyl groups and the resulting impact on crystallization of the PEG sequences, the observations are consistent with expectation. Furthermore, the higher melting points and enthalpies of the deprotected polyols are most likely due to interaction of neighbouring hydroxyl groups, forming hydrogen bonds in the bulk. The gradual change of the thermal properties with EEGE comonomer fraction once again supports random comonomer incorporation in the chain.

Conclusion

We have described a convenient synthesis for linear, functional PEG-copolymers with a single orthogonal amino or allyl function in the α -position and an adjustable number of hydroxyl-groups in the polymer backbone. Particularly the orthogonal character of the functional groups and the excellent water solubility of the functional PEG structures bear promise for new pharmaceutical and biomedical applications, e.g., in PEGylation. The single amino-moiety as well as the allyl group can be specifically addressed in a variety of reactions and can therefore be utilized to obtain well-defined polymer-biomolecule conjugates and for surface modification of biomaterials. In contrast to PEG, the systems reported here possess a varying number of hydroxyl functionalities within the chain. This also results in adjustable thermal properties. Further studies on the bioconjugation of the novel PEG-like materials are in progress.

Supporting Information

Experimental

Bn₂NP(EO₁₉₃-co-EEGE₃₄) (15% EEGE incorporation). 193 mg *N,N*-Dibenzyl-2-aminoethanol ($8.02 \cdot 10^{-4}$ mol, 1,1 eq.) was dissolved in 5 mL benzene in a Schlenk flask and 121 mg of cesium hydroxide ($7.29 \cdot 10^{-4}$ mol 1 eq) was added. The mixture was stirred at 60 °C under argon for 1 hour and evacuated at 90 °C (10^{-2} mbar) for two hours to remove benzene and water, forming the cesium alkoxide, which was then dissolved in dry DMSO (20 wt%). In a separate setup, 20 mL dry THF was cryo-transferred into a 250 mL-Schlenk flask. 6.19 g EO (7 mL, 0.14 mol, 193 eq.) were cryo-transferred to a graduated ampoule (at -80 °C), dried over CaH₂ and then cryo-transferred into the flask containing THF to produce an approximately 50 weight % solution. Subsequently 3.62 g EEGE (0.024 mol, 34 eq.) were added via syringe and the mixture was warmed to RT. The initiator was introduced via canula and the flask was double-sealed with electrical tape. Subsequently, the reaction solution was heated to 90 °C and stirred for 12 hours. Precipitation in cold diethyl ether resulted in the pure polymer (¹H NMR = Bn₂NP(EO₁₉₃-co-EEGE₃₂)). Yield: 95%.

¹³C NMR spectroscopy

N,N-Dibenzyl-poly(ethylene oxide-co-ethoxyethyl glycidyl ether): ¹³C NMR (300 MHz, DMSO-*d*₆): δ = 139.52, 128.43, 128.12, 126.75 (aromatic), 99.18 (d, OCH(CH₃)O), 78.46-77.59 (OCH₂CHO), 72.33 (CH₂CH₂OH), 70.60-68.75 (OCH₂CH₂OCH₂CHO), 64.46 (d, CHCH₂O), 60.19 (OCH₂CH₃), 60.10 (CH₂CH₂OH), 58.01 (NCH₂Ph), 52.09 (NCH₂CH₂), 19.71 (CHCH₃), 15.17 (CH₂CH₃).

Allyloxy-poly(ethylene oxide-co-ethoxyethyl glycidyl ether): ¹³C NMR (300 MHz, DMSO-*d*₆): δ = 135.28 (CH=CH₂), 116.22 (CH=CH₂), 99.18 (d, OCH(CH₃)O), 78.46-77.59 (OCH₂CHO), 72.33 (CH₂CH₂OH), 71.05 (CH₂=CHCH₂O), 70.60-68.75 (OCH₂CH₂OCH₂CHO), 64.46 (d, CHCH₂O), 60.19 (OCH₂CH₃), 60.10 (CH₂CH₂OH), 19.71 (CHCH₃), 15.17 (CH₂CH₃).

N,N-Dibenzyl-poly(ethylene oxide-co-glycerol): ¹³C NMR (300 MHz, DMSO-*d*₆): δ = 139.52, 128.43, 128.12, 126.75 (aromatic), 80.11-79.30 (OCH₂CHO), 72.33 (CH₂CH₂OH), 71.15-68.75 (OCH₂CH₂OCH₂CHO), 60.10 (CH₂CH₂OH), 58.01 (NCH₂Ph), 52.09 (NCH₂CH₂).

Triad Sequence Analysis

The triad sequence analysis was conducted in analogy to previous works on other EO-copolymers, especially on EO/PO random copolymers. This system was first analysed by Whipple and Green³⁵, and a detailed characterization can also be found in several articles by Guyot et al.³⁰ Possible monomer triads are shown below.

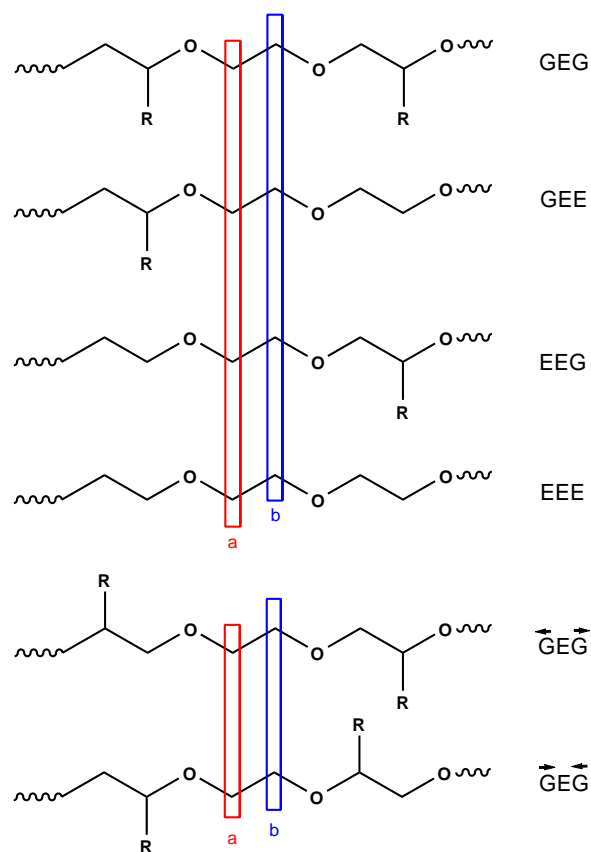


Figure S1. Possible triad sequence distribution, with R = ethoxy-ethyl-protecting group and E = EO unit and G = EEGE/G-units, respectively.

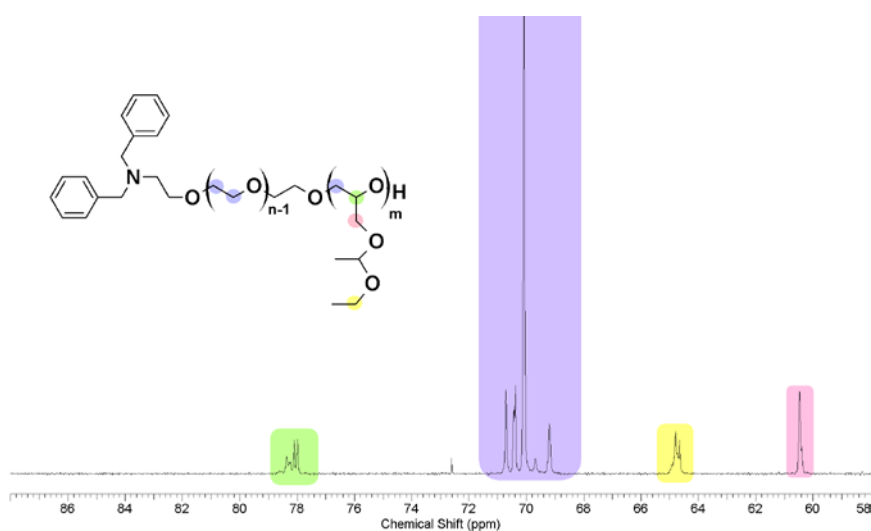


Figure S2. Zoom into ^{13}C -spectrum of entry 4 $\text{Bn}_2\text{NP}(\text{EO}_{307}\text{-co-EEGE}_{90})$ in $\text{DMSO-}d_6$, showing the E-centered triads (71-68 ppm) overlapping with the methylene-carbon from the EEGE-units (purple) and the G-centered triads (78 ppm, green), caused by the methin-carbon.

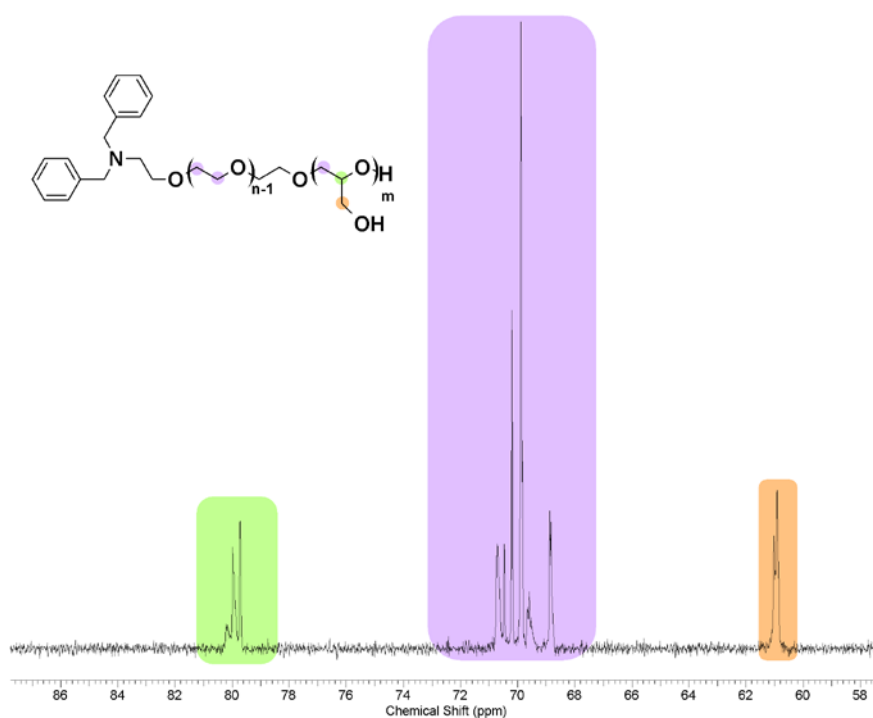


Figure S3. Zoom into the ^{13}C NMR spectrum of entry **5d** $Bn_2NP(EO_{245}\text{-}co\text{-}G_{154})$ in $DMSO-d_6$, showing the E-centered triads (71-68 ppm) overlapping with the methylene-carbon of the EEGE-units (purple) and the G-centered triads (80 ppm, green), in comparison to the previous spectrum: note that the signal at 64 ppm corresponding to the protecting group has disappeared.

Size exclusion chromatography

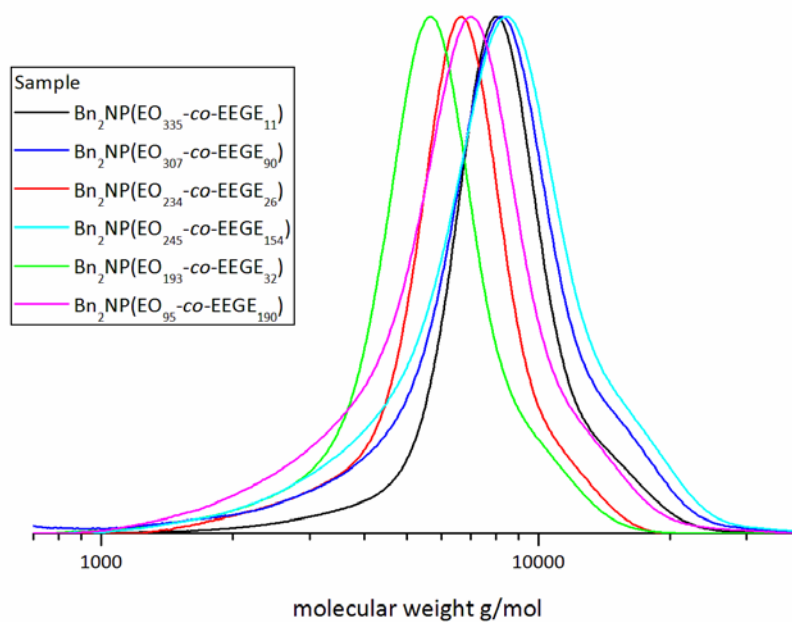


Figure S4. Molecular weight distributions of samples **1** to **6** obtained by SEC in DMF vs. PEG-standards.

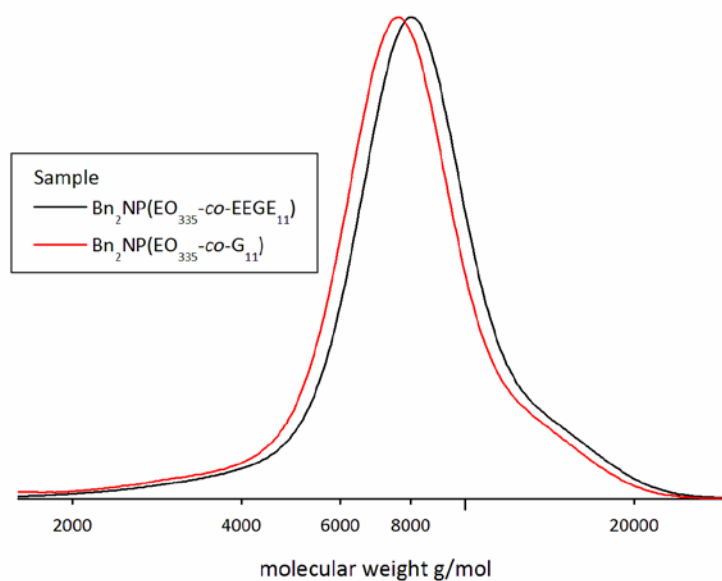


Figure S5. Molecular weight distribution of sample **1** before and after (**1d**) acidic deprotection of the acetals.

Thermal properties

The effects of comonomer incorporation on the morphology of the highly crystalline PEG are already obvious from the appearance of the materials. While copolymers **1** and **7** (3 and 2.5% EEGE-incorporation) were obtained as colourless powders, all other materials (**2-6** and **3d-6d**, 10-65% incorporation) were highly viscous liquids. Samples **2d**, **7d** and **8d** revealed a waxy consistency.



Figure S6. 1) Sample Allyl-P(EO_{120} -*co*-EEGE₃) 2) Allyl-P(EO_{101} -*co*-EEGE₆) 3) $\text{Bn}_2\text{NP}(\text{EO}_{307}$ -*co*-EEGE₉₀)

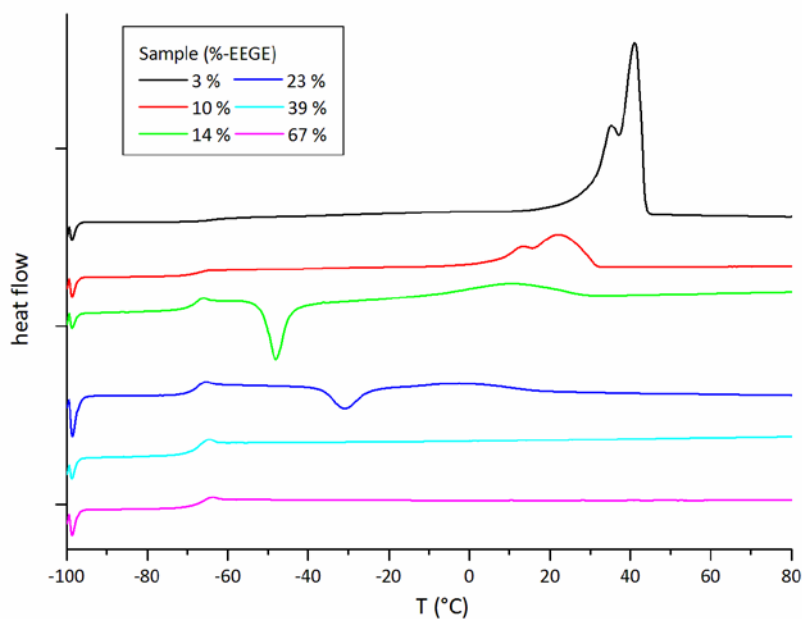


Figure S7. DSC-heating curves for samples 1 to 6. The decrease in the melting enthalpy as well as the increasing T_g can be clearly observed. Additionally, samples 2 and 3 also show recrystallization events.

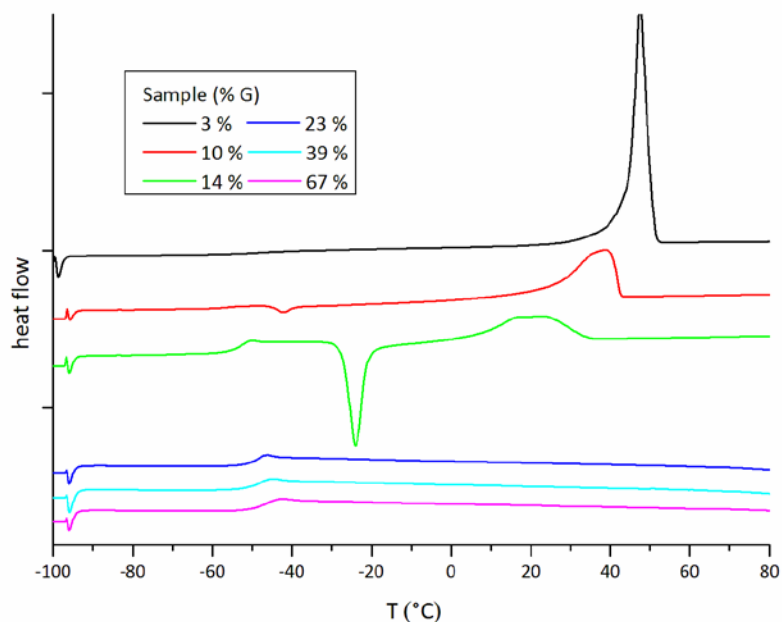


Figure S8. DSC-heating curves of sample 1d to 6d. Samples 1 to 3 show a melting peak, whereas sample 2 and 3 also reveal a recrystallization peak. The T_g increases with increasing amount of glycerol units incorporated. For incorporation exceeding 20% no crystallization is observed. A detailed discussion is given in the main manuscript.

MALDI-TOF

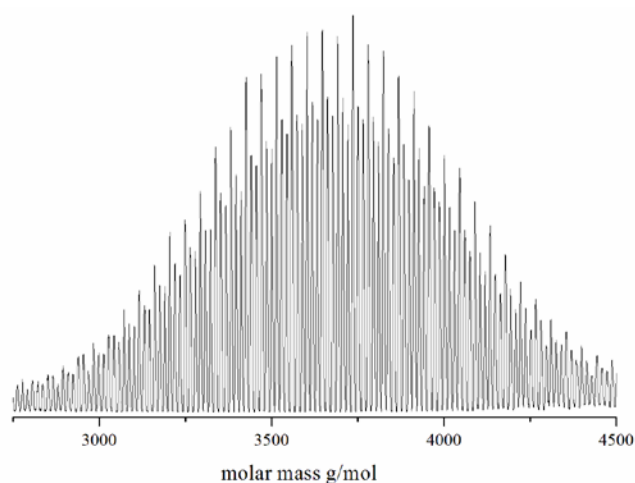


Figure S9. Molar mass distribution of sample 7d.

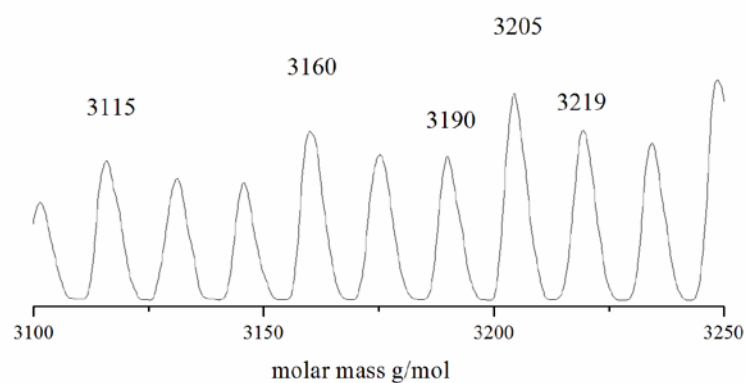


Figure S10. Zoomed region of the spectra shown in Figure 9 (sample 7d), the values are assigned to the initiator + monomer combinations given below.

Molecular weights

Initiator: 102,13 g/mol

EO: 44,05 g/mol

G: 74,08 g/mol

Cs⁺: 132,91 g/mol

3115	Initiator + 62 EO + 2 G + Cs ⁺
3160	Initiator + 63 EO + 2 G + Cs ⁺
3190	Initiator + 62 EO + 3 G + Cs ⁺
3205	Initiator + 64 EO + 2 G + Cs ⁺
3219	Initiator + 61 EO + 4 G + Cs ⁺

1. Zalipsky, S. *Adv. Drug Delivery Rev.* **1995**, 16, (2-3), 157-182.
2. Merrill, E. W., *Poly(ethylene glycol) Chemistry: Biotechnical and Biomedical Applications*. 1 ed.; Plenum Press: New York, 1992.
3. Roberts, M. J.; Bentley, M. D.; Harris, J. M. *Adv. Drug Delivery Rev.* **2002**, 54, (4), 459-476.
4. Caliceti, P.; Veronese, F. M. *Adv. Drug Delivery Rev.* **2003**, 55, (10), 1261-1277.
5. Tao, L.; Geng, J.; Chen, G.; Xu, Y.; Ladmiral, V.; Mantovani, G.; Haddleton, D. M. *Chem. Commun.* **2007**, (33).
6. Hiroyuki, Y.; Toshiyuki, S.; Takaaki, A.; Masaki, K.; Hisao, N.; Motoo, Y. *Biochimica et Biophysica Acta (BBA) - General Subjects* **2008**, 1780, (4), 680-686.
7. Thompson, M. S.; Vadala, T. P.; Vadala, M. L.; Lin, Y.; Riffle, J. S. *Polymer* **2008**, 49, (2), 345-373.
8. Wurm, F.; Klos, J.; Räder, H. J.; Frey, H. *J. Am. Chem. Soc.* **2009**, 131, 7954-7955.
9. Kainthan, R. K.; Hester, S. R.; Levin, E.; Devine, D. V.; Brooks, D. E. *Biomaterials* **2007**, 28, (31), 4581-4590.
10. Kainthan, R. K.; Muliawan, E. B.; Hatzikiriakos, S. G.; Brooks, D. E. *Macromolecules* **2006**, 39, (22), 7708-7717.
11. Kainthan, R. K.; Janzen, J.; Levin, E.; Devine, D. V.; Brooks, D. E. *Biomacromolecules* **2006**, 7, (3), 703-709.
12. Tokar, R.; Kubisa, P.; Penczek, S.; Dworak, A. *Macromolecules* **1994**, 27, (2), 320-322.
13. Dworak, A.; Walach, W.; Trzebicka, B. *Macromol. Chem. Phys.* **1995**, 196, (6), 1963-1970.
14. Sunder, A.; Hanselmann, R.; Frey, H.; Mulhaupt, R. *Macromolecules* **1999**, 32, (13), 4240-4246.
15. Sunder, A.; Heinemann, J.; Frey, H. *Eur. Polym. J.* **2000**, 6, (14), 2499-2506.
16. Kautz, H.; Sunder, A.; Frey, H. *Macromol. Symp.* **2001**, 163, 67-74.
17. Taton, D.; Le Borgne, A.; Sepulchre, M.; Spassky, N. *Macromol. Chem. Phys.* **1994**, 195, (1), 139-148.
18. Keul, H.; Möller, M. *J. Polym. Sci., Part A: Polym. Chem.* **2009**, 47, (13), 3209-3231.
19. Dimitrov, P.; Rangelov, S.; Dworak, A.; Tsvetanov, C. B. *Macromolecules* **2004**, 37, (3), 1000-1008.
20. Dimitrov, P.; Utrata-Wesolek, A.; Rangelov, S.; Walach, W.; Trzebicka, B.; Dworak, A. *Polymer* **2006**, 47, (14), 4905-4915.
21. Dworak, A.; Trzebicka, B.; Wałach, W.; Utrata, A.; Tsvetanov, C. *Macromol. Symp.* **2004**, 210, (1), 419-426.
22. Jamróz-Piegza, M.; Walach, W.; Dworak, A.; Trzebicka, B. *J. Colloid Interface Sci.* **2008**, 325, (1), 141-148.

23. Halacheva, S.; Rangelov, S.; Tsvetanov, C. *Macromolecules* **2006**, 39, (20), 6845-6852.
24. Erberich, M.; Keul, H.; Möller, M. *Macromolecules* **2007**, 40, (9), 3070-3079.
25. Dworak, A.; Baran, G. y.; Trzebicka, B.; Walach, W. *React. Funct. Polym.* **1999**, 42, (1), 31-36.
26. Sun, R.; Wang, G.; Liu, C.; Huang, J. *J. Polym. Sci., Part A: Polym. Chem.* **2009**, 47, (7), 1930-1938.
27. Huang, J.; Li, Z.; Xu, X.; Ren, Y.; Huang, J. *J. Polym. Sci., Part A: Polym. Chem.* **2006**, 44, (11), 3684-3691.
28. Li, Z.; Chau, Y. *Bioconjugate Chem.* **2009**, 20, (4), 780-789.
29. Fitton, A. O.; Hill, J.; Jane, D. E.; Millar, R. *Synthesis* **1987**, (12), 1140-1142.
30. Hamaide, T.; Goux, A.; Llauro, M.-F.; Spitz, R.; Guyot, A. *Angew. Makromol. Chem.* **1996**, 237, (1), 55-77.
31. Heatley, F.; Yu, G.-e.; Booth, C.; Blease, T. G. *Eur. Polym. J.* **1991**, 27, (7), 573-579.
32. Billouard, C.; Carlotti, S.; Desbois, P.; Deffieux, A. *Macromolecules* **2004**, 37, (11), 4038-4043.
33. Wurm, F.; Nieberle, J.; Frey, H. *Macromolecules* **2008**, 41, (4), 1184-1188.
34. Fuller, C. S. *Chem. Rev.* **1940**, 26, (2), 143-167.
35. Whipple, E. B.; Green, P. J. *Macromolecules* **1973**, 6, (1), 38-42.

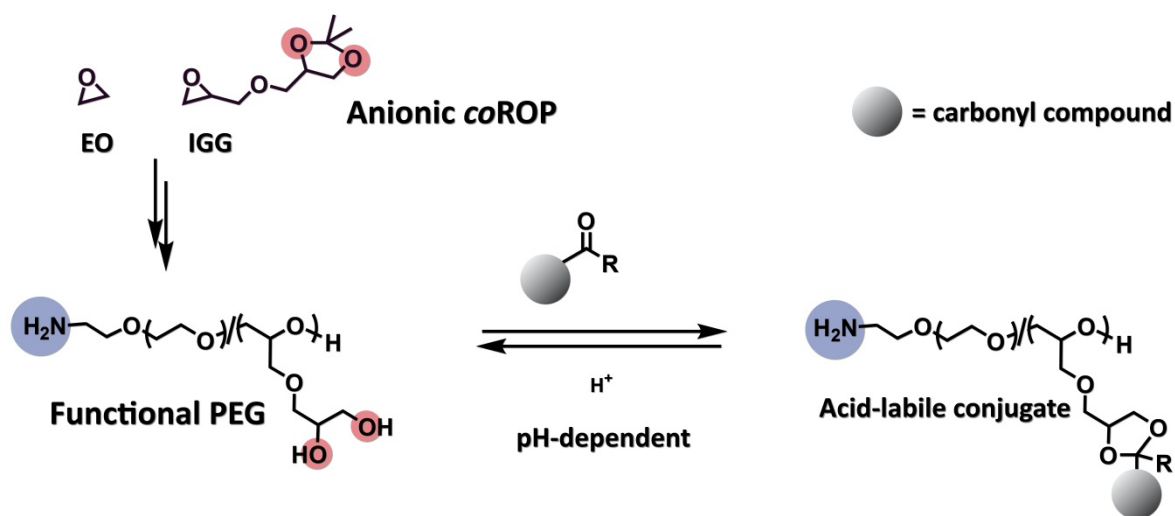
Chapter 2.2:

“Functional Poly(ethylene glycol)”: PEG-based Random Copolymers with 1,2-Diol Side Chains and Terminal Amino Functionality

“Functional Poly(ethylene glycol)”: PEG-based Random Copolymers with 1,2-Diol Side Chains and Terminal Amino Functionality

Christine Mangold, Frederik Wurm, Boris Obermeier, Holger Frey

Published in *Macromolecules* **2010**, 43, (20), 8511-8518.



Keywords: anionic polymerization, poly(ethylene oxide), PEG, polyether, random copolymer

Abstract

A series of poly(ethylene glycol-*co*-isopropylidene glyceryl glycidyl ether) (P(EO-*co*-IGG)) random copolymers with different fractions of 1,2-isopropylidene glyceryl glycidyl ether (IGG) units was synthesized. After acidic hydrolysis a new type of “functional PEGs”, namely poly(ethylene glycol-*co*-glyceryl glycerol) (P(EO-*co*-GG)) was obtained. Using an initiator that releases a terminal amino moiety after deprotection, functional end groups with orthogonal reactivity to the in-chain groups were obtained. All polymers showed narrow molecular weight distributions (1.07-1.19), and control of the molecular weights was achieved in the range of 5 000 to 30 000 g/mol. Random incorporation of both comonomers was verified by monitoring the copolymerization kinetics via real-time ¹H NMR spectroscopy during the polymerization and by characterization of the triad sequence distribution, relying on ¹³C NMR analysis. Using the 1,2 diol-component of the side chains allows for attachment and facile acid-catalyzed release of molecules bearing ketone/aldehyde functionalities. This renders the materials potentially useful as support for reagents, drugs or catalysts. This was demonstrated using benzaldehyde as a model compound. DSC was carried out on all samples, showing amorphous structures upon incorporation of IGG fractions exceeding 15%.

Introduction

Poly(ethylene oxide) (PEO) is undoubtedly the most important polymer for biomedical applications today. This is based on two major key features: on the one hand PEO shows excellent solubility in aqueous media, and second PEO is biocompatible, possessing low immunogenicity and antigenicity.¹ Therefore PEO, or poly(ethylene glycol) (PEG), which mostly refers to PEO with a molecular weight below 20 000 g/mol and its anionic or cationic derivatives are used in numerous cosmetic² and also pharmaceutical products. Furthermore, molecular hybrids of PEG and peptide or protein drugs play an important role to enhance circulation times. The covalent linkage of monofunctional PEG (mPEG) to a variety of different biomolecules is known as PEGylation and represents a well-established method today,^{3, 4} which is already standard practice for different medications. The introduction of functional groups other than hydroxyl to obtain mono- or difunctional PEG derivatives can either be realized by a suitable initiator system or via appropriate terminating agents in the anionic ring-opening polymerization of ethylene oxide (EO). A detailed overview has been given by Riffle et al.⁵ A newly developed initiator, which allows the introduction of a terminal amino moiety by catalytic hydrogenation subsequent to the polymerization was recently introduced by our group.⁶ The preparation of well-defined PEGs with more than two functional groups that are randomly distributed at the polyether backbone requires a comonomer bearing a protecting group, which must be stable under the strongly basic reaction conditions of the oxyanionic polymerization and can be removed quantitatively in postpolymerization reactions. Suitable comonomers are glycidyl ethers, which release one hydroxyl function per monomer unit upon acidic hydrolysis or catalytic hydrogenolysis. At present the most prominent glycidyl ether is ethoxy ethyl glycidyl ether (EEGE), which was first mentioned by Fitton et al.⁷ and has been employed by several groups⁸⁻¹⁰ to obtain block^{11, 12} and recently also random copolymers with EO.¹³⁻¹⁵ Möller et al. have reported an elegant synthesis of copolymers using various glycidyl ethers for the orthogonal deprotection of the hydroxyl functionality.¹⁶ For the introduction of other functional groups two different methods are possible: The first option is the derivatization of hydroxyl-functionalized polymers in subsequent polymer modification reactions.¹³ In this case the degree of functionalization strongly depends on the yields and selectivity of the respective modification reactions, often leading to inhomogeneous product mixtures. An alternative approach to functional PEG-copolymers relies on the copolymerization of protected epoxide comonomers. In this context, we recently reported the use of the protected amino analogue of glycidol to introduce multiple amino groups via random copolymerization.¹⁷ While polymerization of the above-mentioned “classical” glycidyl ethers results in linear poly(glycerol)s (*linPG*) after deprotection, the use of 1,2-isopropylidene glyceryl glycidyl ether (IGG),¹⁸ a monomer that was recently developed in our group, permits the introduction of glycerol side chains with two adjacent hydroxyl functions for each IGG unit incorporated after acidic hydrolysis of

the acetal protective groups. To date, the IGG monomer has only been employed in the synthesis of block copolymers or served as precursor for the synthesis of linear-hyperbranched PEG-*b*-*hb*poly(glycerol) (PG) copolymers.¹⁹ However, the presence of two vicinal hydroxyl groups also opens a general pathway for attachment to the chain and facile, acid catalyzed release of any molecule with a ketone or aldehyde functionality via formation of the cyclic acetal or ketal, respectively. This leads to various interesting applications, such as transport and controlled release of drugs or other biomolecules and furthermore the use of these novel polymers as polymeric support for organic synthesis.

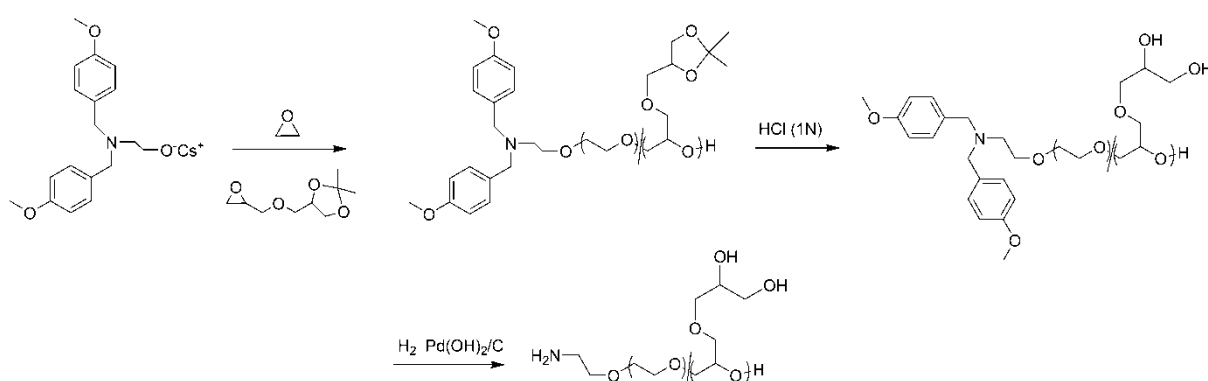


Figure 1. Reaction sequence for the synthesis of the random P(EO-co-IGG)-copolymers bearing one single terminal amino- and multiple 1,2-diol side groups.

In the current work we have studied the random copolymerization of the recently introduced, protected comonomer IGG with ethylene oxide by anionic ring opening copolymerization. Subsequent acidic hydrolysis results in PEG-copolymers with 1,2-diol side chains (Fig. 1). Detailed characterization focusing on polymerization kinetics, polymer microstructure and thermal properties is presented. With this work we aim at the following issues: (i) Can both comonomers be copolymerized in a random manner, despite the steric bulk of the IGG comonomer and the high reactivity of EO? (ii) How does copolymerization influence the materials properties of the “functional PEGs” in comparison to PEG? (iii) Can the resulting copolymers be employed for the reversible attachment and acid-catalyzed liberation of a model drug?

Experimental Section

Instrumentation

^1H NMR spectra (300 MHz and 400 MHz) and ^{13}C NMR spectra (75.5 MHz) were recorded using a Bruker AC300 or a Bruker AMX400. All spectra were referenced internally to residual proton signals of the deuterated solvent. For SEC measurements in DMF (containing 0.25 g/L of lithium bromide as an additive) an Agilent 1100 Series was used as an integrated instrument, including a PSS HEMA column ($10^6/10^5/10^4$ g/mol), a UV (275 nm) and a RI detector. Calibration was carried out using poly(ethylene oxide) standards provided by Polymer Standards Service. DSC measurements were performed using a Perkin-Elmer 7 series thermal analysis system and a Perkin Elmer Thermal Analysis Controller TAC 7/DX in the temperature range from -100 to 80 °C at heating rates of 10 K·min $^{-1}$ under nitrogen. Matrix-assisted laser desorption and ionization time-of-flight (MALDI-ToF) measurements were performed on a Shimadzu Axima CFR MALDI-TOF mass spectrometer using potassium trifluoro- acetic acid as a cationizing agent and dithranol (1,8,9-trishydroxy-anthracene) as a matrix.

Reagents

All solvents and reagents were purchased from Acros Organics and used as received, unless otherwise stated. Chloroform- d_1 and DMSO- d_6 were purchased from Deutero GmbH. 1,2-isopropylidene glyceryl glycidyl ether was prepared according to a recently published procedure, dried over CaH_2 , and freshly distilled before use.

***p*-Methoxybenzyl bromide:** 25 g of *p*-methoxy-benzyl alcohol (0.21 mol) and 400 mL of dry diethyl ether were placed in 1-L three-neck round bottom flask and 29 g of phosphorus tribromide (0.11 mol) were added via dropping funnel for 2 h. The reaction mixture was then allowed to stir at room temperature for additional 12 h. 300 g of ice were added to hydrolyse the excess of phosphorus tribromide. The organic and aqueous phases were separated and the aqueous phase was extracted with 2x 200 mL of diethyl ether. The combined organic extracts were washed with 300 mL H_2O and 300 mL of a saturated NaHCO_3 solution, dried with MgSO_4 and concentrated *in vacuo*. A slightly yellow viscous liquid was obtained, which was then distilled at 13 mbar. bp.: 113 °C, yield: 35.5 g (83%) ^1H NMR (300 MHz, CDCl_3): δ (ppm)= 7.33 (d, 2 H, aromatic), 6.88 (d, 2 H, aromatic), 4.51 (s, 2 H, BrCH_2Ph), 3.80 (s, 3 H, OCH_3).

***N,N*-di(*para*-methoxy-benzyl)aminoethanol:** 15 g of the freshly distilled *p*-methoxybenzyl bromide (75 mmol) 2.3 g aminoethanol (37 mmol), 13.8 K_2CO_3 (100 mmol) and 100 mL DMF were refluxed for 24 h. After cooling the reaction mixture to room temperature, the solution was filtrated and 300 mL of diethyl ether were added. The organic phase was then washed with water, a saturated NaHCO_3 solution and dried with MgSO_4 . The organic phase was dried *in vacuo* and a highly viscous liquid was

obtained. The crude mixture was purified by column chromatography using acetic acid ethyl ester and petrol ether as solvents. Yield: 9 g (80% th.) ^1H NMR (300 MHz, CDCl_3): $\delta(\text{ppm})= 7.33$ (d, 4 H, aromatic), 6.88 (d, 4 H, aromatic), 3.80 (s, 6H, OCH_3), 3.60 (s, 4 H, NCH_2Ph), 3.57 (t, 2 H, CH_2OH), 2.65 (t, 2 H, NCH_2).

General Procedure for the Copolymerization of EO and IGG: *N,N*-di(*p*-methoxy-benzyl)-2-aminoethanol was dissolved in benzene in a 250 mL-Schlenk flask and 0.9 equivalents of cesium hydroxide were added. The mixture was stirred at 60 °C under argon for 1 h and evacuated at 90 °C (10^{-2} mbar) for 2 h to remove benzene and water, forming the corresponding cesium alkoxide. Approximately 1 mL dry THF was then cryo-transferred into the Schlenk flask to dissolve the initiator-salt. EO was first cryo-transferred to a graduated ampoule, and then cryo-transferred into the flask containing the initiator in THF (at around -80 °C). Subsequently the second comonomer (IGG) was added via syringe and the mixture was heated to 60 °C and stirred for 18-24 h. Precipitation in cold diethyl ether resulted in the pure copolymers. For polymers with a high fraction of IGG, the polymer solution was dried *in vacuo*. Yields: 95% to quantitative. ^1H NMR (300 MHz, $\text{DMSO}-d_6$): $\delta(\text{ppm})= 7.24$, 6.87 (d, $\text{C}_6\text{H}_4\text{OMe}$), 4.16 (m, acetal-*H*), 3.98 (t, *CHH*-acetal), 3.74 (s, $\text{C}_6\text{H}_4\text{OMe}$), 3.68-3.34 (polyether backbone), 1.3 (d, CH_3 acetal).

***N,N*-Di(*p*-methoxy-benzyl)-poly(ethylene oxide-co-glyceryl glycerol):** The acetal protecting groups were removed by the addition of 1N hydrochloric acid to a 20% solution of the polymer in MeOH/THF 1:1 and about 500 mg of ion exchange resin (Dowex 50WX8). The reaction mixture was stirred at room temperature for 12 h, filtrated (to remove the resin) and concentrated *in vacuo*. Yields: 80-90%. ^1H NMR (300 MHz, $\text{DMSO}-d_6$): $\delta(\text{ppm})= 7.53$, 7.00 (d, $\text{C}_6\text{H}_4\text{OMe}$), 4.01-3.80 (br, OH), 3.74 (s, $\text{C}_6\text{H}_4\text{OMe}$), 3.67-3.09 (polyether backbone).

H_2N -poly(ethylene oxide-co-glyceryl glycerol) or H_2N -poly(ethylene oxide-co-isopropylidene glyceryl glycidyl ether): 1 g sample of copolymer was dissolved in 50 mL methanol (or a methanol/THF-mixture in the case of the IGG-species) and palladium on activated charcoal (10%) was added. The reaction vessel was flushed with hydrogen (8 bar) and the reaction was allowed to stir for 72 h at room temperature. The solution was filtered, concentrated, and precipitated into cold diethyl ether. Yields: quantitative. H_2N -poly(ethylene oxide-co-glyceryl glycerol): ^1H NMR (300 MHz, $\text{DMSO}-d_6$): $\delta(\text{ppm})= 4.54$ (m, OH, position varies dependent on concentration/ temperature etc.), 3.81-3.15 (m, polyether backbone). H_2N -poly(ethylene oxide-co-isopropylidene glyceryl glycidyl ether): ^1H NMR (300 MHz, $\text{DMSO}-d_6$): $\delta(\text{ppm})= 4.16$ (m, acetal-*H*), 3.98 (t, *CHH*-acetal), 3.74 (s, $\text{C}_6\text{H}_4\text{OMe}$), 3.68-3.34 (polyether backbone) 1.3 (d, CH_3 acetal).

***N,N*-Di(*p*-methoxy-benzyl)-poly(ethylene oxide-co-2-phenyl 1,3-dioxolan glycidyl ether):** 1 g of P(EO-co-GG) as well as a tenfold excess (per GG-unit) of benzaldehyde dimethyl acetal was placed in a round bottom flask. A catalytic amount of *p*-toluenesulfonic acid was added and the mixture was

put into an ultrasonic bath at room temperature and under argon atmosphere for 3 h until a homogeneous mixture was obtained. Piperidine was added and all volatile compounds were removed under reduced pressure. The crude product mixture was then dialyzed in THF using benzoylated tubing with a molecular weight cut off (MWCO) of 1000 g/mol. After 72 h THF was removed *in vacuo* and the pure copolymer was obtained. Yield: 80%. ^1H NMR (300 MHz, $\text{DMSO-}d_6$): $\delta(\text{ppm}) = 7.52\text{--}7.33$ (m, arom. side-chain), 7.22, 6.84 (d, $\text{C}_6\text{H}_4\text{OMe}$), 5.74 (d, acetal-H), 4.25–3.25 (m, polyether backbone).

^1H NMR kinetics¹⁷: In a conventional NMR tube a mixture of IGG and EO in $\text{DMSO-}d_6$ was placed under an argon atmosphere, cooled to -196°C and evacuated. The initiator solution was added rapidly to guarantee that the first layer stayed frozen and no reaction took place. Then the tube was evacuated again while freezing the initiator-solution. The NMR-tube was flame-sealed by applying high vacuum. It is of crucial importance to keep both solution-layers frozen until the NMR measurements are started. Immediately after melting and mixing of the two solutions, the first spectrum was recorded. Intervals between two measurements were 5 s within the first minute and extended afterward. A sample of the pure monomer mixture was measured in advance to reduce the necessary time for locking and shimming.

Results and Discussion

Synthesis

To copolymerize two monomers such as EO and IGG with highly diverging boiling points a procedure has to be chosen that levels these differences to a minimum. All reactions were therefore carried out at 60°C *in vacuo*, as reported recently for another EO copolymerization.¹⁹ There appears to be a general bias that the reactivity of ethylene oxide is generally considerably higher than for all other epoxide monomers, such as glycidyl ethers. It is an important objective of this work to clarify this issue by probing the possibility of random copolymerization in this system that combines EO with a bulky epoxide as a comonomer.

As a novel initiator *N,N*-di(*p*-methoxybenzyl)-aminoethanol has been prepared. This initiator has been improved in comparison to the previously mentioned *N,N*-Di-benzyl-aminoethanol by introducing methoxy groups in the para-position of the aromatic system, permitting more facile cleavage, which is due to the inductive effect of the methoxy groups. *N,N*-Di(*p*-methoxybenzyl)-aminoethanol was deprotonated with 0.9 equiv. of cesium hydroxide monohydrate, and the polymerization was carried out in a highly concentrated solution of the two monomers and THF. In the NMR online experiments, which were carried out not only to verify the kinetics of the reaction but also the reactivity of the two comonomers, $\text{DMSO-}d_6$ was used as a solvent. This is mainly due to experimental and security reasons with regard to the higher boiling point of DMSO in comparison to

THF. Depending on the IGG-content of the samples, the copolymers obtained possessed different appearance, ranging from amorphous solids (9% IGG) to highly viscous liquids (53% IGG), in pronounced contrast to PEG, which is a crystalline powder at room temperature. Detailed characterization of the thermal properties is given in a following section subsequent to the structural characterization of the materials.

Completion of the polymerization was monitored via ^1H NMR spectroscopy, relying on the absence of the oxirane signals corresponding to the two monomers after about 24 h stirring at 60 °C. The copolymer composition was also studied by ^1H NMR spectroscopy (Figure 2). Agreement of the IGG fraction incorporated in the random copolymers with the composition of the monomer feed is confirmed by ^1H NMR spectra from the comparison of the polyether backbone-signals with the acetal protons at 4.16 ppm and the methyl signals centered around 1.3 ppm. In addition, from ^1H NMR spectroscopy the number average molecular weight was calculated by integration of the aromatic resonances of the initiator (6.87 ppm), the polyether backbone (3.5 ppm) and the signals referring to IGG-units (1.2 ppm). It should be noted at this point that due to the high molecular weights obtained the error of this method is on the order of 5-10%. Size exclusion chromatography (SEC) was carried out for all copolymer samples, demonstrating narrow molecular weight distributions ($M_w/M_n = 1.08-1.19$). As can be seen from Table 1 the molecular weights obtained from the SEC-measurements using PEG-standards deviate from the values calculated from the ^1H NMR measurements. The deviation is approximately half of the value for the 10% IGG-content samples and becomes gradually more pronounced with increasing amount of IGG incorporated. This is due to the peculiar nature of the molecular weight increase, since the additional groups are located in the side chains, most probably resulting in a stagnating hydrodynamic radius.

Removal of the cyclic protecting group and release of the two adjacent hydroxyl-functionalities in the polymer-backbone was readily achieved under moderately acidic conditions and stirring for 12 h at room temperature. Removal of the protecting groups can be followed by NMR via disappearance of the peaks due to the isopropylidene groups, for instance the acetal proton at 4.16 ppm (^1H NMR, Figure 2) or the corresponding carbon atom and its signal at 99 ppm (^{13}C NMR). After release of the hydroxyl functions, the apparent molecular weights obtained from SEC increase for all P(EG-co-GG) samples, while a decrease would be expected due to the loss of the acetal group. Interestingly, this increase is directly correlated to the IGG-content and therefore to the number of hydroxyl functions formed. This can most likely be attributed to the emerging diol-functions that interact with the SEC columns, thus leading to an apparent increase in the hydrodynamic radii, (compare with Figure 7). The polydispersities remained low after deprotection and were in the range of $M_w/M_n = 1.09-1.19$.

Table 1. Overview of the characterization data for all copolymer samples prepared.

No	composition (th.)	sum (NMR) ^a	IGG/GG-fraction ^a	M_n (NMR)	M_n (SEC) ^b	PDI (SEC) ^b
1	MeOBn ₂ NP(EO ₂₀₀ -IGG ₂₀)	MeOBn ₂ NP(EO ₂₆₅ -IGG ₂₆)	9%	16 500	7 600	1.11
2	MeOBn ₂ NP(EO ₁₆₀ -IGG ₄₀)	MeOBn ₂ NP(EO ₁₈₀ -IGG ₃₂)	14%	14 000	7 000	1.15
3	MeOBn ₂ NP(EO ₄₅ -IGG ₁₅)	MeOBn ₂ NP(EO ₄₇ -IGG ₁₇)	26%	5 300	3 000	1.08
4	MeOBn ₂ NP(EO ₁₀₀ -IGG ₅₀)	MeOBn ₂ NP(EO ₉₀ -IGG ₄₀)	30%	11 800	4 700	1.11
5	MeOBn ₂ NP(EO ₁₀₀ -IGG ₁₀₀)	MeOBn ₂ NP(EO ₁₂₂ -IGG ₁₃₆)	53%	30 000	4 500	1.13
1d	MeOBn ₂ NP(EO ₂₆₅ -GG ₂₆)	MeOBn ₂ NP(EO ₂₆₅ -GG ₂₆)	9%	15 700	8 000	1.15
2d	MeOBn ₂ NP(EO ₁₈₀ -GG ₃₂)	MeOBn ₂ NP(EO ₁₈₀ -GG ₃₂)	14%	12 800	8 700	1.17
3d	MeOBn ₂ NP(EO ₄₇ -GG ₁₇)	MeOBn ₂ NP(EO ₄₇ -GG ₁₇)	26%	4 800	3 700	1.08
4d	MeOBn ₂ NP(EO ₉₀ -GG ₄₀)	MeOBn ₂ NP(EO ₉₀ -GG ₄₀)	30%	10 000	5 800	1.17
5d	MeOBn ₂ NP(EO ₁₀₀ -GG ₁₀₀)	MeOBn ₂ NP(EO ₁₀₀ -GG ₁₀₀)	53%	25 200	5 700	1.18
1dt	H ₂ NP(EO ₂₆₅ -GG ₂₆)	H ₂ NP(EO ₂₆₅ -GG ₂₆)	9%	15 400	8 000	1.15
3dt	H ₂ NP(EO ₄₇ -GG ₁₇)	H ₂ NP(EO ₄₇ -GG ₁₇)	26%	4 500	3 900	1.14
4dt	H ₂ NP(EO ₉₀ -GG ₄₀)	H ₂ NP(EO ₉₀ -GG ₄₀)	30%	9 700	5 600	1.30
1t	H ₂ NP(EO ₂₆₅ -IGG ₂₆)	H ₂ NP(EO ₂₆₅ -IGG ₂₆)	9%	16 200	8 000	1.15
3t	H ₂ NP(EO ₄₅ -IGG ₁₅)	H ₂ NP(EO ₄₇ -IGG ₁₇)	26%	5 000	3 000	1.11
5t	H ₂ NP(EO ₁₂₂ -IGG ₁₃₆)	H ₂ NP(EO ₁₂₂ -IGG ₁₃₆)	53%	27 700	4 400	1.13

^a determined from ¹H NMR (300 MHz, DMSO-*d*₆); ^b M_w determined by SEC-RI in DMF.

Similar to the deprotection of the acetals, the liberation of the terminal amino-moiety by catalytic hydrogenation can be followed via ¹H NMR, monitoring the disappearance of the aromatic signals at 6.86 and 7.24 ppm. The reaction conditions applied for the hydrogenolysis guarantee removal of the benzylic protecting groups at the amine without removal of the isopropylidene protecting groups. Figure 2 shows the respective ¹H NMR spectra of the four different types of functional polyethers that can be synthesized after orthogonal reactions. Depending on the order of the deprotection reactions that can be chosen freely due to their orthogonal character, it is on the one hand possible to obtain P(EO-*co*-GG)-copolymers with glyceryl side chains, where the terminal amine still carries the benzyl protective groups, but on the other hand also P(EO-*co*-IGG)-copolymers with a cleaved amine in terminal position and isopropylidene-protected glyceryl units along the backbone are accessible. Both polymer types can finally be converted into the fully (terminal and in-chain) deprotected polymers (Figure 2).

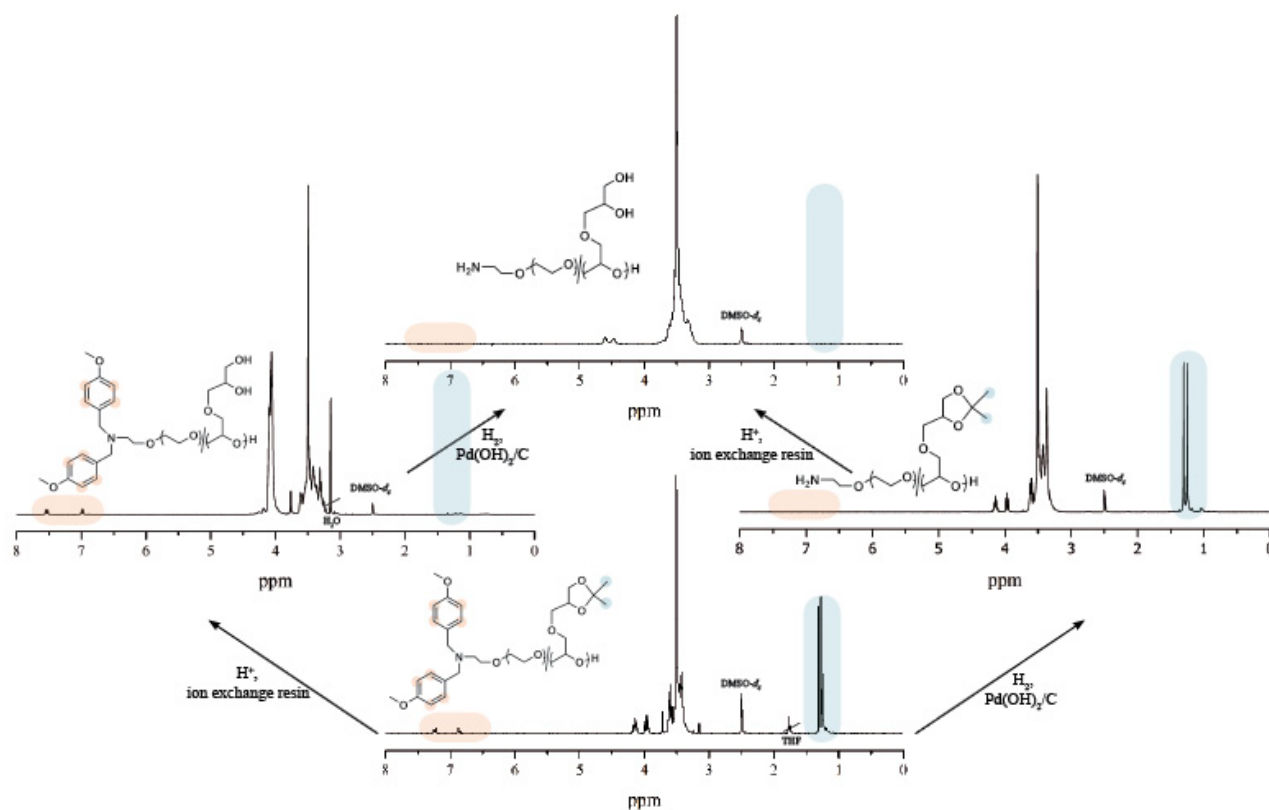


Figure 2. ^1H NMR spectra of the copolymers synthesized; the deprotection steps can be interchanged.

The different possible copolymer structures have also been investigated by MALDI-ToF mass spectrometry. The recorded spectra obtained are quite complex with rather low resolution, but they clearly show the expected pattern for a copolymer with a variety of different possible comonomer combinations. The change in molecular weight after acidic hydrolysis or hydrogenation can also be followed by MALDI-ToF. The corresponding spectra are given in the Supporting Information.

^1H NMR Copolymerization Kinetics

To investigate the copolymerization behavior of EO and IGG we used an experimental procedure that has recently been developed in our group.¹⁹ First a comonomer solution was transferred into a NMR-tube, evacuated, cooled with liquid nitrogen, and the initiator solution was added thereafter. The cold NMR-tubes were evacuated, flame-sealed, and the polymerization was carried out *in vacuo*. Because of experimental reasons the online-kinetic studies were carried out in $\text{DMSO-}d_6$ instead of THF, which usually serves as the solvent in the large-scale polymerizations. To examine the copolymerization kinetics three different temperatures, i.e., 25 °C, 50 °C and 70 °C were applied. The molecular weight distributions of all samples obtained in these online NMR experiments were narrow with PDIs around 1.06. Incorporation of the two comonomers and the growth of the

polyether chain was studied by following the decrease of the epoxide signals located at 2.61 ppm for the four protons of the symmetric EO monomer and at 3.09 ppm for the methine proton of IGG, respectively. All signals are referenced to the aromatic peaks corresponding to the initiator at 6.87 ppm, which were set to 4 and should obviously remain constant in the course of the reaction. The emerging backbone signal at 3.54 ppm overlaps with different signals of the IGG-monomer, which complicates the calculation of the molecular weight. This is unfortunate, since M_n determined in this independent manner could otherwise serve as an affirmation for the molecular weight calculated from the monomer decrease. Plotting the monomer conversion versus molecular weight resulted in a linear graph (see Supporting Information), confirming the living character of the polymerization, as it is expected for the anionic ROP. Figure 3 displays a zoom-in (4.5-2 ppm) of different ^1H NMR-spectra, showing the decreasing signal intensity of the monomer signals and the growing backbone signal. As expected, the rate of the polymerization is significantly influenced by the reaction temperature. While the copolymerization at 50 °C takes approximately 3.5 hours to completion (5 h for the sample with higher molecular weight), approximately one week is required for the polymerization at 25 °C.

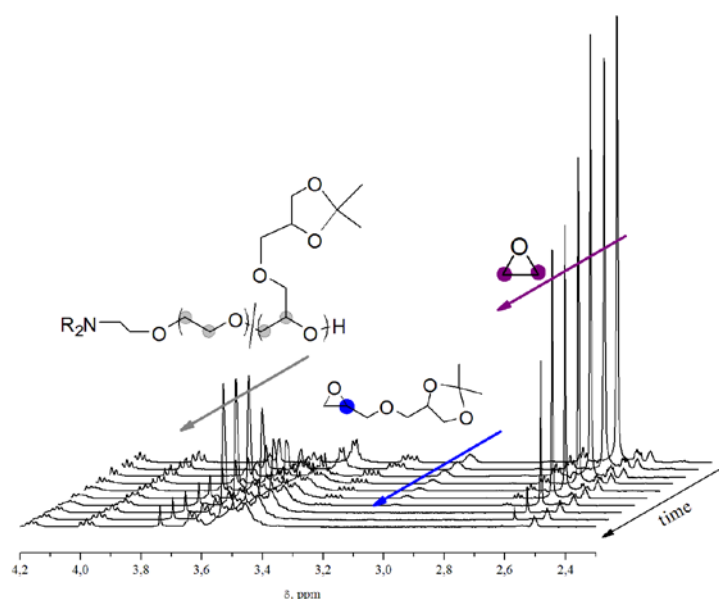


Figure 3. ^1H NMR spectra for the copolymerization of IGG and EO at 50 °C in $\text{DMSO-}d_6$ recorded after 0, 0.1, 2, 13, 21, 26, 87, 115, 190 and 264 minutes, respectively.

At 70 °C the reaction is completed already after one hour, and even the initial spectra taken after a few seconds already reveal signals of the polymer backbone. Figure 4 shows the conversion versus time plot for EO and IGG at different temperatures, as derived from the NMR measurements. The most relevant information clearly derived from the NMR-spectra is that there appears to be little difference in the reactivity of the two monomers, despite the sterically demanding structure of IGG

in comparison to EO. The conversion of both comonomers is virtually identical at all stages of the reaction (Figures 4 and 5). Unexpectedly, in the case of the two low temperature-samples (25 °C and 50 °C) the decrease of the IGG-signal appears to be even faster at the beginning of the reaction than the decrease of the EO-resonances. Figure 5 shows exemplarily the conversion of both comonomers plotted against the overall monomer-consumption for one sample at 50 °C.

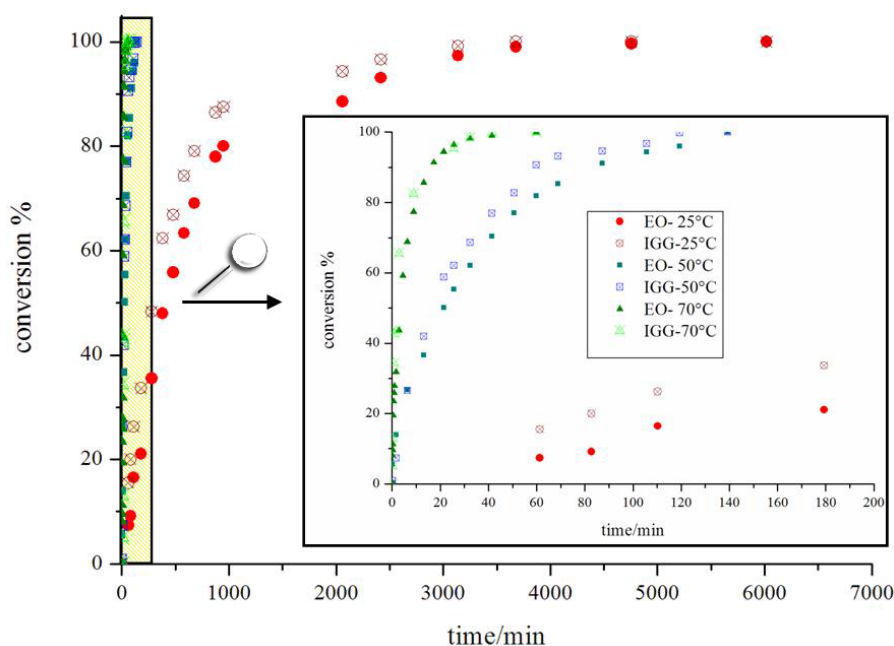


Figure 4. Monomer conversion versus time monitored by ^1H NMR in $\text{DMSO-}d_6$ resulting in polymers with the following final composition: 70 °C (green triangles) $\text{MeOBn}_2\text{NP}(\text{EO}_{61}\text{-IGG}_7)$ (7*), 50 °C (blue squares) $\text{MeOBn}_2\text{NP}(\text{EO}_{31}\text{-IGG}_9)$, 25 °C (red, circles) $\text{MeOBn}_2\text{NP}(\text{EO}_{29}\text{-IGG}_9)$.

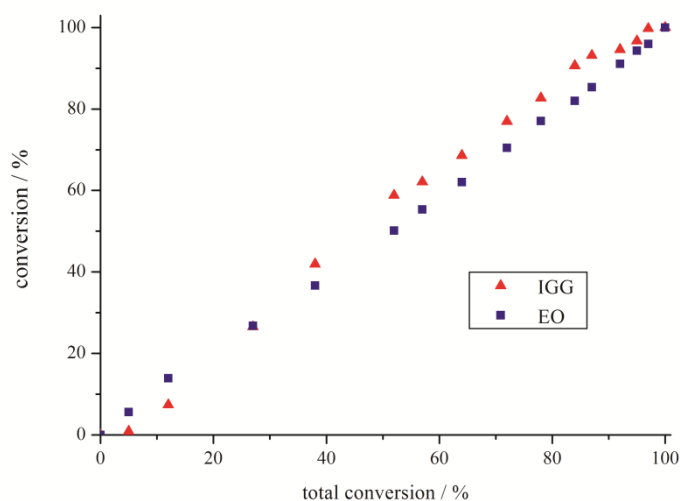


Figure 5. Monomer incorporation (percentage) versus the overall conversion at 50 °C. Final copolymer composition: MeOBn₂P(EO₃₁-IGG₉).

While the decrease of EO is directly related to the total conversion, small fluctuations (to higher but also lower values) are observed for the IGG content. At this point it should be noted that EO is the predominant component in the copolymer studied and that the EO-conversion contributes to a stronger extent to the overall conversion than the conversion of IGG. Therefore little variation of the EO-incorporation is observed. In addition, four proton signals of the two methylene groups of ethylene oxide are used to calculate the decrease of EO in the course of the polymerization, but only one methine signal is used as a reference for the determination of the IGG-conversion. Obviously a larger error is expected in the latter case. Taking the abovementioned considerations into account, it can be concluded that in all cases a linear EO/IGG-conversion is observed, that is the comonomers are incorporated equally, and a random distribution is obtained in the polymer backbone. This unexpected behavior is valid independent of the EO/IGG-ratio and for all temperatures studied.

¹³C NMR Characterization

Random distribution of the comonomer units within the PEG backbone is of crucial importance with respect to potential applications of the functional PEG copolymers. ¹³C NMR analysis permits to investigate the monomer triad sequence distribution, revealing details concerning the incorporation statistics of IGG units. Besides the well-established signal assignment for random copolymers based on propylene oxide and ethylene oxide,²⁰ only few other oxirane monomer combinations have been investigated to date. However, EO has often been assumed to possess considerably higher reactivity than other epoxide monomers, such as glycidyl ethers. To confirm random incorporation, the deprotected copolymer samples were investigated, since fewer side group resonances overlap with the triad signals in question than in the respective acetal-protected copolymers. Figure 6 shows a section of the ¹³C NMR spectra of samples **1**, **2** and **5** with increasing comonomer fraction from spectrum a (front) to c. To keep abbreviations short for the triad sequences, the EO unit is referred to as **E** and the GG (former IGG)-units are indicated as **I**. Two of the side group signals (1 and 2 in Figure 7) resulting from the glycerol unit are located at 63.2 and 72.9 ppm, the other two (4 and 5) overlap with the triad sequence signals of either the two methylene carbon atoms of EO or the one of the GG-unit. Several microstructure-related resonances in the range of 71.1 to 68.7 ppm occur, of which one signal at 69.9 ppm can clearly be assigned to the EEE triad. This signal decreases with increasing GG content, while other triad signals become more pronounced. In addition the signal at 68.9 ppm, which can clearly be assigned to the methylene carbon in proximity of a GG unit (for example IEE) does not only increase, but is split up into several signals with increasing amount of GG units

incorporated (increasing abundance of IEI, IIE and III triads). The same observations are made for the methine carbon of the GG units. The sample with the lowest GG-content shows only one single peak that is assigned to the EIE-triad. This resonance also splits up with increasing GG-content, and the sample with 53% comonomer content shows three signals of different intensities, which is most probably explained by the occurrence of the III, EII and IIE as well as the EIE triads. The two possible end group signals of the primary or secondary carbons linked to the terminal hydroxyl groups cannot be discerned in the spectra due to the low concentration and high molecular weight of the samples.

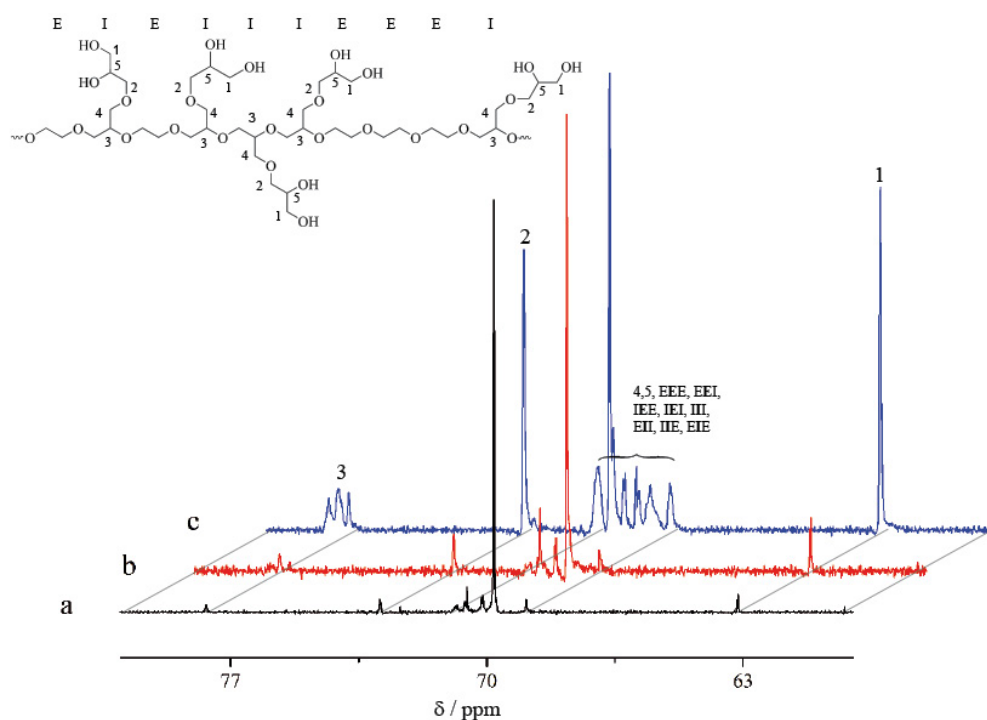


Figure 6. ^{13}C NMR spectra of different P(EO-co-GG) copolymers with different GG fraction of a) 9%, b) 14%, c) 53%.

Although unequivocal assignment of all triad signals was not possible, the spectra permit to exclude the formation of longer runs of one comonomer. All observations confirm random incorporation of the IGG/GG-comonomer units in the PEG-backbone and are in line with the observations from the kinetic studies (vide supra).

Thermal behavior

The thermal properties of the P(EG-co-GG) copolymers are of central interest for future applications in the biomedical field as well as for use as polymer supports for organic synthesis. The thermal characteristics summarized in Table 2 have been studied using differential scanning calorimetry (DSC). The glass transition temperature (T_g) of all samples is higher than for the PEG-homopolymer

(-64 °C²¹ for MPEG-1000). The T_g is -54 °C for sample **1** with an IGG-content of 9% and increases slightly with increasing IGG-incorporation (sample **5** with 53% IGG exhibits a T_g of -49 °C). For the samples with lower molecular weights obtained from the ¹H NMR-kinetic experiments, the T_g s were somewhat lower compared to those of higher molecular weight, but similar IGG-content, which is consistent with expectation. The deprotected analogues exhibit glass transitions that are approximately 5 to 10 °C higher than those of the respective protected polymers, which we ascribe to hydrogen bonding interaction of the 1,2-diol side chains.

Table 2. Thermal properties of poly(ethylene glycol-co-isopropylidene glyceryl glycidyl ether) and poly(ethylene glycol-co-glyceryl glycerol) random copolymers (DSC-measurements).

No.	Formula	IGG/GG fraction	T_g (°C)	T_m (°C)	ΔH (J/g)	T_{rc} (°C)	ΔH_{rc} (J/g)
1	MeOBn ₂ NP(EO ₂₆₅ -IGG ₂₆)	9%	-54	31	35	/	/
2	MeOBn ₂ NP(EO ₁₈₀ -IGG ₃₂)	14%	-51	31	13	/	/
3	MeOBn ₂ NP(EO ₄₇ -IGG ₁₇)	26%	-55	/	/	/	/
4	MeOBn ₂ NP(EO ₉₀ -IGG ₄₀)	30%	-50	/	/	/	/
5	MeOBn ₂ NP(EO ₁₂₂ -IGG ₁₃₆)	53%	-49	/	/	/	/
6*	MeOBn ₂ NP(EO ₈₅ -IGG ₈)	9%	-58	13	39	-33	34
7*	MeOBn ₂ NP(EO ₆₁ -IGG ₇)	10%	-59	14	49	-38	33
8*	MeOBn ₂ NP(EO ₃₁ -IGG ₉)	23%	-51	/	/	/	/
1d	MeOBn ₂ NP(EO ₂₆₅ -GG ₂₆)	9%	-48	44	45	-27	28
2d	MeOBn ₂ NP(EO ₁₈₀ -GG ₃₂)	14%	-42	35	18	-14	17
3d	MeOBn ₂ NP(EO ₄₇ -GG ₁₇)	26%	-38	/	/	/	/
4d	MeOBn ₂ NP(EO ₉₀ -GG ₄₀)	30%	-32	/	/	/	/
5d	MeOBn ₂ NP(EO ₁₀₀ -GG ₁₀₀)	53%	-28	/	/	/	/

^a determined from ¹H NMR (300 MHz, DMSO-*d*₆); ^b glass transition temperature in °C; ^c melting temperature T_m : in °C; ^d melting enthalpy in J/g determined by integration; ^e recrystallization temperature T_{rc} , in °C ^f recrystallization enthalpy in J/g.

Poly(ethylene oxide) is a crystalline polymer with a melting temperature of 66 °C.²² With increasing comonomer content (IGG or GG), T_m is gradually shifted to lower temperatures, until crystallization is completely inhibited, if the incorporated comonomer fraction exceeds 15-20%. For the P(EO-co-IGG)-copolymer series crystallization can be observed up to an IGG-content of as much as 14%, however, the melting temperature is significantly lowered in comparison to PEG (31 °C vs. 66 °C for the

homopolymer). The same observations are made for the deprotected samples, but in this case the melting temperatures are higher and additionally the melting enthalpies exceed those of the protected samples. Thus, a higher fraction of crystalline domains is present, which we ascribe to the lower steric hindrance of the glyceryl units in comparison to the bulky 1,2 isopropylidene glyceryl units, which appear to strongly impede ordering of the chains.

Derivatization

The use of mPEG (5 000 g/mol) as soluble polymeric support in organic synthesis is a widely established method and is also conducted on industrial scale.²³⁻²⁶ Its success as a soluble support is based on its good solubility in water and various other organic solvents, but on the other hand good precipitability in diethyl-ether and 2-propanol.²⁷ However, PEG exhibits low loading capacity, since it possesses only two end groups. It has been suggested that this drawback can be overcome by using hyperbranched poly(glycerol) (*hbPG*),²⁸ which carries multiple hydroxyl groups in either linear or terminal positions. Different reactions have been carried out using PG as support for either reagents or catalysts and utilizing either the single hydroxyl-functionalities²⁹ or the vicinal position³⁰ of the terminal OH-groups. To demonstrate the potential of the synthesized copolymers as soluble polymeric support by the reaction with ketones or aldehydes to the respective acetals, we employed the dimethoxy-acetal derivative of benzaldehyde as a model compound. Removing the evolving methanol in the course of the reaction favors the formation of the polymeric acetal without cross-linking and leads to high yields, which is evidenced by the absence of hydroxyl signals in the ¹H NMR. After dialysis of the crude product, quantitatively acetalized polymers were obtained. Table 3 summarizes the characterization data of the initial and the new polymers with 2-phenyl-1,3-dioxolane (PDG) side groups.

Table 3. Comparison of the characterization data of the initial polymer, the deprotected material and the benzyl-derivatives.

No.	Formula	M _n (NMR) ^a	M _n (SEC)	PDI	T _g (°C) ^b	T _m (°C) ^c	ΔH (J/g) ^d
1	MeOBn ₂ NP(EO ₂₆₅ -IGG ₂₆)	16 500	7 600	1.11	-54	31	35
1d	MeOBn ₂ NP(EO ₂₆₅ -GG ₂₆)	15 700	9 200	1.15	-48	44	45
1b	MeOBn ₂ NP(EO ₂₆₅ -PDG ₂₆)	18 100	7 400	1.16	-49	26	36
3	MeOBn ₂ NP(EO ₄₇ -IGG ₁₇)	5 300	3 000	1.08	-55	/	/
3d	MeOBn ₂ NP(EO ₄₇ -GG ₁₇)	4 800	4 000	1.08	-38	/	/
3b	MeOBn ₂ NP(EO ₄₇ -PDG ₁₇)	6 400	3 000	1.08	-31	/	/

^a determined from ¹H NMR (300 MHz, DMSO-*d*₆); ^b glass transition temperature; ^c melting temperature T_m; ^d melting enthalpy in J/g determined by integration of the melting peak.

The products were characterized by ^1H NMR spectroscopy. The newly emerging acetalic proton leads to signals at 5.78 and 5.69 ppm, and by integration of those and the aromatic signals of the initiator as well as the new aromatic side chains, quantitative derivatization can be confirmed. Corresponding NMR-spectra are shown in the Supporting Information. The molecular weights obtained from SEC-measurements, which should increase by about 88 g/mol per GG-unit decreases slightly, which is consistent with the previously discussed observations made for the IGG-copolymers. Figure 8 shows the shift of the molecular weight obtained from SEC-experiments and the corresponding spectra obtained by MALDI-ToF, confirming the dependence of the apparent molecular weight on the presence of the hydroxyl groups. The MALDI-ToF spectra was depicted, although the complexity of the situation does not allow for distinct assignment of all peaks, but qualitative information regarding the molecular weight can be gained. The glass transition temperature increases significantly by exchanging the isopropylidene side group with a benzylidene side-group. Melting enthalpy and melting points are slightly lower in the case of the PDG-species.

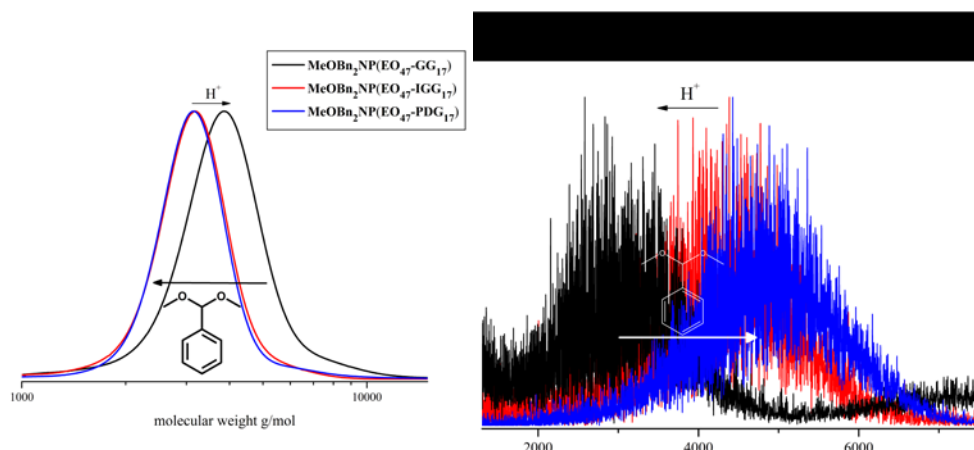


Figure 7. Molecular weight distribution of the samples 3, 3d and 3b from a) SEC-measurements in DMF and b) MALDI-ToF mass spectrometry using trifluoroacetate as a cationizing agent and dithranol (1,8,9-trishydroxy-anthracene) as a matrix.

Conclusion

A novel class of random poly(ethylene glycol)-based random copolymers with predetermined amount of glycerol side chain functionalities, low polydispersities as well as adjustable molecular weights have been synthesized and characterized in detail, focusing on macroscopic materials properties and microstructure. The copolymerization kinetics was investigated by ^1H NMR

spectroscopy using a recently developed online NMR-technique, and ^{13}C NMR measurements were employed to support random incorporation of the two comonomers. Differential scanning calorimetry was carried out on all samples confirming expectation for the thermal properties of random copolymers. Incorporation of the recently developed monomer 1,2-isopropylidene glyceryl glycidyl ether (IGG) allows to obtain one glycerol per comonomer unit upon acidic hydrolysis. Each glyceryl unit offers two vicinal hydroxyl groups, which can serve as diol-component in the reversible formation of a cyclic acetal/ketal. In contrast to *hbPG*, which is used as polymeric support, the number of vicinal hydroxyl groups is adjustable rather independent of the molecular weight of the whole polymer.

This reaction can be used, as it has been shown exemplarily with benzaldehyde, to attach and release molecules that bear aldehyde or ketone functionality. The use of a new initiator *N,N*-di(*p*-methoxybenzyl)aminoethanol leads to the facile introduction of a terminal amino group, which can be recovered by catalytic hydrogenation subsequent to the polymerization. In addition the reaction conditions applied allow to liberate the terminal amino moiety without removal of the acetal protecting groups. This means the in-chain functional groups and the terminal group are orthogonally protected and can be addressed selectively, which is interesting with respect to a variety of applications for bioconjugation, surface modification and drug transport and release.

Acknowledgement

The authors thank Dr. Mihail Mondeshki for NMR measurements and Alina Mohr for technical assistance. C.M., F.W. and B.O acknowledge the POLYMAT graduate school of excellence in the context of MAINZ for valuable financial support. B.O. also acknowledges the Fonds der Chemischen Industrie for a scholarship. F.W. thanks the Alexander-von-Humboldt foundation for a fellowship. H. F. acknowledges the SFB 625 of the DFG for valuable support.

Supporting Information

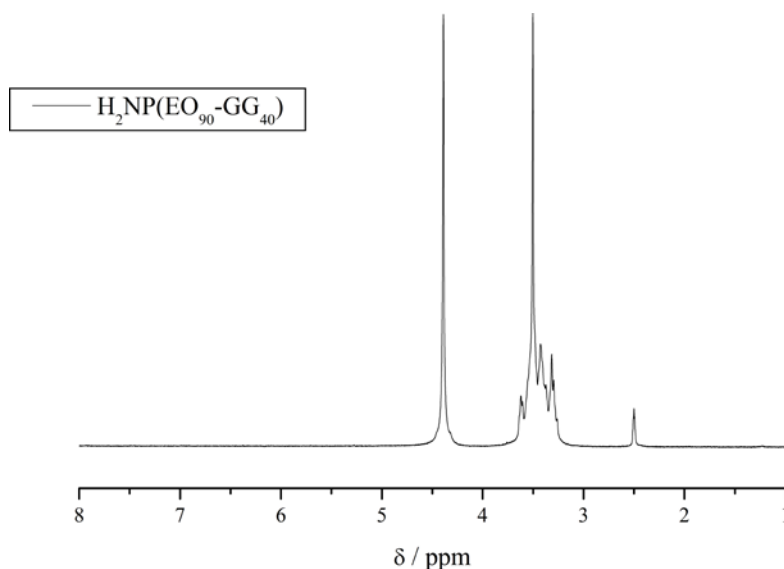
 ^1H NMR characterization

Figure S1. Typical spectrum of a terminally deprotected and in chain deprotected copolymer. Comparison with Figure 2 of the main paper reveals that size, position and shape of the *OH*-signal are dependent on various factors (solvent, fraction of GG, etc.).

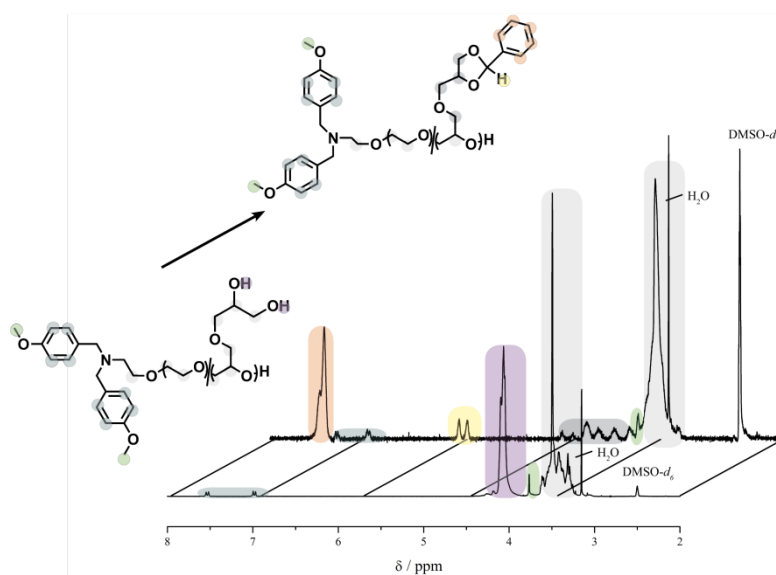


Figure S2. ^1H NMR spectra for the conversion of sample **3d** $\text{MeOBn}_2\text{NP}(\text{EO}_{47}\text{-GG}_{17})$ to sample **3b** $\text{MeOBn}_2\text{NP}(\text{EO}_{47}\text{-PDG}_{17})$.

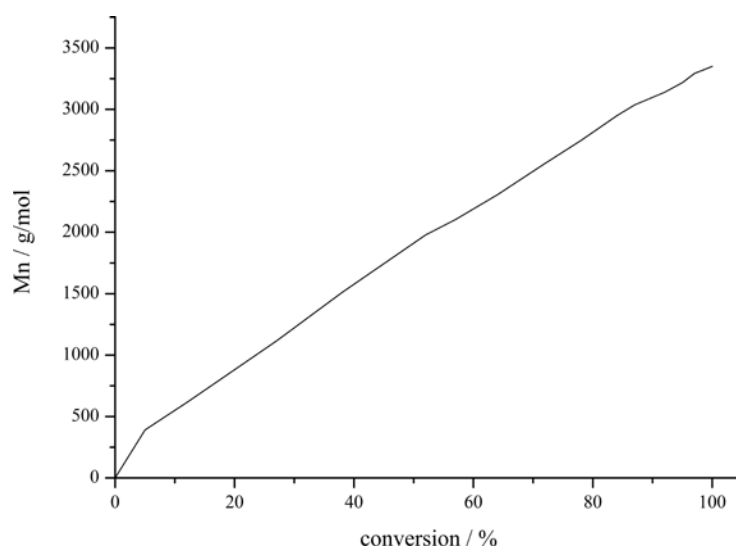
^1H NMR kinetic measurements

Figure S3. Molecular weight versus conversion, as determined by ^1H NMR kinetic measurements for the sample $\text{MeOBn}_2\text{N-P}(\text{EO}_{31}\text{-IGG}_9)$.

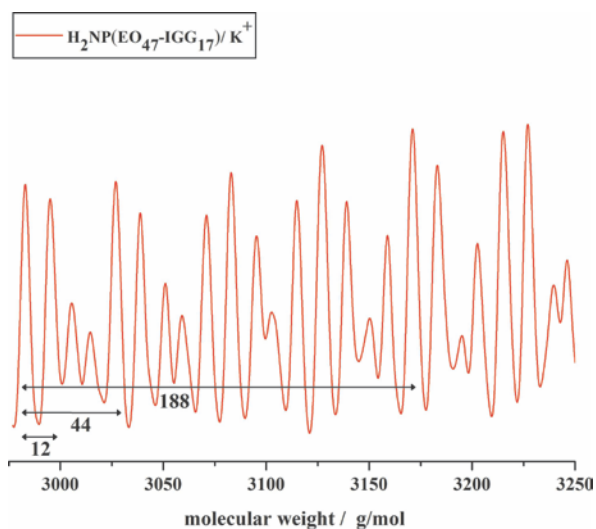
MALDI-ToF mass spectrometry

Figure S4. Zoom into the MALDI-ToF spectrum of sample 3t $\text{H}_2\text{NP}(\text{EO}_{47}\text{-IGG}_{17})$ using trifluoroacetate as a cationizing agent and dithranol as a matrix. a) $\text{EO}_{21}\text{-IGG}_{11}$, b) $\text{EO}_{34}\text{-IGG}_8$, c) $\text{EO}_{30}\text{-IGG}_9$. The smallest distance between two signals is 12 g/mol, which results from the different molecular weights of the two monomer units ($188 \text{ g/mol} - 4 \times 44 \text{ g/mol} = 12 \text{ g/mol}$). All signals in the enhanced region can be assigned to the respective comonomer compositions, which is exemplarily shown for a, b and c, but also for the polymers with a constant number of 10 IGG- but varying number of EO units.

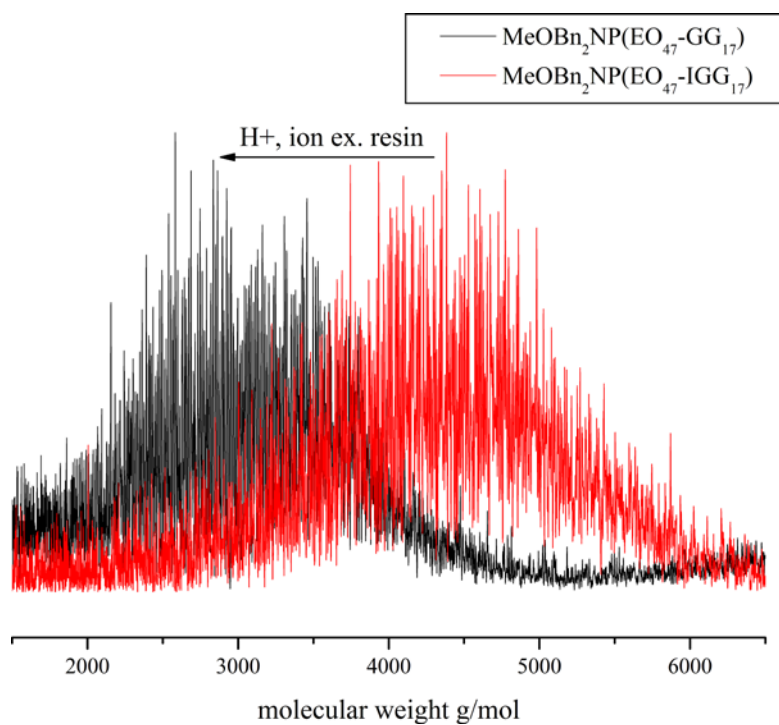


Figure S5. Shift of the molecular weight distribution obtained from MALDI-ToF upon deprotection of the acetalic side groups.

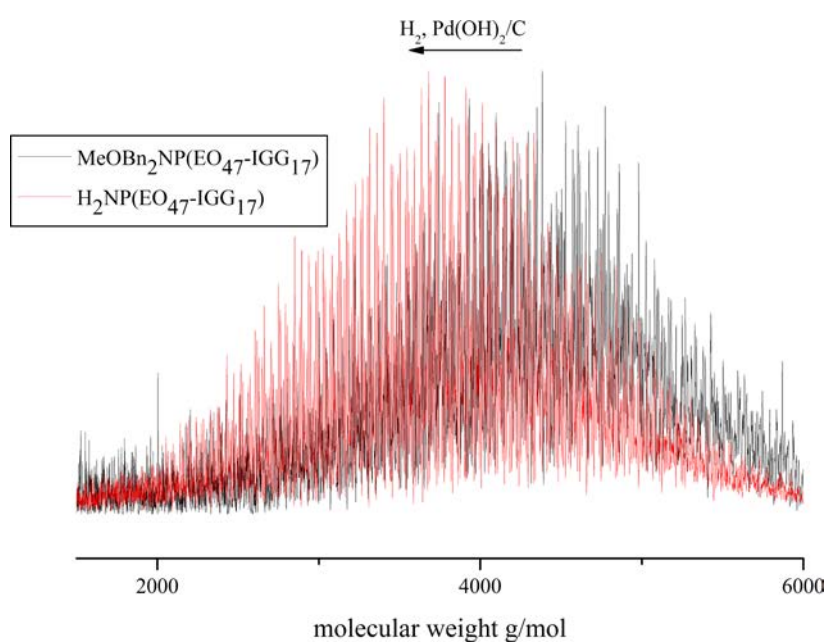


Figure S6. Shift of the molecular weight distribution upon hydrogenation, that is removal of the terminal methoxy-benzyl protecting groups.

1. Zalipsky, S.; Harris, J. M., Introduction to Chemistry and Biological Applications of Poly(ethylene glycol). In *Poly(ethylene glycol)*, American Chemical Society: 1997; Vol. 680, pp 1-13.
2. Fruijtier-Pölloth, C. *Toxicology* **2005**, 214, 1-38.
3. Abuchowski, A.; McCoy, J. R.; Palczuk, N. C.; van Es, T.; Davis, F. F. *J. Biol. Chem.* **1977**, 252, (11), 3582-3586.
4. Davis, F. F. *Adv. Drug Delivery Rev.* **2002**, 54, (4), 457-458.
5. Thompson, M. S.; Vadala, T. P.; Vadala, M. L.; Lin, Y.; Riffle, J. S. *Polymer* **2008**, 49, (2), 345-373.
6. Wurm, F.; Klos, J.; Räder, H. J.; Frey, H. *J. Am. Chem. Soc.* **2009**, 131, 7954-7955.
7. Fitton, A. O.; Hill, J.; Jane, D. E.; Millar, R. *Synthesis* **1987**, (12), 1140-1142.
8. Taton, D.; Le Borgne, A.; Sepulchre, M.; Spassky, N. *Macromol. Chem. Phys.* **1994**, 195, (1), 139-148.
9. Halacheva, S.; Rangelov, S.; Tsvetanov, C. *Macromolecules* **2006**, 39, (20), 6845-6852.
10. Dworak, A.; Baran, G. y.; Trzebicka, B.; Walach, W. *React. Funct. Polym.* **1999**, 42, (1), 31-36.
11. Dworak, A.; Panchev, I.; Trzebicka, B.; Walach, W. *Macromol. Symp.* **2000**, 153, (1), 233-242.
12. Dimitrov, P.; Hasan, E.; Rangelov, S.; Trzebicka, B.; Dworak, A.; Tsvetanov, C. B. *Polymer* **2002**, 43, (25), 7171-7178.
13. Li, Z.; Chau, Y. *Bioconjugate Chem.* **2009**, 20, (4), 780-789.
14. Mangold, C.; Wurm, F.; Obermeier, B.; Frey, H. *Macromol. Rapid Commun.* **2010**, 31, (3), 258-264.
15. Pang, X.; Jing, R.; Huang, J. *Polymer* **2008**, 49, (4), 893-900.
16. Erberich, M.; Keul, H.; Möller, M. *Macromolecules* **2007**, 40, (9), 3070-3079.
17. Obermeier, B.; Wurm, F.; Frey, H. *Macromolecules* **2010**, 43, (5), 2244-2251.
18. Wurm, F.; Nieberle, J.; Frey, H. *Macromolecules* **2008**, 41, (6), 1909-1911.
19. Hofmann, A. M.; Wurm, F.; Hühn, E.; Nawroth, T.; Langguth, P.; Frey, H. *Biomacromolecules* **2010**, 11, (3), 568-574.
20. Hamaide, T.; Goux, A.; Llauro, M.-F.; Spitz, R.; Guyot, A. *Angew. Makromol. Chem.* **1996**, 237, (1), 55-77.
21. Lestel, L.; Guegan, P.; Boileau, S.; Cheradame, H.; Laupretre, F. *Macromolecules* **1992**, 25, (22), 6024-6028.
22. Mandelkern, L. *Chem. Rev.* **1956**, 56, (5), 903-958.
23. Dickerson, T. J.; Reed, N. N.; Janda, K. D. *Chem. Rev.* **2002**, 102, (10), 3325-3344.
24. van Heerbeek, R.; Kamer, P. C. J.; van Leeuwen, P. W. N. M.; Reek, J. N. H. *Chem. Rev.* **2002**, 102, (10), 3717-3756.

25. McNamara, C. A.; Dixon, M. J.; Bradley, M. *Chem. Rev.* **2002**, 102, (10), 3275-3300.
26. Bergbreiter, D. E. *Chem. Rev.* **2002**, 102, (10), 3345-3384.
27. Lu, J.; Toy, P. H. *Chem. Rev.* **2009**, 109, (2), 815-838.
28. Sunder, A.; Hanselmann, R.; Frey, H.; Mülhaupt, R. *Macromolecules* **1999**, 32, (13), 4240-4246.
29. Roller, S.; Siegers, C.; Haag, R. *Tetrahedron* **2004**, 60, (39), 8711-8720.
30. Haag, R.; Stumbe, J. F.; Sunder, A.; Frey, H.; Hebel, A. *Macromolecules* **2000**, 33, (22), 8158-8166.

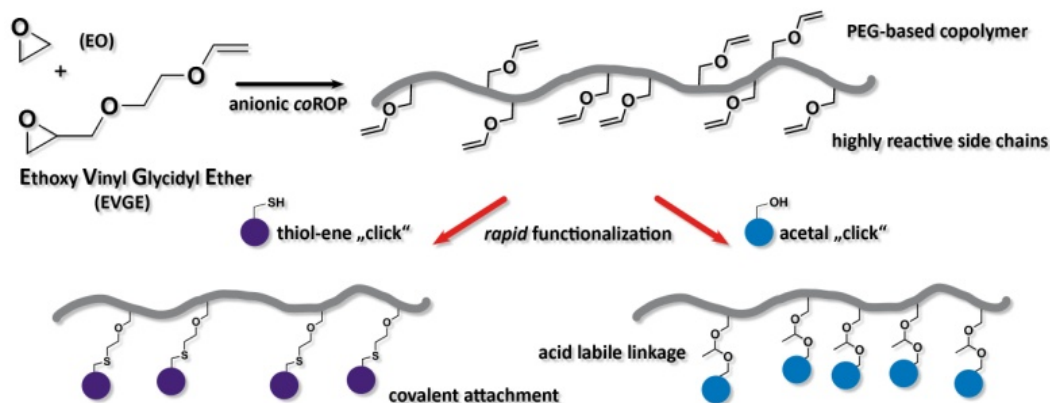
Chapter 2.3:

PEG-based Multifunctional Polyethers with Highly Reactive Vinyl-Ether Side Chains for Click-type Functionalization

PEG-based Multifunctional Polyethers with Highly Reactive Vinyl-Ether Side Chains for Click-type Functionalization

Christine Mangold, Carsten Dingels, Boris Obermeier, Holger Frey, Frederik Wurm

Published in *Macromolecules* **2011**, 44, (16), 6326-6334.



Keywords: anionic polymerization, PEG, polyether, random copolymer, vinyl ether, click-chemistry

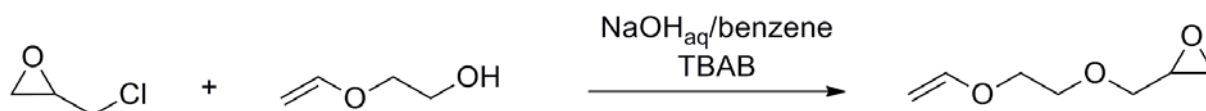
Abstract

Introduction of highly reactive vinyl ether moieties along a poly(ethylene glycol) (PEG) backbone has been realized by copolymerization of the novel epoxide monomer ethoxy vinyl glycidyl ether (EVGE) with ethylene oxide (EO). A series of copolymers with varying structure (block and random) as well as EVGE comonomer content (5-100%) with molecular weights in the range of 3 900-13 200 g/mol and narrow molecular weight distributions ($M_w/M_n = 1.06-1.20$) has been synthesized and characterized with respect to their microstructure and thermal properties. The facile transformation of the vinyl ether side chains in click type reactions was verified by two different post polymerization modification reactions: (i) thiol-ene addition and (ii) acetal formation, employing various model compounds. Both strategies are very efficient, resulting in quantitative conversion. The rapid and complete acetal formation with alcohols results in an acid-labile bond and is thus highly interesting with respect to biomedical applications that require slow or controlled release of a drug, while the thiol-ene addition to a vinyl ether prevents cross-linking efficiently compared to other double bonds.

Introduction

The importance of multifunctional, biocompatible polymer structures is obvious, particularly with respect to binding and release of pharmacologically active agents. Poly(ethylene glycol) (PEG), which exhibits low toxicity and antigenicity,^{1, 2} is used in a broad variety of biomedical applications.^{3, 4} However, the use of PEG is limited by its low loading capacity in drug conjugation, particularly when used as support for low molecular weight drugs. One strategy to increase the functionality of PEG is the synthesis of star- or block copolymers, which often leads to amphiphilicity and requires multistep syntheses. Another, more recent approach for enhancing the functionality of PEG, but leaving the water-solubility and toxicity unchanged, is the random copolymerization with an epoxide comonomer bearing an additional functional group that in most cases has to be protected for the anionic ring opening polymerization (AROP). The most popular protecting groups in AROP are acetals, such as ethoxy ethyl- (for OH-functionalities), as for example in the case of ethoxy ethyl glycidyl ether⁵ (EEGE), a monomer which has been used in a number of reports for the copolymerization with ethylene oxide⁶⁻⁸ either in a random^{9,10, 11} or block-like^{12, 13} manner to achieve linear and also more sophisticated structures.^{14, 15} Other functionalities introduced via the protected-monomer strategy are vicinal diols¹⁶ or amino functionalities,¹⁷ which were reported recently by our group. Currently, for the introduction of functionalities other than hydroxyl groups, different post-polymerization modifications are applied, which exceed a simple one-step deprotection reaction. A comprehensive overview of such reactions has been given by Li and Chau.¹⁸

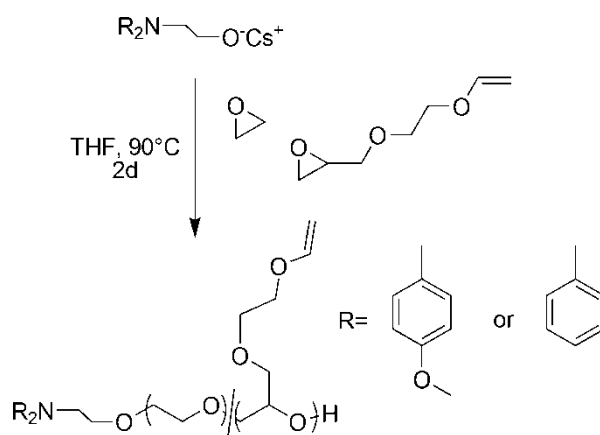
Functional macromolecules that permit facile and complete transformation of side chains play an important role in polymer science with respect to the attachment of drugs, catalyst structures or reagents.¹⁹ To date, the only functional epoxide monomer that contains a stable functional group for AROP, is allyl glycidyl ether (AGE),²⁰⁻²² permitting the introduction of allyl groups. In the current report we present the novel comonomer EVGE for the AROP to introduce vinyl ethers attached randomly along a PEG chain. The monomer is accessible in a simple one-step reaction²³ and can be purified by distillation.



Scheme 1. Ethoxy vinyl glycidyl ether (EVGE), obtained via phase transfer catalysis.

In a single previous work, this compound was used as a crosslinking reagent,²⁴ but to date, no reports on the AROP of the glycidyl ether have been reported. Since vinyl ethers are stable toward carbanionic²⁵ and oxyanionic²⁶ polymerization conditions, this monomer can be employed for AROP. In a recent first account we have demonstrated that EVGE can be homopolymerized and that

multiple attachment of Grubbs' catalyst to the resulting structure is possible.²⁷ The vinyl ether group does not only offer the opportunity for thiol-ene functionalization reactions, but also for the attachment of any molecule possessing an alcohol. The latter modification results in an acetal which allows triggered release of a specified target in acidic conditions. This is a promising approach for the design of novel polymer therapeutics with releasable payloads. There are various examples in literature, where this principle has been realized, but usually multistep procedures are necessary.²⁸ In the current publication we describe the random, anionic ring-opening copolymerization of EVGE with EO (Scheme 2). The resulting polyethers with vinyl ether side chains have been characterized with respect to their thermal behavior and their microstructure, particularly in view of the random incorporation of both comonomers. In addition, postpolymerization modifications were performed, i.e., thiol-ene functionalization with different model compounds, and the kinetics of the resulting acetal formation has been studied, employing ¹H NMR online measurements.



Scheme 2. Synthesis of random copolymers of EO and EVGE by simultaneous reaction of both monomers with the deprotonated initiator.

Experimental Section

Instrumentation

¹H NMR spectra (300 MHz and 400 MHz) and ¹³C NMR spectra (75.5 MHz) were recorded using a Bruker AC300 or a Bruker AMX400. All spectra were referenced internally to residual proton signals of the deuterated solvent. For SEC measurements in DMF (containing 0.25 g/L of lithium bromide as an additive) an Agilent 1100 Series was used as an integrated instrument, including a PSS HEMA column ($10^6/10^5/10^4$ g/mol), a UV- (275 nm) and a RI-detector. Calibration was carried out using poly(ethylene oxide) standards provided by Polymer Standards Service. DSC measurements were performed using a Perkin-Elmer 7 series thermal analysis system and a Perkin Elmer thermal analysis

controller TAC 7/DX in the temperature range from -100 to 80 °C at heating rates of $10 \text{ K}\cdot\text{min}^{-1}$ under nitrogen.

Reagents

Solvents and reagents were purchased from Acros Organics, Sigma Aldrich or Fluka and used as received, unless otherwise stated. Chloroform- d_1 , methanol- d_4 and DMSO- d_6 were purchased from Deutero GmbH. The two different initiators used, di(benzyl)-aminoethanol and di(*p*-methoxybenzyl)amino-ethanol, were synthesized as reported previously.^{14, 16}

Synthesis

Ethoxy vinyl glycidyl ether (EVGE). 2-(vinylloxy)ethanol (10 g, 113.5 mmol) was placed in a 500 mL round bottom flask and dissolved in a mixture of 50% aqueous NaOH (150 mL) and benzene (150 mL). To this mixture 3.5 g (11 mmol) tetrabutylammonium bromide (TBAB) was added and the mixture was stirred quickly with a mechanical stirrer. Subsequently the reaction mixture was cooled with an ice bath, and epichlorohydrin (31.5 g, 340.5 mmol) was slowly added via a dropping funnel. After 24 h reaction time at room temperature, the organic phase was separated from the aqueous phase, washed several times with brine, dried and concentrated *in vacuo* to remove benzene and the excess epichlorohydrin. The resulting slightly yellow residue was distilled under reduced pressure to yield the desired product as a colourless liquid, typically in 70-80% yield (11-13 g). ^1H NMR (CDCl_3 , 300 MHz): δ (ppm) = 6.44 (1H, dd, $\text{CH}_2=\text{CH}$, $J_1=14.3$, $J_2=7$), 4.13 (1H, dd, $\text{CH}_2=\text{CH}$, $J_1=14.3$, $J_2=2.2$), 3.96 (1H, dd, $\text{CH}_2=\text{CH}$, $J_1=7$, $J_2=2.2$), 3.8-3.65 (4H, m, $-\text{O}-\text{CH}_2-\text{CH}_2-\text{O}-$ & CH_2 (glycidyl ether)), 3.38 (2H, dd, CH_2 (glycidyl ether), $J_1=11.8$, $J_2=5.9$), 3.1 (1H, m, CH-epoxide), 2.74 (1H, dd, $\text{CH}_2\text{-epoxide}$, 1H, $J_1=5$, $J_2=4.2$), 2.56 (1H, dd, $\text{CH}_2\text{-epoxide}$, $J_1=5.2$, $J_2=2.6$).

General Procedure for the Copolymerization of EO and EVGE. *N,N*-di(*p*-methoxybenzyl)-2-aminoethanol was dissolved in benzene in a 250 mL-Schlenk flask, and 0.9 equiv. of cesium hydroxide were added. The mixture was stirred under argon for 3 h at room temperature and evacuated at (10^{-2} mbar) for 12 h to remove benzene and water, forming the corresponding cesium alkoxide. Then 20 mL of dry THF was cryo-transferred into the Schlenk flask to dissolve the initiator-salt. EO was first cryo-transferred to a graduated ampule, and subsequently cryo-transferred into the flask containing the initiator in THF (at around -80 °C). The EVGE comonomer was added via syringe and the mixture was heated to 90 °C and stirred for 24-72 h. Precipitation in cold diethyl ether resulted in the pure copolymers. For polymers with a high fraction of EVGE, the polymer solution was dried *in vacuo*. Yields: 95% to quantitative. ^1H NMR (DMSO- d_6 , 300 MHz): δ (ppm) = 7.24, 6.87 (8H, d, $\text{C}_6\text{H}_4\text{OMe}$) in the case of *p*-methoxybenzyl-; without methoxy-group: 7.40-7.15 (10H, m, aromatic), 6.48 (1H/EVGE-unit, dd, $\text{CH}=\text{CH}_2$), 4.16 (1H/EVGE-unit, dd, $\text{CH}=\text{CHH}$), 3.95 (1H/EVGE-unit, dd, $\text{CH}=\text{CHH}$), in the case of methoxy-benzyl: 3.74 (s, $\text{C}_6\text{H}_4\text{OMe}$), 3.68-3.34 (polyether backbone), 2.54 (2H, t, $\text{Bn}_2\text{NCH}_2\text{CH}_2\text{O}-$).

Block copolymer synthesis. 2 g mPEG-5000 was deprotonated with 0.9 equiv. of CsOH·H₂O. The reaction water was removed by azeotropic distillation with benzene. The deprotonated polymer was dissolved in dry DMSO to give a 50% solution. Subsequently EVGE was added to the mixture and the polymerization was allowed to proceed for 12 h at 90 °C. Precipitation in diethyl ether resulted in the pure block copolymer.

Polymer Modification: Thiol-Ene-Functionalization. 0.2 g of the respective copolymer were dissolved in 10 mL DMF and 0.5 to 10 equiv. of benzyl mercaptan and 0.75 equiv. of azobis(isobutyronitrile) (AIBN) with respect to the absolute number of vinyl ether groups, were added. After three freeze-pump-thaw cycles the reaction mixture was heated to 75 °C and stirred for 12 h. The reaction mixture was then dialyzed against THF/MeOH, using benzoylated tubings (MWCO 1500 g/mol), for 2 days. ¹H NMR (CDCl₃-d₁, 300 MHz): δ(ppm) = 7.39-7.10 (initiator & arom. side group), 4.15-3.36 (polyether backbone), 3.70 (s, benzylic), 2.57 (CH₂S-benzyl).

Polymer Modification: Acetal-Formation. 0.2 g of the respective copolymer and 10 equiv. of benzyl alcohol were placed in a round bottom flask and 0.01 equiv. of *p*-toluenesulfonic acid (in relation to the absolute number of vinyl-ether bonds) was added at 0 °C. After 2 h of stirring at RT, the reaction was stopped by the addition of triethylamine, and the mixture was dialyzed against THF (MWCO= 1500 g/mol) for 24-48h, to remove the residual benzyl alcohol and PTSA as well as NEt₃. ¹H NMR (CDCl₃-d₁, 300 MHz): δ(ppm) = 7.36-7.18 (initiator & arom. side-group), 6.80 (d, ini.), 4.82 (m, acetal-H), 4.54 (dd, benzyl-H), 3.68-3.34 (polyether backbone), 2.54 (2H, t, Bn₂NCH₂CH₂O-), 1.33 (d, CH₃).

¹H NMR-Kinetics

30 mg of the copolymer was dissolved in 0.5 mL of deuterated methanol and the first spectrum (t=0) was recorded immediately. Then the respective amount of PTSA were dissolved in 0.2 mL deuterated methanol and added to the polymer solution via syringe. After rapid mixing, ¹H NMR spectra were taken every minute (compare Figure 4).

Results and Discussion

A: Synthesis of P(EO-*co*-EVGE) Copolymers, Characterization and Thermal Properties

Synthesis

The copolymerization of two monomers with highly diverging boiling points requires special reaction conditions. The key for random incorporation of glycidyl ether comonomers is polymerization at an elevated temperature, which was proven in previous works for other glycidyl ethers.^{11, 16, 17, 22, 29} To level the different reactivities of the monomers, the reaction mixture was rapidly heated to 90 °C in a sealed system under vacuum. All polymerizations were carried out in THF and stirred for at least 48 h to guarantee full conversion of both monomers. *N,N*-di(*p*-methoxy-benzyl)-2-amino ethanol and *N,N*-di(benzyl)-2-amino ethanol were used as the respective initiators, since they allow the facile

determination of the molecular weight via ^1H NMR. The aromatic signals of the resulting end group do not interfere with other signals in the spectrum and therefore permit reliable integration of the ^1H NMR spectra for molecular weight determination. In addition, the protective groups can be removed to regenerate a primary amino group in the α -position of the polymer chain. The corresponding initiator was deprotonated with 0.9 equiv. of $\text{CsOH}\cdot\text{H}_2\text{O}$, and the evolving water was azeotropically removed under vacuum in the presence of benzene. As the vinyl ether groups are highly reactive and unstable toward acidic media, the resulting copolymers were either purified by dialysis or precipitation in diethyl ether (for low EVGE-content, compare Experimental Section). Stirring the polymers with acidic ion exchange resin to reprotonate the active species and to remove residual Cs^+ ions leads to the deprotected polymer with $-\text{CH}_2\text{OCH}_2\text{CH}_2\text{OH}$ side chains and a similar structure as linear poly(glycerol); thus, the vinyl ether side chain can also be regarded as an efficient protective group for hydroxyl groups in the AROP. It should also be mentioned here, that the use of acidic media in combination with heat and low pressure can result in crosslinked products for this system.

The EVGE comonomer content has been varied in a systematic manner from 5% to 100%, and Table 1 summarizes the results for the series of copolymers that were prepared in this study with respect to molecular weights and polydispersities. From a comparison of the composition of the monomer feed and the copolymer composition it can clearly be stated that the monomer feed corresponds to the incorporated EO/EVGE-ratio, as determined by ^1H NMR spectroscopy. The copolymers showed good water solubility up to 25% EVGE-content at room temperature, which is crucial for biomedical applications. A typical spectrum of a water soluble copolymer in D_2O is displayed in Figure 1.

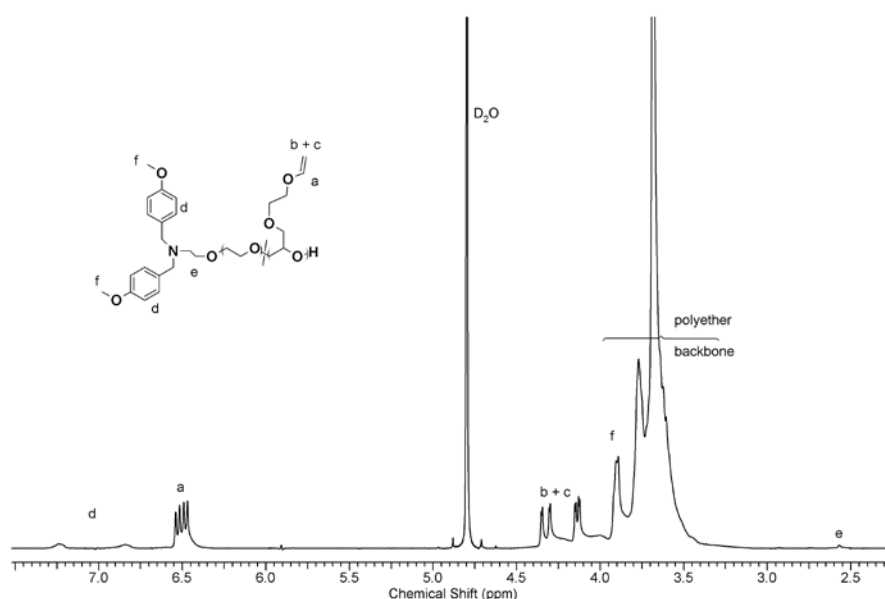


Figure 1. ^1H NMR spectra in $\text{D}_2\text{O}-d_2$ of $\text{P}(\text{EO}_{120}\text{-co-EVGE}_{30})$.

The resonances a, b and c correspond to the vinyl ether groups, and by integration of these signals and comparison to the polyether backbone (3.18-3.79 ppm) and the aromatic end group signals (6.78-7.25 ppm) the copolymer composition can be calculated. The structural parameters given in Table 1 have been determined using ^1H NMR in CDCl_3-d_1 (additional ^{13}C NMR spectra can be found in the Supporting Information)

Table 1. Characterization data for all copolymer samples prepared.

No	monomer feed composition	polymer composition ^a	M_n (NMR) ^a	M_n (SEC) ^b	PDI ^b
1	MeOBn ₂ NP(EO ₁₀₀ - <i>co</i> -EVGE ₁₀)	MeOBn ₂ NP(EO ₁₀₄ - <i>co</i> -EVGE ₆)	5 800	2 400	1.06
2	MeOBn ₂ NP(EO ₁₂₀ - <i>co</i> -EVGE ₁₀)	MeOBn ₂ NP(EO ₁₁₅ - <i>co</i> -EVGE ₁₁)	6 700	2 500	1.08
3	MeOBn ₂ NP(EO ₁₂₀ - <i>co</i> -EVGE ₃₀)	MeOBn ₂ NP(EO ₁₂₀ - <i>co</i> -EVGE ₃₀)	9 900	5 130	1.08
4	MeOBn ₂ NP(EO ₁₀₀ - <i>co</i> -EVGE ₃₀)	MeOBn ₂ NP(EO ₈₉ - <i>co</i> -EVGE ₃₀)	8 500	5 100	1.11
5	Bn ₂ NP(EO ₂₅ - <i>co</i> -EVGE ₂₅)	Bn ₂ NP(EO ₂₃ - <i>co</i> -EVGE ₂₅)	4 600	1 600	1.20
6	Bn ₂ NP(EO ₃₀ - <i>co</i> -EVGE ₉₀)	Bn ₂ NP(EO ₃₁ - <i>co</i> -EVGE ₈₀)	13 200	4 000	1.20
7	Bn ₂ NP(EO ₂ - <i>co</i> -EVGE ₂₀)	Bn ₂ NP(EO ₂ - <i>co</i> -EVGE ₁₅)	2 200	1 600	1.15
8	MeOP(EO ₁₁₄ - <i>block</i> -EVGE ₁₀)	MeOP(EO ₁₁₄ - <i>block</i> -EVGE ₉)	6 300	4 900	1.04
9	Bn ₂ NP(EVGE ₃₀)	Bn ₂ NP(EVGE ₂₇)	3 900	2 300	1.22

^a determined from ^1H NMR (300 MHz, CDCl_3-d_1); ^b determined by SEC-RI in DMF.

The molecular weight distributions obtained from size exclusion chromatography (SEC) measurements (in DMF with PEG-standards) were in the range of $M_w/M_n = 1.06$ to 1.22, as expected for oxyanionic polymerization. The resulting monomodal SEC traces are given in the Supporting Information (Figure S1). The deviation of the molecular weights obtained from NMR and SEC can be explained by the presence of the sidechains, since their mass does not contribute to the overall hydrodynamic radius in the same manner as an increase of the degree of polymerization does, and SEC was calibrated with PEG. Furthermore, incorporation of EVGE units leads to more hydrophobic copolymers, which changes the hydrodynamic radius compared to the PEG-standards in DMF. The comparison reveals an average deviation factor of 2 for our setup.

^{13}C NMR Characterization (Triad Sequence Analysis)

Random distribution of the vinyl ether side chains is essential for use of the EVGE/EO copolymers in any application. The influence of adjacent units on the methylene (and methine) carbon shift in ^{13}C NMR allows for the determination of the microstructure of copolymers. The resulting triad sequence distribution allows to investigate the distribution of two different monomers in the poly(ether) backbone and represents a well-established method for the characterization of

copolymers based on propylene oxide and EO.³⁰ Recently, some other poly(ether)s have been investigated in this manner by our group (EEGE,¹¹ IGG (1,2-isopropylidene glyceryl glycidyl ether),¹⁶ AGE²² and DBAG¹⁷). For all of these monomers and the novel monomer EVGE, this technique clearly evidence the random composition of such epoxide-based copolymers. **Figure 2** displays the relevant region of the ¹³C NMR spectra of several EO/EVGE copolymers, showing the resonances for the respective triads. For brevity, ethylene oxide units are referred to as “E”, while EVGE units are abbreviated with “V”. Both units have two different carbon atoms (a and b or a’ and b’), which are shifted in dependence of the adjacent monomer units.

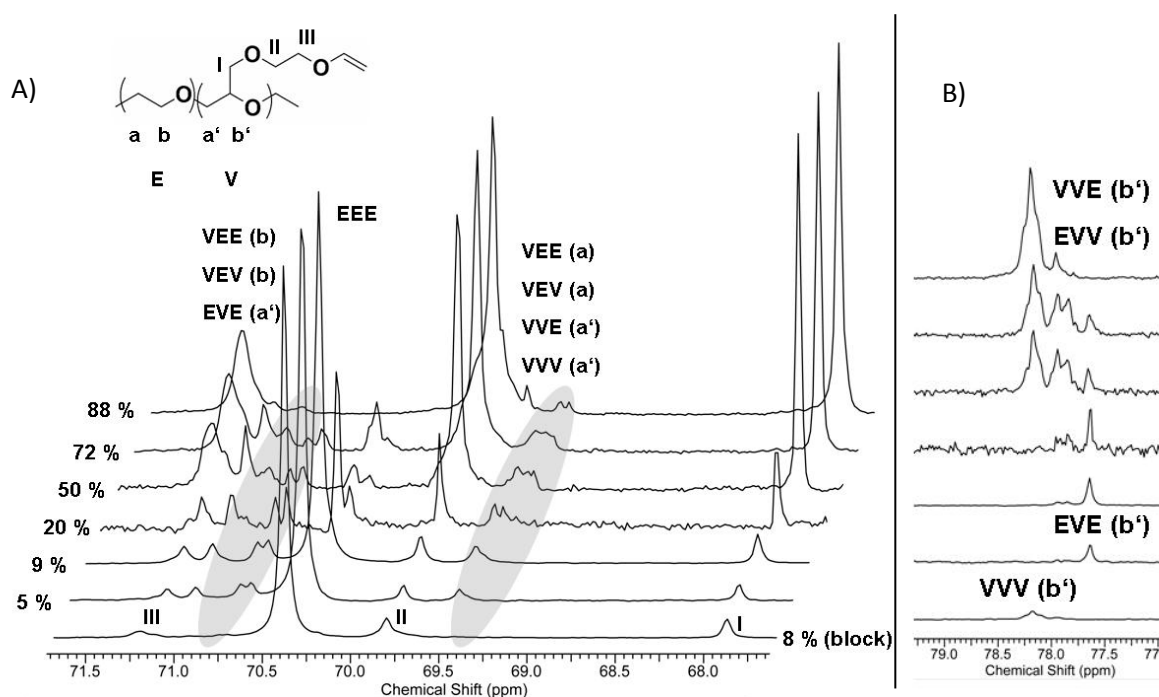


Figure 2. Typical ¹³C NMR spectra in DMSO-*d*₆ of P(EO-*co*-EVGE) copolymers with varying EVGE fraction (in %), and a block copolymer (bottom) from A) 67 to 72 ppm and B) 77 to 79 ppm.

In the ¹³C NMR spectrum of all different copolymers (Figure 2), two regions can be analyzed to determine the distribution of the comonomers via triad analysis: (i) from 69 to 72 ppm and (ii) from 77 to 79 ppm, which stem from the carbon resonances of the polyether backbone. With the block copolymer (8% EVGE) in hand, all signals corresponding to the side group of EVGE (marked with I, II and III) and the methine signal (cf. Figure 2B) can be unequivocally assigned. In addition, the signals of the methylene carbons (a and b) of the EO triads, which are marked with EEE, can be clearly identified. As expected, the spectra of the random copolymers differ significantly from the block copolymer MeOP(EO₁₁₄-*block*-EVGE₉). With increasing EVGE-content several new resonances in the area of the side groups appear, but in addition new signals occur in the regions marked in gray in Figure 2A. These resonances overlap with the side group signals, rendering quantification difficult.

However, from simulated ^{13}C NMR spectra (performed with ChemDraw Ultra 10.0), the triads can be assigned to the respective regions marked in gray. The signals in these regions increase steadily up to 65% EVGE incorporation, while the EEE-triad decreases to the same extent. In the spectrum with 88% EVGE content the signals of the EEE-triad vanishes completely, which is in line with the expectation. Figure 2B gives a zoom into the area for the methine carbons of EVGE. In the case of the block copolymer, the methine-signal of the EVGE-unit (b') is detected as a single signal (Figure 2B, bottom), which can be assigned to the VVV-triad of the P(EVGE) block copolymer. In the case of the random copolymer with only 5% EVGE, the most probable environment for one EVGE unit are two EO units (EVE-triad), and the only signal which appears in the respective region can be assigned to this triad. With increasing incorporation of EVGE, other combinations become likely and at least two other signals appear at 78 ppm. The spectrum of $\text{Bn}_2\text{NP}(\text{EO}_2\text{-co-EVGE}_{15})$ (entry 8, table 1) with 88% EVGE-content exhibits one major signal at the same position as it can be found in the block copolymer, which is again assigned to the VVV triad. The strongest evidence can be found by direct comparison of the two copolymers with approximately the same EVGE incorporation (8-9%), but varying internal structure. While in the block copolymer only four carbon resonances between 72 and 68 ppm are detected, the random copolymer exhibits a considerably more complicated spectrum. The occurrence of triad-signals confirms the random comonomer distribution. This result also is in line with previous works on other glycidyl ether copolymerizations with EO.^{11, 16, 17, 22, 29}

Thermal Behavior

Characterization of the thermal properties was carried out via differential scanning calorimetry (DSC, heating rate 10 K/min). PEG with a molecular weight of 600 g/mol and higher is a crystalline polymer with a melting temperature, which is strongly dependent on the molecular weight of the polymer. PEG-600 has a melting range of 17-22 °C, and with increasing M_w the T_m increases steadily until a maximum of 65 °C³¹ is reached. PEVGE, on the other hand, exhibits an amorphous character and a low T_g (-63 °C, sample 9, Table 1). Incorporation of EVGE-units into the PEG-backbone leads to obvious morphology changes, as the copolymers are obtained as (i) white powder for 5% EVGE incorporation, (ii) sticky solid (at 10% EVGE-incorporation) and (iii) viscous liquids (with more than 25% EVGE incorporated). DSC measurements demonstrate that the polymers with a low content of EVGE (5, 10%) contain a crystalline fraction and show a melting point and related melting enthalpies (compare Table 2). As the number of EVGE monomer units increases, the crystalline domains disappear, and no melting point can be detected via DSC. On the basis of the assumption that the distribution of the EVGE units is completely random, the average number of adjacent EO units is 17 in the case of copolymer 1 and 10 in the case of copolymer 2. The average length of homo-PEG units that is required to obtain a crystalline homopolymer is 13 (this corresponds to PEG-600).³² Thus, the

thermal characteristics reflect the random copolymer structure. The glass transition temperature of the copolymers, on the other hand, decreases only slightly, from -55 °C, to a T_g of -60 °C with increasing amount of EVGE. While a T_g of -55 °C (copolymer 1) can clearly be ascribed to the PEG-domains, the final T_g of copolymer 7 (88% EVGE) corresponds to the PEVGE nature, since the pure homopolymer of EVGE exhibits a T_g of -63 °C. The slight variation of the T_g can be ascribed to differing molecular weights.

Table 2. Thermal properties of poly(ethylene glycol-co-ethoxy vinyl glycidyl ether) with varying amounts of EVGE incorporated.

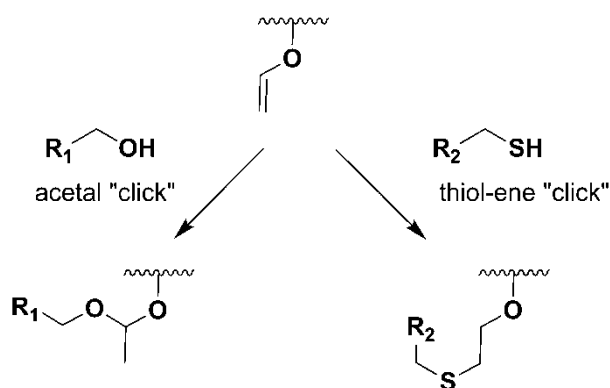
No	polymer composition	EVGE %	T_g^a / °C	T_m^b / °C	ΔH^c / J/g
1	MeOBn ₂ NP(EO ₁₀₄ -co-EVGE ₆)	5	-55	34	74
2	MeOBn ₂ NP(EO ₁₁₅ -co-EVGE ₁₁)	9	-59	16	47
3	MeOBn ₂ NP(EO ₁₂₀ -co-EVGE ₃₀)	20	-58	-	-
4	MeOBn ₂ NP(EO ₈₉ -co-EVGE ₃₀)	25	-58	-	-
5	Bn ₂ NP(EO ₂₃ -co-EVGE ₂₅)	52	-57	-	-
6	Bn ₂ NP(EO ₃₁ -co-EVGE ₈₀)	72	-60	-	-
7	Bn ₂ NP(EO ₂ -co-EVGE ₁₅)	88	-60	-	-
8	MeOP(EO ₁₁₄ -block-EVGE ₉)	8	-55	54	103
9	MeOBn ₂ NP(EVGE ₂₇)	100	-63	-	-
10	mPEG-5000	0	- ^d	61	175

^a glass transition temperature; ^b melting temperature T_m : in °C; ^c melting enthalpy determined by integration. ^d not detectable in this set-up.

Again, a block copolymer PEO-*b*-PEVGE was used to compare two polymers with similar EVGE content, but different structure. Comparing polymer 2 with polymer 8 (both with approximately 8-9% EVGE) clearly shows the presence of a crystalline fraction. However, the melting points differ strongly and the melting enthalpy in the random copolymer is reduced, since the crystalline order is impeded by the presence of the comonomer, as expected. In summary, thermal properties mirror the random incorporation of EVGE into the polymer backbone.

B:“Click” Type Functionalization of the EVGE-Copolymers

Two different types of high-yield transformations have been studied that capitalize on the peculiar reactivity of the vinyl ether side chains of the EVGE comonomer units (Scheme 3).



Scheme 3. Polymer modification reactions employed i) the thiol-ene reaction with compounds bearing a thiol group and ii) acetal formation with alcohols.

Thiol-Ene Reaction

The functionalization of double-bond carrying polymers by thiol-ene “click” reactions has been studied intensively by several groups.³³⁻³⁶ A major issue which has to be considered are undesired cross-linking reactions between the double bonds along the backbone. In the case of the thiol-ene reaction these can be successfully suppressed by using an excess of the thiolcontaining component in the reaction mixture. This necessitates subsequent purification (i.e., dialysis) of the polymers to remove residual thiol. The term “click-reaction”, with respect to polymer modification reactions has recently been subject of an intense discussion. The general requirements of click reactions are high (close to complete) conversion, facile reaction conditions with easily available starting materials, preferably with no solvent involved, and a simple isolation procedure. This general concept was expanded by the authors by introducing the concept of equimolarity, when a simple work-up procedure, such as precipitation, is not possible. This would imply that thiol-ene reactions are no “click-reactions” when employed for polymer modification. However, due to the stability of the vinyl ether radical, no crosslinking of the polymer chains occurs.³⁷ This finding is in good agreement with prior reports on radical polymerization of vinyl ethers,³⁸ which only undergo copolymerization in the presence of a second vinyl monomer with electron withdrawing groups³⁹ or by the introduction of electron acceptors in proximity to the vinyl ether moiety.⁴⁰

In principle, the Markovnikov as well as the anti-Markovnikov addition of the thiol-component is possible, but fundamental studies on thiol-ene reactions involving vinyl ethers have shown that due to the prealignment of the molecules by the oxygen-hydrogen interaction the anti-Markovnikov product is clearly favored over the Markovnikov product, leading to more uniform products compared to allyl-systems.⁴¹ In addition, it should be mentioned that vinyl ethers do not exhibit double bond isomerization, which can be found for the allyl analogues.⁴²

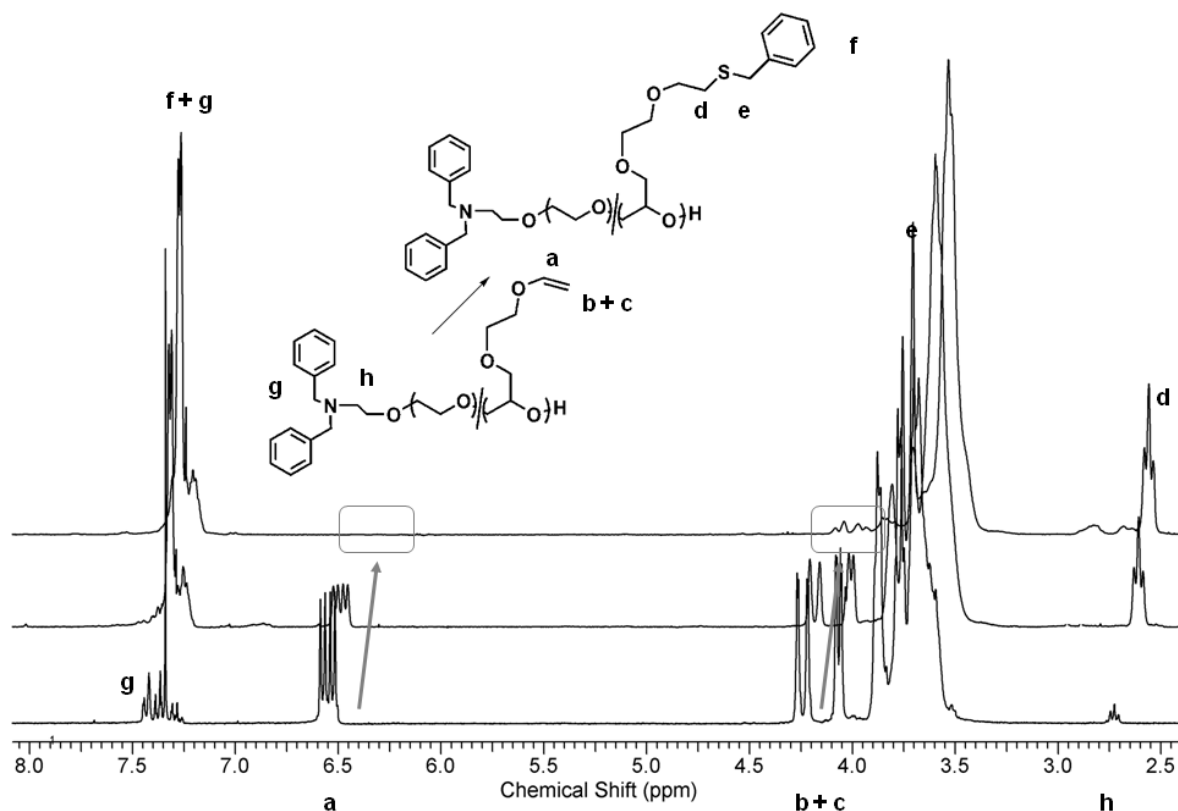


Figure 3. Copolymer **5** in $\text{CDCl}_3\text{-}d_1$ ($\text{Bn}_2\text{P}(\text{EO}_{23}\text{-}co\text{-EVGE}_{25})$) before and after the thiol-ene click reaction with 0.5 and 10 equivalents of added thiol (scale bar corresponds to the top spectrum).

Benzyl mercaptan was chosen as a model compound, since it allows the facile assignment of the relevant resonances in ^1H NMR spectroscopy. The reaction was carried out overnight in DMF at 75°C and after work-up by dialysis (to remove residual DMF) the successful transformation of the vinyl ether can be observed by the (partial) disappearance of the resonances at 6.48, 4.16 and 3.95 ppm, while new resonances are detected due to formation of the thio ether structure. These are, e.g., for mercaptobenzyl alcohol in the aromatic region (c 7.34 ppm), at 3.70 (deriving from the benzylic protons), and at 2.57 ppm (corresponding to CH_2 adjacent to the thioether bond, Figure 3). The comparison of the thio ether signals with the poly(ether) backbone and the initial amount of vinyl ether side chains allows to determine the conversion of the vinyl ether moieties. This demonstrates that attachment of small molecules to the vinyl ether side chains is possible and can in principle be employed for any compound bearing a thiol moiety. Since crosslinking reactions do not occur, it is possible to attach less than one equivalent of the thiol component and this implies that (i) this post polymerization reaction is a real “click reaction” and (ii) the remaining double bonds can be used for further functionalization reactions (compare Figure S7), which is highly interesting with respect to future applications.

Acetal-Formation as a Click-Type Polymer Modification

The general requirements for click reactions and the currently considered criteria for polymer modification reactions have been discussed in the previous section. The first three criteria (high conversion, facile reaction conditions, easily available starting materials) are all met by the acetal formation reaction by addition of an alcohol to a vinyl ether. However, the criteria equimolarity, facile work-up procedure as well as stable end-products, are not fulfilled. The formation of acetals based on vinyl ethers and alcohols is generally fast and proceeds selectively in the absence of water. In the case of low molecular weight compounds, the acetal bond is generated under acidic catalysis from the respective alcohol and the vinyl ether within several minutes without any side-products. Compared to other polymer modification reactions this method allows the facile, rapid and quantitative attachment of alcohols via a pH-labile acetal bond.

Benzyl alcohol was chosen as a model compound and PTSA was added as a catalyst. The reaction was monitored via ^1H NMR, following the disappearance of the vinyl ether signals (compare Supporting Information S5, a,b,c) and the emerging signals at 4.82 (d, acetal), 4.54 (e, benzyl) and 1.33 (f, CH_3) ppm. From a comparison of the acetalic proton and the CH_3 -group integrals to the initial amount of vinyl ether side chains, it can clearly be concluded that this reaction is quantitative and no detectable side reactions occur. Removal of the acidic catalyst was most efficient via dialysis against THF/ NEt_3 . The precipitation of the product in diethyl ether does not guarantee complete removal of the *p*-toluenesulfonic acid (PTSA) and, moreover, crosslinking by trans-acetalization can occur (compare above).

Since the transformation of the vinyl ether groups was found to be very fast, the reaction was investigated by online ^1H NMR kinetics (Figure 4). For the respective measurements, the polymer was dissolved in deuterated methanol, which served both as a solvent and as a reactant. The catalyst was dissolved in MeOD separately. After addition of the acid to the polymer solution NMR-spectra were measured in intervals of 30 s.

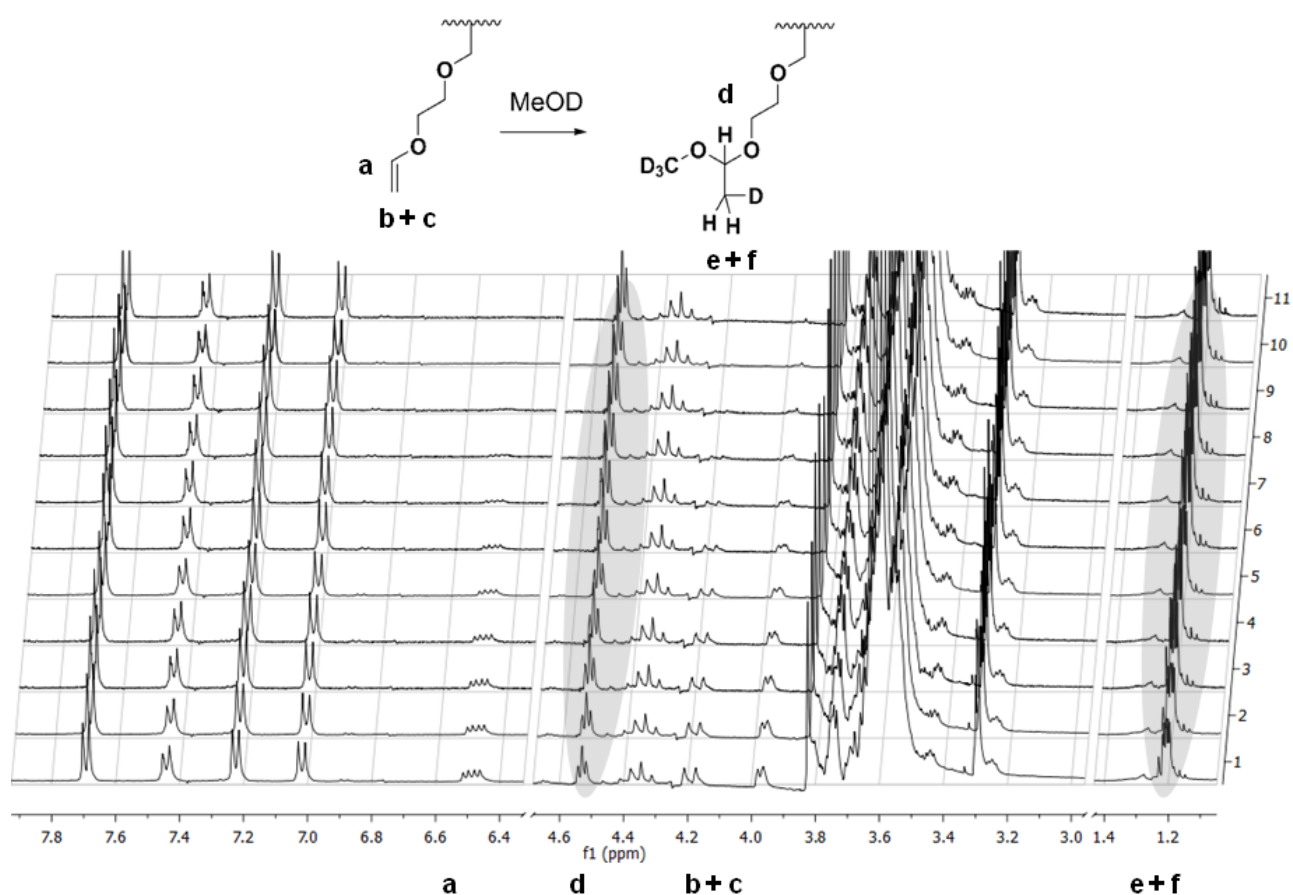


Figure 4. Reaction of copolymer **1** with MeOD- d_4 (4.92 and 3.31 ppm), in the presence of PTSA (7.75, 7.28 and 2.41 ppm). For clarity only the relevant part of the spectrum is shown, additional spectra with the whole ppm range can be found in the SI.

Since the lock and shim process requires approximately 3-5 minutes, the resonance for the acetal proton is already present in the first spectrum. The corresponding signal can be discerned at 4.59 ppm (d) and the corresponding methyl-group signal at 1.26 ppm (e + f). Nevertheless, the reaction can be followed by monitoring the disappearance of the vinyl ether signals at 6.54 (a), 4.26 and 2.04 ppm (b + c). The reaction reached 99% conversion of the vinyl ether bonds within 10 minutes. Note: Even in the presence of trace amounts of water, which is due to the crystallization water of PTSA (not dried prior to the experiment) no cleavage of the acetal bond is found. If the acetal had been opened, the respective resonances for acetaldehyde around 9 ppm (aldehyde) and 2 ppm (methyl-group) would have been detectable. Here, acetal formation at the multifunctional PEG copolymers can be described by first order kinetics, since one of the reagents serves as the solvent and thus the concentration is constant throughout the reaction. A plot of converted vinyl ether groups versus reaction time (shown in Figure 5) supports this assumption.

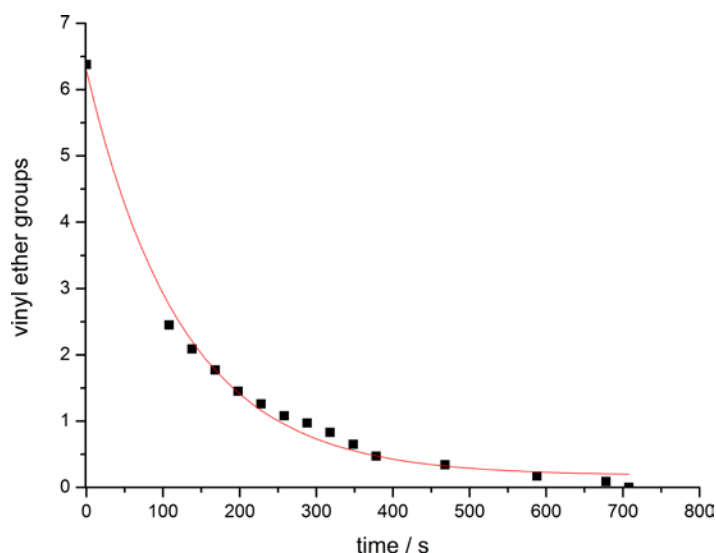


Figure 5. Conversion of vinyl ether groups versus time for the reaction of copolymer **1** with MeOD- d_4 . Black squares: measured values; red line: exponential fit (Origin 7).

The first spectrum from the NMR experiment was obtained at already 61% conversion after approximately 3 minutes. Nevertheless, it is possible to assign these values with an exponential fit and estimate the half life time of the vinyl ether moieties to ca. 80 s. This value depends on the reaction conditions and has to be treated with care, since every alcohol will show a different behavior and methanol was used as a solvent in this case. In addition, both the concentration of the catalyst and of the alcohol represent key parameters for this reaction. Additional measurements were carried out, and the respective spectra are given in the Supporting Information. A comparison of the two kinetics conducted shows that reducing the amount of catalyst/vinyl ether ratio from 1:2.5 to 1:20 prolongs the half life time from 80 to 180 s. The reaction time and conditions will have to be adjusted according to the respective molecule. Further work on a broad range of alcohols is currently in progress.

In summary, these results clearly evidence that the acetal formation at the polymer backbone is a very rapid and selective transformation for polymer modification. In direct comparison with other polymer modification methods, it is facile, leads to high conversion, can be used to attach a variety of molecules bearing a hydroxyl functionality and is therefore as valuable as the widespread thiol-ene modification. It was also proven that in the presence of diluted acids the attached molecules can be released. This allows the attachment of drugs or biomolecules and the triggered release of them in slightly acidic media, as present e.g., in lysosomes. The use of these materials in biomedical applications is subject of ongoing studies in our group.

Conclusion

The importance of functional and biocompatible polymers has increased steadily during the past decade. The materials are obtained either by radical polymerization techniques or end group modification of commercial PEG. Another, straightforward strategy for introducing a broad range of functionalities into the biocompatible PEG backbone is the direct copolymerization of functional comonomers with EO.⁴³ In this work we have introduced the novel monomer EVGE with a vinyl ether group, which copolymerizes with EO in a controlled and random manner. The random distribution of the EVGE comonomer units in the PEG backbone was proven by NMR and DSC measurements. PEG-copolymers with up to 25% vinyl ether content are soluble in aqueous solution, which opens manifold possibilities for biomedical applications.

The PEG-based multifunctional polymers can be derivatized in different ways: (i) by reaction with a thiol a side-chain polythioether is generated and (ii) the reaction with any alcohol results in a side-chain polyacetal. This has been demonstrated by different model reactions and by kinetic NMR measurements. The first transformation results in the stable, covalent attachment of thiols to the PEG-based copolymer, avoiding crosslinking, which represents a hard to exclude side reaction for comparable allyl bonds in poly(allyl glycidyl ether).^{20,41} Thus, this feature represents a significant advantage over the allyl-glycidyl ether (AGE) monomer which has been reported to permit sequential “click” reactions to multifunctional polymers in previous studies.

In addition, the rapid acetal formation (ii), which has, to the best of our knowledge not been applied in a post-polymerization protocol, is highly interesting with respect to polymer therapeutics or hydrogels, due to the facile release of the alcohol in acidic media. In ongoing studies the suitability of these post-polymerization reactions with respect to the attachment of proteins or low molecular weight drugs is investigated and will be presented in near future.

Acknowledgement

The authors thank Alina Mohr for technical assistance. C. M. is a recipient of a fellowship through funding of the Excellence Initiative (DFG/GSC 266). C. D. is grateful to MPG for a scholarship and financial support. B.O. acknowledges the Fonds der Chemischen Industrie for a scholarship. F.W. thanks the Alexander-von-Humboldt foundation for a fellowship. H. F. acknowledges the SFB 625 of the DFG (German Science Foundation) for valuable support.

Supporting Information

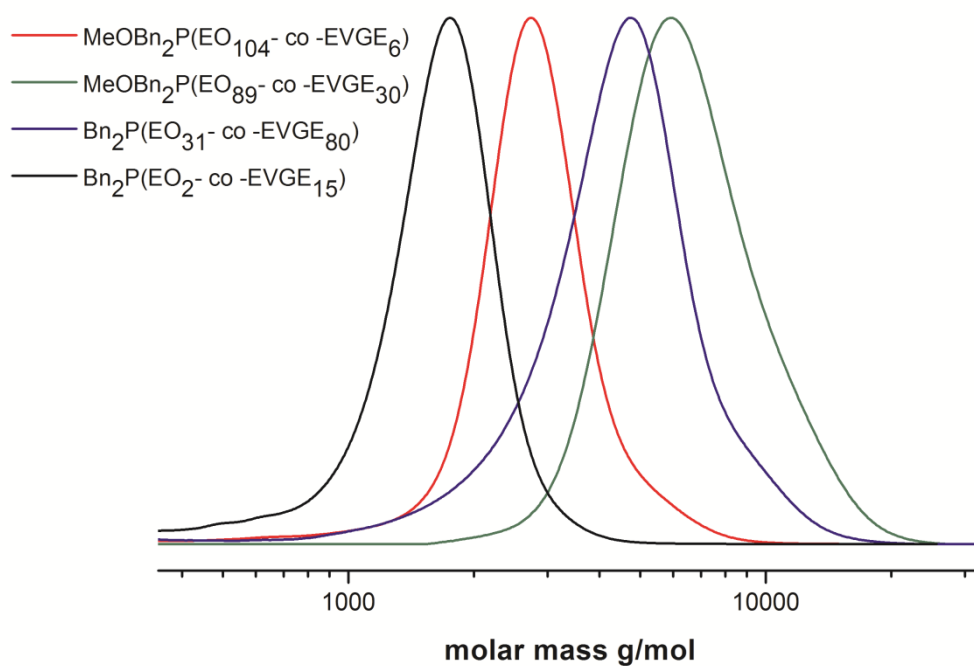


Figure S1. SEC-traces of copolymers **1**, **4**, **6** and **7** with different molecular weights and different content of EVGE.

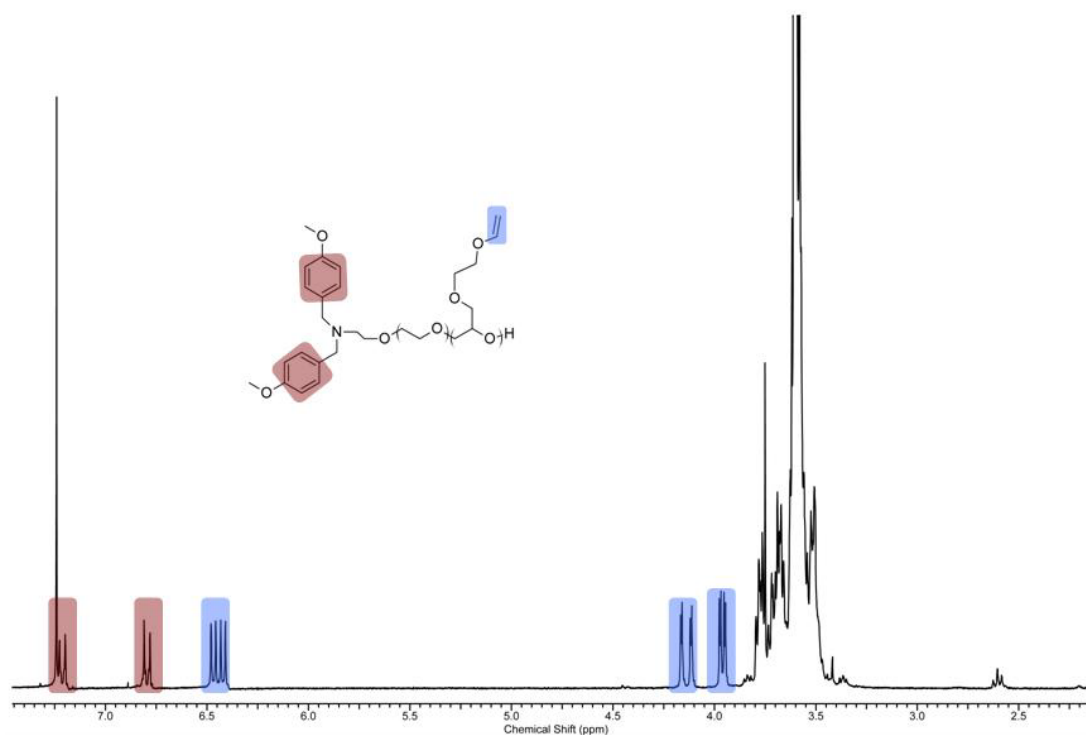


Figure S2. ¹H NMR spectrum of sample MeOBn₂NP(EO₁₀₄-co-EVGE₆)

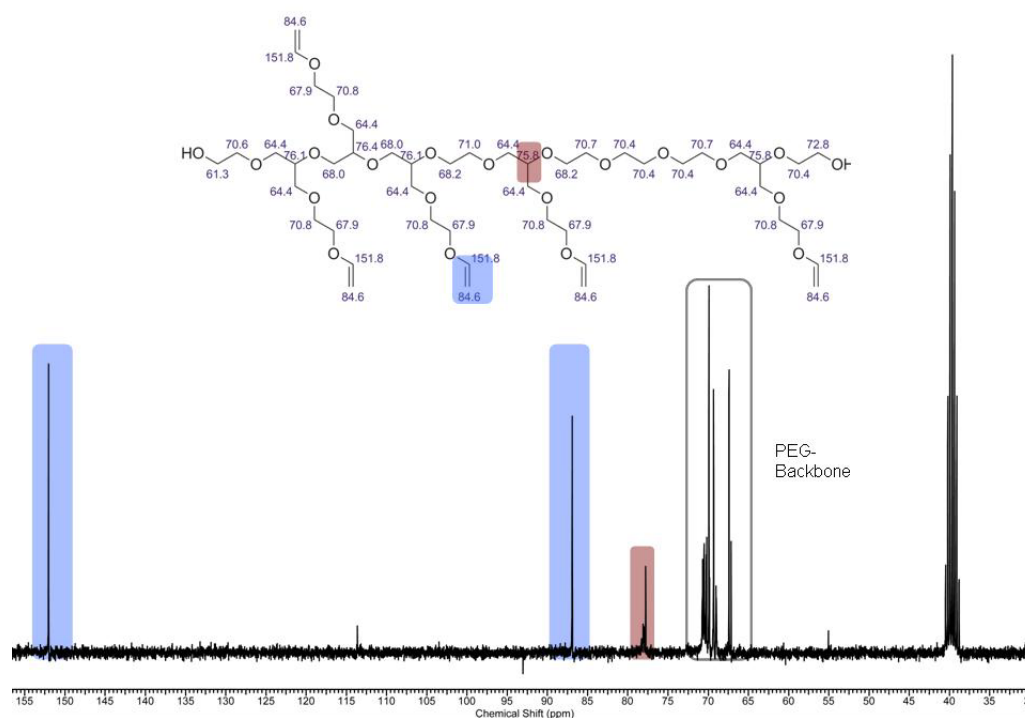


Figure S3. ¹³C-NMR spectrum of sample MeOBn₂NP(EO₈₉-co-EVGE₃₀).

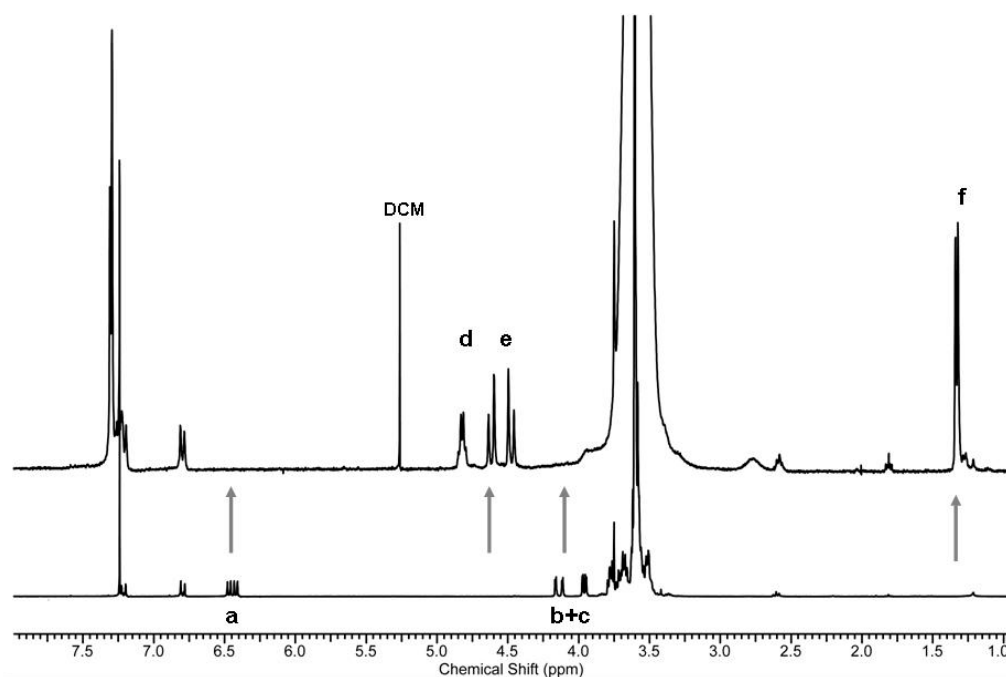


Figure S4. ¹H NMR spectrum of sample MeOBn₂NP(EO₁₁₅-EVGE₁₁) before (bottom) and after click-reaction with benzyl alcohol (top).

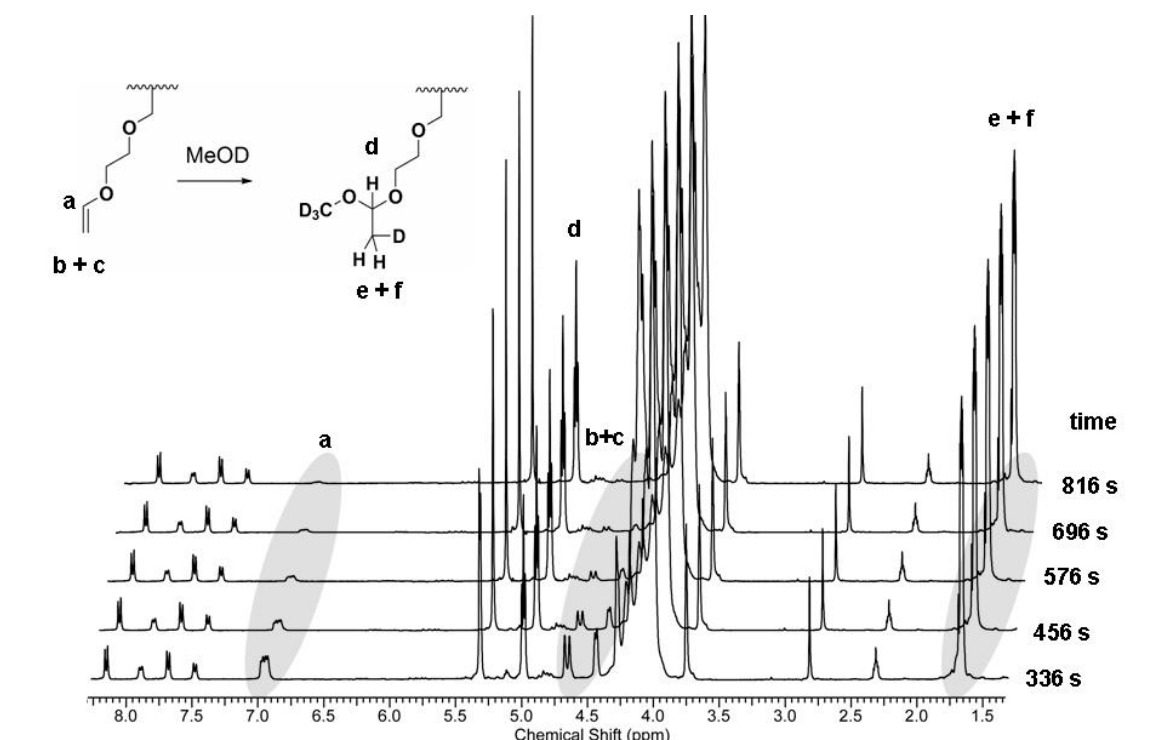


Figure S5. Reaction of copolymer **6** with MeOD (4.92 and 3.31 ppm), in the presence of PTSA (7.75, 7.28 and 2.41 ppm). THF (3.71 and 1.87 ppm) was added as additional reference. The ppm scale corresponds to the upper spectra.

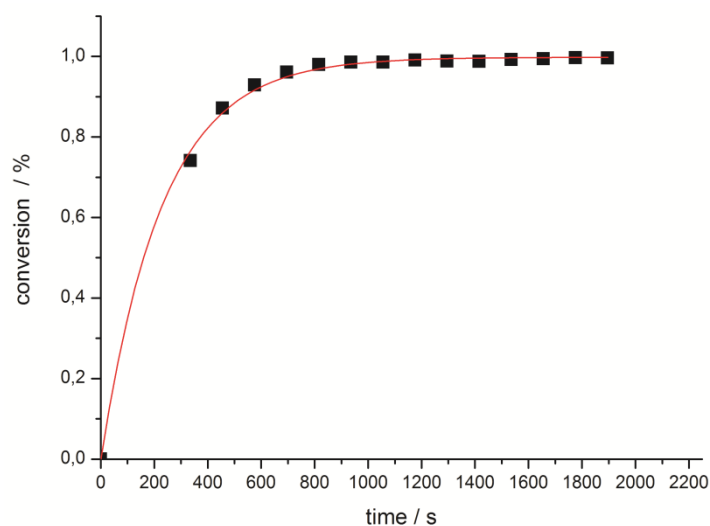


Figure S6. Plot of conversion versus time for the reaction of copolymer **6** with MeOD. Black squares: measured values; red line: exponential fit (Origin 7).

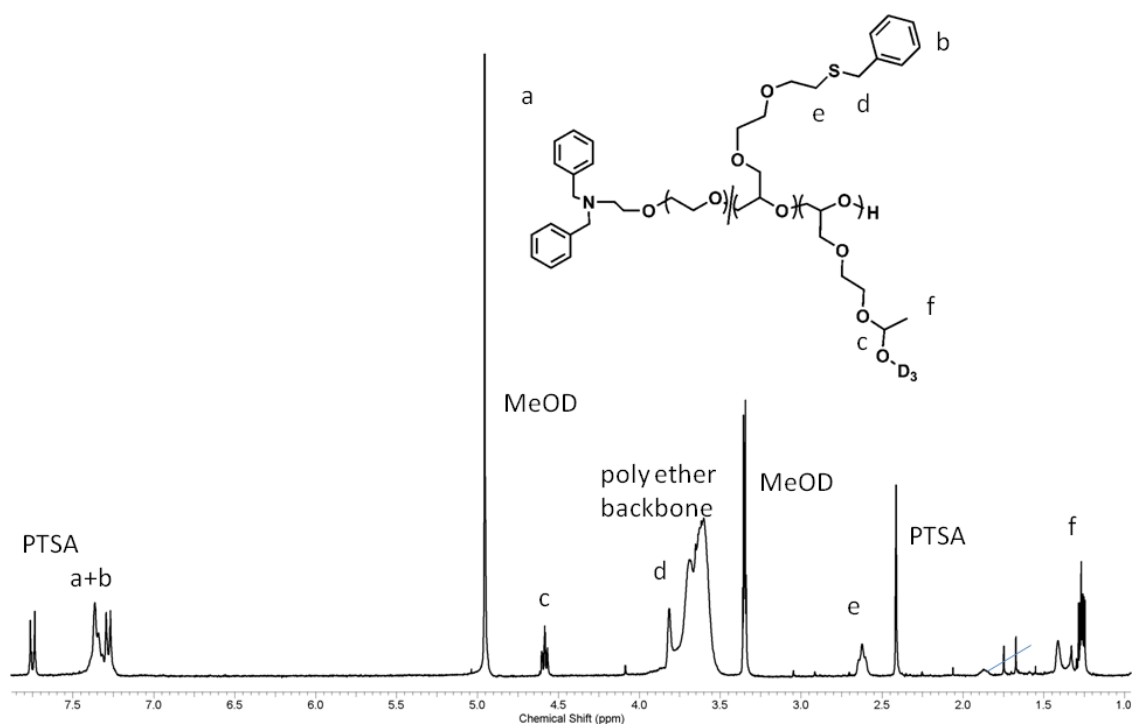


Figure S7. Copolymer **6** first used in thiol-ene click reaction and then transferred into a NMR tube containing MeOD and PTSA. The spectrum displays the non-purified product.

1. Zalipsky, S.; Harris, J. M., Introduction to Chemistry and Biological Applications of Poly(ethylene glycol). In *Poly(ethylene glycol)*, American Chemical Society: 1997; Vol. 680, pp 1-13.
2. Roberts, M. J.; Bentley, M. D.; Harris, J. M. *Adv. Drug Delivery Rev.* **2002**, 54, (4), 459-476.
3. Abuchowski, A.; McCoy, J. R.; Palczuk, N. C.; van Es, T.; Davis, F. F. *J. Biol. Chem.* **1977**, 252, (11), 3582-3586.
4. Davis, F. F. *Adv. Drug Delivery Rev.* **2002**, 54, (4), 457-458.
5. Fitton, A. O.; Hill, J.; Jane, D. E.; Millar, R. *Synthesis* **1987**, (12), 1140-1142.
6. Taton, D.; Le Borgne, A.; Sepulchre, M.; Spassky, N. *Macromol. Chem. Phys.* **1994**, 195, (1), 139-148.
7. Halacheva, S.; Rangelov, S.; Tsvetanov, C. *Macromolecules* **2006**, 39, (20), 6845-6852.
8. Dworak, A.; Panchev, I.; Trzebicka, B.; Walach, W. *Macromolecular Symposia* **2000**, 153, (1), 233-242.
9. Pang, X.; Jing, R.; Huang, J. *Polymer* **2008**, 49, (4), 893-900.

10. Huang, J.; Li, Z.; Xu, X.; Ren, Y.; Huang, J. *J. Polym. Sci., Part A: Polym. Chem.* **2006**, *44*, (11), 3684-3691.
11. Mangold, C.; Wurm, F.; Obermeier, B.; Frey, H. *Macromol. Rapid Commun.* **2010**, *31*, (3), 258-264.
12. Dworak, A.; Baran, G. y.; Trzebicka, B.; Walach, W. *React. Funct. Polym.* **1999**, *42*, (1), 31-36.
13. Dimitrov, P.; Hasan, E.; Rangelov, S.; Trzebicka, B.; Dworak, A.; Tsvetanov, C. B. *Polymer* **2002**, *43*, (25), 7171-7178.
14. Wurm, F.; Klos, J.; Räder, H. J.; Frey, H. *J. Am. Chem. Soc.* **2009**, *131*, 7954-7955.
15. Wurm, F.; Kemmer-Jonas, U.; Frey, H. *Polym. Int.* **2009**, *58*, (9), 989-995.
16. Mangold, C.; Wurm, F.; Obermeier, B.; Frey, H. *Macromolecules* **2010**, *43*, (20), 8511-8518.
17. Obermeier, B.; Wurm, F.; Frey, H. *Macromolecules* **2010**, *43*, (5), 2244-2251.
18. Li, Z.; Chau, Y. *Bioconjugate Chem.* **2009**, *20*, (4), 780-789.
19. Gauthier, M. A.; Gibson, M. I.; Klok, H.-A. *Angew. Chem.* **2009**, *121*, (1), 50-60.
20. Wurm, F.; Schüle, H.; Frey, H. *Macromolecules* **2008**, *41*, (24), 9602-9611.
21. Sunder, A.; Turk, H.; Haag, R.; Frey, H. *Macromolecules* **2000**, *33*, (21), 7682-7692.
22. Obermeier, B.; Frey, H. *Bioconjugate Chem.* **2011**, *22*, (3), 436-444.
23. Belozеров, L. E.; Stankevich, V. K.; Ezhova, L. N.; Balakhchi, G. K.; Trofimov, B. A. *Russ. J. Appl. Chem.* **1994**, *67*, 1231-1232.
24. Annekov, V. V.; Levina, A. S.; Danilovtseva, E. N.; Filina, E. A.; Mikhaleva, E. A.; Zarytova, V. F. *Russ. J. Bioorg. Chem.* **2006**, 32460-32467.
25. Ruckenstein, E.; Zhang, H. *Polym. Bull.* **2001**, *47*, (2), 113-119.
26. Wurm, F.; König, H. M.; Hilf, S.; Kilbinger, A. F. M. *J. Am. Chem. Soc.* **2008**, *130*, (18), 5876-5877.
27. Mangold, C.; Wurm, F.; Kilbinger, A. F. M., Asymmetric Micellization of Organometallic Polyether Block Copolymers. In *Non-Conventional Functional Block Copolymers*, American Chemical Society: 2011; Vol. 1066, pp 103-115.
28. Vetvicka, D.; Hruby, M.; Hovorka, O.; Etrych, T.; Vetric, M.; Kovar, L.; Kovar, M.; Ulbrich, K.; Rihova, B. *Bioconjugate Chem.* **2009**, *20*, (11), 2090-2097.
29. Mangold, C.; Dingels, C.; Obermeier, B.; Frey, H.; Wurm, F. *Macromolecules* **2011**, *44*, (16), 6326-6334.
30. Hamaide, T.; Goux, A.; Llauro, M.-F.; Spitz, R.; Guyot, A. *Angew. Makromol. Chem.* **1996**, *237*, (1), 55-77.
31. Mandelkern, L. *Chem. Rev.* **1956**, *56*, (5), 903-958.
32. Henning, T. *SOFW Journal* **2001**, *127*, 28-35.

33. Herczynska, L.; Lestel, L.; Boileau, S.; Chojnowski, J.; Polowinski, S. *Eur. Polym. J.* **1999**, 35, (6), 1115-1122.
34. Gress, A.; Völkel, A.; Schlaad, H. *Macromolecules* **2007**, 40, (22), 7928-7933.
35. Romani, F.; Passaglia, E.; Aglietto, M.; Ruggeri, G. *Macromol. Chem. Phys.* **1999**, 200, (3), 524-530.
36. Passaglia, E.; Donati, F. *Polymer* **2007**, 48, (1), 35-42.
37. Barner-Kowollik, C.; Du Prez, F. E.; Espeel, P.; Hawker, C. J.; Junkers, T.; Schlaad, H.; Van Camp, W. *Angew. Chem. Int. Ed.* **2011**, 50, (1), 60-62.
38. Mishima, E.; Yamago, S. *Macromol. Rapid Commun.* **2011**, 32, (12), 893-898.
39. Meskini, A.; Raihane, M.; Ameduri, B. *Macromolecules* **2009**, 42, (10), 3532-3539.
40. Lee, J.-Y.; Kim, M.-J.; Jin, M.-K.; Ahn, M.-R. *Bull. Korean Chem. Soc.* **1999**, (20), 1355-1358.
41. Lou, F.-W.; Xu, J.-M.; Liu, B.-K.; Wu, Q.; Pan, Q.; Lin, X.-F. *Tetrahedron Lett.* **2007**, 48, (50), 8815-8818.
42. Koyama, Y.; Umehara, M.; Mizuno, A.; Itaba, M.; Yasukouchi, T.; Natsume, K.; Suginaka, A.; Watanabe, K. *Bioconjugate Chem.* **1996**, 7, (3), 298-301.
43. Obermeier, B.; Wurm, F.; Mangold, C.; Frey, H. *Angew. Chem. Int. Ed.* **2011**, 50, (35), 7988-7997.

Chapter 3.1:

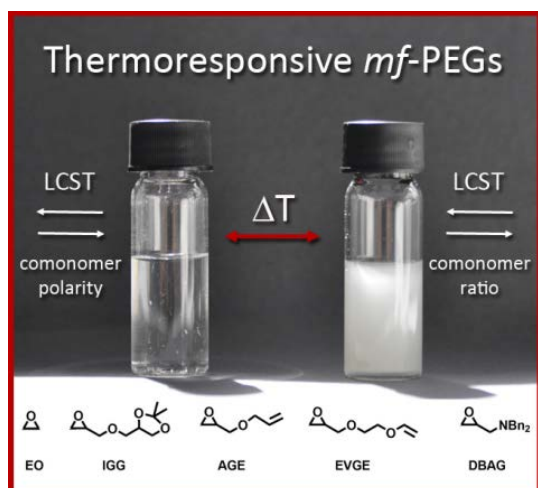
From an Epoxide Monomer Toolkit to Functional PEG Copolymers with Adjustable LCST Behavior

From an Epoxide Monomer Toolkit to Functional PEG Copolymers with Adjustable LCST Behavior

Christine Mangold, Boris Obermeier, Frederik Wurm, Holger Frey

Published in *Macromol. Rapid Commun.* **2011**, 32, (23), 1930-1934.

Novel random copolymers based on ethylene oxide and a functional comonomer exhibit stimuli responsive behavior. The solubility in water can be altered by variation of comonomer hydrophobicity as well as the comonomer content. It was possible to adjust the lower critical solution temperature in the range of 9 to 82 °C. The materials investigated in this study are promising for a variety of biomedical applications.



Keywords: copolymers, LCST, PEG, polyethers, stimuli-sensitive polymers.

Abstract

The LCST behavior of novel PEG-based copolymers bearing multiple functional groups, obtained by anionic ring-opening (co)polymerization (AROP), was investigated. Variable comonomer ratios of EO and the corresponding oxiranes IGG, EVGE, AGE or DBAG, particularly designed to implement functional groups at the PEG backbone, were found to influence the LCST behavior. Sharp transitions from translucent to opaque solutions, comparable to other well-established stimuli-responsive polymers, were observed at temperatures ranging from 9 to 82 °C. The influence of the side group hydrophobicity could be quantified by the comparison of the different copolymer systems observed.

Introduction

Thermoresponsive polymers have gathered enormous attention over the past decade, as they are promising for a variety of uses, especially in the field of biomedical applications. The most prominent polymer exhibiting thermoresponsive behavior is poly(*N*-isopropylacrylamide) (P(NIPAM)).¹ This is mainly due to its lower critical solution temperature (LCST) of 32 °C, which is close to the body temperature and the stability of this value with respect to external influences such as pH or salt concentration.² Another class of materials exhibiting LCST behavior in aqueous solutions are polymers bearing oligo(ethylene glycol) side chains.³ These macromonomer-based comb (co)polymers can either be synthesized by cationic polymerization, as it has been presented by Aoshima and coworkers,⁴ or by (controlled) radical polymerization techniques via the respective (meth)acrylates, i.e. oligo(ethylene glycol) (meth)acrylate (OEG(M)A), studied intensively by Lutz et al.⁵ These OEGMA-based materials are highly versatile, because their LCST can be tailored by the incorporation of different comonomers⁶ or end groups.⁷ Another important aspect is their excellent biocompatibility, which is in line with their poly(ethylene glycol) (PEG)-based side chain structure. Besides these two prominent examples, only a few reports focus on linear poly(glycidyl ether)s, such as poly(glycidyl methyl ether), obtained by anionic polymerization,⁸ with either block⁹- or random structures.¹⁰ In addition to these relatively simple systems, more sophisticated polyether-based architectures exhibiting LCSTs are e.g., hyperbranched¹¹ or star¹² copolymers. Dendronized polymers with PEG side chains showing LCST behavior were recently developed by Schlüter and coworkers.^{13, 14} Although there is an increasing interest in thermoresponsive polymers and their use in biomedical applications,¹⁵ one simple class of polymers has hardly been considered to date, namely random poly(ether)s based on ethylene oxide (EO) and a hydrophobic comonomer. The classical comonomer is propylene oxide (PO), and surprisingly it is rarely mentioned that random P(EO-*co*-PO) copolymers, produced on industrial scale, exhibit tunable LCSTs.^{16, 17}

Very recently, we have been able to develop a variety of different random copolymers of ethylene oxide¹⁸⁻²¹ with multiple functional groups (vicinal diols, vinyl ethers, double bonds or amines) that are randomly distributed in the PEG backbone (compare Scheme 1). These novel multifunctional (*mf*) PEGs²² are promising with respect to biomedical applications, as they are mainly comprised of PEG and permit the multiple (reversible) attachment of biomolecules, such as low molecular weight drugs. As it may be expected, with regard to the well-known PEO-PPO copolymers, these novel materials can exhibit temperature- and composition-dependent water-solubility. In this communication we describe the LCST behavior of these random copolyethers. To the best of our knowledge, this represents the first report on random copolymers based on EO and different oxiranes with a very broad range of adjustable LCSTs.

Experimental Section

Reagents

Solvents and reagents were purchased from Acros Organics, Sigma Aldrich or Fluka and used as received, unless otherwise stated.

Instrumentation

¹H NMR spectra (300 MHz) were recorded using a Bruker AC300 or a Bruker AMX400. All spectra are referenced internally to residual proton signals of the deuterated solvent. For SEC measurements in DMF (containing 0.25 g/L of lithium bromide as an additive) an Agilent 1100 Series was used as an integrated instrument, including a PSS HEMA column (10⁶/10⁵/10⁴ g/mol), a UV (275 nm) and a refractive index (RI) detector. Calibration was carried out using poly(ethylene glycol) standards provided by Polymer Standards Service.

Cloud points were determined in deionized water at varying concentration and observed by optical transmittance of a light beam ($\lambda=632$ nm) through a 1 cm sample quartz cell. The measurements were performed in a Jasco V-630 photospectrometer with a Jasco ETC-717 Peltier element. The intensities of the transmitted light were recorded versus the temperature of the sample cell. The heating/cooling rate was 1 °C min⁻¹ and values were recorded every 0.1 °C.

Results and Discussion

Anionic ring opening polymerization permits the synthesis of well-defined polyethers with narrow molecular weight distributions (MWD) as well as the precise control of molecular weight and comonomer content. All copolymers investigated in this study exhibit polydispersities (PDI, M_w/M_n) below 1.17, the major fraction even below 1.1 (compare Table 1). Such low values are often inaccessible, when employing controlled radical techniques, such as atom transfer radical (co)polymerization (ATRP) in combination with a macromonomer approach. The copolymerization of EO and the respective oxirane was carried out at elevated temperature (60-90 °C) in a sealed system, using either tetrahydrofuran, dimethyl sulfoxid or a mixture of both as solvent(s) (a detailed description can be found in literature²³). The random incorporation of the respective epoxide comonomers in the mainly PEG backbone is of great interest with respect to potential biomedical applications, since block-like structures might form undesired aggregates, whereas the random structure prevents the formation of micelles or other subordinate structures. Detailed microstructure investigation of all new copolymers has been performed, evidencing the random character of the macromolecules. (triad sequence analysis, employing ¹³C NMR and ¹H NMR kinetics of the respective copolymerizations). Although two of the three glycidyl ether comonomers (AGE and IGG), which have been investigated in ¹H NMR kinetics did show polymerization rates equal to ethylene oxide, the amine containing oxirane DBAG was found to be slightly less reactive. However, the P(EO-co-DBAG)

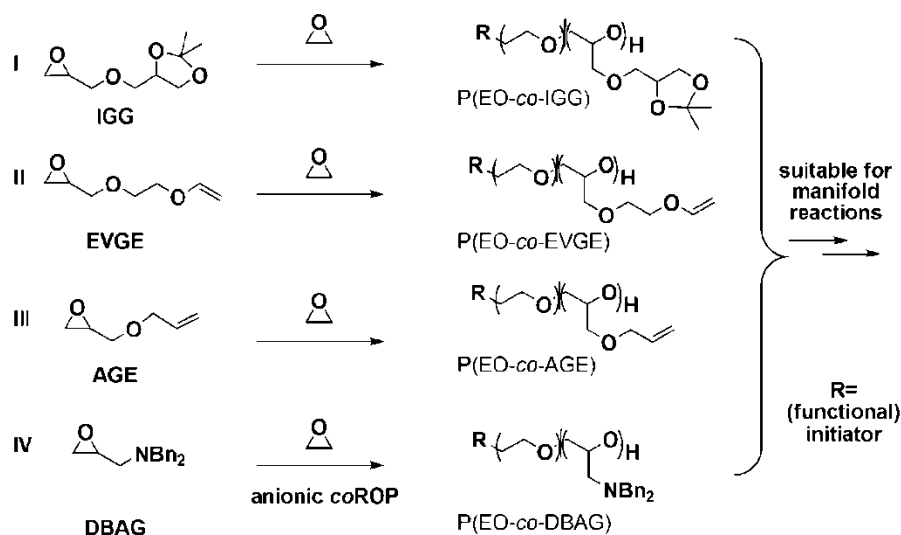
copolymers do not exhibit block-like structures, but a tapered microstructure.¹⁸ In contrast to the glycidyl ether copolymers, which exhibit a “perfect” random structure, their LCST behavior is slightly different, as it will be discussed in the following. Table 1 summarizes the key parameters of the copolymers investigated in this study.

Table 1. Copolymers investigated and their respective cloud point temperatures.

No.	Formula ^{a)}	M _n (SEC) ^{b)} g/mol	PDI ^{b)}	co. content ^{a)} %	LCST-5 ^{c)} °C	LCST-10 ^{d)} °C	LCST-20 ^{e)} °C
1	MeOBn ₂ NP(EO ₂₆₅ -CO-IGG ₂₆)	8 200	1.11	9	80.8	- ^{f)}	-
2	MeOBn ₂ NP(EO ₁₈₀ -CO-IGG ₃₂)	9 750	1.15	15	66.7	-	-
3	MeOBn ₂ NP(EO ₄₇ -CO-IGG ₁₇)	2 800	1.08	27	46.8	48.0	46.9
4	MeOBn ₂ NP(EO ₁₀₄ -CO-EVGE ₆)	2 400	1.06	5	82.5	-	-
5	MeOBn ₂ NP(EO ₁₁₅ -CO-EVGE ₁₁)	2 500	1.08	9	68.7	69.6	-
6	MeOBn ₂ NP(EO ₁₂₀ -CO-EVGE ₃₀)	5 130	1.08	20	31.1	35.3	34.3
7	MeOBn ₂ NP(EO ₈₉ -CO-EVGE ₃₀)	5 100	1.11	25	~ ^{g)}	-	-
8	Bn ₂ NP(EO ₅₂ -CO-AGE ₅)	3 900	1.13	9	72.9	74.5	73.8
9	Bn ₂ NP(EO ₁₀₂ -CO-AGE ₁₆)	4 600	1.11	14	62.4	-	-
10	MeOP(EO ₁₁₄ -CO-AGE ₂₉)	7 000	1.04	20	39.8	-	-
11	MeOP(EO ₁₁₀ -CO-DBAG ₂)	4 900	1.15	2	71.3	-	-
12	MeOP(EO ₁₁₂ -CO-DBAG ₅)	5 400	1.14	4	56.9	57.8	58.1
13	MeOP(EO ₉₀ -CO-DBAG ₁₅)	5 800	1.17	9	21.9	-	-

^{a)}obtained from ¹H NMR, ^{b)}determined by SEC measurements in DMF (RI-signal) ^{c)}5 mg mL⁻¹,

^{d)}10 mg mL⁻¹, ^{e)}20 mg mL⁻¹ solution of the copolymer in deionized water, ^{f)}values were not determined, ^{g)}estimated value obtained from cooling cycle.



Scheme 1. Copolymers investigated in this study. The comonomers used in the anionic ring opening copolymerization with EO are I) isopropylidene glyceryl glycidyl ether (IGG); II) ethoxyl vinyl glycidyl ether (EVGE); III) allyl glycidyl ether (AGE) IV) *N,N*-dibenzyl amino glycidyl (DBAG).

The cloud points of the aqueous polymer solutions have been measured by monitoring the transmittance of a light beam (wavelength 632 nm) through a 1 cm quartz sample cell at a heating (cooling) rate of $1\text{ }^{\circ}\text{C}\cdot\text{min}^{-1}$. The cloud point temperatures of the very sharp transitions from translucent to opaque solutions were defined as the value measured at 50% transmittance. The corresponding figures displaying the transmittance versus temperatures plots for different polymer samples are given in the Supporting Information (Figure S1-S4).

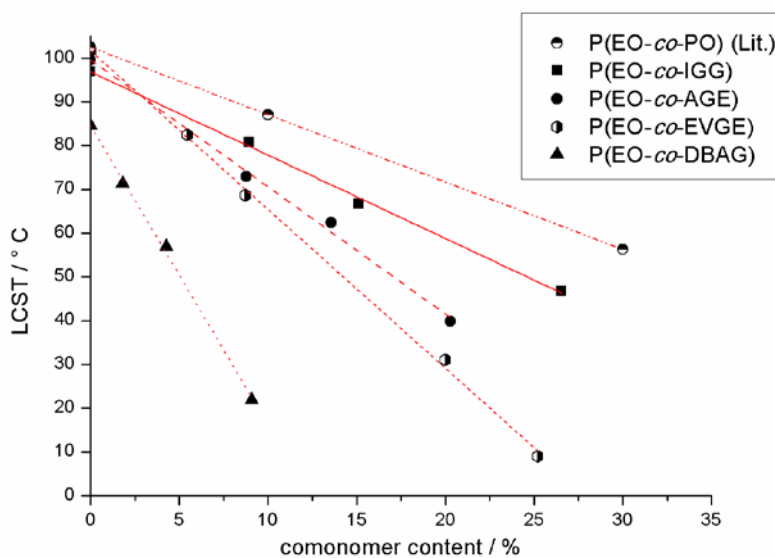


Figure 1. Comparison of LCST versus comonomer content for the different copolymer series. The values were fitted by a linear approach using Origin 8. The values for the PEO-PPO series was calculated from literature.

In the following we will refer to the LCST of the copolymers in a general sense, although we are aware that the term LCST in a strict sense corresponds to the lowest cloud point temperature possible, which is only observed at a certain concentration of a (co)polymer. However, considering the cloud point temperatures of the same copolymer (e.g., Table 1 copolymer **3**, **6**, **8** and **12**) at different concentrations, it can be stated that in the range from 5 to 20 mg mL⁻¹ (which are typical values employed for the investigation of LCST behavior) no significant change could be detected and the LCST, only varying within a few degrees, is almost constant.

A comparison of the LCSTs within one random copolymer series with varying comonomer content reveals that with increasing amount of hydrophobic comonomer incorporated into the PEG backbone the LCST (at a concentration of 5 mg mL⁻¹) decreases steadily. Plotting the LCST versus comonomer content for all different copolymer series clearly shows that this decrease follows a linear behavior (compare Figure 1). This is consistent with the previous report on linear random polyethers, based on EO and PO.¹⁷ While the slopes of the different linear fits vary with respect to the changing hydrophobicity or size of the side chains, the interceptions with the y-axis of the three glycidyl ether copolymer functions give approximately the same values, or they lie within the error margin of the average value (IGG: 97 +/- 3 °C, EVGE: 100 +/- 5 °C, AGE: 102 +/- 2 °C, PO (from literature): 102.5 °C). The interception with the y-axis yields the theoretical LCST of a polymer with 0% of comonomer incorporated (PEG homopolymer) and average value (100 °C) is in good agreement with previous experimental results on PEO-PPO-copolymers shown in Figure 1.²⁴ The interception of the y-axis of the DBAG containing copolymer on the other hand is found at 85 +/- 2 °C and the deviation of 15 °C from the homopolymer value does not lie within the error margin, but might point to another important aspect. We assume that this deviation can be explained by the slightly inhomogeneous microstructure of the DBAG-containing copolymers, leading to the different behavior, which is still linear, but slightly shifted. Thus, this LCST behavior is another indirect proof of random incorporation of the other comonomers during the copolymerization.

The x-axis interception on the other hand, which is of course dependent on the slope of the fitted functions (SI), gives the maximum amount of comonomer, which can be incorporated, until the copolymers become completely insoluble in water (or show a theoretical LCST below 0 °C). For the P(EO-co-IGG) copolymers a maximum of 50% IGG can be incorporated, whereas 34% of AGE, 27% of EVGE and only 12% of DBAG can be introduced into the PEG-backbone. It is instructive to compare these data with the established PEO-PPO copolymers. Applying the linear equation given for the P(EO-co-PO) copolymers by Louai et al.,¹⁷ the calculated x-axis interception is at 66% of PO incorporation for these systems. Other interesting benchmarks are the water solubility of a certain copolymer at room temperature (25 °C) or at body temperature (37 °C), which can easily be

calculated from the linear equation of the fitted values (obtained from Origin 8), which are all given in the Supporting Information (Figure S6-S9). These values, as well as the slopes of the fitted functions correlate with the comonomer hydrophobicity as well as the size of the side group. As it might be expected, the two bulky and hydrophobic benzyl protecting groups show the largest impact on the LCST behavior, as the LCST of the 9% sample is already at 21 °C. The smallest side group (i.e., a methyl group) in the case of PO on the other hand has the smallest influence on lowering the LCST, as it is expected from theoretical considerations. The incorporation of EVGE, which possesses a higher molecular weight side chain (ethoxy vinyl group) than the AGE monomer (allyl group), but shows a presumably similar hydrophobicity, lowers the LCST of the resulting copolymers to a greater extent than AGE. IGG, which is very bulky is an exception in this case, because the presence of oxygen atoms in the side chain enhances water solubility, and therefore the LCST is not lowered to such a strong extent as in the case of the two benzyl protecting groups of DBAG.

An important aspect with regard to biomedical applications of these water soluble multifunctional copolyethers is the influence of an enhanced ionic strength of the medium on the LCST. Thus, the LCST behavior of four copolymers (one for each copolymer series, with approximately the same comonomer content) has been investigated at different salt concentrations. Table 2 summarizes the respective results. In Figure 2 the transmittance of light versus temperature was plotted exemplarily for sample **8** at a concentration of 5 mg mL⁻¹ and with varying salt concentrations (0-10 mg mL⁻¹). An additional graph for copolymer **12** is given in the Supporting Information (Figure S5).

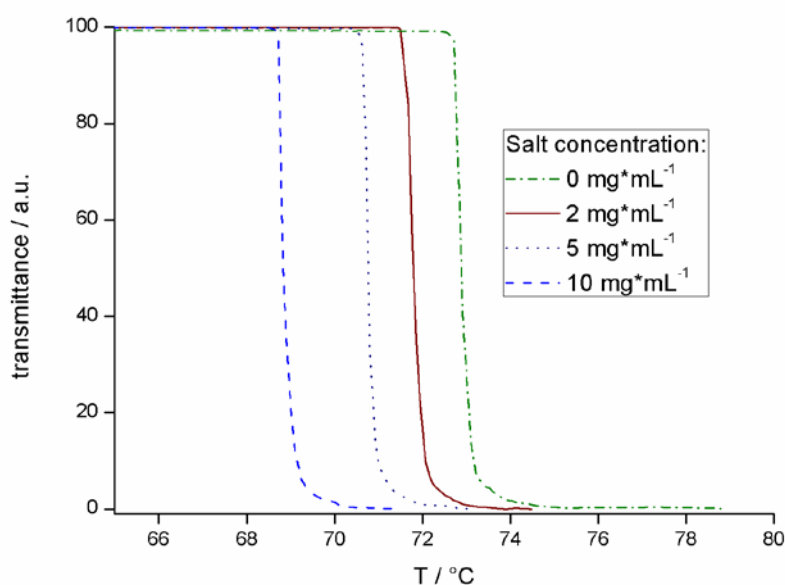


Figure 2. Intensity of transmitted laser light versus the temperature for copolymer **8** at a concentration of 5 mg mL⁻¹ (Bn₂NP(EO₅₂-co-AGE₅)) in aqueous solution with 3 different NaCl concentrations.

In general NaCl is known to lower the LCST of polymers in aqueous solutions, which is due to the disruption of the polymer hydration shell, caused by hydration structures of the salt ions.²⁵ This so-called salting out effect can be observed for a variety of salts, but also for other small molecules.²⁶

Table 2. Copolymers and their respective cloud points at different salt concentrations.

No.	Formula	LCST-0 ^{a)}	LCST-2 ^{b)}	LCST-5 ^{c)}	LCST-10 ^{d)}
		°C	°C	°C	°C
1	MeOBn ₂ NP(EO ₂₆₅ -CO-IGG ₂₆)	80.8	79.9	77.8	75.3
5	MeOBn ₂ NP(EO ₁₁₅ -CO-EVGE ₁₁)	68.7	67.5	66.6	64.4
8	Bn ₂ NP(EO ₅₂ -CO-AGE ₅)	72.9	71.8	70.8	69.6
12	MeOP(EO ₁₁₂ -CO-DBAG ₅)	56.9	56.0	51.8	49.7

Copolymers in aqueous solution with a concentration of 5 mg mL⁻¹ and a salt concentration of: ^{a)}0, ^{b)}2 mg mL⁻¹, ^{c)}5 mg mL⁻¹ and ^{d)}10 mg mL⁻¹ of NaCl.

A comparison of the cloud point temperatures of the copolymers with increasing salt concentration clearly shows that this effect is also present for the different *mf*-PEGs. By changing the salt concentration from 0 to 10 mg mL⁻¹, the LCST is lowered steadily by 2 to 7 °C, depending on the copolymer microstructure. This decrease lies within the values that are usually found for thermo-responsive polymers, such as the “gold standard” P(NIPAM). This indicates that in principle all four copolymer series are suitable for application in physiological media, because the LCSTs are retained under physiological conditions.

Conclusion

In summary, we have shown that various water-soluble functional polyethers, with a predominantly PEG-type structure, exhibit adjustable LCST behavior. In principle any desired LCST can be realized by altering the copolymer composition. In our current study a variation from 9 to 82 °C was achieved for the LCST. Furthermore, it was demonstrated that the LCST values are rather constant with respect to different polymer concentrations and that the LCST is only slightly decreased by the addition of salts. In direct comparison with well-established thermoresponsive polymers, these novel materials exhibit

promising properties for future applications, in particular in the biomedical field, such as their use in temperature-responsive hydrogels, responsive nanoparticles or drug-delivery vessels. The promise of this class of copolymers is also founded on their facile further functionalization or modification and the possibility to use them as building units of stimuli sensitive hydrogels or microgels. We are currently studying variations of the LCST upon click-functionalization of these copolymers.

Acknowledgements

The authors thank Florian Jochum for helpful discussions and Alina Mohr for technical assistance. C. M. is a recipient of a fellowship through funding of the Excellence Initiative (DFG/GSC 266). B.O. acknowledges the Fonds der Chemischen Industrie for a scholarship. F.W. thanks the Alexander-von-Humboldt foundation for a fellowship. H. F. acknowledges the SFB 625 of the DFG (German Science Foundation) for valuable support.

Supporting Information

General Copolymerization Procedure

N,N-di(*p*-methoxy-benzyl)-2-amino ethanol (or dibenzyl(amino ethanol), or methoxy-ethanol) was dissolved in benzene in a 250 mL-Schlenk flask and 0.9 eq. of cesium hydroxide were added. The mixture was stirred at RT under argon for 3 h and evacuated at (10^{-2} mbar) for 12 h to remove benzene and water, forming the corresponding cesium alkoxide. 20 mL of dry THF was then cryo-transferred into the Schlenk flask to dissolve the partially deprotonated initiator. In some cases, especially when copolymerizing AGE and DBAG DMSO was added as well. Ethylene oxide was then first cryo-transferred to a graduated ampoule, and then into the reaction flask (around -80 °C). The second comonomer (IGG, EVGE, DBAG or AGE, respectively) was added via syringe and the mixture was heated to 90 °C and stirred for 24-71 h. Precipitation in cold diethyl ether resulted in the desired copolymers. For polymers with a high fraction of the hydrophobic comonomer, the polymer solution was dried *in vacuo*. Yields: 95% to quantitative. ^1H NMR can be found in the SI.

^1H NMR:

P(EO-*co*-IGG). ^1H NMR (300 MHz, DMSO- d_6 , δ): 7.24, 6.87 (d, $\text{C}_6\text{H}_4\text{OMe}$), 4.16 (m, acetal-*H*), 3.98 (t, *CHH*-acetal), 3.74 (s, $\text{C}_6\text{H}_4\text{OMe}$), 3.68-3.34 (polyether backbone) 1.3 (d, CH_3 acetal) ppm.

P(EO-*co*-EVGE). ^1H NMR (300 MHz, DMSO- d_6 , δ): 7.24, 6.87 (8H, d, $\text{C}_6\text{H}_4\text{OMe}$) in the case of *p*-methoxybenzyl-; without methoxy-group: 7.40-7.15 (10H, m, aromatic), 6.48 (1H/EVGE-unit, dd, $\text{CH}=\text{CH}_2$), 4.16 (1H/EVGE-unit, dd, $\text{CH}=\text{CHH}$), 3.95 (1H/EVGE-unit, dd, $\text{CH}=\text{CHH}$), in the case of methoxy-benzyl: 3.74 (s, $\text{C}_6\text{H}_4\text{OMe}$), 3.68-3.34 (m, polyether backbone), 2.54 (2H, t, $\text{Bn}_2\text{NCH}_2\text{CH}_2\text{O}$ -) ppm.

P(EO-*co*-AGE). ^1H NMR (300 MHz, DMSO- d_6 , δ): 7.38 - 7.16 (10 H, m, aromatic), 5.93-5.77 (1H/AGE unit, m), 5.15 (1H/AGE unit, dd), 3.93 (1H/AGE unit, dd), 3.68-3.34 (polyether backbone) ppm.

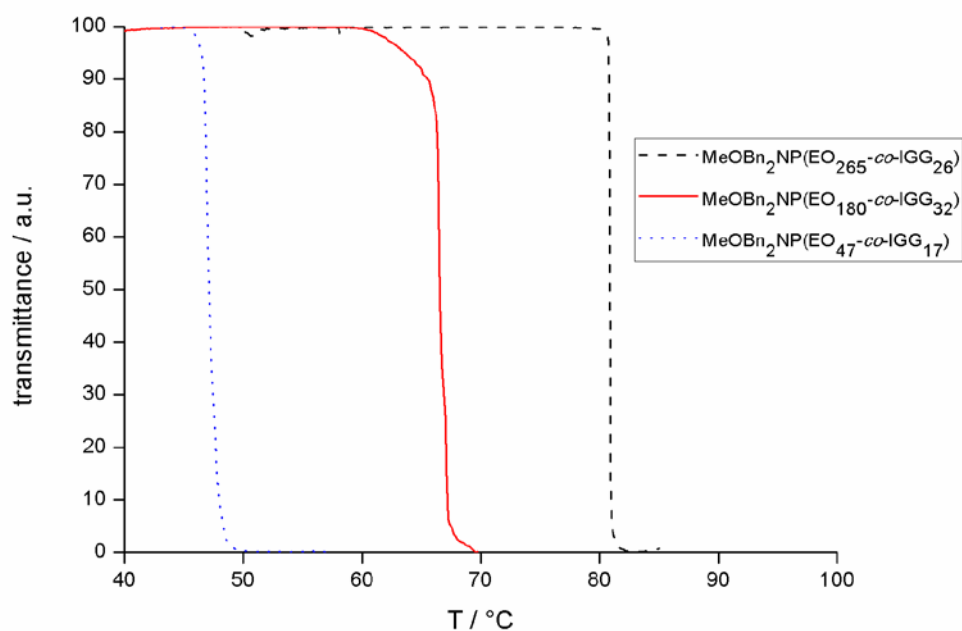


Figure S1. Intensity of transmitted laser light versus the temperature for the copolymer series P(EO-co-IGG) at a concentration of 5 mg mL⁻¹.

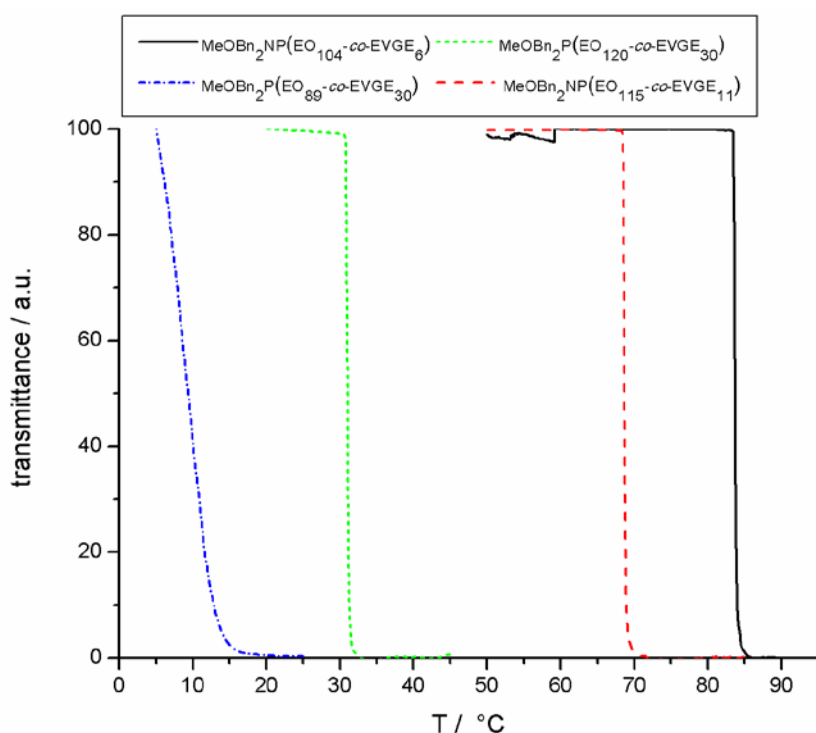


Figure S2. Intensity of transmitted laser light versus the temperature for the copolymer series P(EO-co-EVGE) at a concentration of 5 mg mL⁻¹. The LCST of copolymer 4 could only be estimated, due to water condensation at the quartz cuvette, which disrupted the measurement.

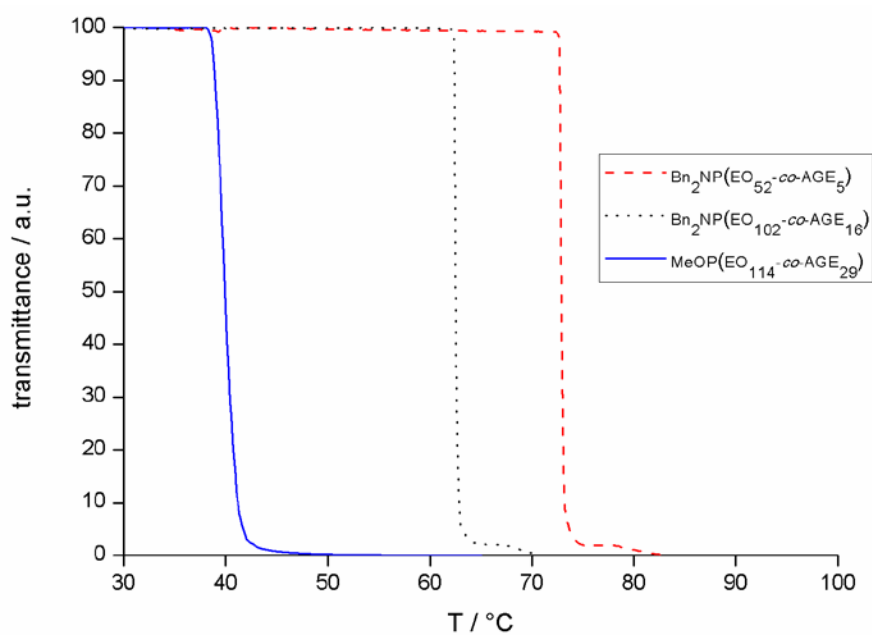


Figure S3. Intensity of transmitted laser light versus the temperature for the copolymer series P(EO-co-AGE) at a concentration of 5 mg mL⁻¹.

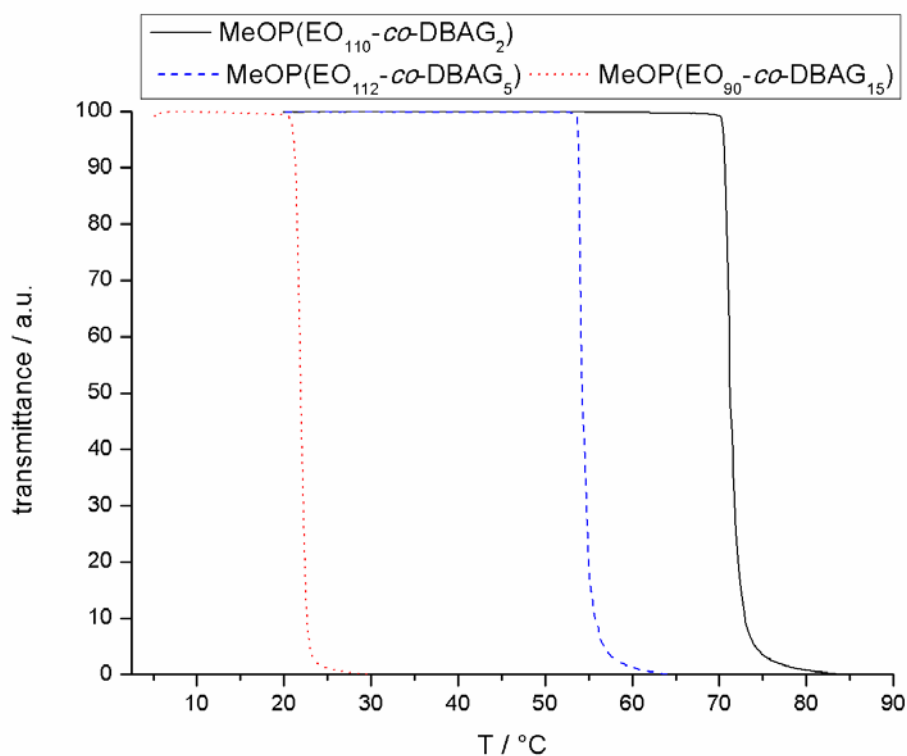


Figure S4. Intensity of transmitted laser light versus the temperature for the copolymer series P(EO-co-DBAG) at a concentration of 5 mg mL⁻¹.

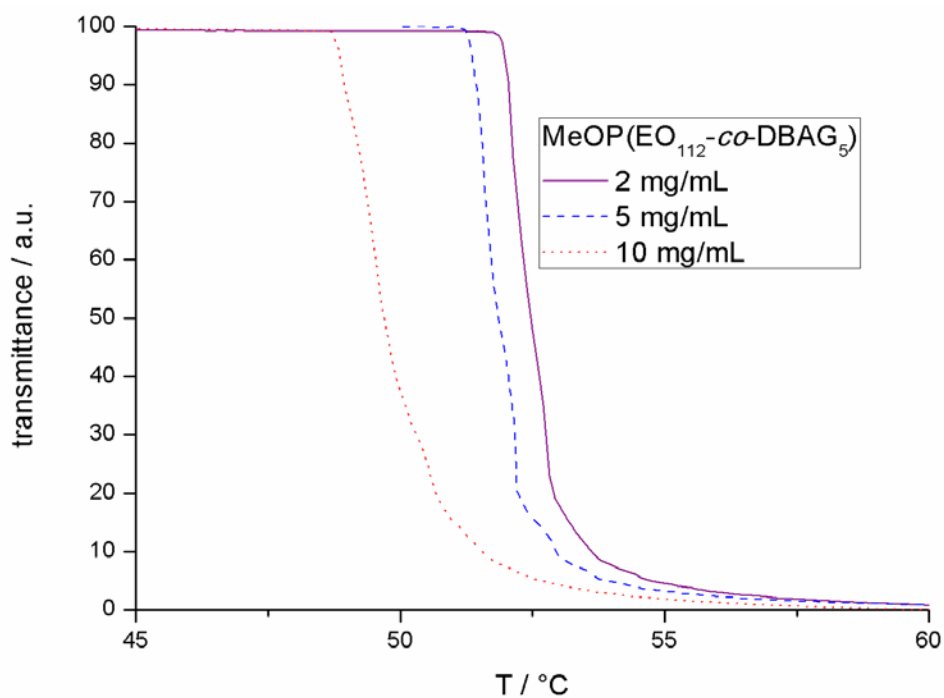


Figure S5. Intensity of transmitted laser light versus the temperature for copolymer **12** at a concentration of 5 mg mL^{-1} ($\text{MeOP}(\text{EO}_{112}\text{-co-DBAG}_5)$) in aqueous solution with 3 different NaCl concentrations.

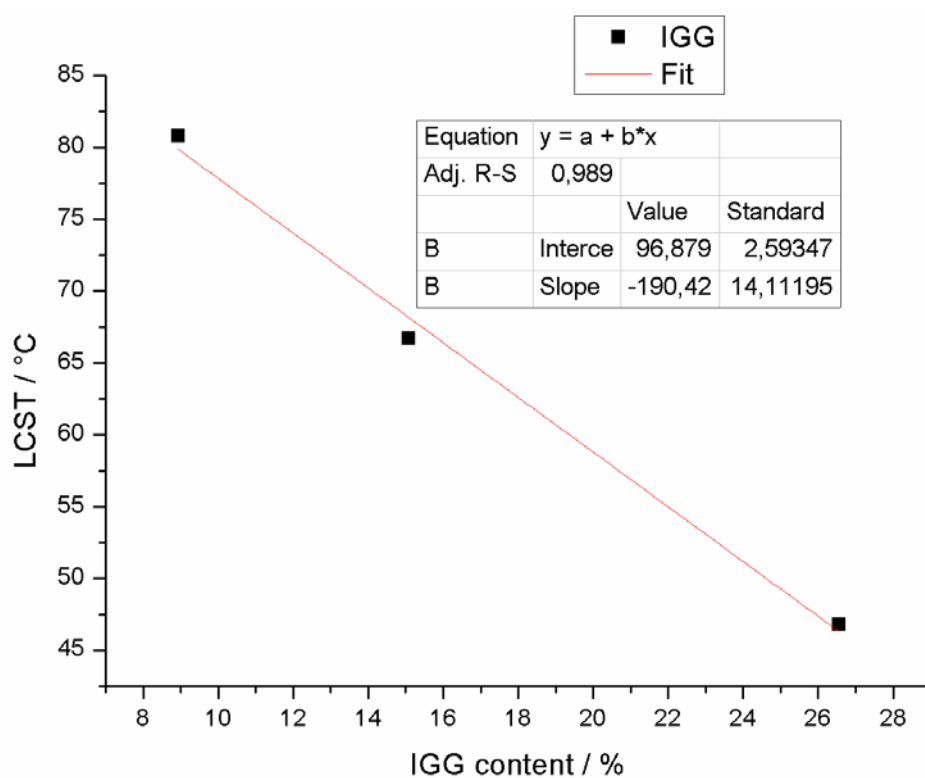


Figure S6. LCST versus IGG content and the corresponding linear fit obtained from Origin 8.

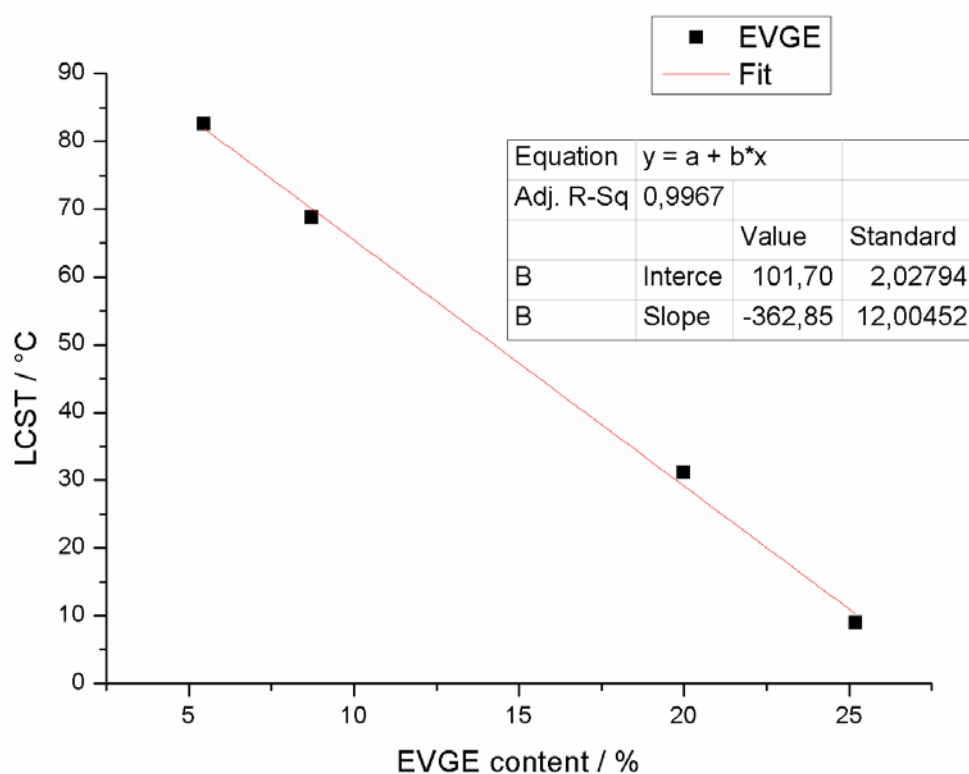


Figure S7. LCST versus EVGE content and the corresponding linear fit obtained from Origin8.

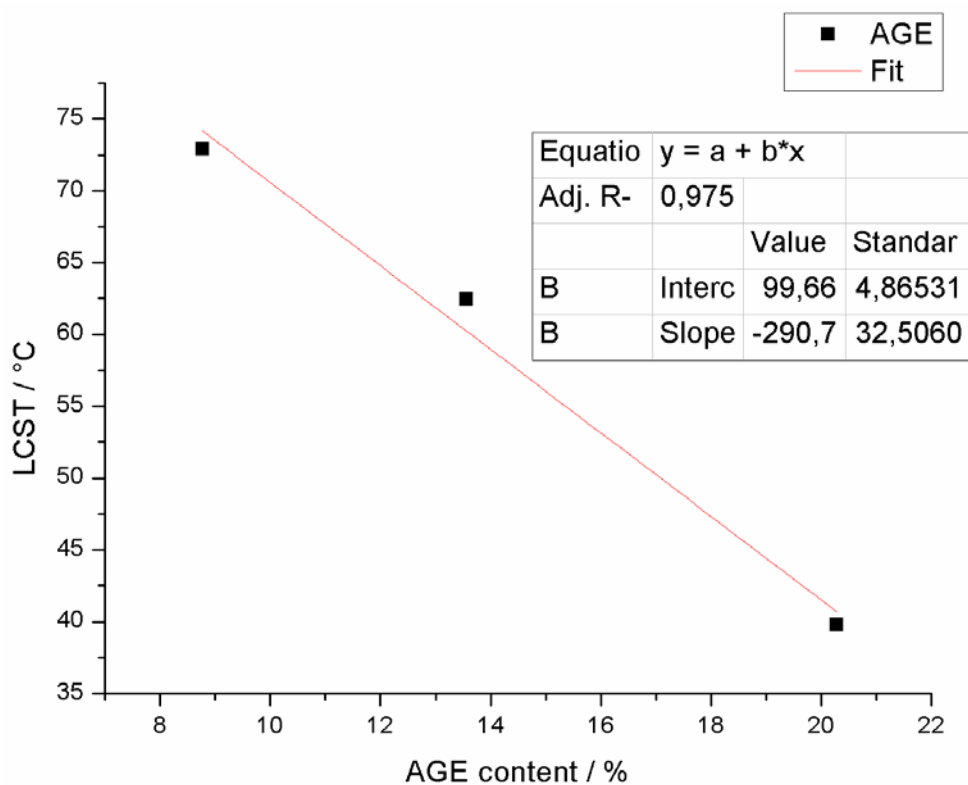


Figure S8. LCST versus AGE content and the corresponding linear fit obtained from Origin8.

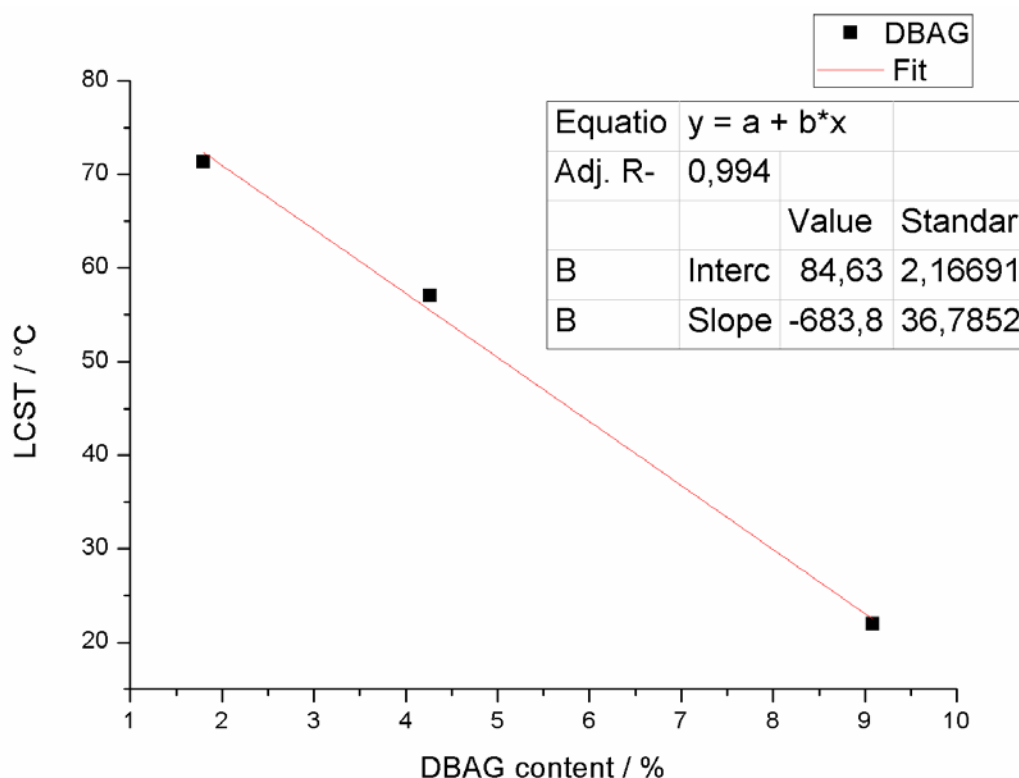


Figure S9. LCST versus DBAG content and the corresponding linear fit obtained from Origin8.

- Schild, H. G. *Prog. Polym. Sci.* **1992**, 17, (2), 163-249.
- Lutz, J.-F.; Akdemir, Ö.; Hoth, A. *J. Am. Chem. Soc.* **2006**, 128, (40), 13046-13047.
- Sugihara, S.; Hashimoto, K.; Okabe, S.; Shibayama, M.; Kanaoka, S.; Aoshima, S. *Macromolecules* **2003**, 37, (2), 336-343.
- Sugihara, S.; Kanaoka, S.; Aoshima, S. *Macromolecules* **2004**, 37, (5), 1711-1719.
- Lutz, J.-F. *Adv. Mater.* **2011**, 23, 2237-2243.
- Lutz, J.-F. o.; Hoth, A. *Macromolecules* **2005**, 39, (2), 893-896.
- Roth, P. J.; Jochum, F. D.; Forst, F. R.; Zentel, R.; Theato, P. *Macromolecules* **2010**, 43, (10), 4638-4645.
- Aoki, S.; Koide, A.; Imabayashi, S.-i.; Watanabe, M. *Chem. Lett.* **2002**, 31, (11), 1128-1129.
- Dimitrov, P.; Rangelov, S.; Dworak, A.; Tsvetanov, C. B. *Macromolecules* **2004**, 37, (3), 1000-1008.
- Weinhart, M.; Becherer, T.; Haag, R. *Chem. Commun.* **2011**, 47, (5), 1553-1555.
- Xia, Y.; Wang, Y.; Wang, Y.; Wang, D.; Deng, H.; Zhuang, Y.; Yan, D.; Zhu, B.; Zhu, X. *Macromol. Chem. Phys.* **2011**, 212, 1056-1062.
- Libera, M.; Trzebicka, B.; Kowalczyk, A.; Walach, W.; Dworak, A. *Polymer* **2011**, 52, (2), 250-257.

13. Li, W.; Wu, D.; Schlüter, A. D.; Zhang, A. *J. Polym. Sci., Part A: Polym. Chem.* **2009**, *47*, (23), 6630-6640.
14. Junk, M. J. N.; Li, W.; Schlüter, A. D.; Wegner, G.; Spiess, H. W.; Zhang, A.; Hinderberger, D. *Macromol. Chem. Phys.* **2011**, *212*, (12), 1229-1235.
15. Gil, E. S.; Hudson, S. M. *Prog. Polym. Sci.* **2004**, *29*, (12), 1173-1222.
16. Bailey, F. E.; Callard, R. W. *J. Appl. Polym. Sci.* **1959**, *1*, (1), 56-62.
17. Louai, A.; Sarazin, D.; Pollet, G.; François, J.; Moreaux, F. *Polymer* **1991**, *32*, (4), 703-712.
18. Obermeier, B.; Wurm, F.; Frey, H. *Macromolecules* **2010**, *43*, (5), 2244-2251.
19. Mangold, C.; Wurm, F.; Obermeier, B.; Frey, H. *Macromolecules* **2010**, *43*, (20), 8511-8518.
20. Obermeier, B.; Frey, H. *Bioconjugate Chem.* **2011**, *22*, (3), 436-444.
21. Mangold, C.; Dingels, C.; Obermeier, B.; Frey, H.; Wurm, F. *Macromolecules* **2011**, *44*, (16), 6326-6334.
22. Obermeier, B.; Wurm, F.; Mangold, C.; Frey, H. *Angew. Chem. Int. Ed.* **2011**, *50*, (35), 7988-7997.
23. Mangold, C.; Wurm, F.; Obermeier, B.; Frey, H. *Macromol. Rapid Commun.* **2010**, *31*, (3), 258-264.
24. Malcolm, G. N.; Rowlinson, J. S. *Trans. Faraday Soc.* **1957**, *53*, 921-931.
25. Van Durme, K.; Rahier, H.; Van Mele, B. *Macromolecules* **2005**, *38*, (24), 10155-10163.
26. Bergbreiter, D. E. *Chem. Rev.* **2002**, *102*, (10), 3345-3384.

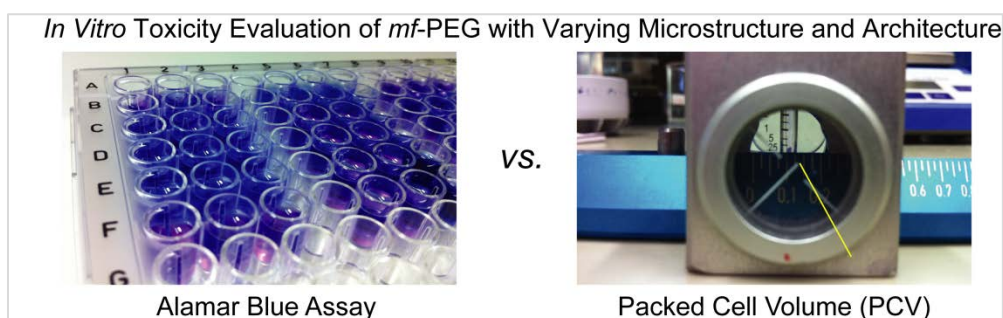
Chapter 3.2:

In Vitro Toxicity Evaluation of mf-PEGs with Varying Microstructure and Architecture

In Vitro Toxicity Evaluation of mf-PEGs with Varying Microstructure and Architecture

Christine Mangold, Richard Oakley, Holger Frey, Florian M. Wurm, Frederik R. Wurm

To be submitted to *Biomaterials*.



Keywords: toxicity, PEG, multifunctional PEG, polyglycerol, polyether

Abstract

Cytotoxicity of several multifunctional poly(ethylene glycol) (*mf*-PEG) copolymers is reported against chinese hamster ovary cells (CHO). Block copolymers with varying polymer architecture and random PEG copolymers with different glycidyl ether-based comonomers are compared. These *mf*-PEGs exhibit additional functionalities in comparison to PEG homopolymers, such as hydroxyl-, allyl-, vinyl-, or amine-moieties. The data is evaluated via the Alamar Blue staining technique and the packed cell volume (PCV) method. In this context not only the different polymers with structural variations at different concentrations and incubation times have been assessed, but also the two different evaluation methods and the comparability of the results obtained. Both methods demonstrate that random copolymers exhibit similarly low toxicity as the standard PEG, while block copolymers show slightly higher toxicity, which can be assigned to the aggregation behavior. In addition, the data confirms that the experimentally more convenient and rapid PCV method provides reliable results for the cytotoxicity of polymers.

Introduction

The understanding of interactions between synthetic compounds and biological systems is a crucial issue for the development of new materials for therapeutics, regenerative medicine or diagnostic purposes.¹ Polymer chemistry offers the possibility to design modern drug carrier conjugates for combating several diseases. The most prominent example is the well-established “PEGylation” (attachment of (multiple) poly(ethylene glycol) (PEG) chains) of pharmaceutically relevant proteins, peptides or low molecular weight drugs.² Polymer conjugation allows for targeted delivery and guarantees prolonged plasma half-life times.³ These challenges call for synthetic strategies that allow precise control over molecular weight, molecular weight distribution (MWD), functionality and architecture of the respective polymers. One of the most important tasks lies in the development of methods to enable site and/or residue specific conjugation of synthetic polymers to peptides, proteins or other biomolecules.⁴

PEG, which exhibits low toxicity and antigenicity,⁵ is used in most biomedical applications. A main reason for that is also the good solubility of PEG in most organic solvents and water. However, its limited loading capacity is often a drawback as the linear polymer chain offers a maximum of two conjugation sites. One possibility to increase the functionality of PEG is the synthesis of block-copolymers,⁶⁻⁹ which often implies undesired amphiphilicity. In some cases, multi-step syntheses are required. A quite novel, potential PEG-substitute which offers a high number of functional groups is poly(glycerol) (PG). PG has been reported to exhibit a similar toxicity profile as PEG.^{10, 11} However, due to the multiple hydroxyl groups in the polymer structure, solubility problems can occur especially, if hydrophobic drug molecules are attached. Besides, the number of functional groups is directly dependent on the molecular weight and cannot be adjusted without changing the molecular weight of the polymer. This problem can be overcome by the synthesis of double hydrophilic di- and triblock copolymers with tailored architecture, e.g., PEG-*block*-PG^{9, 12} or by the random copolymerization of glycidol with ethylene oxide, as presented recently by our group.¹³ In recent work the linear and branched copolymers of EO and glycidol have been reported to show similar toxicity as PEG.^{13, 14}

Other PEG-analogues have also been reported, mainly via radical polymerization of methacrylate monomers, such as oligoethylene glycol methacrylate.¹⁵ However, this common approach results in comb-polymers with a methacrylate backbone and an ester linkage with the PEG-combs, which may be susceptible to hydrolysis. Moreover, in the case of the copolymerization of different methacrylates often gradient or block like copolymers are obtained, due to differing copolymerization behavior of methacrylates with different substituents.¹⁶

Another approach for enhancing the functionality of PEG without introducing amphiphilicity is the random copolymerization with another comonomer that bears a protected functional group,¹⁷⁻¹⁹ or a

functionality that is stable towards the highly basic conditions of anionic ring opening polymerizations (AROP).²⁰ These in-chain functionalities can then be used to increase the number of drug molecules loaded on the polymeric carrier and present an interesting strategy for a polymer therapeutic, so called multifunctional PEGs (*mf*-PEGs). Our group has focused on the synthesis of different *mf*-PEGs²¹ by anionic copolymerization of ethylene oxide and comonomers based on glycidol or glycidyl ethers.

In recent years we have investigated several monomers, such as ethoxy ethyl glycidyl ether (EEGE),²² isopropylidene glyceryl glycidyl ether (IGG),¹⁹ ethoxy vinyl glycidyl ether (EVGE),²⁰ and dibenzylamino glycidol (DBAG).¹⁸ Detailed ¹³C NMR and triad analysis of the comonomer distribution and online ¹H NMR monitoring the decay of both monomers in the course of the polymerization were carried out to investigate the microstructure of the materials.²¹ A very interesting feature of these EO copolymerizations is the proven random character of the resulting *mf*-PEGs in most cases. Only the copolymerization of EO with DBAG, which exhibits bulky benzyl protecting groups led to a copolymer exhibiting a slightly tapered microstructure. This type of microstructure might also be a general feature of epoxides with amine moieties. Very recently, we were able to show that all the above mentioned random copolymers exhibit a lower critical solution temperature (LCST), which can be adjusted by the copolymer ratio and the comonomer hydrophobicity over a broad range of temperatures.²³

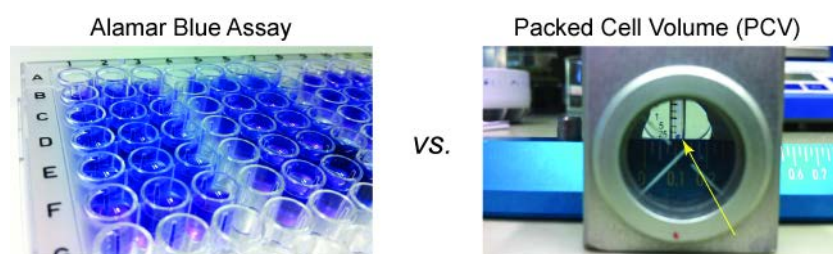
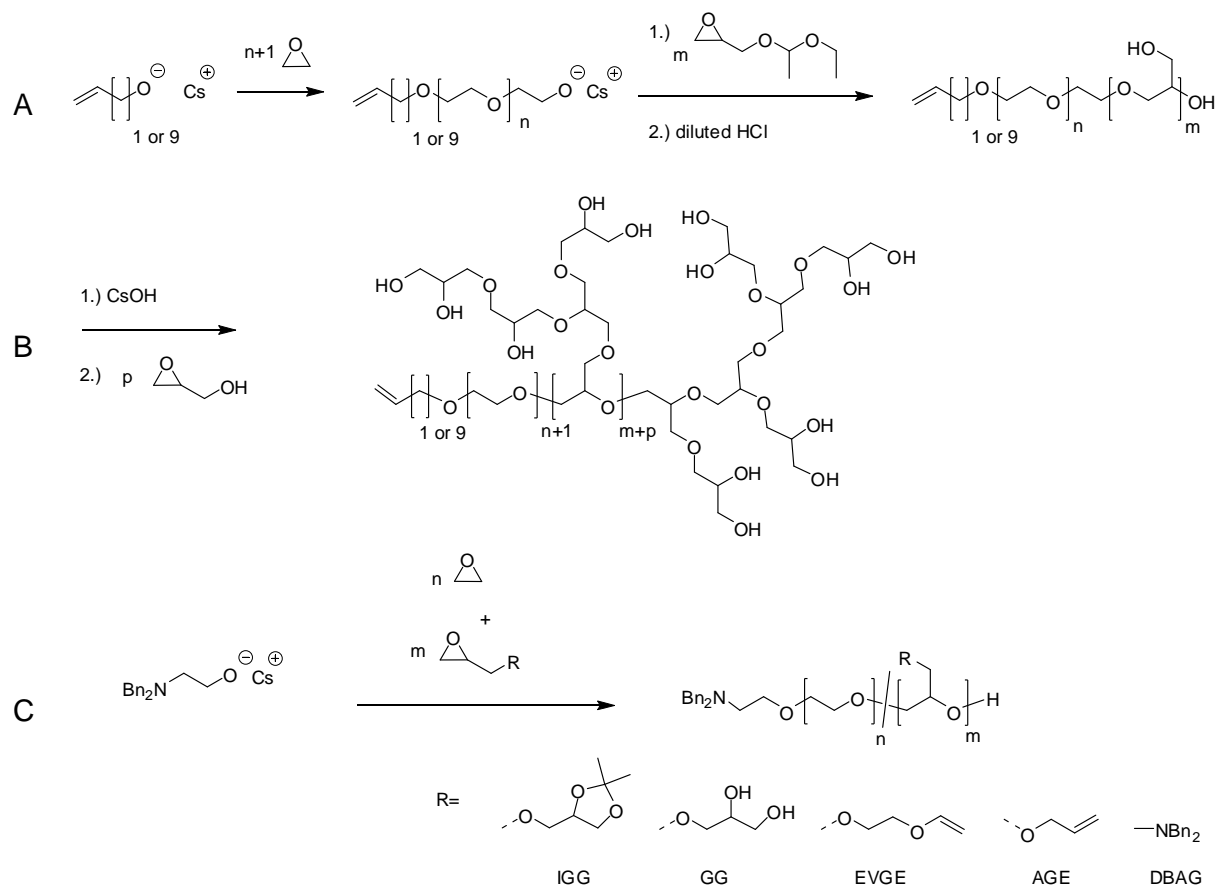


Figure 1: Alamar Blue assay for cytotoxicity in a 96 well plate vs. packed cell volume method for determination of the cell numbers (note: the yellow arrow marks the height of the cell cake in the test tube).

This paper presents the toxicity studies of several *mf*-PEGs with varying macromolecular architecture. We report on the abovementioned linear PEG copolymers, linear PEG-based block copolymers, and linear-hyperbranched block copolymers bearing a single double bond at the linear chain end. For cytotoxicity, PEG and hyperbranched PEGs of different molecular weight were used as reference materials. To the best of our knowledge this is the first report on a systematic, architecturally diverse library of PEG-copolymers with respect to their cytotoxicity. The toxicity of the polymers has been investigated against Chinese hamster ovary (CHO) cells at varying polymer concentrations and time

periods after incubation at 37 °C. The cell numbers were determined by the well-established Alamar blue staining protocol²⁴ for counting viable cells (a measure of mitochondrial activity) with the much more convenient packed cell volume (PCV) method which is the typical method for the determination of the hematocrit value in blood tests (Figure 1) and affords less time as well as experimental effort.²⁵



Scheme 1: Synthetic protocol to *mf*-PEGs prepared in this study, showing the functional groups introduced at the PEG backbone.

Experimental Part

Materials

All solvents and reagents were purchased from Acros Organics and used as received, unless otherwise stated. Chloroform-*d*₁ and DMSO-*d*₆ were purchased from Deutero GmbH. 1,2-Isopropylidene glyceryl glycidyl (IGG),²⁶ ethoxy ethyl glycidyl ether (EEGE),⁷ ethoxy vinyl glycidyl ether (EVGE),²⁰ and dibenzyl amino glycidol (DBAG)¹⁸ were prepared according to recent literature,

dried over CaH_2 , and freshly distilled before use. Polymerization was conducted as reported previously.^{8, 18, 20}

Instrumentation

^1H NMR spectra (300 and 400 MHz) were recorded using a Bruker AC300 or a Bruker AMX400. All spectra were referenced internally to residual proton signals of the deuterated solvent. For SEC measurements in DMF (containing 0.25 g/L of lithium bromide as an additive) an Agilent 1100 Series was used as an integrated instrument, including a PSS HEMA column ($10^6/10^5/10^4$ g/mol), a UV (275 nm) and a RI detector. Calibration was carried out using poly(ethylene oxide) standards provided by Polymer Standards Service

Cell studies, toxicity and degradation studies

Cell culture. Suspension cell cultures of CHO DG44 cells were maintained in square-shaped glass flasks (250 mL) in serum free ProCHO5 cell culture medium (CCM) (Lonza AG, Verviers, Belgium) supplemented with $13.6 \text{ mg}\cdot\text{L}^{-1}$ hypoxanthine, $3.84 \text{ mg}\cdot\text{L}^{-1}$ thymidine and 4 mM glutamine (SAFC Biosciences, St. Louis, MO) as described by Muller et al.²⁷ Cell culture was maintained at 37 °C in a 95% humidified incubator with 5% CO_2 . The cells were passaged every 3 days at a seeding density of $3 \times 10^5 \text{ cells}\cdot\text{mL}^{-1}$.

In vitro assessment of cytotoxicity. In vitro cell viability was investigated against CHO DG44 cells after 3, 5 and 7 days incubation at 37 °C at varying concentrations (0.5 g/L, 1 g/L, 5 g/L) of the respective polymer and was performed as follows. On the day of the experiment, cells were centrifuged and resuspended in ProCHO5 medium to achieve a cell density of $250\,000 \text{ cells}\cdot\text{mL}^{-1}$ in TubeSpin[®] bioreactor 50 tubes (TubeSpin; TPP, Trasadingen, Switzerland). Then, different sterilized 96-well plates (for the different time intervals) were charged with each 50 μL of the cell suspension. The solution was mixed with the appropriate polymer sample dissolved in Milli Q water to afford a polymer concentration in the culture medium of 0.5, 1, or 5 g/L or diluted by the addition of 200 μL Milli Q water (for the control). The well-plate was placed in an incubator for the desired time-interval. Each experiment was carried out as three independent replicates.

AlamarBlue assay:

25 μL of the 10% Alamar blue working solution (Serotec, Oxon, UK) in PBS were added to each well and left for 3 hours in a dark, humidified incubator (37 °C, 5% CO_2). Then, the absorbance was measured by at 540 and 630 nm on a FLUOstar OPTIMA multidetection microplate reader. Calibration was achieved by measuring cell suspensions with known cell numbers and plotted against the read-out.

Packed cell volume:

For PCV measurements, 200 μL of a suspension culture were transferred into a mini PCV tube (Techno Plastics ProductsAG, Trasadingen, Switzerland). The tubes were centrifuged in a

microcentrifuge (Model 5417C, Eppendorf AG, Hamburg, Germany) fitted with a swinging-bucket rotor (Model A-8-11, Eppendorf AG) for 1 min at 2,500g (5,000 rpm) unless otherwise mentioned. For determining the height of the cell pellet, a visual assessment was made using the capillary graduation.

Results and Discussion

A: Polymer Characterization

PEGylation of proteins and other drugs has become a major strategy for combating diseases such as hepatitis or cancer.²⁸ In order to evaluate, whether the newly designed *mf*-PEGs with varying microstructure and architecture are suitable for future drug conjugation and potential application *in vivo*, this paper investigates their cytotoxicity and compares the results to the well-established PEG and the proven biocompatible hyperbranched PG. A famous example for the dependence on architectural variations for a simple polymer structure like PEG on the pharmacological profile of a protein-polymer conjugate, is PEGasys, which is PEGylated interferon.²⁹ This protein is available in two forms, the linear PEGylated and the branched PEGylated protein and it was reported that the branched structure of PEG improves the plasma-half life time of the conjugate significantly. This implies that polymer architecture plays an important role in tailoring the properties of protein-polymer conjugates²⁹ and it is therefore important to investigate the influence of architectural differences on the cytotoxicity.

The polymers were synthesized via anionic ring-opening polymerization (AROP) of EO and the respective comonomers, either applying random copolymerization or by sequential monomer addition in the case of block copolymers. The living character of the anionic ROP permits the synthesis of polymers with narrow molecular weight distributions, which represents one key requirement of polymers for biomedical uses. Linear and linear-hyperbranched block copolymers were synthesized in several steps starting from a functional alcohol which is activated by cesium hydroxide to start the polymerization of EO and subsequently of the second monomer EEGE. The acetal protective groups of P(EEGE) were removed in a following step via acidic hydrolysis resulting in the linear double-hydrophilic block copolymer PEG-*block*-linPG (Scheme 1 A). These block copolymers serve as multifunctional macroinitiators for the multibranching AROP of glycidol to generate the respective linear-hyperbranched block copolymers (Scheme 1 B).

In addition, two different initiators were used: allyl alcohol (**7a**, **8a**) and undecenyl alcohol (**7b**, **8b**); with the longer aliphatic tail the effect of a possible amphiphilicity on cell viability have been investigated.

The second class of polymers investigated herein are random PEG-copolymers, which are prepared in a single step by direct copolymerization of EO with the respective comonomers (IGG, EVGE, DBAG, AGE) at elevated temperatures (Scheme 1 C). In the case of IGG, also a deprotected P(EG-co-GG) was investigated. This material possesses increased hydrophilicity. The DBAG-containing copolymers serve as a negative control due to the presence of the multiple amino groups, which were expected to be cytotoxic (*see below*).

All polymers prepared in the course of this study exhibit a narrow molecular weight distribution (compare Table 1). Table 1 also gives the structure and composition and the (functional) initiator of the polymerization. The benzyl protected amino ethanol is a common initiator that offers the possibility to introduce an amino functionality at the linear chain end after hydrogenation. Using the aromatic signals, the molecular weight determination via end group analysis in ^1H NMR is feasible. Nevertheless, it has to be noted here, that the single amino function may have a slight negative effect on cytotoxicity which should be kept in mind.

Table 1: Characterization data of all (co)polymers

No	Sum	M_n^1	PDI^1	structure	initiator	% ²
1a	P(EG ₁₇₄ -CO-DBAG) ₃	4 810	1.13	random	methoxy ethanol	2
1b	P(EG ₁₃₁ -CO-DBAG) ₇	3 520	1.16	random	methoxy ethanol	5
1c	P(EG ₇₀ -CO-DBAG) ₈	5 150	1.11	random	methoxy ethanol	10
2a	P(EG ₁₃₅ -CO-AGE) ₂	5 400	1.05	random	methoxy ethanol	2
2b	P(EG ₁₀₄ -CO-AGE) ₅	4 600	1.04	random	methoxy ethanol	5
2c	P(EG ₁₃₂ -CO-AGE) ₁₃	5 700	1.04	random	methoxy ethanol	10
2d	P(EG ₁₁₄ -CO-AGE) ₂₉	7 000	1.04	random	methoxy ethanol	20
4a	P(EG ₂₆₅ -CO-IGG) ₂₆	8 200	1.11	random	dibenzylamino ethanol	9
4b	P(EG ₁₈₀ -CO-IGG) ₃₂	9 750	1.11	random	dibenzylamino ethanol	14
4c	P(EG ₁₂₂ -CO-IGG) ₁₃₆	5 300	1.15	random	dibenzylamino ethanol	53
5	P(EG ₁₂₂ -CO-GG) ₁₃₆	7 750	1.18	random	dibenzylamino ethanol	53
6a	P(EG ₁₁₅ -CO-EVGE) ₁₁	2 500	1.08	random	dibenzylamino ethanol	9
6b	PEG ₁₁₃ - <i>b</i> -PEVGE ₁₁	5 500	1.05	lin block	methanol	10
7a	A-PEG ₁₂₀ - <i>b</i> -linPG ₃₇	7 800	1.10	lin block	allyl alcohol	30
7b	U-PEG ₁₀₇ - <i>b</i> -linPG ₃₂	7 000	1.15	lin block	undecenyl alcohol	30
8a	A-PEG ₁₂₀ - <i>b</i> -hbPG ₉₀	12 000	1.23	lin-hb block	allyl alcohol	75
8b	U-PEG ₁₀₇ - <i>b</i> -hbPG ₈₁	12 000	1.22	lin-hb block	undecenyl alcohol	75
9a	hbPG ₄₁	3 000	1.28	hb	trimethylolpropane	100
9b	hbPG ₁₃₅	10 000	1.34	hb	trimethylolpropane	100
10	mPEG ₁₁₃	4 800	1.05	lin	methanol	0

1: molecular weights determined by GPC vs. PEO standards

2: percentage comonomer (determined by ¹H NMR).

B: Cytotoxicity tests using the Alamar Blue assay.

The CHO suspension cell cultures were maintained in square-shaped glass flasks in serum free ProCHO5 cell culture medium supplemented with 13.6 mg·L⁻¹ hypoxanthine, 3.84 mg·L⁻¹ thymidine and 4 mM glutamine. The cell culture was maintained at 37 °C in a 95% humidified incubator with 5% CO₂. The cells were passaged every 3 days at a seeding density of 3x10⁵ cells·mL⁻¹. For cytotoxicity tests, the cells were diluted to a concentration of 250 000 cells·mL⁻¹ and the respective polymer solution was added. All (co)polymer/cell mixtures were incubated at 37 °C in 96 well plates at different polymer concentrations of 0.5 g/L, 1 g/L, and 5 g/L. The cells were analyzed after 3, 5, and 7 days, respectively. As reference PG as well as PEG, which have been proven to be biocompatible, are investigated in the same study. Figure 2 shows the cell viability measured by the Alamar blue assay after 3 days incubation time at a polymer concentration of 0.5 g/L.

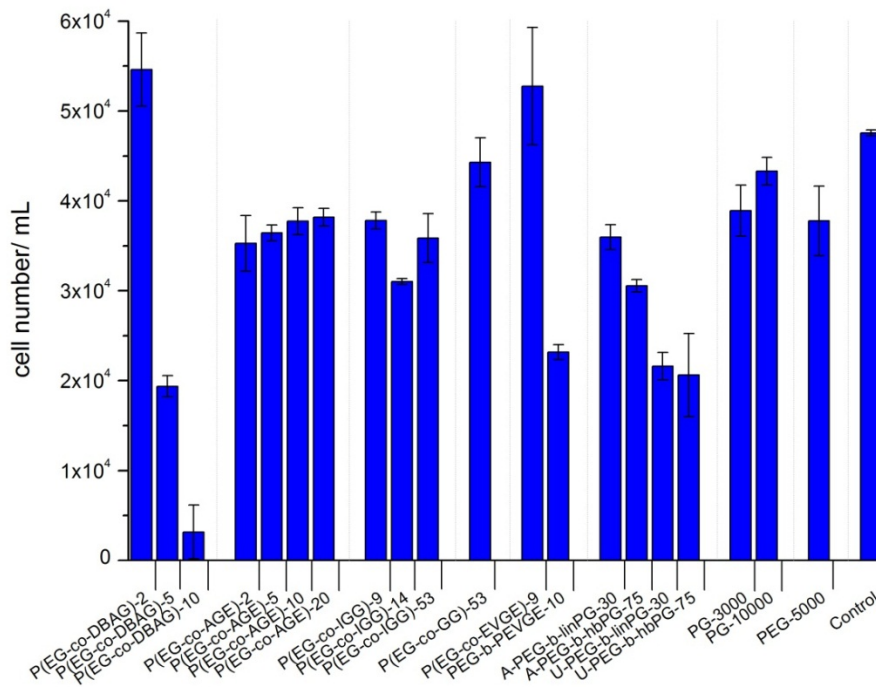


Figure 2: Cell viability after 3 days incubation at 37 °C at a polymer concentration of 0.5 g/L (Alamar blue assay).

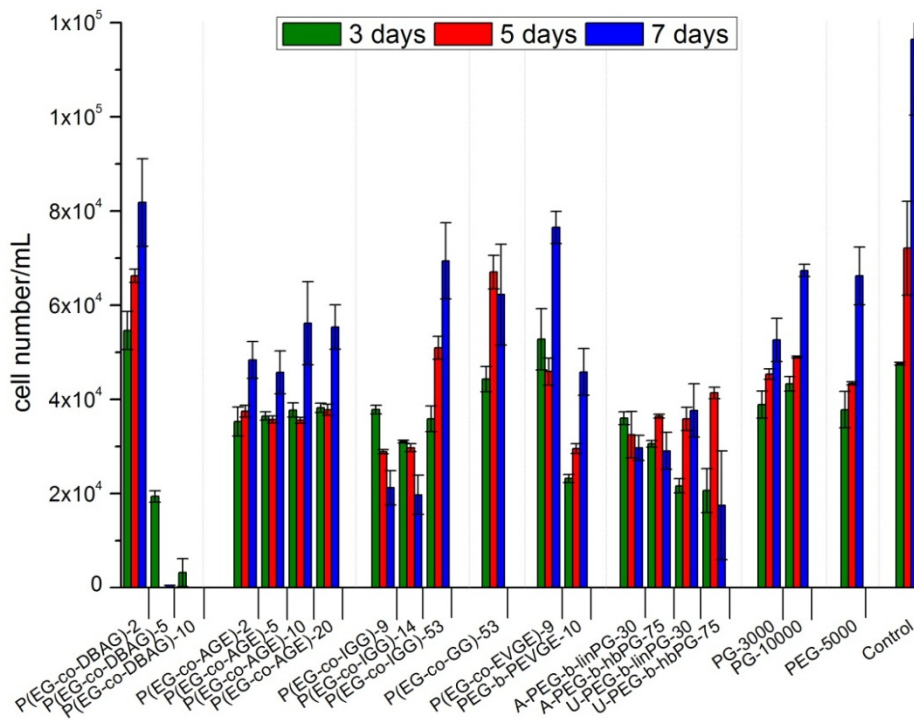


Figure 3: Cell viability after 3, 5, and 7 days incubation at 37 °C at a polymer concentration of 0.5 (Alamar blue assay).

The samples were also investigated after 3, 5, and 7 days. A general trend was observed: for most polymers the cell number steadily increased over time, meaning that proliferation is possible in the presence of the polymers. Interestingly, most polymers show a similar toxicity compared to PEG or hyperbranched PG. However, the rate of cell growth is lower in all cases compared to the control without polymer (Figure 3). Only the block copolymers show a rather constant value in cell numbers, i.e., the materials impeded the proliferation. Interestingly for PEG-*b*-PEVGE an increase in cell numbers is observed in comparison to the random copolymers. This could be attributed to the relatively short second block of PEVGE.

Furthermore, the effect of polymer concentration on cell viability has been investigated (Figure 4). As expected from theory in most cases for higher concentration, the polymers become more toxic and cell proliferation is slower.

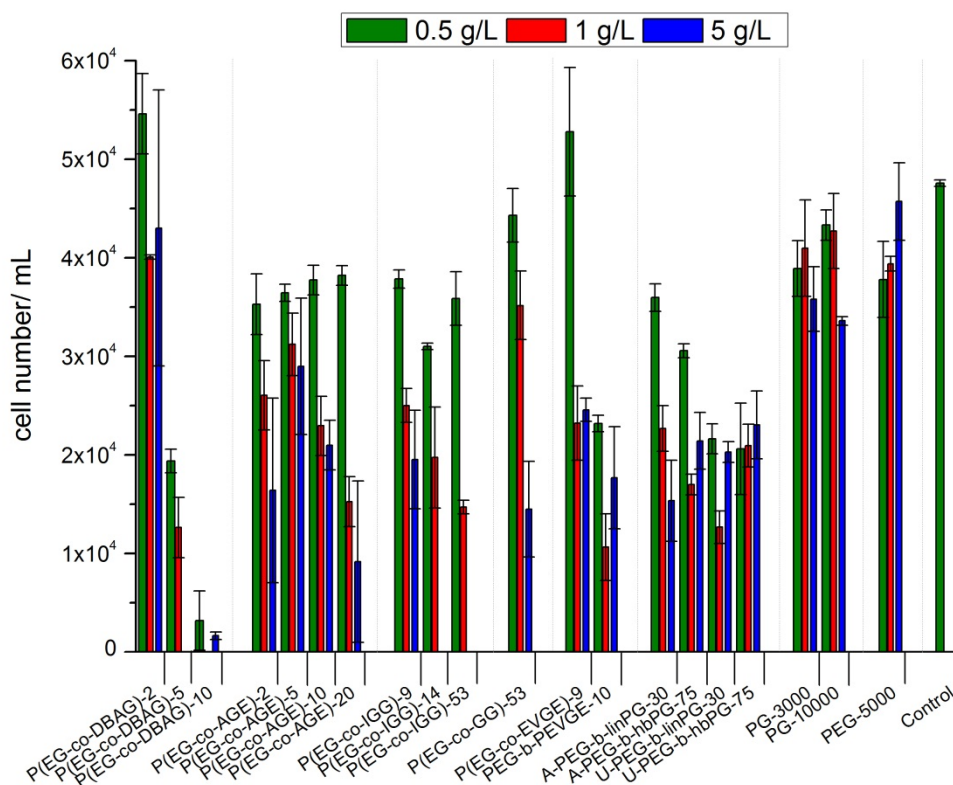


Figure 4: Cell viability after 3 days incubation at 37°C at different polymer concentrations of 0.5, 1 g/L, and 5 g/L (Alamar blue assay).

From Figures 2-4 several general trends can clearly be identified, which will be supported by the following experiments (note: the numbers in the polymer sums represent the percentage of

comonomer): 1.) All random copolymers exhibit similar toxicity compared to PEG and hyperbranched PG; only the DBAG-containing copolymers become toxic when a certain amount of amine groups is present in the polymer structure. This finding was expected and suggests that for biomedical application of these copolymers the amine group should be converted into an amide, which is expected to be non-toxic. However, the polyamine could be an interesting candidate for applications in gene delivery as poly(ethylene imine)-substitute.^{30, 31} 2.) The block copolymers have a higher toxicity than the random copolymers. In detail, the undecenyl initiated U-PEG-*b*-PGs and PEG-*b*-PEVGE block copolymers show higher toxicity which is attributed to the amphiphilic structure of the polymer. The comparable A-PEG-*b*-PGs copolymers which are initiated by allyl alcohol showed slightly higher toxicity than PEG and the respective random copolymers.

It has to be noted at this point that all polymers investigated in this study are known to exhibit an LCST exceeding 37 °C to guarantee a stable solution under physiological conditions. Only sample **4c** (P(EG₁₂₂-*co*-IGG)₁₃₆) with 53% IGG incorporated exhibits an LCST of 9 °C. In this case the cells were mixed with the cold polymer solution, which started to cloud immediately after the addition. The high increase in cell numbers from 3 to 7 days for this sample could be explained by precipitation of the polymer over time. However, after three days the suspension was still stable and the toxicity values are comparable to the other IGG-containing copolymers as expected.

C: Cytotoxicity tests using the PCV method.

One major aim of this work besides the study of the toxicity of the mf-PEG structures was also a comparison of the convenient PCV method for the determination of cell numbers with the abovementioned more established Alamar Blue assay. The UV assay is a useful method for many samples, if an automated plate reader is at hand. We planned to investigate, whether the experimentally simple and cost-efficient PCV method is a suitable substitute for the conventional assay. The PCV method is widely employed for blood analysis. Typically, an aliquot of 50 mL of blood is centrifuged in a special capillary. Then the height of the cell pellet within the capillary is measured and expressed as the packed cell volume or more convenient as the hematocrit, i.e. the fraction of blood occupied by cells. Typical PCV values for blood range from 30–50%. For cultivated cells the PCV is much lower and as a consequence lower amounts and special PCV tubes have to be used. In our laboratory PCV is the standard method to determine the cell numbers for CHO cells and others, as reported previously.²⁵

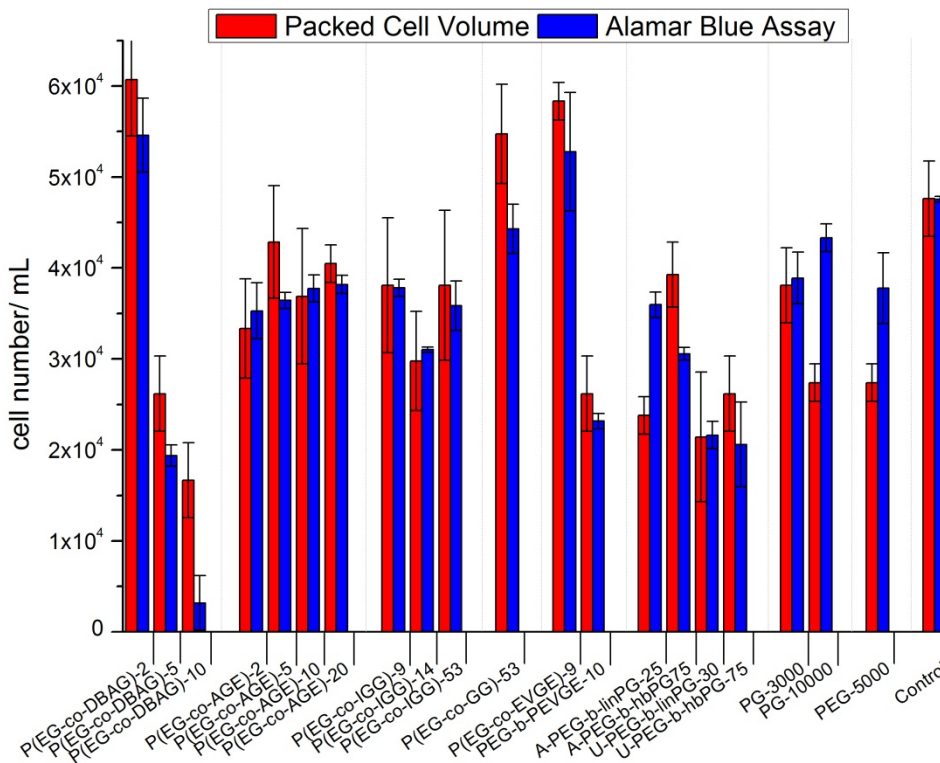


Figure 5: Comparison between the Alamar Blue UV read-out for cell viability and the packed cell volume method.

From Figure 5 it can be derived that the PCV results are very close to the results determined by the Alamar Blue staining method. As a matter of fact, the experimentally determined errors of the PCV values are higher than for the staining protocol stemming from the simple read-out of a cell pellet for the determination of the relatively low cell number in the case of the toxicity measurements compared to blood tests or the previously reported cell growth of CHO cells and other.²⁵

Figure 6 shows the cell numbers determined by the PCV method over a period of several days. As above, the proliferation of cells can be proven with this experiment and the overall trend of both methods, i.e. by Alamar Blue staining and PCV is the same.

Figure 7 shows the comparison of the cell numbers determined by PCV at different polymer concentrations. An interesting finding is that these results corroborate with the results from the Alamar blue assay for all concentrations, however, the comparison between PEG and the copolymers seems to be different in this case. A deviation in cytotoxicity might be explained by the impact of the dead cell volume.

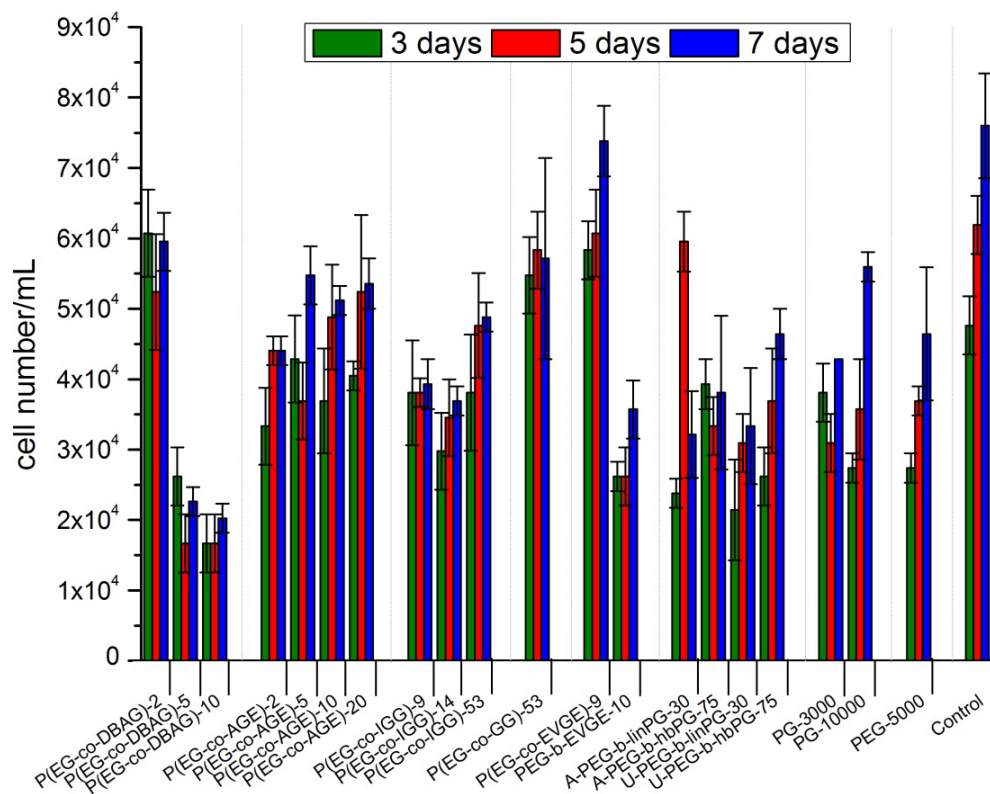


Figure 6: Cell viability measured by PCV at a polymer concentration of 0.5 g/L over several days.

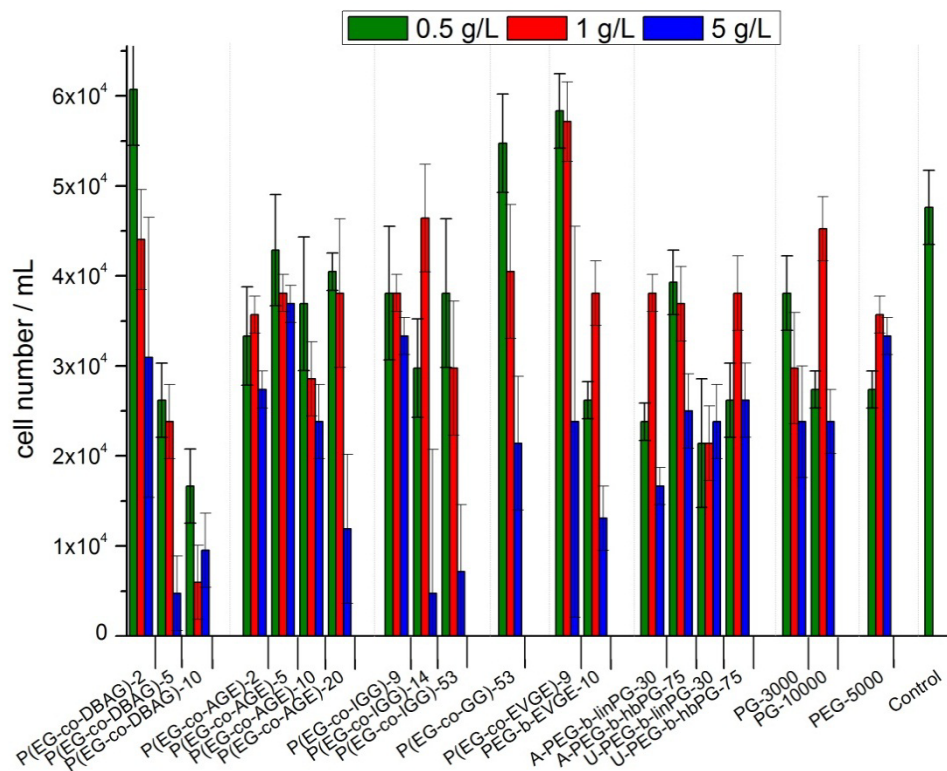


Figure 7: Cell viability after 3 days measured by the PCV method at varying polymer concentrations.

Summary

In summary we have obtained cytotoxicity data for a broad range of *mf*-PEGs with varying architecture and microstructure based on several comonomers. For the abovementioned data it can be stated that the random copolymers exhibit similar toxicity as PEG or hyperbranched PG, or lie within the error margin determined for the two methods presented herein.

In addition, the Alamar Blue assay for the determination of cell numbers has been compared to the more convenient PCV protocol. Interestingly, both methods give reasonable and comparable results for the cytotoxicity of the investigated copolymers. Even for rather cytotoxic materials PCV gives reliable results even when the “dead cell material” is counted while the Alamar Blue redox reaction can only be conducted by living cells. We believe that with these results the *mf*-PEGs will find use in future drug/ protein conjugates (polymer therapeutics) and that, moreover, the simple PCV method can be more established for cytotoxicity measurements.

Acknowledgment

C.M. is a recipient of a fellowship through funding of the Excellence Initiative (DFG/GSC 266). F.W. thanks the Alexander-von-Humboldt foundation for a fellowship and the Max Planck Graduate Center (MPGC) for support. H.F. acknowledges the SFB 625 of the DFG (German Science Foundation) for valuable support.

1. Wurm, F.; Klok, H.-A. *Chimia* **2011**, 65, (9), 659-662.
2. Roberts, M. J.; Bentley, M. D.; Harris, J. M. *Adv. Drug Deliver. Rev.* **2002**, 54, (4), 459-476.
3. Caliceti, P.; Veronese, F. M. *Adv. Drug Deliver. Rev.* **2003**, 55, (10), 1261-1277.
4. Gauthier, M. A.; Klok, H.-A. *Chem. Commun.* **2008**, (23), 2591-2611.
5. Veronese, F. M.; Pasut, G. *Drug Discov. Today* **2005**, 10, (21), 1451-1458.
6. Dworak, A.; Panchev, I.; Trzebicka, B.; Walach, W. *Macromol. Symp.* **2000**, 153, (1), 233-242.
7. Taton, D.; Le Borgne, A.; Sepulchre, M.; Spassky, N. *Macromol. Chem. Phys.* **1994**, 195, (1), 139-148.
8. Wurm, F.; Klos, J.; Räder, H. J.; Frey, H. J. *Am. Chem. Soc.* **2009**, 131, (23), 7954-7955.
9. Wilms, D.; Wurm, F.; Nieberle, J.; Bohm, P.; Kemmer-Jonas, U.; Frey, H. *Macromolecules* **2009**, 42, (9), 3230-3236.
10. Kainthan, R. K.; Brooks, D. E. *Biomaterials* **2007**, 28, (32), 4779-4787.
11. Wilms, D.; Stiriba, S.-E.; Frey, H. *Acc. Chem. Res.* **2009**, 43, (1), 129-141.
12. Wurm, F.; Nieberle, J.; Frey, H. *Macromolecules* **2008**, 41, (4), 1184-1188.
13. Wilms, D.; Schömer, M.; Wurm, F.; Hermanns, M. I.; Kirkpatrick, C. J.; Frey, H. *Macromol. Rapid Comm.* **2010**, 31, (20), 1811-1815.

14. Zhou, P.; Li, Z.; Chau, Y. *Eur. J. Pharm. Sci.* **41**, (3-4), 464-472.
15. Broyer, R. M.; Grover, G. N.; Maynard, H. D. *Chem. Commun.* **2011**, 47, (8), 2212-2226.
16. Matyjaszewski, K.; Xia, J. *Chem. Rev.* **2001**, 101, (9), 2921-2990.
17. Li, Z.; Chau, Y. *Bioconjugate Chem.* **2009**, 20, (4), 780-789.
18. Obermeier, B.; Wurm, F.; Frey, H. *Macromolecules* **2010**, 43, (5), 2244-2251.
19. Mangold, C.; Wurm, F.; Obermeier, B.; Frey, H. *Macromolecules* **2010**, 43, (20), 8511-8518.
20. Mangold, C.; Dingels, C.; Obermeier, B.; Frey, H.; Wurm, F. *Macromolecules* **2011**, 44, (16), 6326-6334.
21. Obermeier, B.; Wurm, F.; Mangold, C.; Frey, H. *Angew. Chem. Int. Ed.* **2011**, 50, (35), 7988-7997.
22. Mangold, C.; Wurm, F.; Obermeier, B.; Frey, H. *Macromol. Rapid Comm.* **2010**, 31, (3), 258-264.
23. Mangold, C.; Obermeier, B.; Wurm, F.; Frey, H. *Macromol. Rapid Comm.* **2011**, 32, (23), 1930-1934.
24. Page, B.; Noel, C. *Int. J. Oncol.* **1993**, 3, 473-476.
25. Stettler, M.; Jaccard, N.; Hacker, D.; Jesus, M. D.; Wurm, F. M.; Jordan, M. *Biotechnol. Bioeng.* **2006**, 95, (6), 1228-1233.
26. Wurm, F.; Nieberle, J.; Frey, H. *Macromolecules* **2008**, 41, (6), 1909-1911.
27. Muller, N.; Girard, P.; Hacker, D. L.; Jordan, M.; Wurm, F. M. *Biotechnol. Bioeng.* **2005**, 89, (4), 400-406.
28. Alconcel, S. N. S.; Baas, A. S.; Maynard, H. D. *Polym. Chem.* **2011**, 2, (7), 1442-1448.
29. Bailon, P.; Palleroni, A.; Schaffer, C. A.; Spence, C. L.; Fung, W.-J.; Porter, J. E.; Ehrlich, G. K.; Pan, W.; Xu, Z.-X.; Modi, M. W.; Farid, A.; Berthold, W.; Graves, M. *Bioconjugate Chem.* **2001**, 12, (2), 195-202.
30. Lampela, P.; Räisänen, J.; Männistö, P. T.; Ylä-Herttuala, S.; Raasmaja, A. *The Journal of Gene Medicine* **2002**, 4, (2), 205-214.
31. Kim, Y. H.; Park, J. H.; Lee, M.; Kim, Y.-H.; Park, T. G.; Kim, S. W. *J. Controlled Release* **2005**, 103, (1), 209-219.

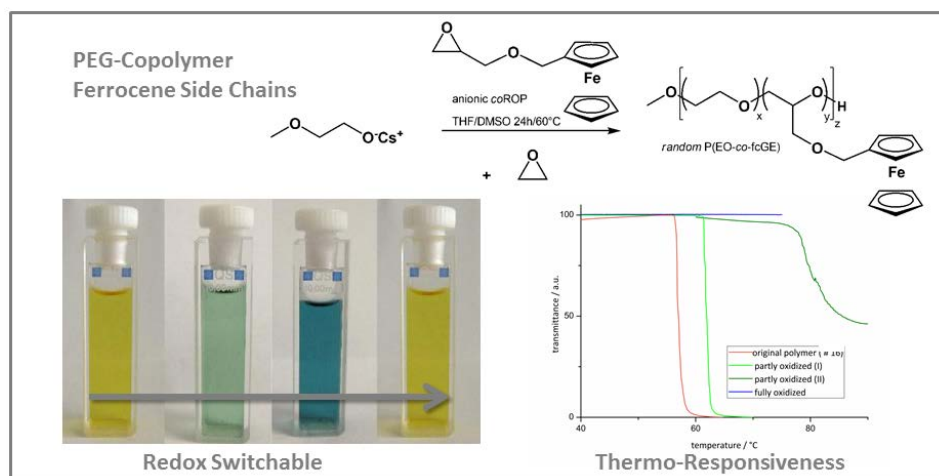
Chapter 4.1:

Thermo-Responsive Ferrocene-Containing Poly(ethylene glycol)

Thermo-Responsive Ferrocene-Containing Poly(ethylene glycol)

Christine Mangold, Sandra Ritz, Holger Frey, Frederik Wurm

To be submitted to *Macromolecules*.



Keywords: anionic polymerization, poly(ethylene oxide), (PEG), polyether, ferrocene, stimuli-responsive

Abstract

Ethylene oxide (EO) was copolymerized with the novel monomer ferrocenyl glycidyl ether (fcGE) to generate electro active, water-soluble and thermo-responsive poly(ethylene glycol)-derived copolyethers. Molecular weights were varied from 2 000 to 10 000 g mol⁻¹, obtaining narrow molecular weight distributions ($M_w/M_n = 1.07$ to 1.20). The incorporation of ferrocene (fc) was adjusted from 3 to 30 mol%, obtaining water soluble materials up to 10 mol% incorporation of the apolar ferrocenyl comonomer. Cyclovoltammetry experiments revealed that the iron centers can be oxidized reversibly, and all copolyethers synthesized exhibit a lower critical solution temperature (LCST), in accordance with previous works on random copolyethers. Moreover, the LCST is tunable by oxidation/reduction of ferrocene. In addition, toxicity tests were carried out with HeLA cell lines and revealed good biocompatibility in the case of low amounts of fcGE incorporated (below 5%) and a highly cytostatic behaviour, when higher fc content is present. The novel copolyethers are promising for biomedical applications or for redox sensors.

Introduction

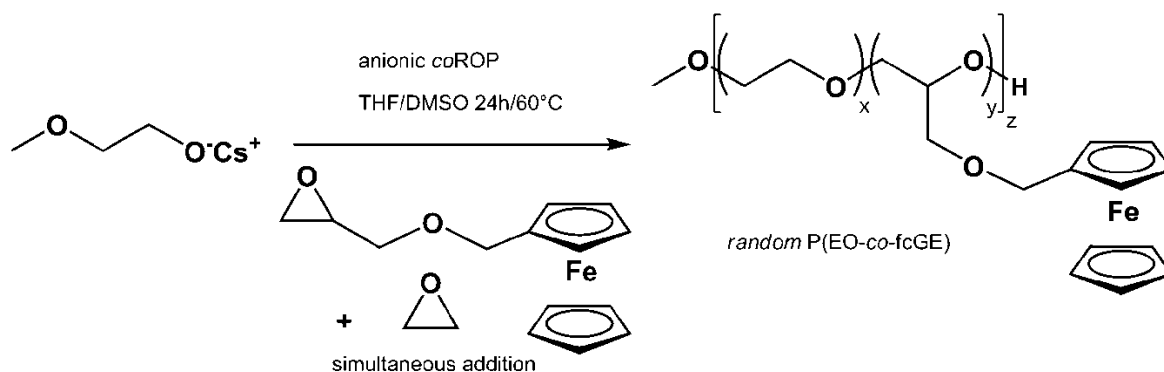
Ferrocene (fc)-containing polymers¹ are interesting materials relying on their unique physical and chemical properties such as redox-² and/or stimuli-responsive behavior.^{3, 4} Fc-derivatives are used in (electro)catalysis⁵ and in non-linear optical polymers.⁶ In addition, fc-containing materials are also important for biomedical uses, since ferrocenyl moieties exhibit antineoplastic properties,^{7, 8} and the redox-potential enables their utilization as amperometric glucose-sensors.⁹ Ferrocenyl groups can be incorporated into polymers either in the side chains or directly in the polymer backbone.¹⁰⁻¹³ Manners and coworkers intensively studied the controlled ring opening polymerization of *ansa*-metallocenophanes^{14, 15} leading to poly(metallocenes) via different polymerization techniques and with variable bridging elements.¹ These elegant works rely on strict Schlenk techniques during monomer preparation and the resulting polymers are usually not water-soluble and have to be converted via post polymerization modification into their water-soluble counterparts.¹⁶

Other groups emphasized the polymerization of monomers with fc as side chain substituents, such as vinylferrocene¹² or ferrocenylmethyl (meth)acrylate.^{13, 17-19} Very recently a series of (meth)acrylate (MA) based monomers with varying spacers between fc and the MA-unit have been introduced by Laschewsky and coworkers.²⁰ Another fruitful approach to incorporate fc moieties in polymers can be achieved via polymerization by hydrosilylation^{21, 22} or by introduction of amide linkages after polymerization.²³

Most of the abovementioned materials are organo-soluble, however, water-soluble fc-containing polymers can be synthesized by different approaches. The first one relies on the synthesis of block-copolymers carrying water-soluble segments such as poly(2-(*N,N*-dimethylamino)ethyl methacrylate) (at pH: 8),²⁴ or poly(ethylene glycol) (PEG) and subsequent attachment or polymerization of the fc-containing block.^{25, 26} However, block copolymers show aggregation in different solvents can be an undesired behavior in many applications. The second approach relies on the polymerization of fc-containing monomers, with hydrophilic side chains, such as oligo(ethylene glycol)²⁷ or poly(electrolytes),^{28, 29} which lead to aqueous solubility with decreased aggregation behavior.

A versatile, yet unexplored approach is the (co)polymerization of designed fc-based monomers with a hydrophilic comonomer resulting in water-soluble (random) copolymers. To the best of our knowledge this approach has not been realized to date. In this work we present the first poly(ethylene glycol)-based copolymers bearing ferrocenyl side chains. The synthesis relies on the anionic (co)polymerization of ferrocenyl-glycidyl ether (fcGE, **1**) with ethylene oxide (EO) (**Scheme 1**). The polymer structures have been studied with respect to water solubility, thermo-responsive behavior³⁰ and toxicity as a function of the ferrocene content. This LCST behavior can be switched off by oxidation of the iron centers, which means that multi-responsive structures³¹ are obtained. In addition, the water-soluble copolymers were investigated with respect to their cytotoxicity and it

was proven that the polymers with low fc content are not toxic rendering them very interesting candidates for biomedical applications, but higher fc containing materials could be interesting candidates as efficient cytostatic materials.



Scheme 1. Strategy for the synthesis of water-soluble polymers containing ferrocene by employing the novel comonomer ferrocenyl glycidyl ether (fcGE).

Experimental Section.

Instrumentation

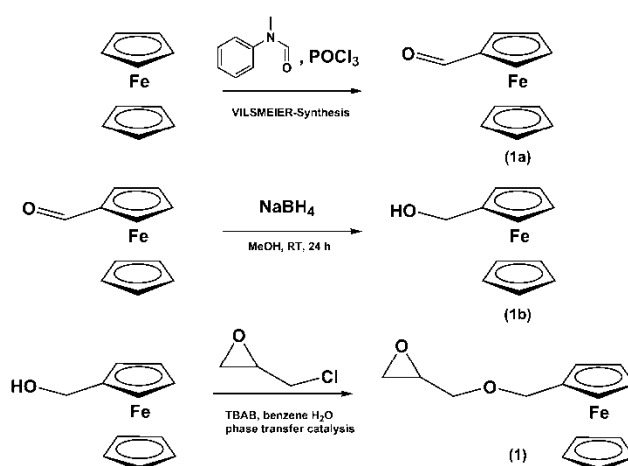
^1H NMR spectra (300 MHz and 400 MHz) and ^{13}C NMR spectra (75.5 MHz) were recorded using a Bruker AC300 or a Bruker AMX400. All spectra were referenced internally to residual proton signals of the deuterated solvent. For SEC measurements in DMF (containing 0.25 g/L of lithium bromide as an additive) an Agilent 1100 Series was used as an integrated instrument, including a PSS HEMA column ($10^6/10^5/10^4$ g/mol), a UV- (275 nm) and a RI-detector. Calibration was carried out using poly(ethylene oxide) standards provided by Polymer Standards Service. DSC measurements were performed using a Perkin-Elmer 7 series thermal analysis system and a Perkin Elmer Thermal Analysis Controller TAC 7/DX in the temperature range from -100 to 80 °C. Heating rates of 10 K min^{-1} were employed under nitrogen. Cloud points were determined in deionized water and observed by optical transmittance of a light beam ($\lambda = 632$ nm) through a 1 cm sample quartz cell. The measurements were performed in a Jasco V-630 photospectrometer with a Jasco ETC-717 Peltier element. The intensity of the transmitted light was recorded versus the temperature of the sample cell. The heating/cooling rate was 1 °C min^{-1} and values were recorded every 0.1 °C. Cyclic voltammetry (CV) was performed using a BAS CV-50 W potentiostat using dichloromethane as a solvent under an inert atmosphere (N_2). The supporting electrolyte was tetrabutylammonium hexafluorophosphate (TBAH [0.1 M]). All experiments were performed at 25 °C, in a conventional three-electrode cell using a platinum working electrode ($A \frac{1}{4} 0.02$ cm^2). All potentials are referred to a saturated calomel reference electrode (SCE). A coiled platinum wire was used as counter electrode.

Reagents

Solvents and reagents were purchased from Acros Organics, Sigma Aldrich or Fluka and used as received, unless otherwise stated. Chloroform- d_1 , methanol- d_4 and DMSO- d_6 were purchased from Deutero GmbH. Ferrocenecarboxaldehyde and ferrocenemethanol were synthesized according to reported procedures.³²

Synthesis

Synthesis ferrocenyl glycidyl ether (fcGE, 1). The glycidyl ether was obtained in analogy to the procedures reported for other functional oxiranes.³³ In a typical reaction 5 g ferrocenemethanol (0.023 mol) were placed in a round bottom flask and 100 mL benzene and 100 mL of a 50% NaOH solution were added. 1 g of tetrabutyl ammoniumbromide (TBAB) was added as a phase transfer catalyst. To this mixture an excess of epichlorohydrin (4.3 g, 0.046 mol) was added, while cooling the reaction mixture with ice. The solution was allowed to warm up to room temperature and rapidly stirred for 24 h. The progress of the reaction was followed by thin layer chromatography. The organic phase was washed with brine and NaHCO_3 -solution and the solvent was removed under vacuum. The crude product was purified by column chromatography using ethyl acetate and petroleum ether (3:7) as eluents. Besides the desired product (ferrocenyl glycidyl ether; $R_f = 0.5$), unreacted starting material (ferrocenemethanol; $R_f = 0.2$) could be recovered and reused. The product was obtained as orange solid in typical yields of 70-80%. $^1\text{H NMR}$ (300 MHz, CDCl_3): δ (ppm) = 4.27-4.13 (m, 4 H, cp), 3.97 (d, 7 H, cp and CH_2 -cp), 3.48-3.43 (dd, 1 H, CHCHHO), 3.20-3.14 (dd, 1 H, CHCHHO), 2.87 (q, 1 H, methine), 2.29-2.17 (m, 2 H, epoxide). The synthetic strategy is shown in **Scheme 2**. For a detailed assignment of the protons compare **Figure 1**.



Scheme 2. Sequence for the synthesis of the novel epoxide monomer ferrocenyl glycidyl ether (fc-GE).

General procedure for the copolymerization with EO (P(EO-co-fcGE)). Methoxy ethanol and 0.9 equivalents of cesium hydroxide monohydrate were placed in a 250 mL Schlenk flask and benzene was added. The mixture was stirred at 60 °C under argon atmosphere for 1 h and evacuated at 60 °C (10^{-2} mbar) for 12 h to remove benzene and water to generate the corresponding cesium alkoxide. Subsequently, approximately 20 mL dry THF were cryo-transferred into the Schlenk flask. EO was cryo-transferred to a graduated ampoule, and then cryo-transferred into the reaction flask containing the initiator in THF. Subsequently, the second comonomer, fcGE, was added via syringe in a 50 wt% solution in anhydrous DMSO. The mixture was heated to 60°C and stirred for at least 12 to 24 h. The polymer solution was dried *in vacuo*, and precipitated into cold diethyl ether to remove residual DMSO. The polymer was obtained as an orange powder or viscous liquid depending on the fc content. Yields: 60-90%. ^1H NMR (300 MHz, DMSO- d_6): δ (ppm) = 4.24-4.16 (m, 4 H, cp), 4.07 (d, 7 H, cp and CH_2 -cp), 3.68-3.45 (br, polyether backbone), 3.33 (s, 3 H, CH_3). For a detailed assignment compare Supporting Information **Figure S3**.

Cytotoxicity studies.

The effect of fc containing PEG-copolymers on the viability of a human cervical cancer cell line (HeLa cells) was measured with a commercial luminescence assay CellTiter-Glo[®] (Promega, Germany). The assay based on the enzymatic reaction of Luciferase transferring luciferin and ATP, supplied by the living cells, to oxyluciferin and luminescence is used as a measure of cell proliferation and cytotoxicity).

HeLa cells were cultured in Dulbecco's modified eagle medium (DMEM), supplemented with 10% FCS, 100 units penicillin and 100 mg·mL⁻¹ streptomycin, $2 \cdot 10^{-3}$ M L-glutamine (all from Invitrogen, Germany). Cells were grown in a humidified incubator at 37 °C and 5% CO₂. For determining the cell viability, HeLa cells were seeded at a density of 20 000 cells·cm⁻² ($6 \cdot 10^4$ cells·mL⁻¹) in 96-well plates (black, opaque-walled, Corning, Netherlands). FcGE copolymers (100 mg/mL) were solved in sterile water (Ampuwa[®], pH 7.4, Fresenius Kabi, Germany) and the indicated concentrations were produced by a serial dilution in cell culture medium (DMEM, 10% FCS). After 24 h, the culture medium was replaced by fcGE copolymer supplemented medium (200 μL , DMEM, 10 % FCS) or medium without compound (DMEM, 10 % FCS) as a specific control for 100% cell viability. The cells were treated for 24 h or 48 h and the number of viable cells were determined by the CellTiter-Glo[®] assay following the manufacturers' instructions. Briefly, cell culture medium with compound was replaced by 100 μL CellTiter-Glo[®] reagent. The 96-well plates were mixed for 2 minutes and incubated for 10 minutes at room temperature. During this time, the cytosolic ATP was released for the enzymatic reaction. The luminescence was detected with a plate reader (Infinite M1000, Tecan, Germany) using i-control software (Tecan, Germany). The values represent the mean \pm SD of four replicates and were plotted relative to the untreated cells.

Results and Discussion

A: Monomer and Polymer Synthesis.

Water-soluble fc-containing polymers with aliphatic polyether backbone are of interest for sensing and biomedical applications. The incorporation of fc into a water-soluble polymer backbone (viz. PEG) has been realized by copolymerization of a newly designed monomer with EO, which guarantees preservation of the metallocene during the anionic ring opening polymerization of the oxirane. The monomer (fcGE, **1**) was synthesized in a three step protocol (Scheme 2), starting with a VILSMEIER-synthesis, to ferrocenecarboxaldehyde (1a). The aldehyde was transformed into the corresponding alcohol (ferrocenemethanol (1b)) by reduction with LiAlH_4 , which was subsequently used in a phase transfer catalyzed nucleophilic substitution reaction with epichlorohydrin to yield fcGE. This procedure was carried out in analogy to synthetic protocols of other previously described functional epoxides^{33, 34} (note: 1a and 1b are also commercially available). The monomer was obtained in overall good yields (up to 80%) and purified by column chromatography. **Figure 1** shows the ^1H NMR spectrum of **1** in benzene and the signal assignments were determined using COSY (**Figure S1**, Supporting Information). ^{13}C NMR spectra with the respective assignment can also be found in the Supporting Information of this manuscript (**Figure S2**).

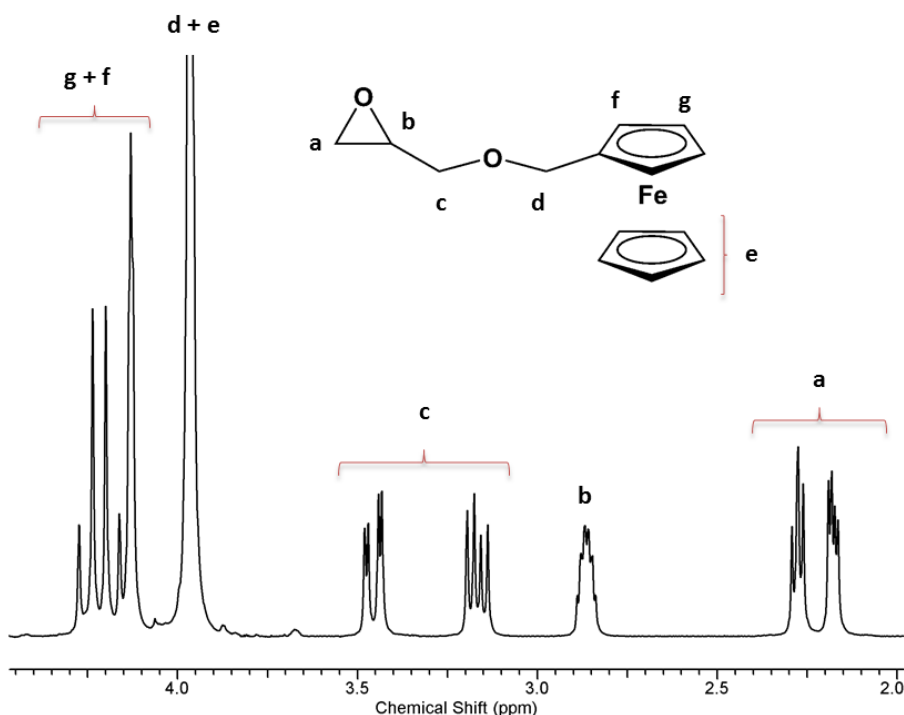


Figure 1. Detailed assignment of respective protons of ferrocenyl glycidyl ether in ^1H NMR.

The polymer synthesis was carried out in analogy to previous works on random poly(ether)s.³⁵⁻³⁸ The cesium salt of methoxyethanol was used as the initiator and a mixture of THF and DMSO as well as a reaction time of 12-24 h were found to be the best polymerization conditions with respect to

complete conversion. With a fc content of more than 28% incorporated in the PEG-backbone, the polymers are no longer soluble in water, therefore the focus was set to ratios with lower fc content to guarantee water solubility. All polymers synthesized in this study exhibit narrow molecular weight distributions (in the range of M_w/M_n : 1.07-1.20, compare Table 1) and monomodal SEC-traces (compare **Figure 2**). This means that the fc moiety is stable towards the highly basic conditions applied during the polymerization of EO and fcGE and no undesired side reactions leading to crosslinking occur. This may be expected, since other fc-based monomers are also used in (carb-) anionic polymerizations.¹²

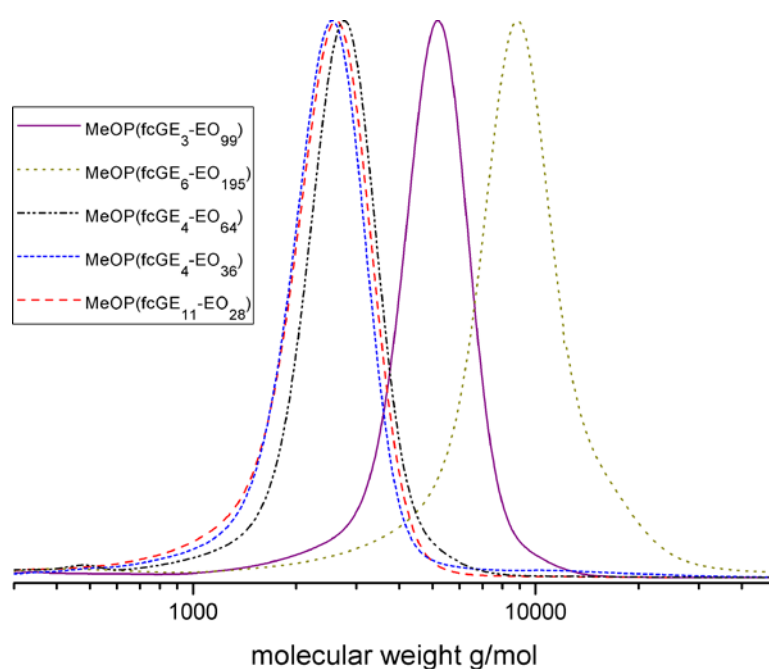


Figure 2. SEC traces of different P(EO-co-fcGE) copolymers, showing monomodal molecular weight distributions and low PDIs. Characterization data are summarized in Table 1.

The molecular weights of the polymers as well as the comonomer content were determined by ^1H NMR spectroscopy. The methyl group of the initiator can be used as a reference signal and is compared to the integral of the resonances of the polyether backbone between 3.68 and 3.45 ppm as well as the signals resulting from the cyclopentadienyl (cp) rings of the fc-moieties at 4.24-4.16 and 4.07 ppm (**Figure S3**). The molecular weights obtained correspond to the theoretical values. This is good agreement with the condition found for anionic polymerization.

An overview of all polymer samples prepared is given in **Table 1**. A comparison of the molecular weights determined via end group analysis from ^1H NMR spectroscopy and SEC measurements shows a deviation between the two values which can be ascribed to the high molecular weight of the fc-side chains. The SEC calibration (PEG standards) underestimates the molecular weight, which we ascribe to the fact that the large fc moieties do not contribute to the hydrodynamic radii. In most of

the cases it can be observed that an increasing content of fcGE leads to an increasing derivation. This effect was already observed for other P(EO-co-glycidyl ether) copolymers.³⁹

Table 1. Molecular weight data for the ferrocene-containing copolymers synthesized in this study by anionic ROP.

No.	Formula ^a	fcGE/EO(%)	M _n (g/mol) ^a	M _n (g/mol) ^b	PDI ^b
P1	MeOP(EO ₉₉ -CO-fcGE ₃)	2.8	5 200	4 700	1.10
P2	MeOP(EO ₁₉₅ -CO-fcGE ₆)	2.9	10 200	8 100	1.20
P3	MeOP(EO ₆₄ -CO-fcGE ₄)	6.3	3 900	2 600	1.07
P4	MeOP(EO ₃₆ -CO-fcGE ₄)	9.5	2 500	2 300	1.16
P5	MeOP(EO ₂₈ -CO-fcGE ₁₁)	28	4 200	2 200	1.15

^adetermined via endgroup analysis from ¹H NMR in DMSO-*d*₆, ^bdetermined from size exclusion chromatography in DMF vs. PEG-standards using the RI-signal.

B. Materials Properties of the Copolymers

Thermal Analysis. Thermal analysis of the copolymers was carried out using differential scanning calorimetry (DSC). The results are summarized in **Table 2**. As expected, the glass transition temperatures (T_g) for all polymers determined are close to the value of PEG (-56 °C), as most polymers contain a major fraction of PEG. Only in the case of copolymer **P5** a slight increase of the T_g can be observed.

Table 2. Thermal data of the copolymers synthesized in this study.

No.	Formula	fcGE/EO (%)	T _g (°C) ^a	T _m (°C) ^b	ΔH (J/g) ^c
P1	MeOP(EO ₉₉ -CO-fcGE ₃)	2.8	-56	43	82
P2	MeOP(EO ₁₉₅ -CO-fcGE ₆)	2.9	-54	42	72
P3	MeOP(EO ₆₄ -CO-fcGE ₄)	6.3	-56	27	48
P4	MeOP(EO ₃₆ -CO-fcGE ₄)	9.5	-59	14	40
P5	MeOP(EO ₂₈ -CO-fcGE ₁₁)	28	-49	/	/

^aglass transition temperature, ^bmelting temperature T_m; ^cmelting enthalpy determined by integration of the melting peak.

Considering the melting behavior of the copolymers a clear trend is observed. PEG is a crystalline material with a melting temperature of ca. 65 °C.⁴⁰ The degree of crystallization of the copolymers is gradually lowered by the incorporation of the comonomer, which disturbs the crystallization of the PEG-domains. This can already be estimated from the physical appearance of the copolymers, as they

are either obtained as orange powder for low fc content or deep orange, sticky solids. In a previous work it was estimated that approximately 13 adjacent EO units are needed (i.e. PEG with a molecular weight of 600 g/mol)^{34, 41} to observe crystallization in random PEG copolymer structures, which is still the case for copolymer **P4** (with an average of 10 adjacent EO units) but not observable for copolymer **P5**. As it was shown in previous works, DSC measurements can be used as an indicator for the random incorporation of glycidyl ether moieties. Incorporation of 28% of comonomer is required to suppress the crystallization of the PEG chains completely. From the thermal properties (Table 2), a first indication of a random comonomer distribution or only slightly tapered structure of the copolymers is given.

Lower Critical Solution Temperature (LCST) Behavior. Very recently we showed that different copolymers based on EO and varied concentration of hydrophobic glycidyl ethers exhibit a tunable thermo-responsive behavior.³⁰ It was demonstrated that the LCST can be varied by two different parameters, the first being the comonomer hydrophobicity and secondly the comonomer content. With increasing content of hydrophobic comonomer and with increasing hydrophobicity of the comonomer the LCST is lowered gradually, as it would be expected. All fc containing copolymers have been investigated with respect to their LCST behavior at a concentration of 5 mg/mL, and the results are summarized in **Table 3**.

Table 3. LCST-values of different P(EO-co-fcGE)-copolymers.

No.	Formula ^a	fcGE/EO (%) ^a	LCST (°C) ^b
P1	MeOP(EO ₉₉ -co-fcGE ₃)	2.8	82.2
P2	MeOP(EO ₁₉₅ -co-fcGE ₆)	2.9	69.1
P3	MeOP(EO ₆₄ -co-fcGE ₄)	6.3	61.8
P4	MeOP(EO ₃₆ -co-fcGE ₄)	9.5	50
P5	MeOP(EO ₂₈ -co-fcGE ₁₁)	28	-

^a obtained from ¹H NMR, ^b 5 mg mL⁻¹ solution of the copolymer in deionized water.

The cloud points of the aqueous polymer solutions have been measured by monitoring the transmittance of a light beam (wavelength 632 nm) through a 1 cm quartz sample cell at a heating (cooling) rate of 1 °C min⁻¹. The cloud point temperatures of the very sharp transitions from translucent to opaque solutions were defined as the value measured at 50% transmittance. The respective graphs of the turbidimetry measurements can be found in the Supporting Information (**Figure S4**).

The LCST values of different copolymers with similar molecular weights were plotted against the comonomer content and a linear relationship between comonomer content and cloud point can be observed. Comparing the slope of the fitted line with the values from literature³⁰ gives a clear hint with respect to the hydrophobicity of fcGE. It was found that the gradient of the line and therefore the hydrophobicity of ferrocenyl glycidyl ether is situated between ethoxy vinyl glycidyl ether³⁴ and dibenzyl amino glycidol.^{30, 35} Furthermore, it was found that in the case of perfectly random copolymers, the interception with the y-axis is situated around 100 °C, as it is also present in PEG-homopolymers. For the fcGE containing copolymers the interception was found to be at 94 +/- 6 °C, which gives another hint for the random distribution of the fc moieties.

The fc groups at the polymer backbone can be further used to tune the LCST behavior of a given polymer sample by an external stimulus. First, β -cyclodextrin (β -CD) was added to the aqueous polymer solution since it is known from literature that inclusion complexes with fc are generated in this case. The addition of β -CD led to a shift of the respective LCST to slightly higher values. This unexpectedly small influence on the cloud point (increase by ca. 5 °C) can most probably be ascribed to the temperature-dependence of this host-guest complex⁴² as well as steric reasons. The respective experimental details can be found in the Supporting Information (**Figure S6**).⁴³

A strong influence on the LCST was observed by oxidation of fc using silver(I) triflate ($\text{AgCF}_3\text{O}_3\text{S}$). Upon addition of the oxidizing agent, the yellow color vanished and a greenish to blue solution resulted (compare **Figure S7**). The formation of silver(0) was observed, and after filtration from the precipitate the clear solutions were measured in turbidimetry experiments again. With increasing fc-oxidation level, higher LCST values were detected, until finally a fully water-soluble polymer without LCST behavior was obtained (compare **Figure S8**). Further, this effect is reversible by the reduction of the iron center using sodium thiosulfate ($\text{Na}_2\text{S}_2\text{O}_3$). The LCST values obtained after reduction reached similar values as for the pristine solutions, although it is important to mention that the salt concentration had an influence on the LCST ("salting out effect").⁴⁴ Intensive studies on the direct correlation of the oxidation state and the LCST behavior are currently under way.

Cyclic Voltammetry Measurements. Fc can be oxidized reversibly by applying a cyclic potential and this redox-active behavior can be studied by cyclic voltammetry. To demonstrate that the fc-moieties attached to a polar polyether backbone can be addressed, we investigated two polymers with different fc content. The samples **P1** and **P5** with the lowest and the highest amount of fc incorporated have been dissolved in dichloromethane with 0.1 M conducting salt (tetrabutylammonium hexafluorophosphate) at a concentration of 5 mg/mL. **Figure 3** shows the cyclic voltammogram of both polymers at a scan rate of 0.5 V/s.

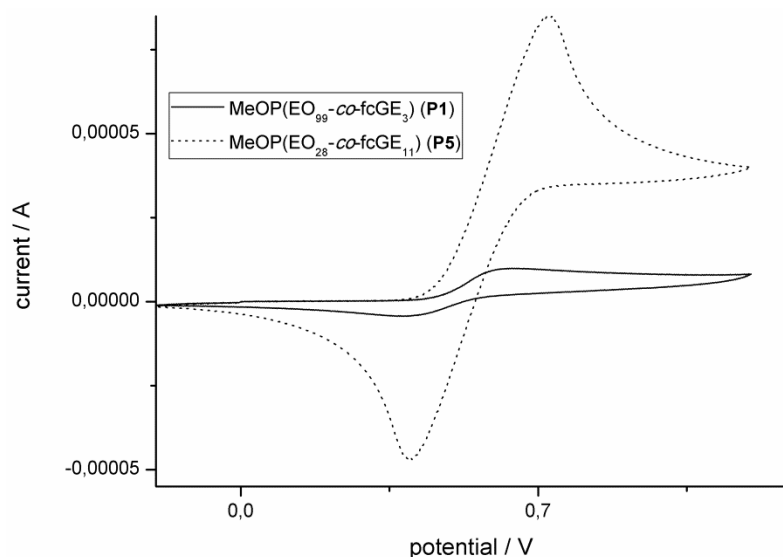


Figure 3. Cyclic voltammogram of **P1** and **P5** at a scan rate of 0.5 V/s.

It can be seen that at a similar weight fraction (targeted: 5 mg/mL) different maximum currents can be detected. For **P1**, 5 mg/mL correspond to $2.9 \cdot 10^{-6}$ mol of fc units/mL, while for **P5** 5 mg/mL correspond to $1.31 \cdot 10^{-5}$ mol of fc units/mL, which is in accordance with the different maximum currents which can be observed. Another information which can be obtained from the cyclic voltammogram is that in this case oxidation is a homogeneous process and no stepwise oxidation is observed, as for example reported for poly(ferrocenylsilane)s.⁴⁵

C: Toxicity Studies.

Toxicity studies of PEG-copolymers are a crucial part of the materials properties with respect to the potential applications. As it was shown recently, many P(EO-co-GE)s exhibit similar toxicity as PEG, we were interested on the effect of fc moieties at the PEG backbone. Ferrocenium salts are known to be cytostatic and have recently been investigated with respect to a potential use in anticancer therapy.^{46, 47}

The toxicity of the P(EO-co-fcGE)s was investigated against a human cervical cancer cell line (HeLa) from a concentration range of $1 \mu\text{g}\cdot\text{mL}^{-1}$ to $1000 \mu\text{g}\cdot\text{mL}^{-1}$ by measuring the ATP content of viable cells in relation to untreated cells. The results are displayed in **Figure 4**. While the two copolymers with less than 5 mol% fcGE units included show good biocompatibility comparable to the PEG homopolymer, the two copolymers with higher fcGE incorporation (6.3 and 9.5%) are effective cytostatics with increasing concentration. These results are in good agreement with expectation, as an increasing weight fraction of copolymer translates to a higher molar amount of fc in the solution, which can be oxidized to ferrocenium ions that act as a cytostatic.

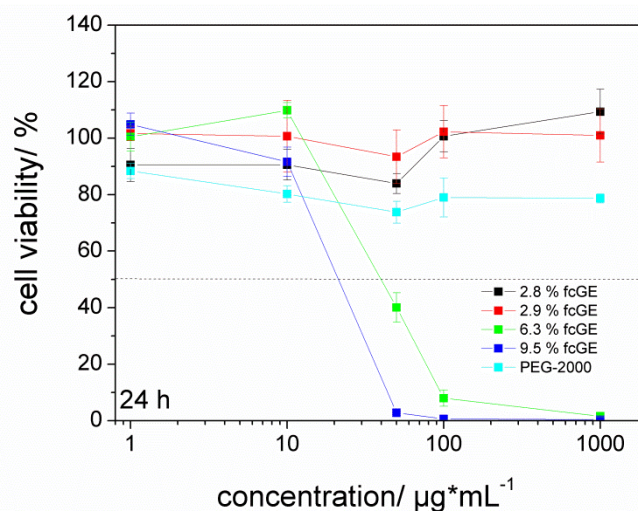


Figure 4. Cell viability of HeLa cells treated with fc-containing PEG-copolymers after 24 h of incubation. Untreated cells were set to 100%. The experiment was done in duplicate with $n = 4$.

With respect to biomedical applications these novel water-soluble polymers might be interesting for PEGylation⁴⁸-like applications, however enabling tracking of the polymer molecules due to the fc-moieties, provided polymers with low iron content are used. Copolyethers with high iron content might be interesting in application like polymeric cytostatics and are currently under investigation for this purpose.

Conclusion

In summary, the first synthesis of water-soluble poly(ether)-based ferrocene containing polyethers with PEG like structure has been presented. The polymers were synthesized via anionic *co*-ROP of EO and fcGE to yield narrowly distributed random copolymers. The copolymers were investigated in detail via NMR spectroscopy and DSC suggesting a random incorporation of fcGE into the poly(ether)-backbone. The copolymers exhibit thermo-responsive behavior, which can be further tailored either by the addition of β -cyclodextrin or by oxidation of the fc moieties. The toxicity of these materials was investigated against HeLa cells, and it was found that for a very low incorporation of fc-moieties the polymers are comparable to PEG, while higher fc concentrations lead to efficient cytostatics. We believe that these PEG-derived copolymers with pending ferrocene units possess intriguing potential due to their possible application in the biomedical field, e.g., for sensing, detection, and as potential polymer therapeutics.

Acknowledgement

The authors thank Alina Mohr for technical assistance. C. M. is recipient of a fellowship through funding of the German Excellence Initiative (DFG/GSC 266). F.W. thanks the Alexander-von-Humboldt

foundation for a fellowship. H.F. acknowledges the Fonds der Chemischen Industrie and the SFB 625 for support.

Supporting Information

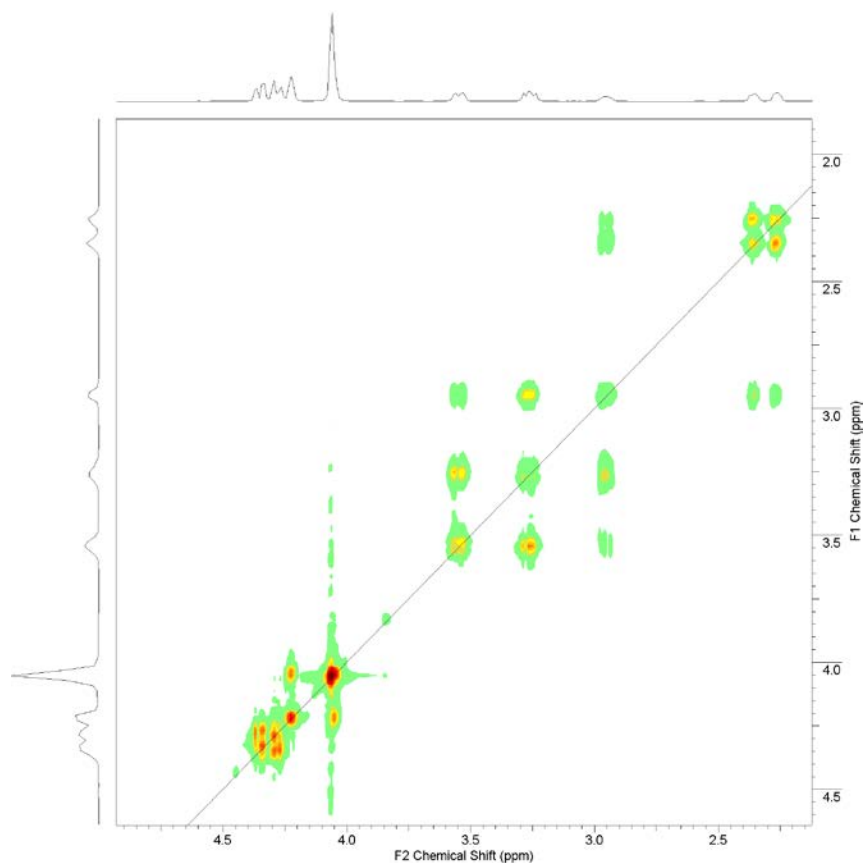


Figure S1. COSY of fcGE revealing the correlation of different protons.

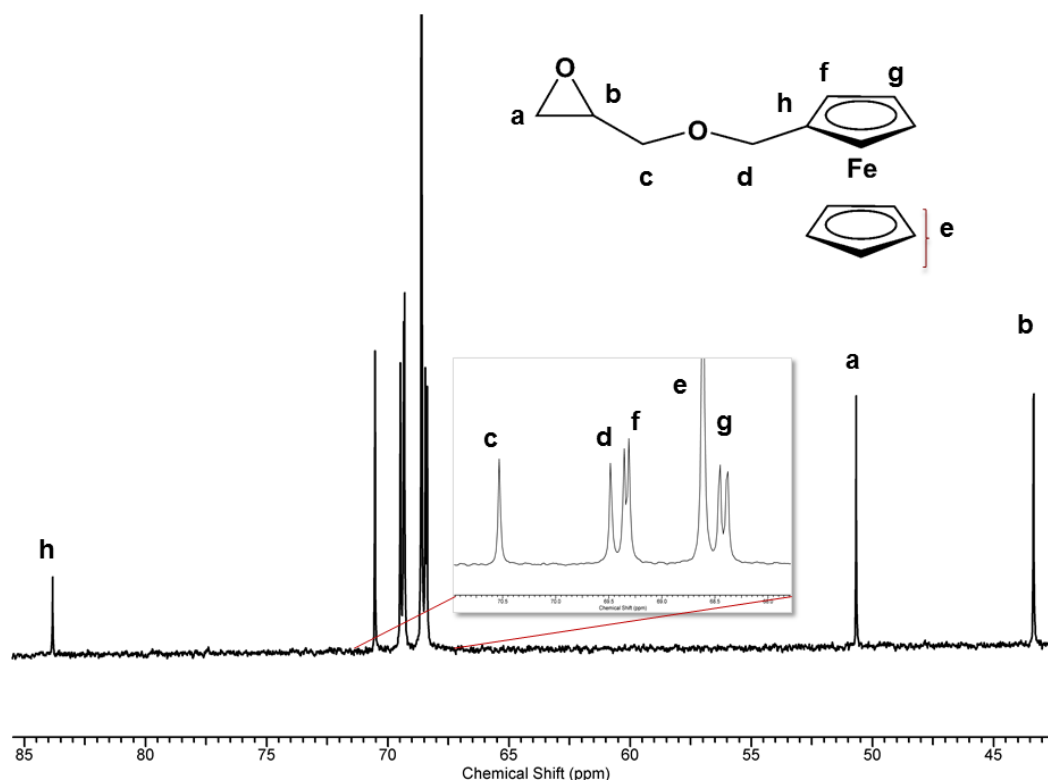


Figure S2. ^{13}C NMR of fcGE with peak assignment.

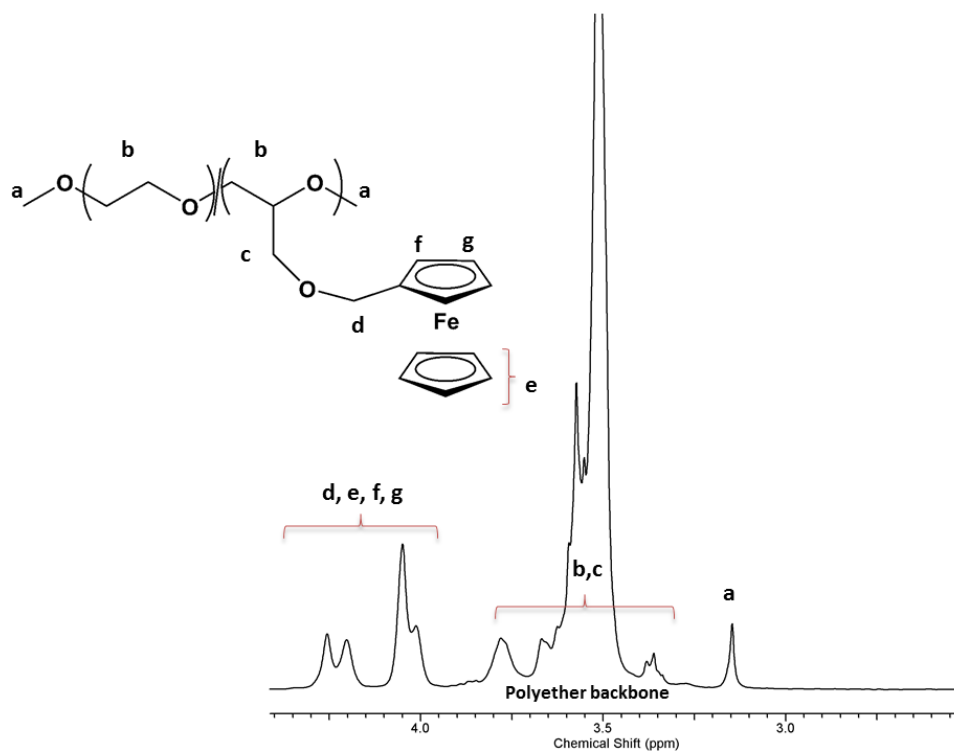


Figure S3. Peak assignment of P(EO-co-fcGE)/sample **P3** in ^1H NMR.

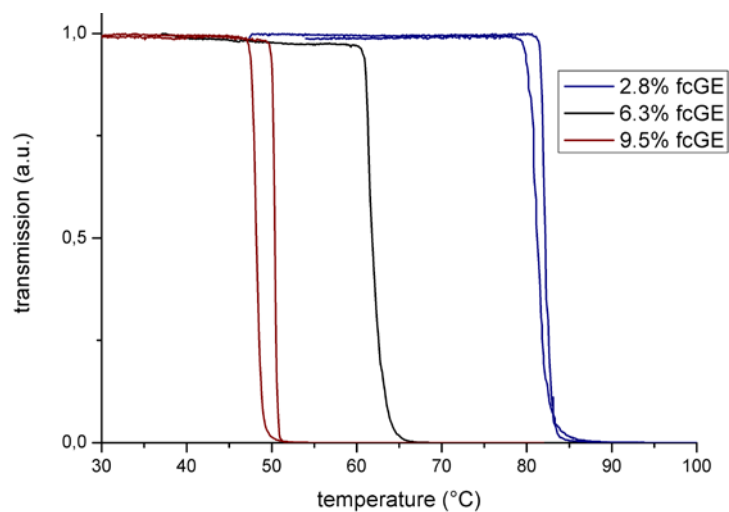


Figure S4. Cloud point measurements exhibit reversible LCST behavior.

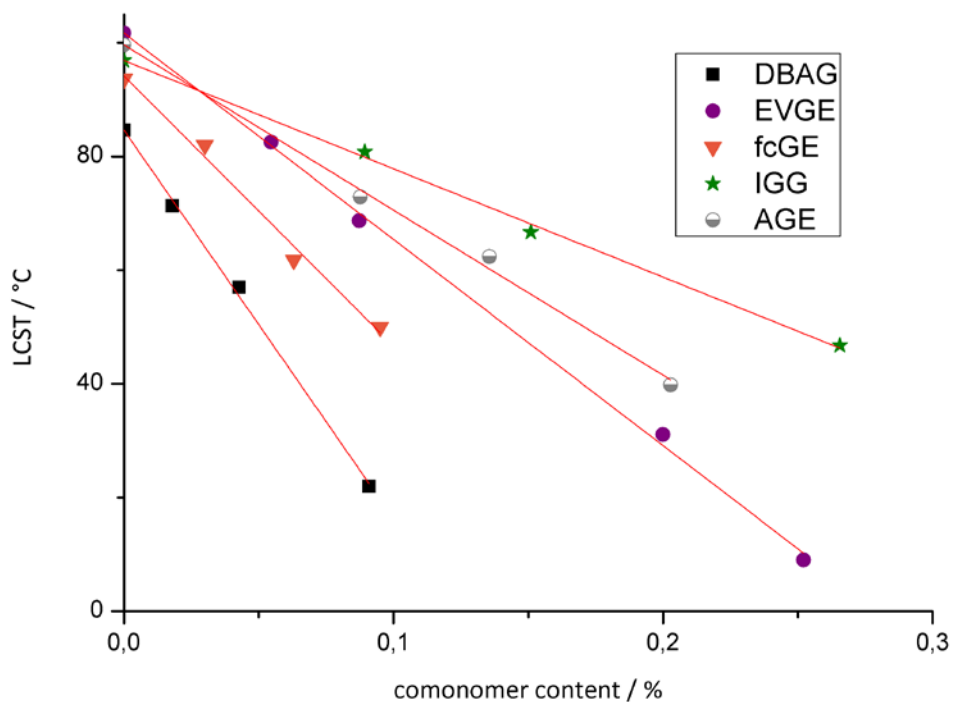


Figure S5. LCST temperature versus comonomer content of P(EO-co-fcGE) copolymer and other previously described copolyethers.³⁰

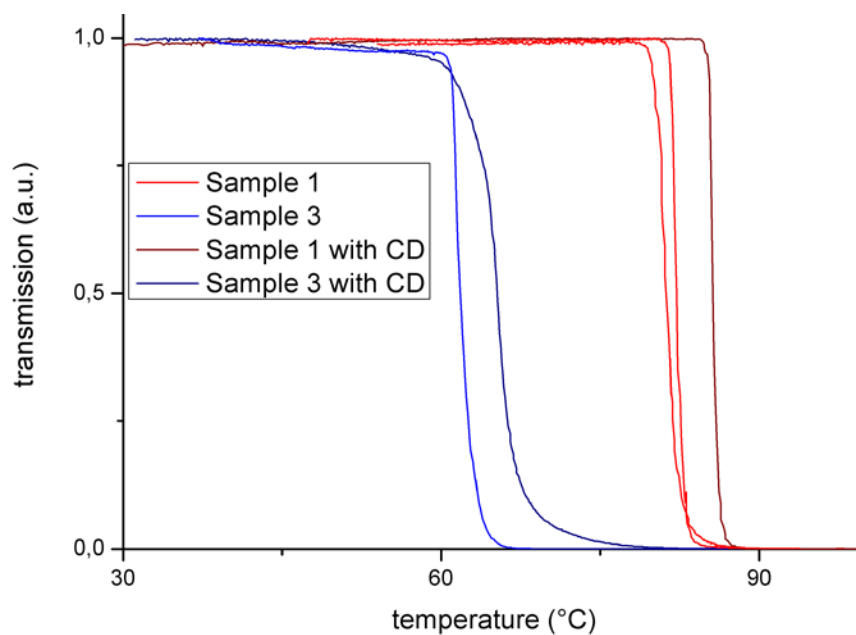


Figure S6. Cloud point measurements before and after treatment with β -cyclodextrin.



Figure S7. A colour change is observed after addition of oxidative reagents.

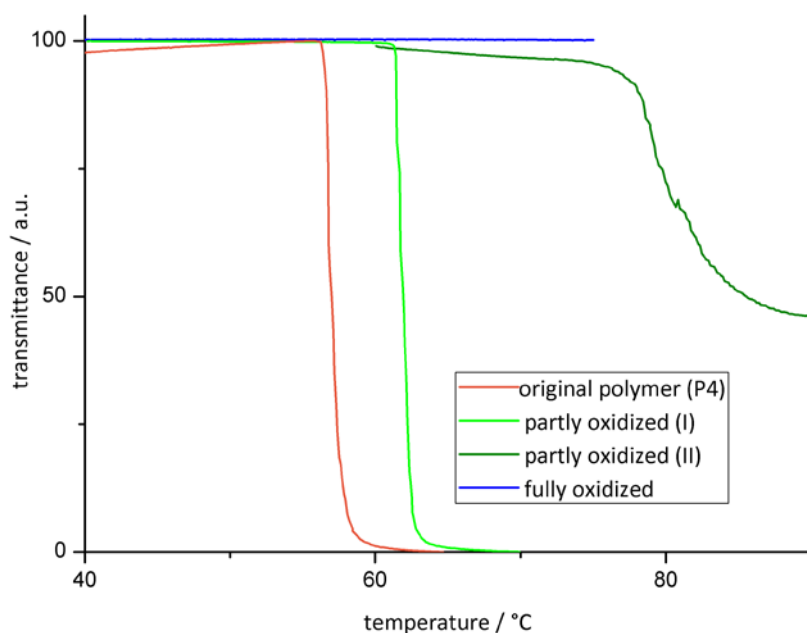


Figure S8. By the addition of oxidizing agents the LCST can be altered until finally the thermo-responsive behavior disappears.

1. Nguyen, P.; Gomez-Elipe, P.; Manners, I. *Chem. Rev.* **1999**, 99, (6), 1515-1548.
2. Frede, M.; Steckhan, E. *Tetrahedron Lett.* **1991**, 32, (38), 5063-5066.
3. Arimoto, F. S.; Haven, A. C. *J. Am. Chem. Soc.* **1955**, 77, (23), 6295-6297.
4. Eloi, J.-C.; Rider, D. A.; Cambridge, G.; Whittell, G. R.; Winnik, M. A.; Manners, I. *J. Am. Chem. Soc.* **2011**, 133, (23), 8903-8913.
5. Durkee, D. A.; Eitouni, H. B.; Gomez, E. D.; Ellsworth, M. W.; Bell, A. T.; Balsara, N. P. *Adv. Mater.* **2005**, 17, (16), 2003-2006.
6. Wright, M. E.; Toplikar, E. G.; Kubin, R. F.; Seltzer, M. D. *Macromolecules* **1992**, 25, (6), 1838-1839.

7. Top, S.; Dauer, B.; Vaissermann, J.; Jaouen, G. *J. Organomet. Chem.* **1997**, 541, (1-2), 355-361.
8. Top, S.; Vessières, A.; Leclercq, G.; Quivy, J.; Tang, J.; Vaissermann, J.; Huché, M.; Jaouen, G. *Chem. Eur. J.* **2003**, 9, (21), 5223-5236.
9. Foulds, N. C.; Lowe, C. R. *Anal. Chem.* **1988**, 60, (22), 2473-2478.
10. Rehahn, M., Organic-Inorganic Hybrid Polymers. In *Synthesis of Polymers*, Schlüter, A.-D., Ed. Wiley-VCH: Weinheim, Germany, 1999; p 319.
11. Gallei, M.; Schmidt, B. V. K. J.; Klein, R.; Rehahn, M. *Macromol. Rapid Commun.* **2009**, 30, (17), 1463-1469.
12. Gallei, M.; Klein, R.; Rehahn, M. *Macromolecules* **2010**, 43, (4), 1844-1854.
13. Gallei, M.; Tockner, S.; Klein, R.; Rehahn, M. *Macromol. Rapid Commun.* **2010**, 31, (9-10), 889-896.
14. Foucher, D. A.; Tang, B. Z.; Manners, I. *J. Am. Chem. Soc.* **1992**, 114, (15), 6246-6248.
15. Manners, I. *Can. J. Chem.* **1998**, 76, (4), 371-381.
16. Wang, Z.; Masson, G.; Peiris, F. C.; Ozin, G. A.; Manners, I. *Chem. Eur. J.* **2007**, 13, (33), 9372-9383.
17. Pittman, C. U.; Lai, J. C.; Vanderpool, D. P. *Macromolecules* **1970**, 3, (1), 105-107.
18. Pittman, C. U.; Hirao, A. *J. Polym. Sci. Polym. Chem. Ed.* **1977**, 15, (7), 1677-1686.
19. Pittman, C. U.; Hirao, A. *J. Polym. Sci. Polym. Chem. Ed.* **1978**, 16, (6), 1197-1209.
20. Herfurth, C.; Voll, D.; Buller, J.; Weiss, J.; Barner-Kowollik, C.; Laschewsky, A. *J. Polym. Sci., Part A: Polym. Chem.* **2012**, 50, (1), 108-118.
21. Wurm, F.; Villanueva, F. J. L.; Frey, H. *J. Polym. Sci., Part A: Polym. Chem.* **2009**, 47, (10), 2518-2528.
22. Hale, P. D.; Boguslavsky, L. I.; Inagaki, T.; Lee, H. S.; Skotheim, T. A.; Karan, H. I.; Okamoto, Y. *Molecular Crystals and Liquid Crystals Incorporating Nonlinear Optics* **1990**, 190, (1), 251-258.
23. Swarts, J. C. *Macromol. Symp.* **2002**, 186, (1), 123-128.
24. Wang, X.-S.; Winnik, M. A.; Manners, I. *Macromol. Rapid Commun.* **2002**, 23, (3), 210-213.
25. Gohy, J.-F.; Lohmeijer, B. G. G.; Alexeev, A.; Wang, X.-S.; Manners, I.; Winnik, M. A.; Schubert, U. S. *Chem. Eur. J.* **2004**, 10, (17), 4315-4323.
26. Resendes, R.; Massey, J.; Dorn, H.; Winnik, M. A.; Manners, I. *Macromolecules* **2000**, 33, (1), 8-10.
27. Power-Billard, K. N.; Manners, I. *Macromolecules* **1999**, 32, (1), 26-31.
28. Power-Billard, K. N.; Spontak, R. J.; Manners, I. *Angew. Chem. Int. Ed.* **2004**, 43, (10), 1260-1264.
29. Yang, W.; Zhou, H.; Sun, C. *Macromol. Rapid Commun.* **2007**, 28, (3), 265-270.

30. Mangold, C.; Obermeier, B.; Wurm, F.; Frey, H. *Macromol. Rapid Commun.* **2011**, 32, (23), 1930-1934.
31. Schattling, P.; Jochum, F. D.; Theato, P. *Chem. Commun.* **2011**, 47, (31).
32. Broadhead, G. D.; Osgerby, J. M.; Pauson, P. L. *J. Chem. Soc.* **1958**, 650-656.
33. Wurm, F.; Nieberle, J.; Frey, H. *Macromolecules* **2008**, 41, (6), 1909-1911.
34. Mangold, C.; Dingels, C.; Obermeier, B.; Frey, H.; Wurm, F. *Macromolecules* **2011**, 44, (16), 6326-6334.
35. Obermeier, B.; Wurm, F.; Frey, H. *Macromolecules* **2010**, 43, (5), 2244-2251.
36. Mangold, C.; Wurm, F.; Obermeier, B.; Frey, H. *Macromolecules* **2010**, 43, (20), 8511-8518.
37. Mangold, C.; Wurm, F.; Obermeier, B.; Frey, H. *Macromol. Rapid Commun.* **2010**, 31, (3), 258-264.
38. Obermeier, B.; Frey, H. *Bioconjugate Chem.* **2011**, 22, (3), 436-444.
39. Obermeier, B.; Wurm, F.; Mangold, C.; Frey, H. *Angew. Chem. Int. Ed.* **2011**, 50, (35), 7988-7997.
40. Fuller, C. S. *Chem. Rev.* **1940**, 26, (2), 143-167.
41. Henning, T. *SOFW Journal* **2001**, 127, 28-35.
42. Rekharsky, M. V.; Inoue, Y. *Chem. Rev.* **1998**, 98, (5), 1875-1918.
43. Giannotti, M.; Lv, H.; Ma, Y.; Steenvoorden, M.; Overweg, A.; Roerdink, M.; Hempenius, M.; Vancso, G. J. *Inorg. Organomet. Polym. Mater.* **2005**, 15, (4), 527-540.
44. Zhang, Y.; Furyk, S.; Bergbreiter, D. E.; Cremer, P. S. *J. Am. Chem. Soc.* **2005**, 127, (41), 14505-14510.
45. Whittell, G. R.; Manners, I. *Adv. Mater.* **2007**, 19, (21), 3439-3468.
46. Wasczak, M. D.; Lee, C. C.; Hall, I. H.; Carroll, P. J.; Sneddon, L. G. *Angew. Chem.* **1997**, 109, (20), 2300-2302.
47. Köpf-Maier, P.; Köpf, H.; Neuse, E. W.; Köpf, H. *Angew. Chem.* **1984**, 96, (6), 446-447.
48. Abuchowski, A.; McCoy, J. R.; Palczuk, N. C.; van Es, T.; Davis, F. F. *J. Biol. Chem.* **1977**, 252, (11), 3582-3586.

Chapter 4.2:

Asymmetric Micellization of Organometallic Polyether Block Copolymers

Asymmetric Micellization of Organometallic Polyether Block Copolymers

Christine Mangold, Frederik Wurm and Andreas F. M. Kilbinger

Published in: *Non-Conventional Functional Block Copolymers*, American Chemical Society: 2011; Vol. 1066, 103-115.



Abstract

Anionic ring-opening polymerization was applied for the synthesis of several di- and triblock copolymers bearing a variable amount of vinyl-ether moieties. These vinyl ethers were reacted with Grubbs' catalyst to generate an organometallic copolymer via a stable Fischer carbene. The block copolymers were investigated via TEM for their aggregation behavior.

Introduction

The synthesis of block copolymers can be regarded as one of the key-features of macromolecular science. Block copolymers offer a tremendous field for applications mostly due to the possibility of combining different characteristics of the respective homopolymers, but also due to incompatibility of both segments resulting in a great variety of supramolecular aggregates.¹ Within the field of block copolymers, linear diblock copolymers are the most investigated class and their supramolecular structures in solution and in bulk have been studied in detail and are well-understood. Research in this field covers not only coiled block copolymers, but also other types of block copolymers like rod-coil block copolymers²⁻⁴ or nonlinear block copolymers, i.e. stars⁵ or highly branched segments.⁶ Introducing a third block results in terpolymers and the variety of possible superstructures increases even further.⁷ Until now there are only few literature examples focussing on the aggregation behaviour of block terpolymers in comparison to the abundance of reports investigating diblock copolymers.

In the last decades the synthesis of asymmetric nanoparticles, which are often called “Janus-particles”, have gathered increased attention. Since de Gennes’ Nobel lecture in 1991, in which he presented the term “Janus grains”,⁸ different areas of researchers have focussed on the synthesis of asymmetric particles. Macroscopic, microscopic and nanoscopic particles have been prepared in which certain parts of their surface differ in chemical composition, polarity, color, or any other property. Spherical, cylindrical, disc-like, snowman-, hamburger-, and raspberry-like structures have been synthesized from organic as well as inorganic materials, or even as hybrids of both. The term “Janus” originates from the two-faced Roman god Janus, the god of the doors. Even in modern culture, the month of January, the first month of the New Year, and the janitor, who is a caretaker of doors and halls, remind us of this ancient Roman god. Janus is depicted as a double-headed god who represents dichotomy. Some recent reviews give an overview on different Janus particles in detail.⁹⁻¹¹ Within this field of research, linear and miktoarm ABC-block terpolymers have been used for the construction of multicompartment micelles, which are also referred to as janus micelles. Linear ABC-block terpolymers have been ordered in the bulk or on solid surfaces to prepare janus micelles, which are asymmetric star copolymers, after physical cross-linking. Since the first mention of janus micelles, janus discs and janus cylinders have also been reported and generated increased academic as well as technological interest.^{9,12}

We recently presented the first Janus particles which are based on an amphiphilic polyether diblock copolymer undergoing a cross metathesis reaction with Grubbs’ first generation catalyst.¹³ In addition to the unexpected formation of asymmetric aggregates this technique allows TEM staining of polymers by the attachment of the electron rich ruthenium to the “invisible” polyether chain. A principal problem in analyzing supramolecular polymeric or compartmented structures is their visualization. Typically, scanning force microscopy (SFM) or transmission electron microscopy (TEM) can be employed. The differentiation between individual compartments or constituents of the supramolecular assembly can be particularly difficult or impossible. In many cases where transmission electron microscopy is used for visualization of polymeric structures, heavy metal staining agents are employed to increase the image contrast between areas of different chemical composition.¹⁴ The most common examples are osmium tetroxide which has been widely employed as a stain for unsaturated polymers, ruthenium tetroxide for saturated and unsaturated polymers or phosphotungstic acid which is especially useful for polyamide staining.¹⁴

To our surprise, the commercially available ruthenium carbene catalysts reported by Grubbs et al.¹⁵⁻¹⁷ have to date not been employed in TEM staining of polymers. Compared to the highly toxic and volatile osmium tetroxide they offer lower toxicity and easier handling at lower cost.

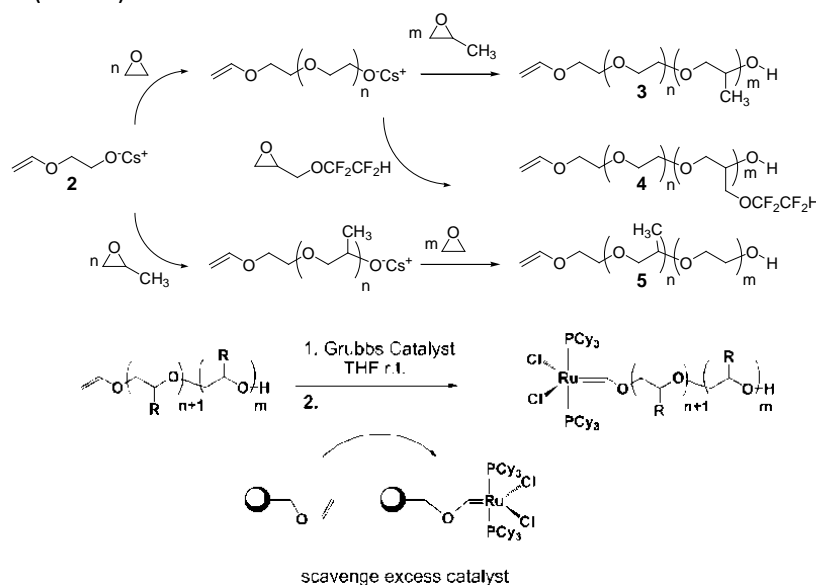
This chapter will summarize the results for the previously mentioned diblock copolymers based on poly(ethylene oxide) (PEO) and poly(propylene oxide) (PPO)¹³ and will introduce a novel block

copolymer with a highly hydrophobic block based on glycidyl-(1,1,2,2-tetrafluoro-ethyl)-ether. In addition we will present some first results on ABC-block terpolymer systems with a variable number of organometallic moieties attached to a polyether backbone via cross metathesis.¹⁸

Results and discussion

Diblock copolymers. All polymers presented herein rely on classical anionic ring-opening polymerization (ROP) of epoxides initiated by cesium alkoxides.

We used the cesium salt of 2-(vinylxy)ethanol (**2**) for the synthesis of diblock copolymers based on PEO and PPO via anionic polymerization bearing a single vinyl ether at the polyether chain end, either at the hydrophobic (PPO) (**5**) or hydrophilic (PEO) (**3**) end by variation of the monomer addition sequence. These narrowly distributed block copolymers were subsequently modified with a ruthenium carbene complex, namely the first generation Grubbs catalyst (**1**) to introduce an organometallic moiety at the chain end via a stable Fischer carbene linkage. It has been well established that vinyl ethers react with ruthenium carbene catalysts to form Fischer carbene-type complexes that are effectively inactive for further olefin metathesis reactions.¹⁹ Reactions of this type are therefore often used for the non-functional chain termination of ring opening metathesis polymerizations (ROMP).



Scheme 1. *Top:* Synthesis of diblock copolymers. *Bottom:* General procedure for cross metathesis of vinyl ether group(s) with Grubbs catalyst.

We also synthesized a hitherto unknown block copolymer, poly(ethylene oxide)-*block*-poly(glycidyl 1,1,2,2-tetrafluoro-ethyl ether) (**4**), again carrying a vinyl ether moiety at the hydrophilic chain end. The molecular weights of the narrow polydispersity block copolymers ranged from ca. 4 200-6 000 g mol⁻¹ (Table 1).

The synthesis of the diblock copolymers and their modification are shown in Scheme 1. Their supramolecular aggregation in water was monitored via transmission electron microscopy. A high contrast of the micelles was expected due to the presence of the electron-rich ruthenium in the micelle.

Solutions of unmodified polymers **3**, **4** and **5** were prepared in THF (1 mg mL^{-1}), which is a good solvent for all segments. They were then further diluted with water to induce micellation. Due to lack of contrast the micelles could be observed using TEM.

Addition of an excess of **1** to the THF solutions of **3**, **4** and **5** resulted in an olefin metathesis reaction at the chain end of the block copolymers. This leads to the formation of a Fischer-type carbene, which is indicated by the color change from purple to light brown. This reaction sequence allows the covalent attachment of the Grubbs catalyst to the block copolymer chain end (Scheme 1). After dilution with water and removal of the insoluble excess of **1**, TEM images were recorded of all three solutions, which revealed dark spherical objects with enhanced contrast compared to the TEM grid (not shown). We believe that parts of the ruthenium catalyst **1** were dissolved in the hydrophobic core of the formed micelles, leading to non-specific staining.

To remove virtually all excess of catalyst **1**, we prepared a scavenger resin which was functionalized with vinyl ether groups.¹³ In a subsequent experiment we added an excess of **1** to THF solutions of **3**, **4** and **5**, followed by the removal of the excess by the addition of the scavenger resin. For polymer **5** dark spherical micelles were observed, as the organometallic group and the PPO-block form the micellar core, while PEO solubilizes the aggregate in the corona (Figure 2, A). For polymers **3** and **4** interestingly non-symmetrical aggregates (Figure 2, B, C) were observed which coexisted with supermicelles (Figure 2, D,E,F) as reported for other Janus micelles (for detailed information on aggregation model see reference¹³).

To further investigate the micellization and staining process, we modified the terminal vinyl-bond by the addition of bromine and visualized the micelles from the aqueous solution via TEM. As expected, all diblock copolymers, regardless if modified on the hydrophilic or hydrophobic chain end, aggregate to conventional spherical micelles with a slightly increased TEM-contrast, which is due to the presence of the bromides at the chain end (Figure 2).

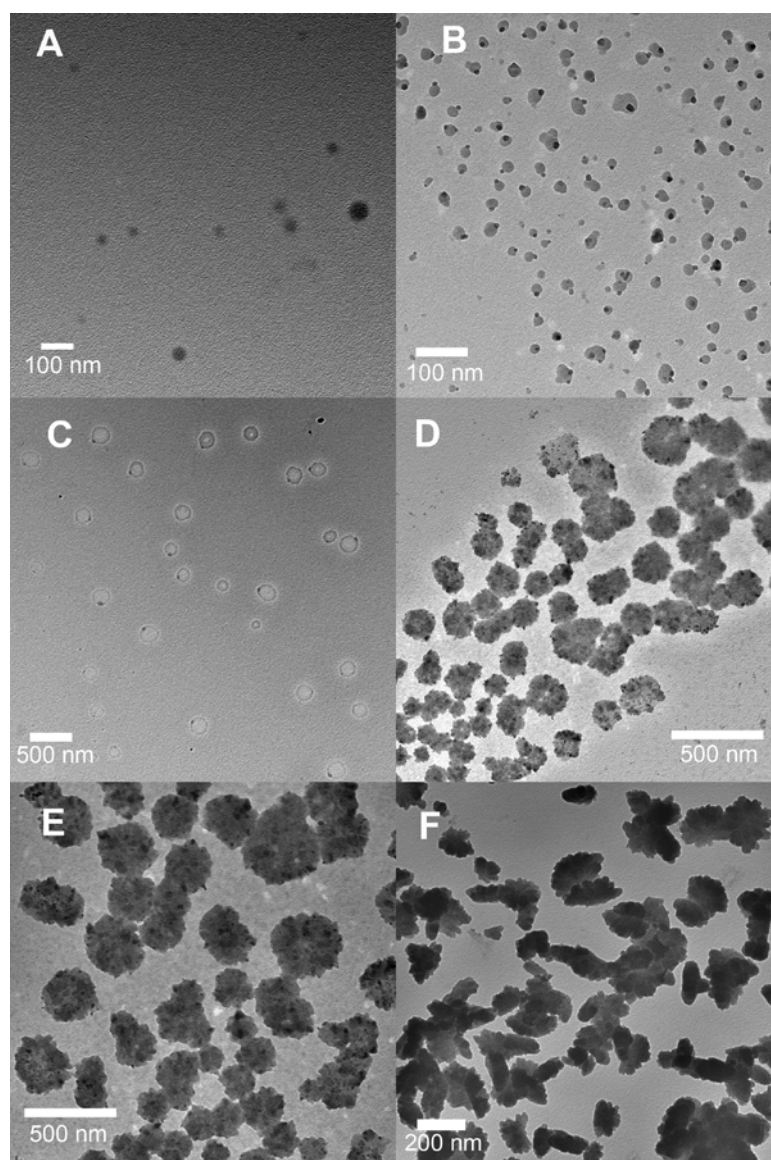


Figure 1. TEM images of block copolymers **3,4,5** reacted with Grubbs catalyst 1st generation dropcast from an aqueous solution. A:**5-Ru**. B:**3-Ru**. C:**4-Ru**. D: supermicelles of **3-Ru** E: zoom into supermicelles of **3-Ru** F: supermicelles **4-Ru**.

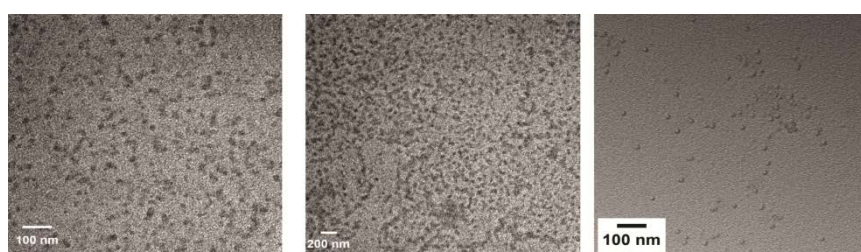


Figure 2. TEM pictures of brominated diblock copolymers *left: Br-3, middle: Br-5, right: Br-4*.

This led us to the conclusion that cross metathesis between the terminal vinyl group and the carbene catalyst, does not only enhance the TEM contrast but in addition has a strong influence on the

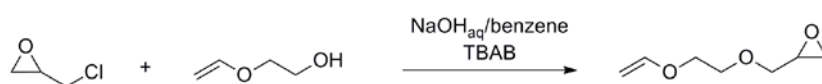
aggregation behavior of the materials. It has to be pointed out that the strongly hydrophobic character and the quite high molecular weight of the Grubbs catalyst (ca. 800 g/mol) generate an ABC-system similar to an ABC-terpolymer with the organometallic unit representing a segment of similar molecular weight as the hydrophobic PPO-block. By decreasing the molecular weight of the “covalent stain” to bromine, conventional micellization was observed with a slight staining effect.

Table 1: Molecular weight data for diblock copolymers.

#	M_n (SEC) ¹	PDI ¹
3 Vinyl-PEO ₁₀₂ -PPO ₁₅	5 300	1.06
4 Vinyl-PEO ₉₆ -PTFGE ₁₀	6 000	1.07
5 Vinyl-PPO ₁₃ -PEO ₇₄	4 200	1.05

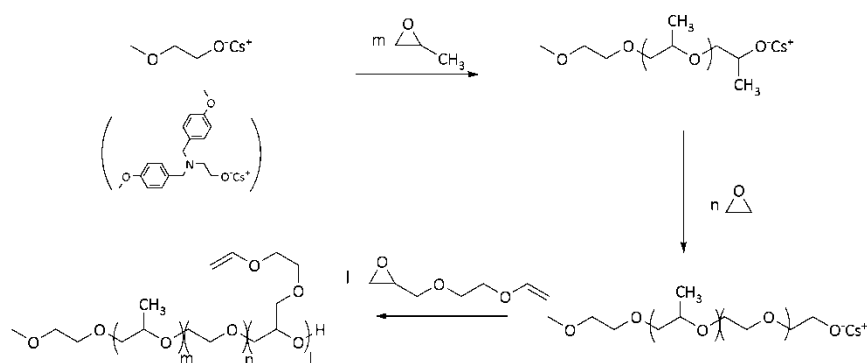
1: determined via SEC in DMF vs PEO Standards.

Terblock copolymers. In a following step the findings from the abovementioned diblock copolymer systems bearing only one organometallic side chain were extended to a block terpolymer system with a variable number of vinyl groups for attachment of the Fischer carbene. For this purpose we designed a novel monomer for anionic ROP, i.e. ethoxy vinyl glycidyl ether (EVGE). The monomer can be conveniently synthesized from epichlorohydrin and 2-(vinylloxy)ethanol under phase-transfer conditions as reported for other glycidyl ethers before^{20, 21} (Scheme 2) and was isolated by fractionated distillation.



Scheme 2. Synthesis of ethoxy vinyl glycidyl ether under phase transfer conditions (TBAB= tetrabutylammonium bromide).

ABC-terpolymers were then synthesized with propylene oxide as the first, ethylene oxide as the second, and EVGE as the last block by sequential anionic ROP. By the degree of polymerization of EVGE the number of possible metathesis sites can be adjusted. Scheme 3 shows the synthetic strategy and Figure 4 shows the SEC elugrams of the block copolymer after each block.



Scheme 3: Synthesis of ABC-triblock terpolymers bearing several vinyl ether groups along the backbone.

As it can be clearly seen narrow molecular weight distributions are obtained for all blocks. Table 2 summarizes the molecular weight data. Figure 5 shows the ^1H NMR spectra for all stages of the polymerization from which the degree of polymerization of the terpolymer can be calculated accurately by comparison to the methyl group of the initiator (in this case methoxy ethanol). Furthermore the ^1H NMR spectra prove the successful incorporation of EVGE with retention of its vinyl-functionality. The respective resonances for the vinyl protons appear at ca. 6.5 ppm and between 4.1 and 4.0 ppm. In addition to the non-functional methoxyethanol which was applied as the initiator, we also applied *N,N*-dibenzylaminoethanol as an initiator²² to introduce an additional aminofunctionality allowing orthogonal reactivity (not presented in this manuscript).

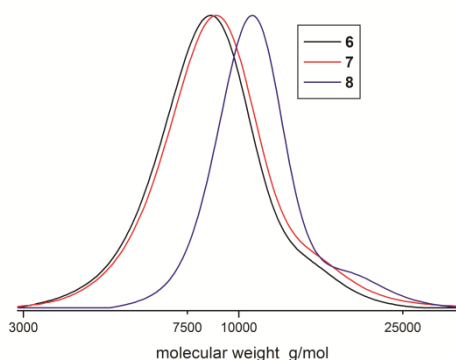


Figure 3. Molecular weight distribution of samples 6-8 in THF. Additional data is given in Table 2.

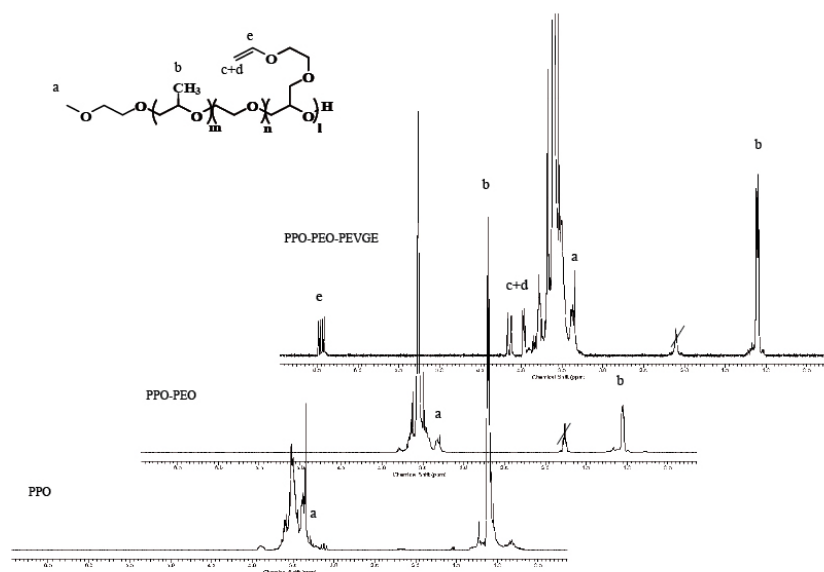


Figure 4. ^1H NMR spectra (CDCl_3 , 300 MHz) of samples taken after polymerization of each block; lower spectrum: PPO-OH, middle: PPO-*b*-PEO-OH, top: PPO-*b*-PEO-*b*-PEVGE-OH.

MALDI-ToF MS further confirmed the successful incorporation of all monomers into the polymer as the distances for all monomer repeat units can be found in the spectrum. Figure 6 shows a zoomed-in section of a typical mass spectrum of an ABC-terpolymer, highlighting its complex features due to the presence of three distinct distributions.

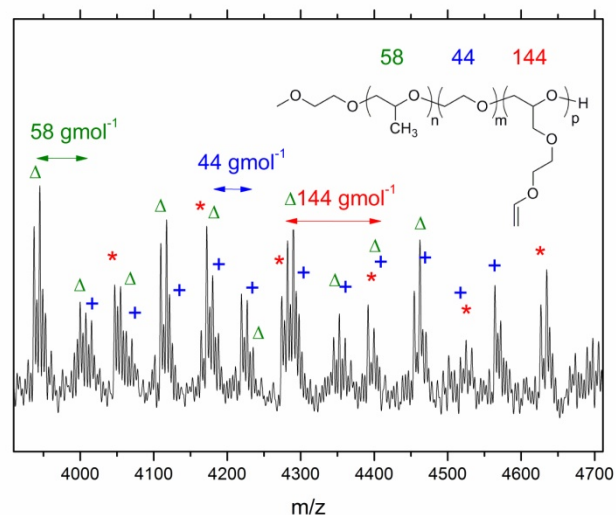


Figure 5. Zoom into a MALDI-ToF spectrum of the terpolymer PPO-*b*-PEO-*b*-PEVGE (measured with CHCA as matrix and KTFA as a cationizing agent; triangles represent the monomer distance for PO (58 g/mol), stars the distance for EVGE (144 g/mol) and the crosses represent the EO distance of 44 g/mol).

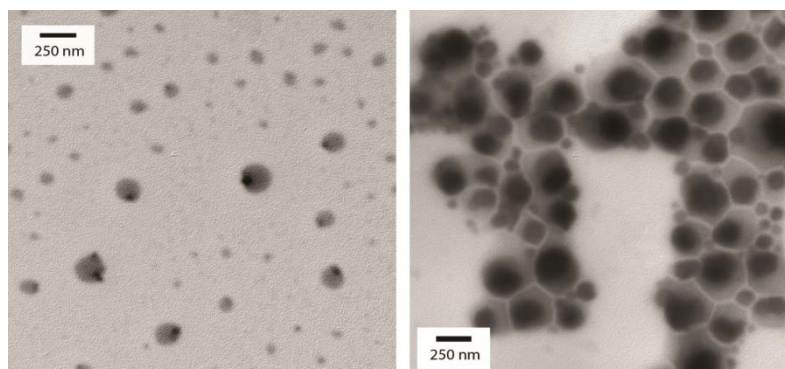


Figure 6. TEM images of block copolymer **6** reacted with Grubbs' 1st generation catalyst dropcast from an aqueous solution. Left: unimers which coexist with supermicelles (right).

In contrast to the AB-linear block copolymers, with only one Grubbs catalyst attached at the chain-end, the aggregation behavior of the triblock terpolymers as investigated by TEM was found to be more complex. A similar staining procedure was applied as reported above, i.e. addition of an excess of **1** and subsequent treatment with the vinyl-ether-modified scavenger resin. In contrast to the abovementioned process for the diblock copolymers, the formation of the Fischer carbene, showed slow kinetics, which were investigated in detail by time-resolved ¹H NMR experiments (data not shown here); thus, the reaction time was extended to several hours to guarantee a nearly quantitative (up to 90%) conversion of all vinyl-ether moieties.

Table 2: Molecular weight data of ABC-terpolymers

#	M _n (NMR) ¹	PDI ²
6 PPO ₁₅ - <i>b</i> -PEO ₁₅₆ - <i>b</i> -PEVGE _{1.5}	7 800	1.11
7 PPO ₁₅ - <i>b</i> -PEO ₁₅₆ - <i>b</i> -PEVGE ₆	8 500	1.09
8 PPO ₁₅ - <i>b</i> -PEO ₁₅₆ - <i>b</i> -PEVGE ₁₆	11 800	1.09 ³

1: determined from ¹H NMR by comparison to the initiator protons. 2: Determined via SEC in THF vs. PEO-standards. 3: Showed a slightly bimodal distribution.

Copolymer **6**, whose microstructure is close to copolymer **3**, forms similar aggregates, as can be seen in Figure 7. This finding is consistent with theoretical expectations. The vinyl-units of the terpolymers **7** and **8** were also reacted to the corresponding organometallic polymers, but did not exhibit reproducible structures in TEM. This might be ascribed to the very high molecular weight of the organometallic block, which seems to suppress the influence of the two other blocks. We found that

our previous procedure used to visualize such structures in TEM is not suitable for these terpolymers as the water-solubility after modification is low. Ongoing studies investigate the variation of block ratios to obtain reliable results. Nevertheless, this first example proves the versatility of this approach to generate novel organometallic polymers with a nonconventional aggregation into asymmetric micelles, induced by olefin metathesis. In addition, by using EVGE as comonomer, one is still able to introduce an orthogonal by the initiator, e.g. amines or other chelating groups could be possible.

Conclusions

In summary, we have developed a versatile method for polymer staining using a ruthenium based irreversible olefin metathesis reaction which can be triggered along the polymer backbone by either initiating with a vinyl ether-based alcohol or by incorporation of a vinyl ether containing monomer into the polymer structure. Efficient removal of any excess of the Grubbs catalyst was performed by a specially designed scavenger resin, making specific staining visible. This scavenger resin could be also applied as a convenient protocol for removing the carbene catalyst from conventional metathesis reactions to prevent other purification steps such as chromatography.

The organometallic polyether block copolymers exhibit interesting supramolecular structures which are strongly influenced by the attached ruthenium moieties. In addition, first results of novel triblock terpolymers with variable amount of vinyl were presented.

While further and more detailed studies are currently undertaken, we assume that for larger polymers the effect on new architectures is negligible and pure staining can be observed due to the high contrast of ruthenium in TEM. This observation renders the described method highly versatile and applicable to many other materials, avoiding very toxic or radioactive reagents relying on well-established olefin metathesis.

Experimental

Instrumentation. ^1H NMR spectra (300 MHz) were recorded using a Bruker AC300. All spectra were referenced internally to residual proton signals of the deuterated solvent. Size exclusion chromatography (SEC) measurements were carried out in THF on an instrument consisting of a Waters 717 plus autosampler, a TSP Spectra Series P 100 pump, a set of three PSS SDV columns (104/500/50Å), and RI and UV detectors. All SEC diagrams rely on the RI detector signal, and the molecular weights refer to linear poly ethylene oxide (PEO) standards provided by Polymer Standards Service. Matrix-assisted laser desorption and ionization time-of-flight (MALDI-ToF) measurements were performed on a Shimadzu Axima CFR MALDI-TOF mass spectrometer equipped with a nitrogen laser delivering 3ns laser pulses at 337nm. α -cyano-4-hydroxy cinnamic acid (CHCA)

was used as matrix. Samples were prepared by dissolving the polymer in acetonitrile at a concentration of 1g/L. A 10 μ L aliquot of this solution was added to 10 μ L of a 10g/L solution of the matrix and 1 μ L of a solution of KTFA (0.1M in water as cationization agent). A 1 μ L aliquot of the mixture was applied to a multistage target and allowed to dry to create a thin matrix/analyte film. The samples were measured in positive ion and in linear or reflection mode of the spectrometer. A Philips EM 420 transmission electron microscope using a LaB6 cathode at an acceleration voltage of 120 kV was used to obtain TEM-images. TEM grids (carbon film on copper, 300 mesh) were obtained from Electron Microscopy Sciences, Hatfield, PA, USA.

Reagents. All solvents and reagents were purchased from Acros Organics and used as received, unless otherwise stated. Chloroform- d_1 was purchased from Deutero GmbH. Polymerization procedure for the diblock copolymers based on PEO and PPO and scavenger resin can be found elsewhere.¹³

Ethoxy vinyl glycidyl ether (EVGE). 2-(vinylloxy)ethanol (10 g, 113.5 mmol) was placed in a 500 mL round bottom flask and dissolved in a mixture of 50% aqueous NaOH (150 mL) and benzene (150 mL). To this mixture tetrabutylammonium bromide (3.5 g, 11 mmol) was added and the mixture was stirred quickly with a mechanical stirrer. Then the reaction mixture was cooled with an ice bath and epichlorohydrin (31.5 g, 340.5 mmol) was slowly added via a dropping funnel. After 24h reaction time at room temperature, the organic phase was separated from the aqueous phase, washed several times with brine, dried and concentrated *in vacuo* to remove benzene and the excess epichlorohydrin. The resulting slightly yellow residue was distilled under reduced pressure to yield the desired product as a colorless liquid in typically in 70-80% yield (11-13 g). H NMR (CDCl₃, 300 MHz): δ = 6.44 (dd, CH₂=CH, J₁=14.3, J₂=7), 4.13 (dd, CH₂=CH, J₁=14.3, J₂=2.2), 3.96 (dd, CH₂=CH, J₁=7, J₂=2.2), 3.8-3.65 (m, -O-CH₂-CH₂-O- 4H & CH₂ (glycidyl ether) 1H), 3.38 (dd, CH₂ (glycidyl ether), 1 H, J₁=11.8, J₂=5.9), 3.1 (m, CH-epoxide, 1H), 2.74 (dd, CH₂-epoxide, 1H, J₁=5, J₂=4.2), 2.56 (dd, CH₂-epoxide, 1H, J₁=5.2, J₂=2.6).

General procedure for the synthesis of the terpolymers P(PO-block-EO-block-EVGE). The corresponding initiator was dissolved in benzene in a 250 mL-Schlenk flask and 0.9 equivalents of cesium hydroxide were added. The mixture was stirred at 60 °C under argon for 1 h and evacuated at (10⁻² mbar) for 6 h to remove benzene and water, forming the corresponding cesium alkoxide. Propylene oxide was first cryo transferred into a graduated ampoule and then into the Schlenck flask. The polymerization was carried out at 60°C. After 24h approximately 15 mL dry THF was cryo-transferred into the Schlenk flask. Ethylene oxide was first cryo-transferred to a graduated ampoule, and then cryo-transferred into the flask containing PO-Oligomers. The mixture was again heated to 60 °C and stirred for 12h. Before the addition of EVGE, it was dried with CaH₂ and distilled freshly. The third monomer was added using a syringe and the solution was heated to 90°C for additional

12h. Precipitation in cold diethyl ether resulted in the pure copolymers. Yields: 95% to quantitative. ^1H NMR (300 MHz, CDCl_3): δ = 6.46 (dd, $\text{H}_2\text{C}=\text{CH}$), 4.15 (dd, $\text{HHC}=\text{CH}$), 3.97 (dd, $\text{HHC}=\text{CH}$), 3.68-3.34 (polyether backbone) 1.15 (m, CH_3). Additional signals occur in dependence of initiator: $(\text{MeOBn})_2\text{NC}_2\text{H}_4\text{OH}$: 7.21 (d, 2H, arom.) 6.81 (d, 2H, arom.), 3.76 (s, 6H, OCH_3), 3.60 (s, 4H, NCH_2Ph), 3.57 (t, 2H, CH_2OH) 2.60 (t, 2H, $\text{NCH}_2\text{CH}_2\text{O}$ -).

Staining and Micellization via Grubbs' Catalyst: For staining with the 1st generation Grubbs' catalyst, the calculated amount of polymer (ca. 5 mg) was dissolved in degassed THF (concentration ca. 50 mg mL^{-1}) and 1.1 eq. Grubbs' catalyst was added. The mixture was placed on an orbital shaker for 2 to 4 hours.

Without a scavenger resin: After the desired reaction time, degassed water (5 mL) was added to the polymer solution it was allowed to equilibrate at room temperature for 1 h and then ca. 2 μL were transferred on a TEM-copper grid and dried over night in vacuo.

With scavenger resin: The mixture was diluted with THF to approx. 10 mg mL^{-1} , the calculated amount of scavenger resin (2 eq excess, at theor. 100% degree of functionalization) was added and the mixture was placed on an orbital shaker for an additional 2-4 hours. Finally, the resin was removed by filtration and the solution was concentrated again to approx. 50 mg mL^{-1} , diluted with water (100-200 μL of THF solution was diluted with 5 mL of water), equilibrated for 0.5 - 3h at room temperature and then drop cast onto a TEM grid and dried overnight *in vacuo*.

Acknowledgements

The authors thank Prof. Holger Frey for his support. A.F.M.K. acknowledges the "Fonds der chemischen Industrie" for valuable financial support. F.W. is grateful to the Alexander von Humboldt-Stiftung for Feodor-Lynen research fellowship.

1. Bates, F. S.; Fredrickson, G. H. *Phys. Today* **1999**, 52, (2), 32-38.
2. Lee, M.; Cho, B.-K.; Zin, W.-C. *Chem. Rev.* **2001**, 101, (12), 3869-3892.
3. Olsen, B. D.; Segalman, R. A. *Mater. Sci. Eng., R* **2008**, 62, (2), 37-66.
4. König, H.; Kilbinger, A. *Angew. Chem. Int. Ed.* **2007**, 46, (44), 8334-8340.
5. Hadjichristidis, N. *J. Polym. Sci., Part A: Polym. Chem.* **1999**, 37, (7), 857-871.
6. Wurm, F.; Frey, H. *J. Polym. Sci., Part A: Polym. Chem.* In Press, Corrected Proof.
7. Hadjichristidis, N.; Iatrou, H.; Pitsikalis, M.; Pispas, S.; Avgeropoulos, A. *Prog. Polym. Sci.* **2005**, 30, (7), 725-782.
8. de Gennes, P. G. *Rev. Mod. Phys.* **1992**, 64, (3), 645.

9. Wurm, F.; Kilbinger, A. *Angew. Chem. Int. Ed.* **2009**, 48, 8412-8421.
10. Walther, A.; Müller, A. H. E. *Soft Matter* **2008**, 4, (4), 663-668.
11. Perro, A.; Reculusa, S.; Ravaine, S.; Bourgeat-Lami, E.; Duguet, E. *J. Mater. Chem.* **2005**, 15, (35-36), 3745-3760.
12. Nie, L.; Liu, S.; Shen, W.; Chen, D.; Jiang, M. *Angew. Chem. Int. Ed.* **2007**, 46, (33), 6321-6324.
13. Wurm, F.; Nieberle, J.; Frey, H. *Macromolecules* **2008**, 41, (4), 1184-1188.
14. Smith, R. W.; Bryg, V. *Rubber Chem. Technol.* **2006**, 79, (3), 520-540.
15. Nguyen, S. T.; Grubbs, R. H.; Ziller, J. W. *J. Am. Chem. Soc.* **1993**, 115, (21), 9858-9859.
16. Schwab, P.; Grubbs, R. H.; Ziller, J. W. *J. Am. Chem. Soc.* **1996**, 118, (1), 100-110.
17. Nguyen, S. T.; Johnson, L. K.; Grubbs, R. H.; Ziller, J. W. *J. Am. Chem. Soc.* **1992**, 114, (10), 3974-3975.
18. Wurm, F. *Polym. Prepr. (Am. Chem. Soc., Div. Polym. Chem.)* **2010**, 51, (1), 322-323.
19. Grubbs, R. H.; Chang, S. *Tetrahedron* **1998**, 54, (18), 4413-4450.
20. Wurm, F.; Nieberle, J.; Frey, H. *Macromolecules* **2008**, 41, (6), 1909-1911.
21. Obermeier, B.; Wurm, F.; Frey, H. *Macromolecules* **2008**, 41, (5), 2244-2251.
22. Wurm, F.; Klos, J.; Räder, H. J.; Frey, H. *J. Am. Chem. Soc.* **2009**, 131, (23), 7954-7955.

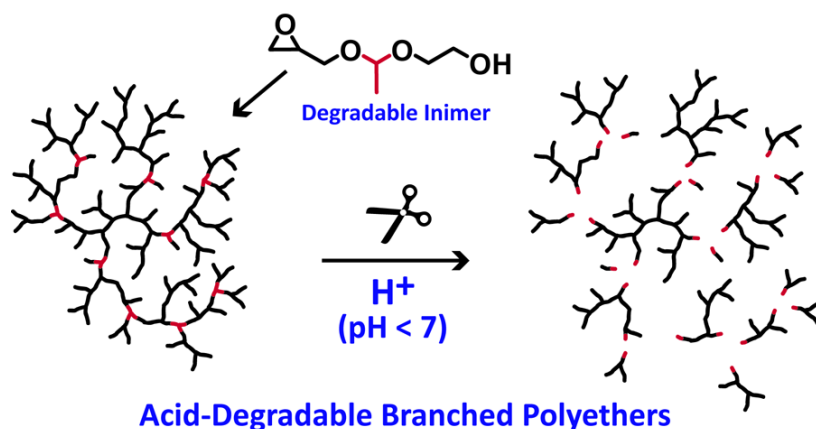
Chapter 5:

Branched Acid-Degradable, Biocompatible Polyether-Based Copolymers by Anionic Ring-Opening Polymerization Using an Epoxide Inimer

Branched Acid-Degradable, Biocompatible Polyether-Based Copolymers by Anionic Ring-Opening Polymerization Using an Epoxide Inimer

Christine Mangold, Christoph Schüll, Carsten Dingels, Holger Frey

To be submitted to *Macromolecules*.



Keywords: anionic polymerization, PEG, polyglycerol, hyperbranched polymers, degradable polymers, acid-labile

Abstract

The introduction of acid-degradable acetal moieties into a hyperbranched polyether backbone has been realized by the design of a novel epoxide-based degradable inimer. This new monomer, viz. glycoloxy ethyl glycidyl ether (GEGE) has been copolymerized in the anionic ring opening polymerization (AROP) with either ethylene oxide (EO) or glycidol, yielding branched polyethers, i.e. (P(EO-*co*-GEGE) and P(G-*co*-GEGE)) with varying structure and an adjustable amount of acid-cleavable acetal units incorporated. In addition, a novel class of multi-arm star polymers P(G-*co*-GEGE-*g*-EO) with acid-labile polyether core and PEG side chains was synthesized by using the P(G-*co*-GEGE) copolymers as multifunctional macroinitiators for AROP of EO. The new materials were characterized in detail, revealing relatively narrow molecular weight distributions. The degradation of these polymers was analysed via SEC and ^1H NMR spectroscopy.

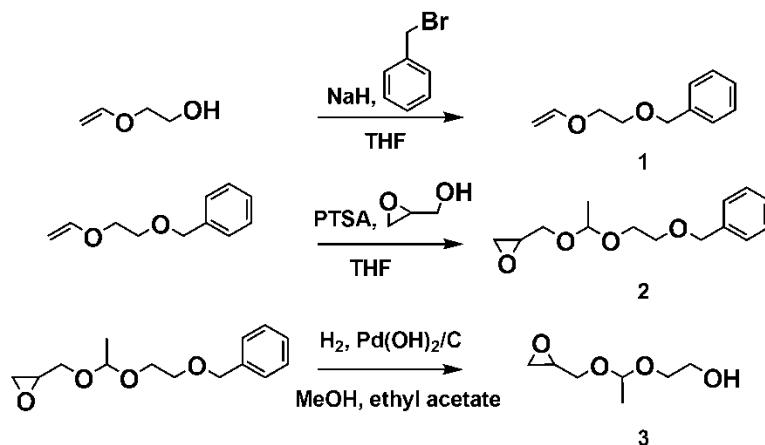
Introduction

The use of biocompatible, non-degradable polymers in biomedical stealth applications, such as PEGylation¹ is a well-established concept, which is widely used in academia, but also finds increasing application in the pharmaceutical industry. A well-known example is PegasysTM, which is PEGylated interferon used for the treatment of hepatitis C.² Although PEGylation and similar concepts based on linking polymers with protein or drugs are of increasing importance in future biomedical applications, the use of polymer-drug (or polymer-protein conjugates) is currently limited to a maximum molecular weight of the conjugated chain, which is given by the eventuality of renal clearance. In the case of the widely used poly(ethylene glycol) (PEG), often referred to as “gold-standard” of all biocompatible polymers, the molecular weight (for biomedical uses) will be limited to a maximum of 40 000 g/mol.³ This value translates to a hydrodynamic radius of 3.5 nm and varies in dependence of the class of polymers. Therefore, it is an important challenge to develop biocompatible polymers that degrade under physiological conditions. An acidic degradation mechanism of the respective polymer is often favored,⁴ due to the low pH-values present in lysosomes or cancer cells.⁵

Synthetic routes for acid-degradable PEG have been described in a few works to date, employing varying synthetic strategies. All of the different routes applied rely on post-polymerization reactions,⁶ and commonly an acetal moiety is used to guarantee the acid labile character. The most prominent example of an acid-labile PEG is “APEG”, developed by Brocchini and Duncan, which is obtained by the acid-catalyzed reaction of diols with vinyl-ether moieties, forming an acetal moiety.⁷ It has to be mentioned that this poly-addition of small oligo(ethylene glycol)-units yields degradable PEG-based polymers, but an unavoidable drawback is the broad molecular weight distributions of the polymers obtained due to the polycondensation kinetics employed.^{8,9} This might be undesired for application in biomedicine. Another approach was developed by Taton and coworkers,¹⁰ who designed acid degradable PEG-based arborescent polymers, using an acid cleavable branching unit and repetitive ethylene oxide (EO) polymerization. This elegant method yields high molecular weight polymers with narrow molecular weight distributions, but a demanding reaction sequence is required, comparable to a dendrimer synthesis. A similar concept was introduced by Hawker and coworkers in recent work, who designed a novel initiator that is suitable for anionic ring opening polymerization of ethylene oxide bearing an acetal moiety, which could be transformed into a nitroxide mediated polymerization (NMP)-initiator. This initiator was then utilized to synthesize a block copolymer with one central cleavable moiety. The report did not focus on biocompatible materials, and to date only poly(styrene) has been introduced as a second block.¹¹

In this work, a novel acetal-containing inimer for anionic ring-opening polymerization (AROP) and its use for the preparation of different polyether structures is described. To the best of our knowledge,

there has been no effort to design an epoxide based monomer that is suitable for anionic ring opening (multibranching) polymerization and enables the introduction of acid-labile groups into a PEG-backbone in a direct manner. The novel acetal-containing epoxide monomer with an initiator moiety, glycoloxy ethyl glycidyl ether (GEGE, **3**) can be synthesized in three reaction steps (compare **Scheme 1**). Besides, it possesses all characteristics of a degradable inimer,⁶ a concept first mentioned by Matyjaszewski et al. in an ATRP work.^{12, 13}



Scheme 1. Synthetic strategy for the novel inimer glycoloxy ethyl glycidyl ether (GEGE).

In this report the synthesis and characterization of degradable polyether architectures, obtained by facile copolymerization of the novel compound glycoloxy ethyl glycidyl ether (GEGE) with ethylene oxide (EO) and glycidol (G) is described. GEGE has been used for copolymerization i) with ethylene oxide and ii) glycidol to obtain either degradable poly(ethylene oxide -*co*- glycoloxy ethyl glycidyl ether) (P(EO-*co*-GEGE)) or poly(glycerol-*co*-glycoloxy ethyl glycidyl ether) (P(G-*co*-GEGE)). The obtained highly branched polyether polyol architectures were characterized in detail using SEC and NMR spectroscopy. In addition, these PEG/PG-based polymers were probed with respect to their degradability, revealing a strong pH-dependency on the degradation kinetics. These materials, which are highly interesting for biomedical applications are currently tested with respect to their biocompatibility and future applications in the field of biomedicine.

Experimental Section

Instrumentation

¹H NMR spectra (300 MHz and 400 MHz) and ¹³C NMR spectra (75.5 MHz) were recorded using a Bruker AC300 or a Bruker AMX400. All spectra were referenced internally to residual proton signals of the deuterated solvent. For SEC measurements in DMF (containing 0.25 g/L of lithium bromide as an additive) an Agilent 1100 Series was used as an integrated instrument, including a PSS HEMA

column ($10^6/10^5/10^4$ g/mol), a UV- (275 nm) and RI-detector. Calibration was carried out using poly(ethylene oxide) standards provided by Polymer Standards Service (PSS Mainz).

Reagents

Solvents and reagents were purchased from Acros Organics, Sigma Aldrich or Fluka and used as received, unless otherwise stated. Chloroform- d_1 , methanol- d_4 and DMSO- d_6 were purchased from Deutero GmbH.

Synthesis of *N,N*-Di(*p*-methoxy)-benzyl tris(hydroxymethyl) aminomethane (MeOBn₂TRIS). 20 g of freshly distilled *p*-methoxy benzyl bromide (0.1 mol) 5.5 g (0.045 mol) tris(hydroxymethyl)-aminomethane (TRIS), and K₂CO₃ (100 mmol) in DMF were refluxed for 24 h. After cooling to RT, the solution was filtrated and DMF was removed *in vacuo*. 300 mL of CHCl₃ were added and the organic phase was washed with water, a saturated NaHCO₃-solution and dried with MgSO₄. The solvent was then removed *in vacuo* and a highly viscous, slightly yellow liquid was obtained. The crude product mixture was purified by recrystallization from petroleum ether and ethyl acetate. Yield: 60%. ¹H NMR (300 MHz, DMSO- d_6): δ (ppm) = 7.12 (d, 4H, aromatic), 6.72 (d, 4H, aromatic) 4.24 (t, 3H, OH), 3.85 (s, 4H, PhCH₂N), 3.65 (s, 6H, OMe) 3.46 (d, 6H, CCH₂OH).

Synthesis of *N,N*-Dibenzyl tris(hydroxymethyl) aminomethane (Bn₂TRIS).¹⁴ 17 g benzyl bromide (0.1 mol), 5.5 g (0.045 mol) tris(hydroxymethyl) aminomethane, 13.8 K₂CO₃ (100 mmol) and 150 mL DMF were refluxed for 24 h. After cooling the reaction mixture to room temperature, the solution was filtrated and DMF was removed *in vacuo*. 300 mL of CHCl₃ were added and the organic phase was washed with water (3x 200 mL), saturated NaHCO₃-solution and dried with MgSO₄. The solvent was removed *in vacuo* and a highly viscous, slightly yellow liquid was obtained. The crude product mixture was purified by recrystallization from ethyl acetate, giving a white solid of the desired product which was dried under vacuum. ¹H NMR (300 MHz, DMSO- d_6): δ (ppm) = 7.28-7.02 (m, 10H, aromatic), 4.34-4.26 (br, 3H, OH), 3.99-3.91 (4H, PhCH₂N), 3.55-3.45 (d, 6H, CCH₂OH). ¹³C NMR (75 MHz, DMSO- d_6): δ (ppm) = 142.6, 128.1, 127.7, 126.0 (C_{arom.}), 65.4 (Bn₂NC), 60.8 (CH₂OH), 53.7 (PhCH₂).

Synthesis of glycoloxy ethyl glycidyl ether (GEGE). 15 g of ethylene glycol mono vinyl ether (0.17 mol) was placed in a two neck round bottom flask in 100 mL THF. 8 g NaH (60% in paraffin oil, approx. 1.2 eq.), was washed with petroleum ether to obtain the pure hydride and added to the solution. The reaction mixture was allowed to stir for 1 h at 60 °C and 34 g of benzyl bromide (0.20 mol) was added subsequently. After refluxing for 24 h the emerging NaBr was removed by filtration and THF as well as the excess of benzyl bromide were removed *in vacuo*. **1** was obtained as a yellow oil; yield: quantitative.

The crude product was then reacted with glycidol in analogy to the established synthesis of ethoxy ethyl glycidyl ether (EEGE).¹⁵ In a typical procedure 5 g of **1**, and 2.1 g of glycidol in dry THF (40 mL) as well as 0.5 g of freshly dried *p*-toluene sulfonic acid were placed in a round bottom flask and stirred for 5-10 h. Formation of the product (**2**) was monitored by thin layer chromatography (TLC). The crude product mixture was purified by column chromatography using a mixture of ethyl acetate and petroleum ether as eluent. Yield: 60-80%.

1 g of **2** in 60 mL ethyl acetate/methanol (5:1) and 100 mg of Pd(OH)₂/C were placed in a round bottom flask under argon atmosphere. H₂ was bubbled through the solution and the reaction mixture was stirred for 6-10 h under an H₂ atmosphere (1 bar). Product formation was monitored by TLC. The crude product mixture was purified by column chromatography (ethyl acetate/petroleum ether) and GEGE (**3**) was obtained as colourless liquid. Yield: 50-67%. ¹H NMR (300 MHz, CDCl₃): δ (ppm) = 4.78 (m, 1H, acetalic), 3.89-3.37 (m, 6H, CH₂O), 3.13 (m, 1H, methine/epoxide), 2.80 (m, 1H, methylene/epoxide-1), 2.62 (m, 1H, methylene/epoxide-2), 1.33 (m, 3H, CH₃-acetal).

Synthesis of poly(ethylene oxide -co- glycoloxy ethyl glycidyl ether) (P(EO-co-GEGE)). General procedure for the copolymerization: *N,N*-Di(*p*-methoxy)-benzyl tris(hydroxymethyl) aminomethane and 1.5 equivalents of cesium hydroxide monohydrate (50% of hydroxyl groups) were placed in a 250 mL-Schlenk flask and benzene was added. The mixture was stirred at 60 °C under argon atmosphere for 1 h and evacuated at 60 °C (10⁻² mbar) for 12 h to remove benzene and water, forming the corresponding cesium alkoxide. Then approximately 20 mL dry THF were cryo-transferred into the Schlenk flask. EO was cryo-transferred to a graduated ampoule, and then cryo-transferred into the reaction flask containing the initiator in THF. Subsequently, the second comonomer, GEGE, was added via syringe in a 50 wt% solution in anhydrous DMSO. The mixture was heated to 60 °C and stirred for 12 h. The polymer solution was dried *in vacuo*, and repeatedly precipitated into cold diethyl ether. Yields: 30-60% (after 2-3 precipitation steps). ¹H NMR (300 MHz, DMSO-*d*₆): δ (ppm) = 7.12 (d, 4H, aromatic), 6.72 (d, 4H, aromatic), 4.66 (m, 1H, acetalic and 1OH), 3.82 (s, 4H, PhCH₂N), 3.71-3.16 (br, polyether backbone), 1.18 (m, 3H, CH₃-acetal).

Synthesis of poly(glycerol-co-glycoloxy ethyl glycidyl ether) (P(G-co-GEGE)). General procedure for the copolymerization: *N,N*-dibenzyl tris(hydroxymethyl) aminomethane and 0.3 equivalents of cesium hydroxide monohydrate (25% of OH groups) and 2 mL of benzene were placed in a Schlenk flask and stirred for 30 min at room temperature. All solvents were removed under reduced pressure and the initiator salt was dried at 90 °C for 4 h under high vacuum. The initiator salt was dissolved in diglyme and a mixture of glycidol and GEGE in diglyme was slowly added under argon atmosphere using a syringe pump. The reaction was terminated by adding methanol. The mixture was concentrated and precipitated into and excess of cold diethyl ether. Yields: 70-80%. ¹H NMR

(300 MHz, MeOH- d_4): δ (ppm) = 7.35-7.05 (10H, aromatic), 4.79 (m, 1H, acetal), 4.02 (s, 4H, PhCH₂N), 3.95-3.45 (br, polyether backbone), 1.32 (m, 3H, CH₃-acetal).

Synthesis of poly(glycerol-co-glycoloxy ethyl glycidyl ether –graft-ethylene oxide) (P(G-co-GEGE-g-EO)). General procedure for the polymerization: 100 mg P(G-co-GEGE) copolymer and 0.1 equivalents of cesium hydroxide monohydrate (referenced to the total amount of OH groups) were placed in a 250 mL-Schlenk flask and benzene was added. After stirring for 1 h at 60 °C, the residual water and benzene were removed by evaporation. The macroinitiator was dried overnight and then approximately 20 mL dry THF were cryo-transferred into the Schlenk flask. The respective amount of EO was cryo-transferred to a graduated ampoule, and then cryo-transferred into the reaction flask containing the initiator in THF. The polymerization was carried out at 60 °C for 12 h and the multi-arm star copolymers were obtained by precipitation into cold diethyl ether. ¹H NMR (300 MHz, CDCl₃): δ (ppm) = 7.21-7.02 (d, 10H, aromatic) 4.66 (m, 1H/ GEGE unit, acetalic), 3.82 (s, 4H, PhCH₂N), 3.71-3.16 (br, polyether backbone), 1.44 (m, 3H/ GEGE unit, CH₃-acetal).

Results and Discussion

A: Monomer Synthesis

One major challenge in synthesizing a PEG/PG-based polymer with acid labile groups in the backbone in a single reaction step is the synthesis of a suitable monomer. For the introduction of acetal groups into a polyether backbone a so-called “degradable inimer” is needed. This concept has been employed in one case by Matyjaszewski et al., who synthesized different inimers suitable for ATRP.^{12, 13} Transferring this idea to oxy-anionic polymerization a monomer is needed, which combines the characteristics of EEGE, additionally possessing an acid-labile moiety and of glycidol, a latent AB₂ monomer that can serve both as an initiator and a monomer.

Using a latent AB₂ monomer is advantageous, since every branching unit generates an additional hydroxyl moiety at the polymer periphery. This is beneficial with respect to the conjugation of functional molecules, e.g., drugs or target functionalities, as there is a significant increase in conjugation capacity. This is in correspondence with a recently developed concept, which has been employed for the synthesis of branched PEG.¹⁶ Besides the need for an inimer-type molecule the cleavable functional group needs to be stable under the strongly basic reaction conditions applied in the anionic ring-opening polymerization process. The acetal moiety has been proven to be highly efficient in the carb-¹⁷ and oxy-anionic polymerization process, e.g., in the synthesis of linear PG, which can be derived from a poly(ethoxy ethyl glycidyl ether) (P(EEGE)) precursor.¹⁸⁻²⁰ Based on these design principles, we have synthesized glycoloxy ethyl glycidyl ether (GEGE, Scheme 1).

Protection of the focal hydroxyl functionality, which is required as a starting point in the multibranching reaction requires a protective group that is cleavable without applying very acidic or basic pH values. At low pH-values the desired acetal moiety would be cleaved, and at basic conditions ring-opening at the epoxide might occur. Thus, the benzyl group has been chosen as a suitable protecting group and has been introduced via the reaction of benzyl bromide with ethyl mono vinyl ether. In analogy to the established synthesis of EEGE, **1** ((2-(vinylxy)ethoxy)methylbenzene) was then reacted with glycidol to introduce the desired oxirane functionality (**2**) for AROP.¹⁵ To release the hydroxyl group in the last reaction step, the benzyl protective group was removed using catalytic hydrogenation (**3**). Although hydrogenation of the benzyl protecting group does not interfere with the stability of the acetal group, appropriate reaction conditions had to be found to prevent ring-opening of the oxirane. By adjustment of the solvents employed (ethyl acetate/ methanol, 5:1), catalyst stoichiometry (Pd(OH)₂/C, 5%), concentration (10 wt%), H₂-pressure (1 bar) and reaction time (6-10 h, followed by thin layer chromatography, TLC) yields up to 67% could be obtained in the critical final reaction step. The complete synthetic procedure is summarized in Scheme 1.

Detailed studies revealed that under these conditions no ring-opening of the oxirane, resulting in an unsymmetric acetal-containing diol occurred (cf. **Scheme S1**, Supporting Information). GEGE was identified using ¹H and ¹³C NMR spectroscopy. Detailed characterization data of all reaction steps can be found in the Supporting Information.

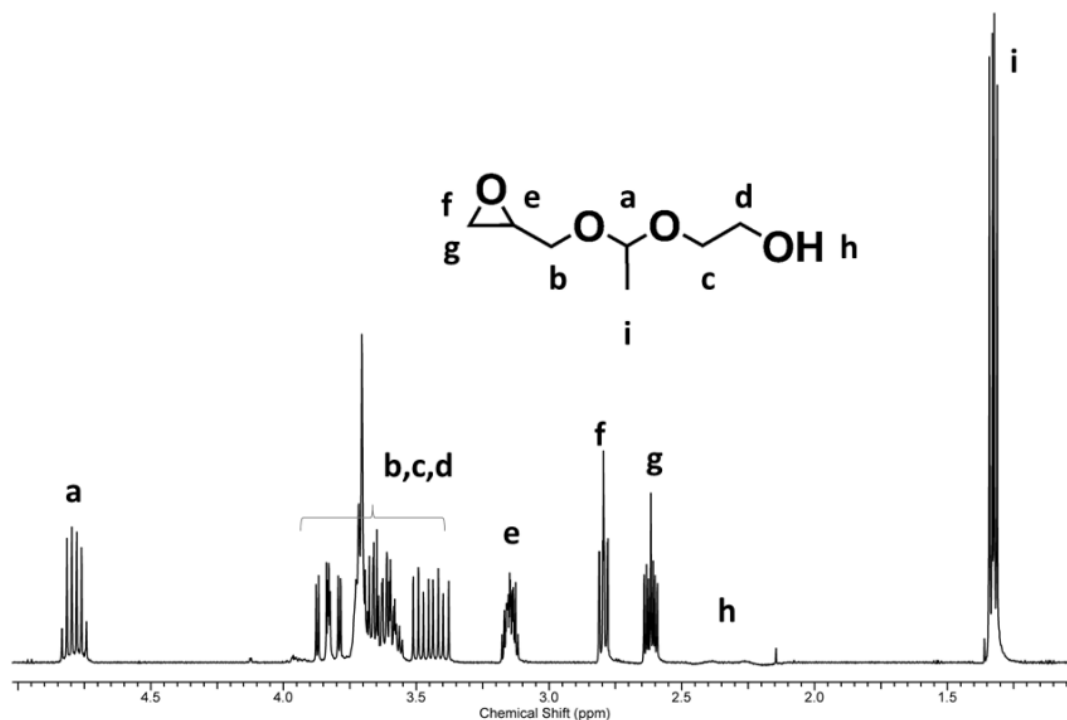


Figure 1. ¹H NMR of glycoloxy ethyl glycidyl ether in CDCl₃ (300 MHz).

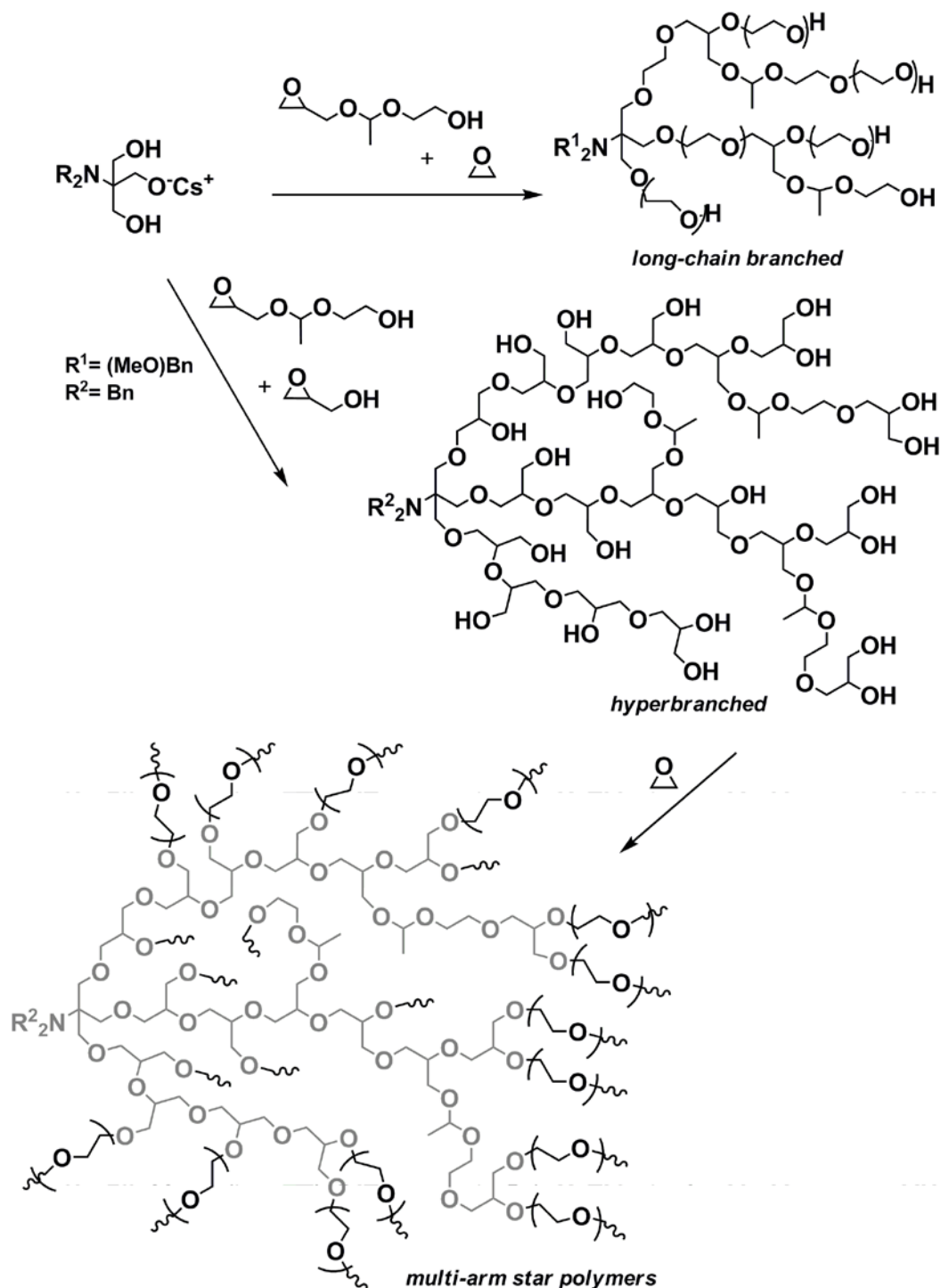
In **Figure 1**, the ^1H NMR spectrum of GEGE is displayed. All signals are assigned to the respective protons. Due to the different stereocenters of the molecule, the signals split up in accordance with the signals found for EEGE, which is a structurally similar compound.^{15, 19} Strong evidence for the successful introduction of the acetal moiety is provided by the corresponding signals at 4.80 (acetalic proton) and 1.33 ppm (methyl group) as well as the oxirane signals at 3.14, 2.80 and 2.61 ppm. The integral ratio of 1 (acetalic proton) to 1 (epoxide proton) to 3 (methyl group) remains constant after hydrogenation, confirming the success of the reaction. The monomer yield after three reaction steps is in the range of 30-50%.

B: Polymer Synthesis and Characterization

Three different branched polyether architectures that are valuable for potential biomedical applications have been synthesized using GEGE as a key building block. GEGE was copolymerized with ethylene oxide (EO) and glycidol (G), respectively to obtain long-chain branched ($\text{P}(\text{EO}_n\text{-co-GEGE}_m)$) and hyperbranched ($\text{P}(\text{G}_n\text{-co-GEGE}_m)$) polyether polyols. In order to obtain acid labile star polymers, PEO chains were initiated from $\text{P}(\text{G}_n\text{-co-GEGE}_m)$ core molecules to obtain multi-arm star polymers $\text{P}(\text{G}_n\text{-co-GEGE}_m\text{-}g\text{-EO}_k)$. An overview of the different polymer topologies synthesized is given in **Scheme 2**. The corresponding data, which will be discussed in the following paragraphs, are summarized in **Table 1**.

[P(EO-co-GEGE)]. For the copolymerization of GEGE with EO, the alkoxide of the newly developed initiator *N,N*-Di(*p*-methoxy)-benzyl tris(hydroxymethyl) aminomethane ((MeOBn₂)NTRIS) was prepared. This initiator allows to obtain a single amino moiety in the branched polymers by hydrogenation of the benzyl protecting groups. In contrast to its analogues^{19, 21, 22} it bears three hydroxyl-groups, which is important for the ring opening multibranching polymerization (ROMBP) of glycidol.^{23, 24} The copolymerization of different glycidyl ethers (ABR-monomers) with the latent AB₂ monomer glycidol and additional theoretical considerations regarding the degree of branching (DB) have been published by Sunder et al.²⁵ In contrast to the system described in this early work, no slow monomer addition (SMA) could be used in the copolymerization of the functional glycidol analogue GEGE with EO (system (ii)). For experimental reasons, there is no possibility to introduce the gaseous, highly toxic EO (bp. 11 °C) steadily into a reaction flask with an inside temperature of 60 °C without severe safety issues. Therefore, both monomers were added to the initiator salt in a one-pot reaction, in analogy to a previously described procedure.¹⁶ Since GEGE is a inimer that can act as an initiator, the formation of small oligomeric side products was observed. This is in accordance with the findings for the EO/glycidol copolymers investigated by Wilms et al.¹⁶ However, the low molecular

weight side products can conveniently be removed by precipitation into cold diethyl ether. SEC-traces of polymer no. 3 before and after precipitation are exemplified in the Supporting Information (**Figure S4**). In all cases, narrow molecular weight distributions were obtained ($M_w/M_n < 1.3$). The molecular weights of the polymers ranged between 1 800 and 2 200 g mol^{-1} . The amount of GEGE was varied from 5 to 20 mol%.



Scheme 2. Three different polymer classes prepared: (i) long-chain branched ($\text{P}(\text{EO}_n\text{-co-GEGE}_m)$), (ii) hyperbranched ($\text{P}(\text{G}_n\text{-co-GEGE}_m)$), and (iii) multi-arm star ($\text{P}(\text{G}_n\text{-co-GEGE}_m\text{-g-EO}_k)$) polyethers.

Incorporation of the novel comonomer GEGE was confirmed via ^1H NMR spectroscopy. By comparing the signals of the polyether backbone, the signals of incorporated GEGE (acetal at 4.66 ppm and CH_3 -group at 1.18 ppm) and the aromatic signals of the initiator (7.14 and 6.69 ppm, in $\text{DMSO-}d_6$) (compare also **Figure 4**), the comonomer ratio can be calculated. Additionally, ^{13}C NMR can be employed to verify the incorporation of the acetal moiety into the branched polymer structure. In addition to the acetal resonances that occur at 101.7 (acetalic proton) and 20.3 ppm (methyl group), different repeat units can be identified with signals at 79.3, 73.3 and 66.1 ppm, which confirm the existence of dendritic and various linear repeat units that originate from the GEGE fraction (Figure S4, Supporting Information).

Table 1. Overview on three different copolymer classes synthesized in this study.

No	Formula (NMR)	% GEGE (NMR)	M_n g/mol (NMR)	M_n g/mol (SEC)	PDI (SEC)
1	$(\text{MeOBn})_2\text{NTrisP}(\text{EO}_{129}\text{-CO-GEGE}_8)$	5.8	6 900	2 200	1.3
2	$(\text{MeOBn})_2\text{NTrisP}(\text{EO}_{129}\text{-CO-GEGE}_{13})$	9.2	7 800	2 400	1.4
3	$(\text{MeOBn})_2\text{NTrisP}(\text{EO}_{131}\text{-CO-GEGE}_{15})$	10.3	8 200	1 800	1.3
4	$\text{Bn}_2\text{NTrisP}(\text{G}_{58}\text{-CO-GEGE}_4)$	6.4	4 900	2 300	1.9
5	$\text{Bn}_2\text{NTrisP}(\text{G}_{34}\text{-CO-GEGE}_{11})$	24.4	4 300	2 400	1.8
6	$\text{Bn}_2\text{NTrisP}(\text{G}_{20}\text{-CO-GEGE}_{19})$	38.7	4 100	3 100	1.6
7	$\text{Bn}_2\text{NTrisP}(\text{G}_{34}\text{-CO-GEGE}_{11}\text{-}g\text{-EO}_{147})$	5.7	10 700	5 800	1.4
8	$\text{Bn}_2\text{NTrisP}(\text{G}_{20}\text{-CO-GEGE}_{19}\text{-}g\text{-EO}_{153})$	9.8	10 800	5 200	1.6

^{a)} ^1H NMR in $\text{DMSO-}d_6$, ^{b)} obtained from the RI-detector signal of SEC, measured in DMF using PEG-standards.

The benzyl protected initiator provides the opportunity to determine the molecular weight of the polymer. However, it should be emphasized, that due to the formation of the oligomeric side products, the determination of the molecular weight by the use of the initiator protons results in a certain inaccuracy, since some of the polymers might originate from self-initiation and thus *N,N*-Di(*p*-methoxy)-benzyl tris(hydroxymethyl) aminomethane might not be incorporated in all polymer chains. In addition, the targeted molecular weight does not correspond to the obtained molecular weight, which was also observed for similar systems.¹⁶ These drawbacks given by the utilization of ethylene oxide as a comonomer are avoided when employing glycidol as comonomer (see following paragraph). However, it is important to show that in principle copolymerization with EO is feasible, due to the high acceptance of PEG for biomedical stealth applications. Still, the polymerization set-up

needs to be adjusted to obtain better control over molecular weight. The development of new polymerization routes is currently subject of investigation. The characterization data of all P(EO-co-GEGE) copolymers synthesized is summarized in Table 1.

[P(G-co-GEGE)]. Hyperbranched polyglycerol (*hbPG*) can be synthesized with control over a broad range of molecular weights ($5\text{-}25\text{ kg mol}^{-1}$) and low to narrow polydispersities ($M_w/M_n = 1.3\text{-}1.8$) by applying the slow monomer-addition (SMA) technique for the ring-opening multibranching polymerization (ROMBP) of the latent AB_2 monomer glycidol.^{16, 23} The structural analogy of glycidol and GEGE allows for the controlled incorporation of GEGE into the *hbPG* scaffold and thus the introduction of a tailored number of acid-cleavable moieties. Polyglycerol (PG) in general is a highly suitable polymer class for biomedical applications, as it has been described in several works, e.g., Brooks and coworkers evaluated the biocompatibility of PGs with varying architecture and molecular weights.²⁶⁻²⁸ By slow addition of a mixture of glycidol and GEGE in high dilution to the partial deprotonated initiator Bn_2TRIS , several poly(glycerol-co-glycoloxy ethyl glycidyl ether) (P(G-co-GEGE)) copolymers with varying GEGE-content were synthesized (compare **Table 1**, entry 4-6).

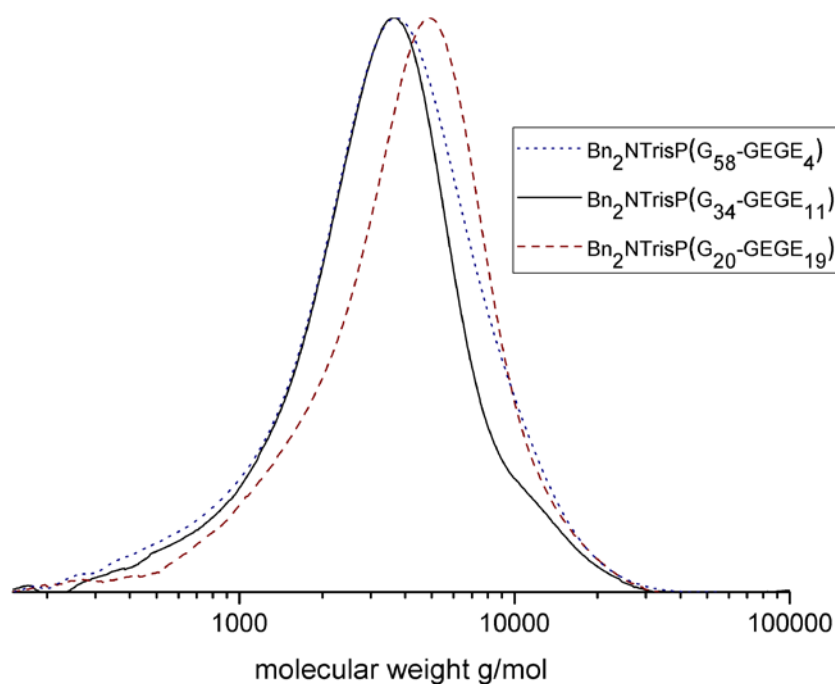


Figure 2. SEC traces of polymer 4-6 after precipitation in DMF using the RI-signal.

The molecular weight of the polymers was characterized using SEC and 1H NMR spectroscopy. In the 1H NMR spectrum (**Figure S5**, Supporting Information), the incorporation of GEGE into *hbPG* can be quantified by comparing the integrals of the initiator (7.44 to 7.07 ppm), the signal of the acetal proton of GEGE (4.82 ppm) and the methyl group (1.35 ppm). Overall, we find good agreement

between the targeted values and the data obtained by NMR spectroscopy for all polymers (GEGE-content = 5-38%). This is in accordance with the control over the copolymerization reaction in contrast to the above-mentioned findings for the copolymerization with EO. Since no oligomeric side products were found, full conversion of the benzyl-protected amine initiator is supposed. Thus, the number average molecular weight of the polymers can be calculated from a comparison of the signals of the initiator and the polyether backbone (4.11 to 3.42 ppm). The comonomer incorporation can also be proven by ^{13}C NMR, and the respective signals corresponding to the GEGE-units are identified in **Figure S6** of the Supporting Information. Due to the overlapping signals of the dendritic and linear units originating from the two comonomers (GEGE and glycidol) a calculation of the degree of branching cannot be carried out, as described in literature.^{16, 23} In the SEC analysis, the molecular weight is usually underestimated compared to results from ^1H NMR and the targeted values, since the branched architecture and the presence of multiple hydroxyl functionality within P(G-co-GEGE) lead to a decreased hydrodynamic volume compared to conventional linear PEGs, which were used for SEC calibration. The P(G-co-GEGE) copolymers show narrow to moderate PDIs ($M_w/M_n = 1.6-1.9$), with a monomodal distribution, as it can be seen from the SEC traces in **Figure 2**. These values are slightly higher than for conventional *hbPG* polymers, but still acceptable for some biomedical applications.⁹ Although the use of glycidol as comonomer resulted in controlled polymerization conditions, the maximum molecular weight that can be achieved, is still limited. An additional class of degradable polymers has been synthesized and is discussed in detail in the following paragraph.

[P(G-co-GEGE-*g*-EO)]. Due to the limitation in achievable molecular weights of P(G-co-GEGE) (around 2 000 g/mol) and P(EO-co-GEGE) (2 000 to 3 000 g/mol), poly(ethylene glycol) (PEG) was grafted from P(G-GEGE), to obtain novel polyether-based multi-arm star polymers poly(glycerol-co-glycoloxy ethyl glycidyl ether-*graft*- ethylene oxide) (P(G-co-GEGE-*g*-EO). The use of PG as a core for the synthesis of multi-arm-star polymers with a polyether structure has first been described by our group.²⁹⁻³¹ In analogy to this work the degree of deprotonation was kept low to guarantee the good solvation of the P(G-co-GEGE) copolymers, which were used as macro-initiators in this case. Exemplary, the molecular weight increase from sample **6** to **8** by grafting EO onto the P(G-co-GEGE)-core is shown in Figure 3.

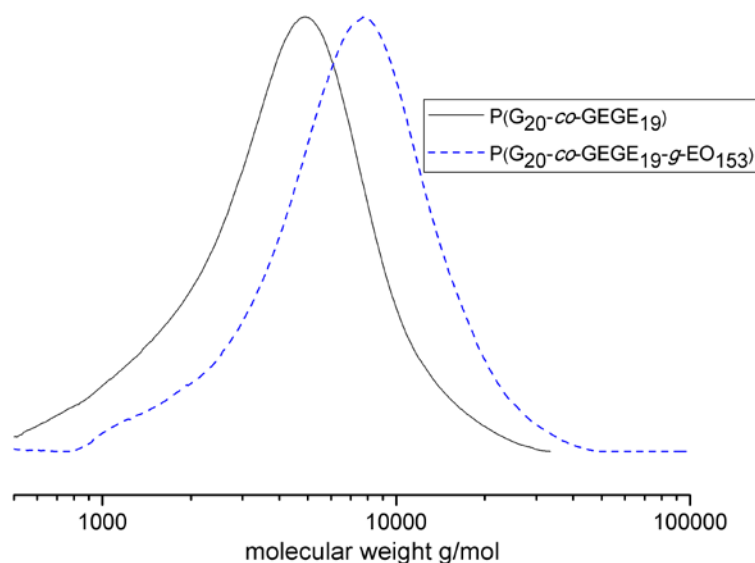


Figure 3. SEC traces of polymer no. **6** ($\text{Bn}_2\text{NTrisP}(\text{G}_{20}\text{-co-GEGE}_{19})$) and **8** ($\text{Bn}_2\text{NTrisP}(\text{G}_{20}\text{-co-GEGE}_{19}\text{-g-EO}_{153})$) in DMF (refractive index detector).

The PEO multi-arm star polymers exhibit molecular weights exceeding 10 000 g/mol, which can be derived from NMR by comparison of the signals of the initiator protons to the polyether backbone in analogy to the two previously described polymer classes. Exemplarily, one ^1H NMR spectrum can be found in the Supporting Information (**Figure S6**). The spectrum was measured in CDCl_3 and the solubility in this solvent confirms successful grafting of PEG, since PG and the $\text{P}(\text{G-co-GEGE})$ -copolymers are insoluble in CDCl_3 . The PDIs obtained from SEC remain constant, compared to the hyperbranched precursors ($M_w/M_n < 1.6$). Similar to the hyperbranched structures described above, a strong deviation of the molecular weight obtained from NMR and the molecular weight obtained by SEC is observed, due to the globular structure of the polymers, which is referenced to linear PEG standards. Besides enhancing the molecular weight of the polymers, the grafting of PEG onto the polyethers will also result in larger fragments formed during the degradation process of the copolymers.

C: Degradation Studies

To confirm the pH-sensitive degradation of the polymers, it is important to demonstrate that the polymers are stable at neutral pH (pH=7) at room temperature. To this end, polymer **2** was kept in D_2O for several weeks. **Figure 4** displays the corresponding ^1H NMR spectrum. Besides the signals resulting from the polyether backbone (3.5 – 4.1 ppm) and the signals of the initiator (7.44 to 7.07 ppm), the signal of the acetal proton (c), which overlaps with the signal resulting from residual water and the methyl group (d) remains visible, and the integrals of these resonances remain constant over time. In addition, the absence of acetic aldehyde, which would be formed during degradation of the

polymers and would be observable at 2.12 and 9.58 ppm (in D₂O, compare degradation kinetics), verifies the stability of the polymers in aqueous solution at pH=7.

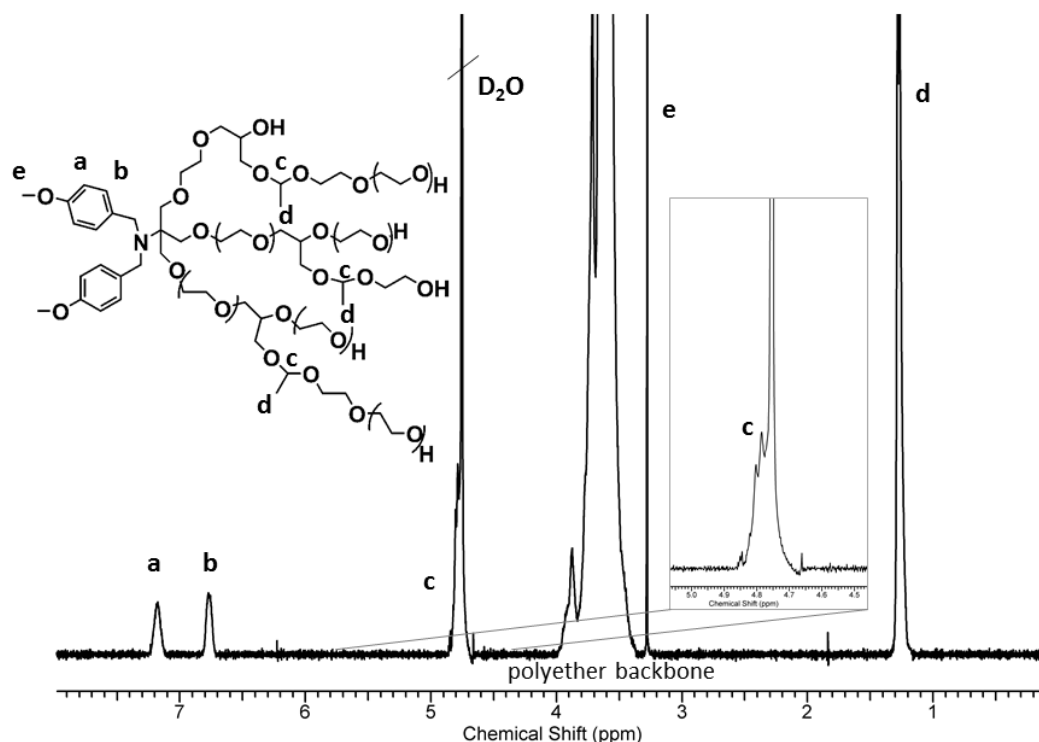


Figure 4. ¹H NMR spectrum (300 MHz, D₂O) of (MeOBn)₂NTrisP(EO₁₂₉-co-GEGE₁₃)/ polymer after 2 weeks.

The polymers obtained have been investigated with respect to their degradation kinetics at room temperature using SEC measurements. For this purpose, sample **3** was dissolved in different buffer solutions. Aliquots have been measured by SEC after 1-24 h and up to 16 days. At pH=7.4 no degradation was observed. At pH 2 the polymer degraded completely within 2 h, while at pH 4 the polymer was degraded after 2 d. The respective SEC curves are given in the Supporting Information (**Figure S7**). Interestingly, the SEC-traces become bimodal after degradation, which can be explained by the presence of a core molecule and lower molecular weight fragments. This can be rationalized by the fact that during the addition of the GEGE-comonomer two different hydroxyl groups are formed, one at the end of acid-labile acetal moiety and a second one covalently connected to the core molecule. As the probability for the addition of other monomers is the same for both hydroxyl groups, only half of the growing arms will be degradable afterwards, which results in the formation of two degradation modes.

However, studying the degradation using SEC-traces does not allow for quantitative investigation of the degradation kinetics, since the intensity of the RI-signals is not only related to the polymer

concentration, but is also dependent on the molecular weight of the fragments. Therefore, we employed ^1H NMR spectroscopy in deuterated water at different pH-values to determine the degradation behavior. All samples were kept at 37 °C to mimic physiological conditions. Sample 6 was measured in acidic D_2O (pH 4). A clear decrease of the acetal group concentration was observed within the first 8 h (compare **Figure S8**), but after 50% the degradation stagnated completely. This was explained by the presence of acetic aldehyde, which is formed during the degradation process. Possessing a boiling point of 20 °C it should be released from the NMR tube, but due to the small surface area in the NMR tube and the good water solubility of acetaldehyde it was found to remain within the solution and prevented further degradation due to the resulting acetalization/hydrolysis equilibrium. The reaction set-up had to be changed and the samples were stirred in a round bottom flask and the degradation of the polymers is observed, without stagnation. In **Figure 5** the degradation of polymer no 5 is shown at different pH-values.

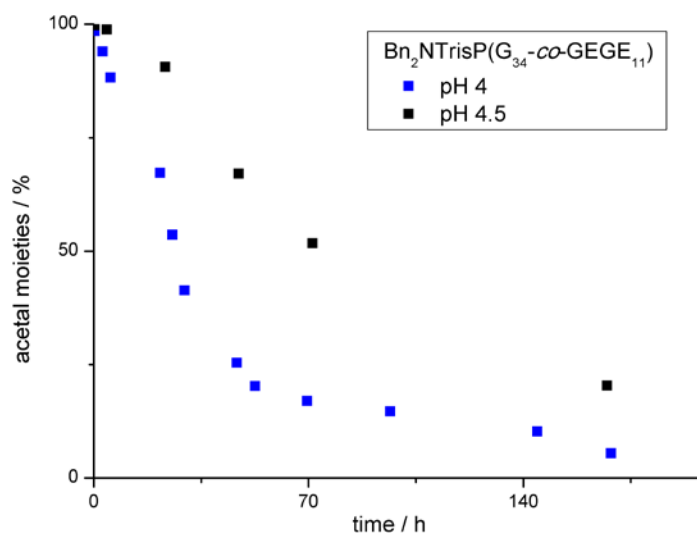


Figure 5. Acetal moieties versus time obtained for polymer 5 from ^1H NMR kinetics ($\text{Bn}_2\text{NTrisP}(\text{G}_{34}\text{-CO-GEGE}_{11})$) at pH 4 and 4.5 at 37 °C.

A strong dependence of the degradation kinetics on the pH is observed. Using an exponential decay to fit the slopes, the half life time of the acetal groups can be calculated using Origin software (compare **Figure S10**, Supporting Information). At pH 4.5 $t_{1/2}$ is approximately 76 h, while at pH 4 $t_{1/2}$ is less than half with 26 h.

With the respect to biomedical applications, these materials are interesting, since no degradation is observed at pH 7 or higher. This means that for instance in the blood stream no molecular weight loss of the polyethers would occur. However, in tissues with lower pH value, a decrease in the molecular weight and therefore an increase in the activity of the drug/protein attached should be

observed. The covalent attachment of multiple reactive molecules (proteins or drugs) to the hydroxyl end groups is currently under investigation.

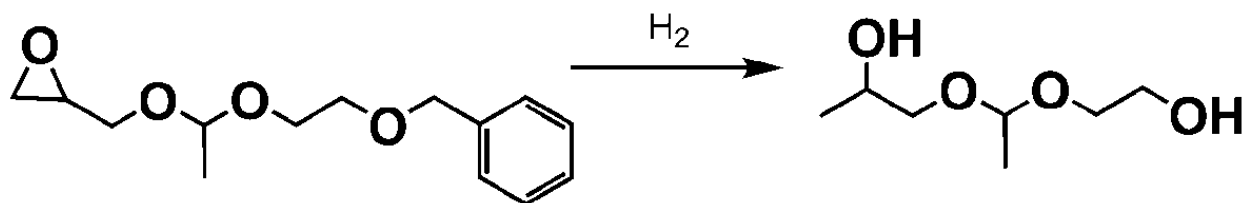
Conclusion

We have developed an epoxide-based acid labile inimer, permitting the one-step synthesis of acid-degradable, branched PEG. To the best of our knowledge this represents the first synthesis of an acetal-containing inimer that is applicable for the synthesis of branched, degradable and biocompatible polyethers. With regard to the initially mentioned limitation of the molecular weight, these polymers are promising concerning the combination of two properties: degradability and biocompatibility. The branched polyethers obtained showed moderate to narrow PDIs ($M_w/M_n < 1.9$), and control over molecular weight was obtained by slow monomer addition. Probing the degradability of the novel compounds revealed a strong pH-dependence of the half-life time of these polymers. On the one hand these materials can be used as carrier molecules and on the other hand an enhanced release of the active reagent at the respective site, after acidic degradation, can be obtained. Since PG has been proven to be biocompatible²⁷ and exhibits a toxicity profile comparable to PEG, the novel structures are promising due to the acid-labile acetal moiety. Toxicity tests for the new materials are currently under way. We believe that pH-responsive materials are a promising development of conventional PEG and PG-based structures for pharmaceutical application.

Acknowledgement

The authors thank Alina Mohr, Tim Dumschlaff, Jochen Willersinn and Margarete Deptolla for technical assistance. C. M. and C.S. are recipients of a fellowship through funding of the Excellence Initiative (DFG/GSC 266). H.F. acknowledges the Fonds der Chemischen Industrie and the SFB 625 for support.

Supporting Information



Scheme S1. Formation of the undesired side product 1-(1-(2-hydroxyethoxy)ethoxy)propan-2-ol observed during hydrogenolysis due to undesired epoxide ring-opening.

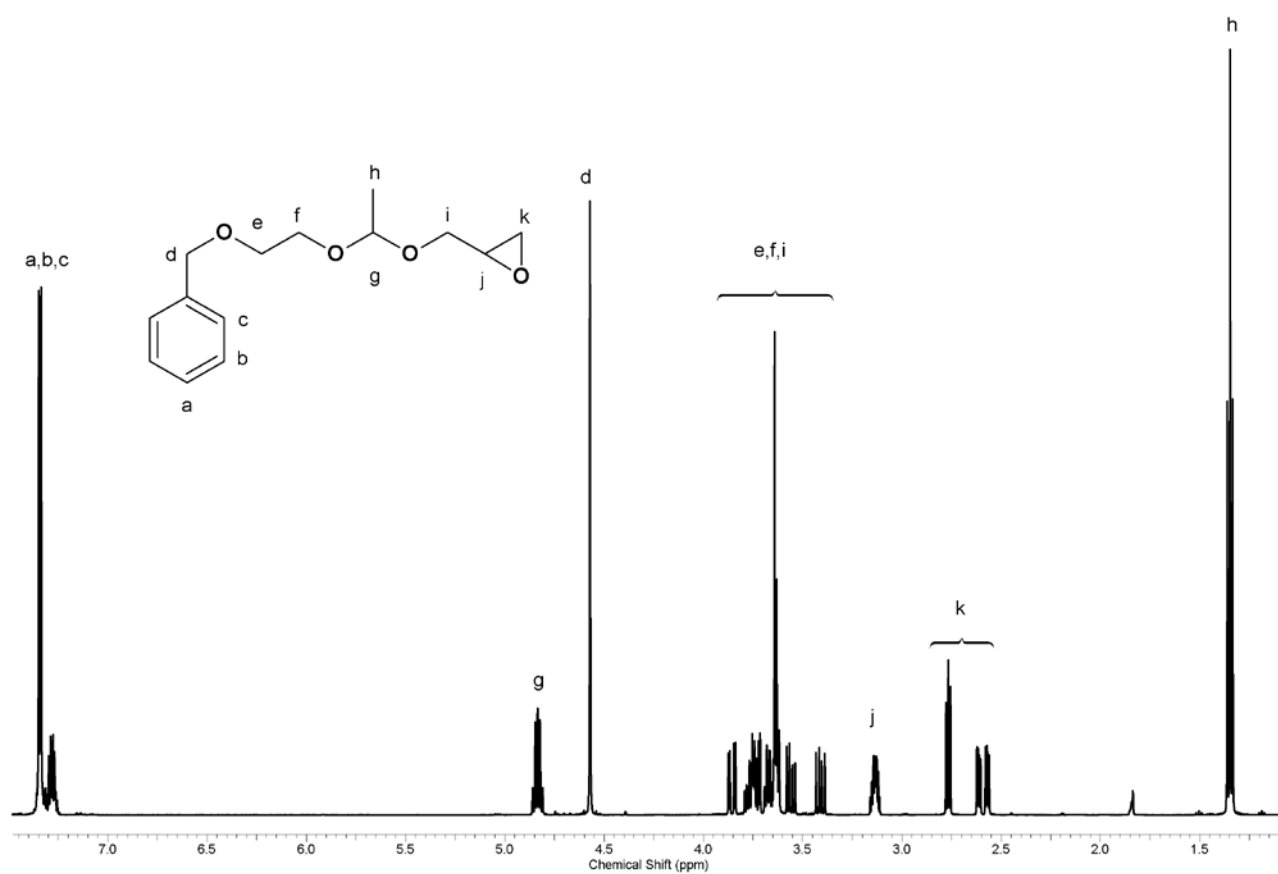


Figure S1. ¹H NMR spectrum of the intermediate product (2, cf. Scheme 1) prior to hydrogenation.

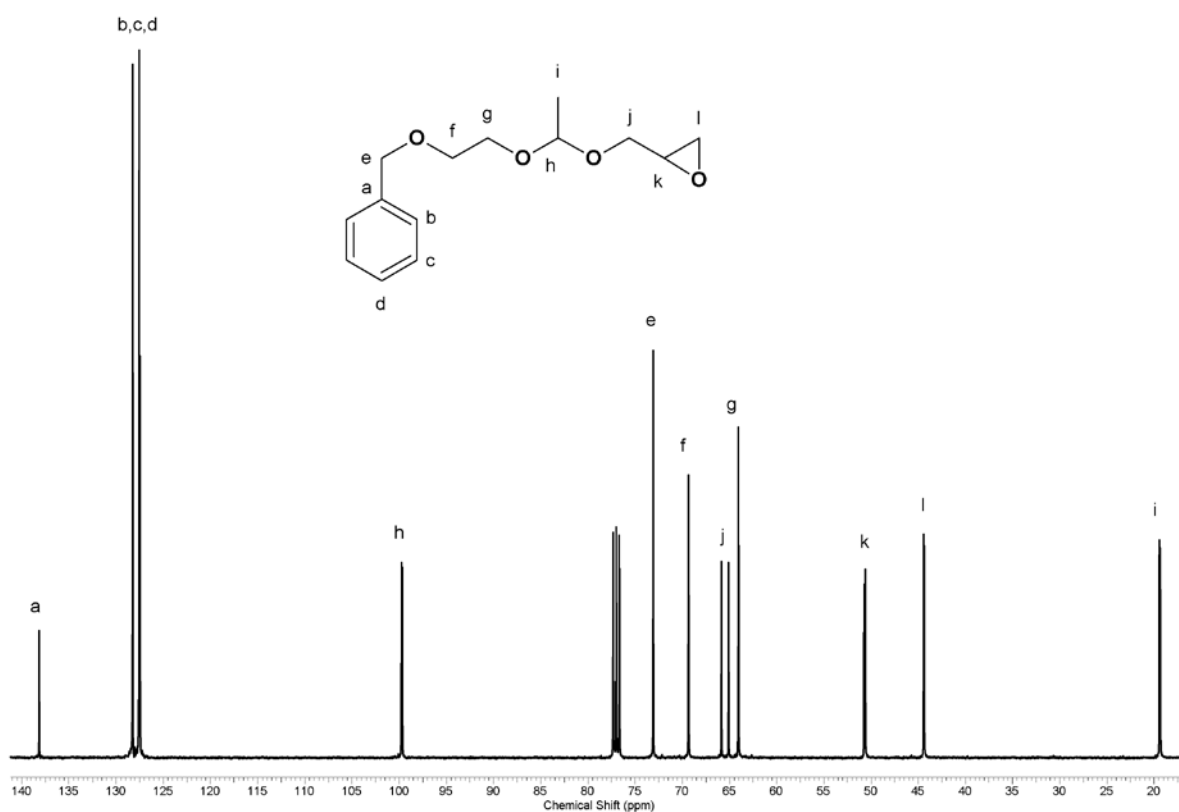


Figure S2. ¹³C NMR spectrum of the intermediate compound (2) prior to hydrogenation.

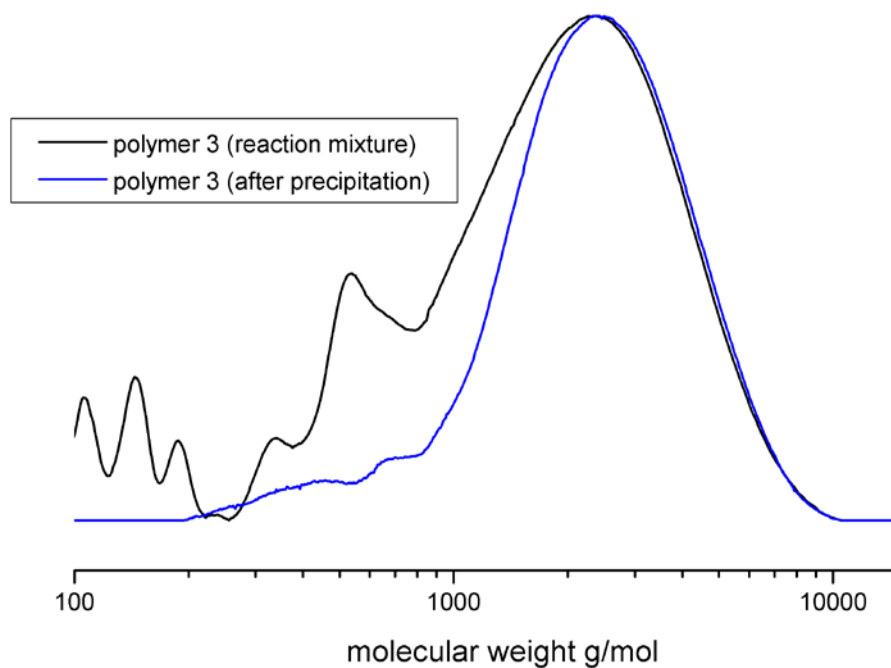


Figure S3. SEC traces of polymer no. 3 ((MeOBn)₂NTrisP(EO₁₃₁-co-GE₁₅)) before and after precipitation, demonstrating removal of oligomers.

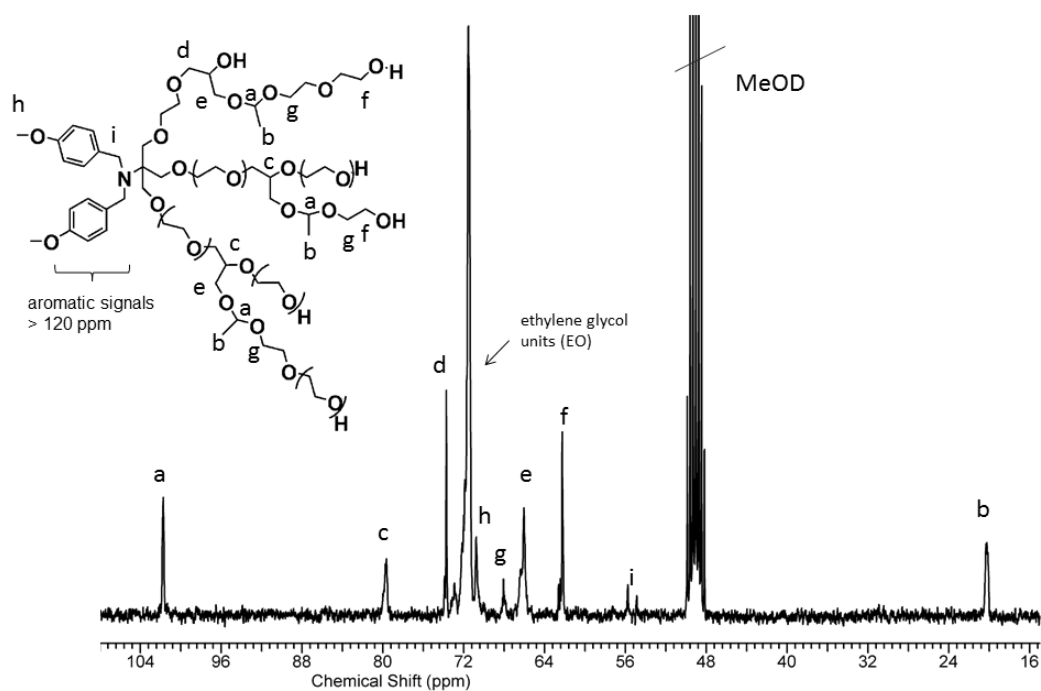


Figure S4. Assignment of the different carbon atoms in ^{13}C NMR spectrum of polymer sample 2 ((MeOBn) $_2$ NTrisP(EO $_{129}$ -CO-GE $_{13}$)) in MeOD.

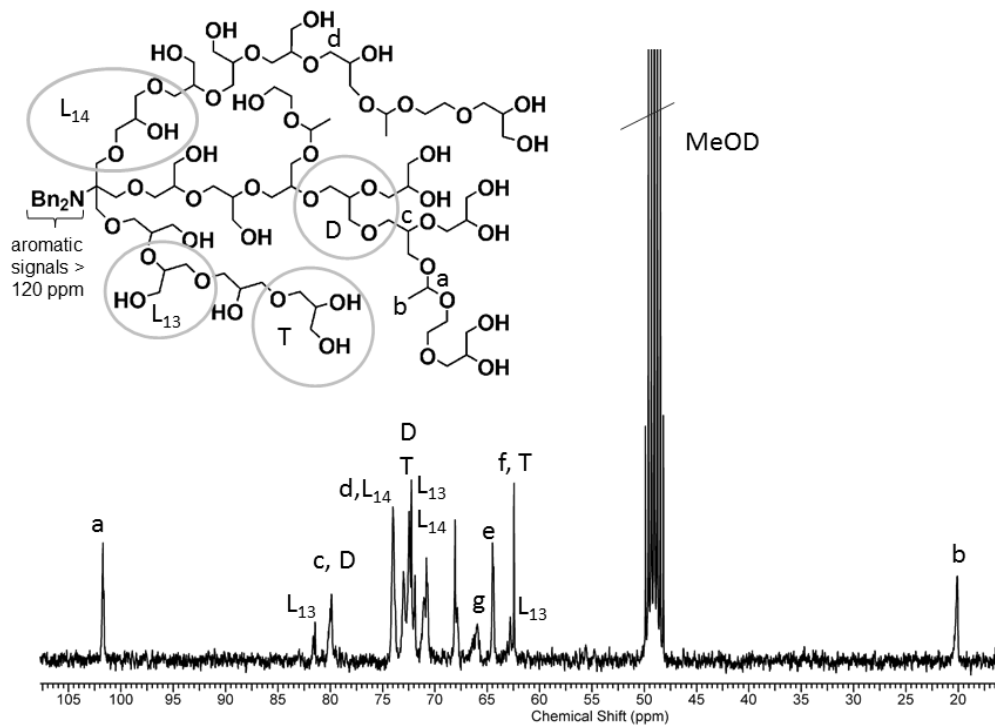


Figure S5. Assignment of the different carbon atoms in ^{13}C NMR of polymer no. 5 Bn $_2$ NTrisP(G $_{34}$ -CO-GE $_{11}$) in MeOD. For the assignment of the carbon atoms of PG in ^{13}C NMR, compare Sunder et al.¹

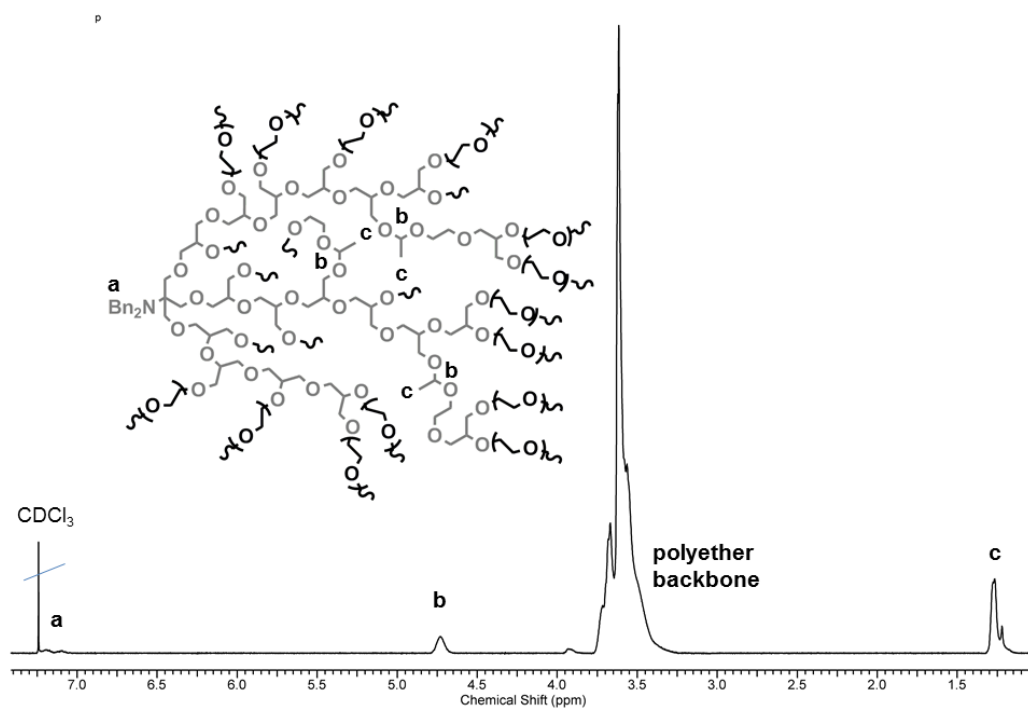


Figure S6. Assignment of ^1H NMR spectrum of degradable multi-arm star polymer **8** $\text{Bn}_2\text{NTrisP}(\text{G}_{20}\text{-co-GEGE}_{19}\text{-g-EO}_{153})$ in CDCl_3 .

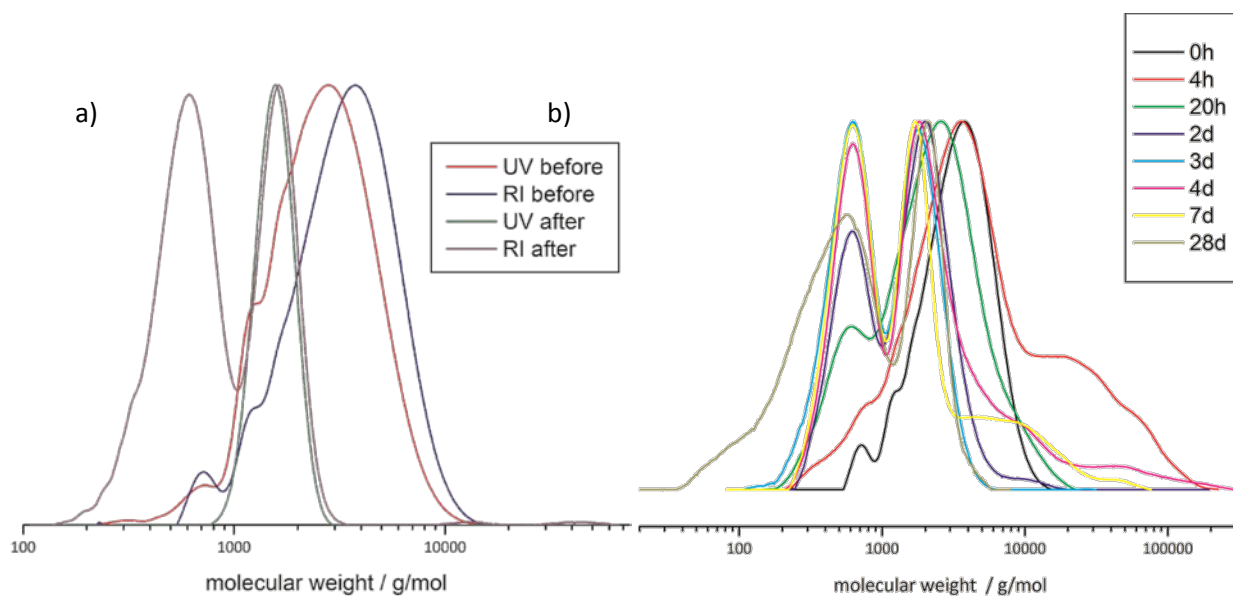


Figure S7. a) SEC-trace of polymer no **3** $(\text{MeOBn})_2\text{NTrisP}(\text{EO}_{131}\text{-co-GEGE}_{15})$ before and after treatment with pH 2 and b) pH 4 at various times.

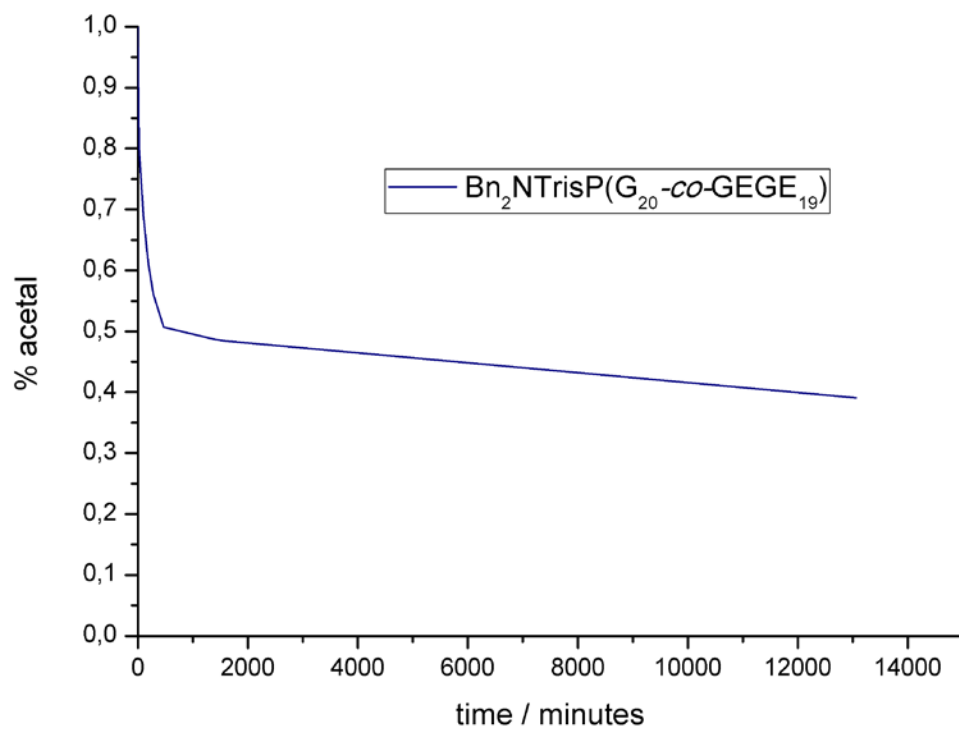


Figure S8. Amount of acetal functionalities (%) versus time of polymer **6** ($\text{Bn}_2\text{NTrisP}(\text{G}_{20}\text{-co-GEGE}_{19})$) at pH 4, recorded in a closed NMR tube (normalized to initial acetal signal).

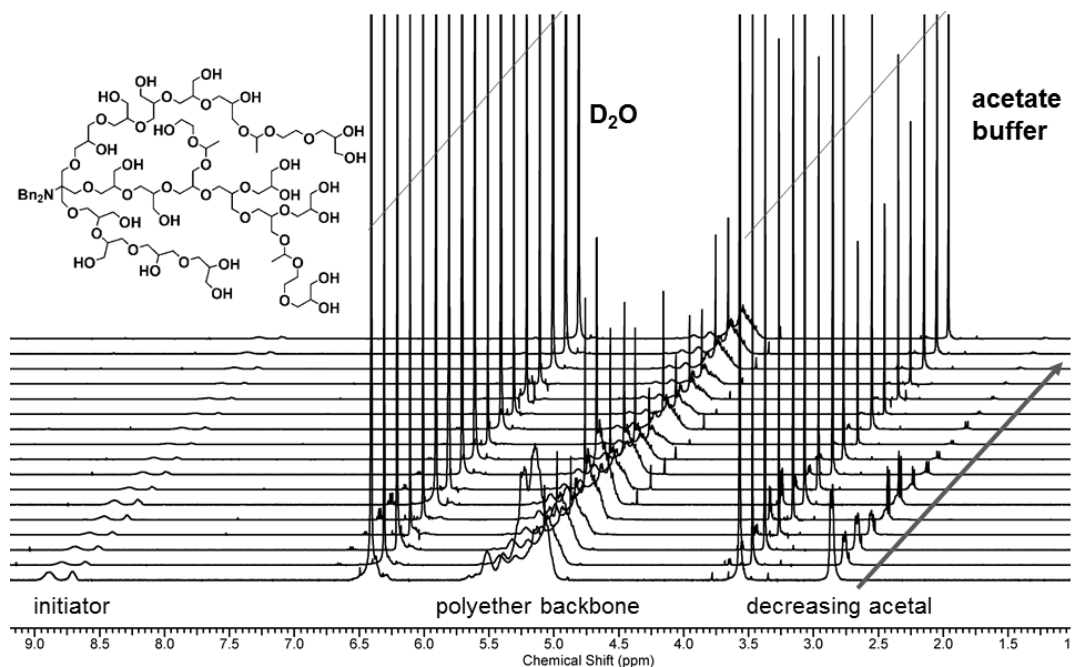


Figure S9. ^1H NMR kinetics of polymer **5** ($\text{Bn}_2\text{NTrisP}(\text{G}_{34}\text{-co-GEGE}_{11})$) in pH 4 (D_2O , 300 MHz)

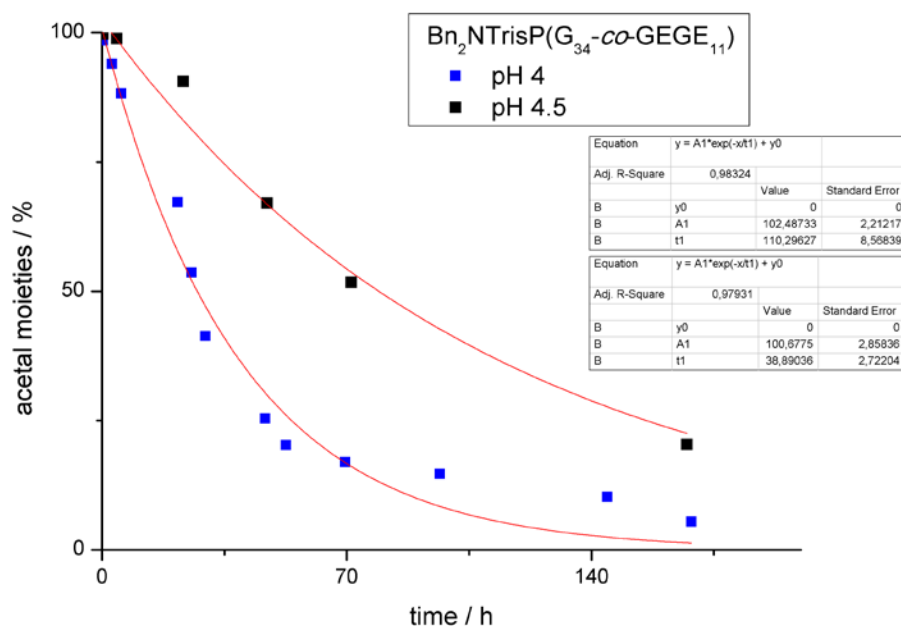


Figure S10. Acetal moieties versus time obtained from the ^1H NMR kinetics of polymer **5** ($\text{Bn}_2\text{NTrisP}(\text{G}_{34}\text{-co-GEGE}_{11})$) in pH 4 (blue symbols) and pH 4.5 at 37°C . The half-life time can be calculated from the equation: $t_{1/2} = t1 * \ln 2$.

1. Abuchowski, A.; McCoy, J. R.; Palczuk, N. C.; van Es, T.; Davis, F. F. *J. Biol. Chem.* **1977**, *252*, (11), 3582-3586.
2. Bailon, P.; Palleroni, A.; Schaffer, C. A.; Spence, C. L.; Fung, W.-J.; Porter, J. E.; Ehrlich, G. K.; Pan, W.; Xu, Z.-X.; Modi, M. W.; Farid, A.; Berthold, W.; Graves, M. *Bioconjugate Chem.* **2001**, *12*, (2), 195-202.
3. Knop, K.; Hoogenboom, R.; Fischer, D.; Schubert, U. S. *Angew. Chem.* **2010**, *122*, (36), 6430-6452.
4. Braunová, A.; Pechar, M.; Laga, R.; Ulbrich, K. *Macromol. Chem. Phys.* **2007**, *208*, (24), 2642-2653.
5. Tannock, I. F.; Rotin, D. *Cancer Research* **1989**, *49*, (16), 4373-4384.
6. Reid, B.; Tzeng, S.; Warren, A.; Kozielski, K.; Elisseff, J. *Macromolecules* **2010**, *43*, (23), 9588-9590.
7. Rickerby, J.; Prabhakar, R.; Ali, M.; Knowles, J.; Brocchini, S. *J. Mater. Chem.* **2005**, *15*, (18), 1849-1856.
8. Tomlinson, R.; Heller, J.; Brocchini, S.; Duncan, R. *Bioconjugate Chem.* **2003**, *14*, (6), 1096-1106.
9. Tomlinson, R.; Klee, M.; Garrett, S.; Heller, J.; Duncan, R.; Brocchini, S. *Macromolecules* **2001**, *35*, (2), 473-480.

10. Feng, X.; Chaikof, E. L.; Absalon, C.; Drummond, C.; Taton, D.; Gnanou, Y. *Macromol. Rapid Commun.* **2011**, 32, (21), 1722-1728.
11. Satoh, K.; Poelma, J. E.; Campos, L. M.; Stahl, B.; Hawker, C. J. *Polym. Chem.* **2012**.
12. Tsarevsky, N. V.; Huang, J.; Matyjaszewski, K. J. *Polym. Sci., Part A: Polym. Chem.* **2009**, 47, (24), 6839-6851.
13. Rikkou-Kalourkoti, M.; Matyjaszewski, K.; Patrickios, C. S. *Macromolecules* **2012**, 45, (3), 1313-1320.
14. Weibel, N.; Charbonniere, L. c.; Ziesel, R. *Tetrahedron Lett.* **2006**, 47, (11), 1793-1796.
15. Fitton, A. O.; Hill, J.; Jane, D. E.; Millar, R. *Synthesis* **1987**, (12), 1140-1142.
16. Wilms, D.; Schömer, M.; Wurm, F.; Hermanns, M. I.; Kirkpatrick, C. J.; Frey, H. *Macromol. Rapid Commun.* **2010**, 31, (20), 1811-1815.
17. Tonhauser, C.; Wilms, D.; Wurm, F.; Berger-Nicoletti, E.; Maskos, M.; Löwe, H.; Frey, H. *Macromolecules* **2010**, 43, (13), 5582-5588.
18. Hans, M.; Keul, H.; Möller, M. *Polymer* **2009**, 50, (5), 1103-1108.
19. Mangold, C.; Wurm, F.; Obermeier, B.; Frey, H. *Macromol. Rapid Commun.* **2010**, 31, (3), 258-264.
20. Gervais, M.; Brocas, A.-L.; Cendejas, G.; Deffieux, A.; Carlotti, S. *Macromolecules* **2010**, 43, (4), 1778-1784.
21. Burakowska, E.; Haag, R. *Macromolecules* **2009**, 42, (15), 5545-5550.
22. Mangold, C.; Wurm, F.; Obermeier, B.; Frey, H. *Macromolecules* **2010**, 43, (20), 8511-8518.
23. Sunder, A.; Hanselmann, R.; Frey, H.; Mülhaupt, R. *Macromolecules* **1999**, 32, (13), 4240-4246.
24. Hanselmann, R.; Holter, D.; Frey, H. *Macromolecules* **1998**, 31, (12), 3790-3801.
25. Sunder, A.; Turk, H.; Haag, R.; Frey, H. *Macromolecules* **2000**, 33, (21), 7682-7692.
26. Kainthan, R. K.; Janzen, J.; Levin, E.; Devine, D. V.; Brooks, D. E. *Biomacromolecules* **2006**, 7, (3), 703-709.
27. Kainthan, R. K.; Hester, S. R.; Levin, E.; Devine, D. V.; Brooks, D. E. *Biomaterials* **2007**, 28, (31), 4581-4590.
28. Kainthan, R. K.; Brooks, D. E. *Biomaterials* **2007**, 28, (32), 4779-4787.
29. Doycheva, M.; Berger-Nicoletti, E.; Wurm, F.; Frey, H. *Macromol. Chem. Phys.* **2009**, 211, (1), 35-44.
30. Knischka, R.; Lutz, P. J.; Sunder, A.; Mülhaupt, R.; Frey, H. *Macromolecules* **1999**, 33, (2), 315-320.
31. Sunder, A.; Mülhaupt, R.; Frey, H. *Macromolecules* **1999**, 33, (2), 309-314.
